ACTA PHARMACEUTICA SCIENCIA

International Journal in Pharmaceutical Sciences, Published Quarterly

ISSN: 2636-8552
e-ISSN: 1307-2080,
Volume: 63, No: 2, 2025
Formerly: Eczacılık Bülteni / Acta Pharmaceutica Turcica
Founded in 1953 by Kasım Cemal GÜVEN

ACTA PHARMACEUTICA SCIENCIA

International Journal in Pharmaceutical Sciences
is Published Quarterly
ISSN: 2636-8552
e-ISSN: 1307-2080,
Volume: 63, No: 2, 2025
Formerly: Eczacılık Bülteni/Acta Pharmaceutica Turcica
Founded in 1953 by Kasım Cemal Güven

Address
İstanbul Medipol Üniversitesi
Kavacık Güney Kampüsü
Göztepe Mah. Atatürk Cad.
No: 40 34810 Beykoz/İSTANBUL
Tel: 0216 681 51 00

E-mail
editor@actapharmsci.com
secretary@actapharmsci.com

Web site
http://www.actapharmsci.com

Contents

Aims and Scope of Acta Pharmaceutica Sciencia

Acta Pharmaceutica Sciencia is a continuation of the former "Eczacılık Bülteni" which was first published in 1953 by Prof. Dr. Kasım Cemal GÜVEN's editorship. At that time, "Eczacılık Bülteni" hosted scientific papers from the School of Medicine-Pharmacy at İstanbul University, Türkiye.

In 1984, the name of the journal was changed to "Acta Pharmaceutica Turcica" and it became a journal for national and international manuscripts, in all fields of pharmaceutical sciences in both English and Turkish. (1984-1995, edited by Prof. Dr. Kasım Cemal GÜVEN, 1995-2001, edited by Prof. Dr. Erden GÜLER, 2002-2011, edited by Prof. Dr. Kasım Cemal GÜVEN)

Since 2006, the journal has been published only in English with the name, "Acta Pharmaceutica Sciencia" which represents internationally accepted high-level scientific standards. The journal has been published quarterly except for an interval from 2002 to 2009 in which its issues were released at intervals of four months. The publication was also temporarily discontinued at the end of 2011 but since 2016, Acta Pharmaceutica Sciencia has continued publication with the reestablished Editorial Board and also with the support of you as precious scientists.

Yours Faithfully

Prof. Dr. Gülden Zehra OMURTAG
Editor

INSTRUCTIONS FOR AUTHORS

Manuscripts must be prepared using the manuscript template.

Manuscripts should contain the following elements in the following order:

Abstract

Keywords

Introduction (without author names and affiliations)

Methodology

Results and Discussion

Statement of Ethics

Conflict of Interest Statement

Author Contributions

Funding Sources

Acknowledgments

References

*Obligatory files are manuscript main document, title page, ethical approval, tables, figures for submission. If exist, supplementary files should also be added.

1. Scope and Editorial Policy

1.1 Scope of the Journal

Acta Pharmaceutica Sciencia (Acta Pharm. Sci.), formerly known as Bulletin of Pharmacy and Acta Pharmaceutica Turcica is a peer-reviewed scientific journal publishing current research and reviews covering all fields of pharmaceutical sciences since 1953.

The original articles accepted for publication must be unpublished work and should contain data that have not been published elsewhere as a whole or a part. The reviews must provide critical evaluation of the state of knowledge related with the subject.

All manuscripts have to be written in clear and concise English.

Including the October 2023 issue, the journal has started to be published online only. It will also publish special issues for national or international scientific meetings and activities in the interested field.

1.2 Manuscript Categories

Manuscripts can be submitted as Original Articles or Review Articles.

Original Articles are definitive accounts of significant, original studies. They are expected to present important new data or provide a fresh approach to an established subject.

Each issue comprises 14 original articles and 1 review article, or 15 original articles in the absence of a review article.

1.3 Prior Publication

Authors should submit only original work that has not been previously published and is not under consideration for publication elsewhere. Academic theses, including those on the Web or at a college Web site, are not considered to be prior publication.

1.4 Patents and Intellectual Property

Authors need to resolve all patent and intellectual property issues. Acceptance and publication will not be delayed for pending or unresolved issues of this type. Note that Accepted manuscripts and online manuscripts are considered published documents.

1.5 Professional Ethics

The editorial board pursue the best practice guidelines of the Committee on Publication Ethics (COPE). To guaranty the integrity of the published papers, *Acta. Pharm. Sci.* editors are guided for using COPE's flowcharts whenever they suspect an ethical issue about the paper they process.

Editors, reviewers, and authors are expected to adhere to internationally accepted criteria for scientific publishing. Helsinki declaration is applied and accepted for the ethical standards of the journal.

World Medical Association. (2001). World Medical Association Declaration of Helsinki. Ethical principles for medical research involving human subjects. Bulletin of the World Health Organization, 79(4), 373-374.

1.5.1 Author Consent

Submitting authors are reminded that the consent of all coauthors must be obtained prior to the submission of manuscripts. If an author is removed after submission, the submitting author must obtain the removed author's consent for the change by e-mail to the assigned editor.

1.5.2 Plagiarism

Manuscripts must be original in concept, content, and writing. It is not appropriate for an author to reuse wording from other publications, including their own previous work, whether or not that publication is cited. Suspected plagiarism should be reported immediately to the editorial office, and the report should specifically indicate the plagiarized material within the manuscript. *Acta Pharmaceutica Sciencia* uses iThenticate or Turnitin software to screen submitted manuscripts for similarity to published material. The maximum allowed plagiarism percentage is 20% or less. Please note that your manuscript may be screened during the submission process.

1.5.3 Use of Human or Animal Subjects

For research involving biological samples obtained from animals or human subjects, editors reserve the right to request additional information from authors. Studies submitted for publication must provide evidence that the described experimental activities have undergone local institutional review, ensuring the safety and humane usage of animal subjects. In the case of human subjects, authors must also provide a statement that study samples were obtained with the informed consent of the volunteers, or, in the absence of that, under the authority of the institutional board that approved the use of such material. Authors are requested to declare the identification or case number of institution approval as well as the name of the licensing committee in a statement placed in the section of 'Statement of Ethics'.

World Medical Association Declaration of Helsinki. Ethical principles for medical research involving human subjects. Bulletin of the World Health Organization, 2001;79(4),373-374.

1.6 Issue Frequency

The Journal publishes 4 issues per year.

2. Preparing the Manuscript

2.1 General Considerations

Manuscripts should be kept to a minimum length. Authors should write in clear, concise English, employing an editing service if necessary. For professional assistance with improving English and/or the figures, or formatting in the manuscript before submission please contact to editorial office by e-mail.

The responsibility for all aspects of manuscript preparation rests with the authors. Applying extensive changes or rewriting of the manuscript will not be undertaken by the editors.

It is best to use the font "Times New Roman", 11 font size, and all kinds of articles must be 1.5 spaced including text, references, tables, and legends.

Ensure that all special characters (e.g., Greek characters, math symbols) are present in the body of the text as characters and not as graphic representations. Be sure that all characters are correctly represented throughout the manuscript—e.g., 1 (one) and l (letter l), 0 (zero) and O (letter o).

All text (including the abstract, all sections of the body of the paper, figure captions, scheme or chart titles, and footnotes and references) and tables should be in one file. Graphics may be included with the text or uploaded as separate files. Manuscripts that do not adhere to the guidelines may be returned to authors for correction.

Use A4 page size with all pages oriented vertically. Set a 2.5 cm margin on each side. There are no page limitations; however, the length should be kept to a minimum. The experimental procedures for all experimental steps must be clearly and fully included in the experimental section of the manuscripts.

2.1.1 Nomenclature

It is the responsibility of the authors to provide correct nomenclature. It is acceptable to use semisynthetic or generic names for certain specialized classes of compounds, such as steroids, peptides, carbohydrates, etc. In such a case, the name should conform to the generally accepted nomenclature conventions for the compound class. Chemical names for drugs are preferred. If these are not practical, generic names, or names approved by the World Health Organization, may be used.

Authors may find the following sources useful for recommended nomenclature:

- The ACS Style Guide; Coghill, A. M., Garson, L. R., Eds.; American Chemical Society: Washington DC, 2006.
- Enzyme Nomenclature; Webb, E. C., Ed.; Academic Press: Orlando, 1992.
- IUPHAR database of receptors and ion channels (http://www.guidetopharmacology.org/).

2.1.2 Compound Code Numbers

Code numbers (including peptides) assigned to a compound may be used as follows:

- Once in the manuscript title, when placed in parentheses AFTER the chemical or descriptive name.
- Once in the abstract.

- Once in the text (includes legends) and once to label a structure. Code numbers in the text must correspond to structures or, if used only once, the chemical name must be provided before the parenthesized code number, e.g., "chemical name (JEM-398)." If appearing a second time in the text, a bold Arabic number must be assigned on first usage, followed by the parenthesized code number, e.g., "1 (JEM-398)." Subsequently, only the bold Arabic number may be used. All code numbers in the text must have a citation to a publication or a patent on first appearance.

Compounds widely employed as research tools and recognized primarily by code numbers may be designated in the manuscript by code numbers without the above restrictions. Their chemical name or structure should be provided as above. Editors have the discretion of determining which code numbers are considered widely employed.

2.1.3 Trademark Names

Trademark names for reagents or drugs must be used only in the experimental section. Do not use trademark or service mark symbols.

2.1.4 Interference Compounds

Active compounds from any source must be examined for known classes of assay interference compounds and this analysis must be provided in the General Experimental section. Many of these compounds have been classified as Pan Assay Interference Compounds (PAINS; see Baell & Holloway, J. Med. Chem. 2010, 53, 2719-2740). These compounds shown to display misleading assay readouts by a variety of mechanisms by forming reactive compounds. Provide firm experimental evidence in at least two different assays that reported compounds with potential PAINS liability are specifically active and their apparent activity is not an artifact.

2.2 Manuscript Organization

Sections: (Capital letters should be used in) Abstract, Introduction, Methodology, Results and Discussion, Statement of Ethics, Conflict of Interest Statement, Author Contributions, Funding Sources, Acknowledgments.

2.2.1 Title Page

The title of the manuscript should reflect the purposes and findings of the work in order to provide maximum information in a computerized title search. The title should be concise and informative. Minimal use of nonfunctional words is encouraged. The title should be concise and informative. Only commonly employed abbreviations (e.g., DNA, RNA, ATP) are acceptable. Code numbers

for compounds may be used in a manuscript title when placed in parentheses AFTER the chemical or descriptive name. *Only the first letter of the first word of the title must be capitalized.*

Authors' Names and Affiliations: The authors' full first names, middle initials, last names (with capital letters for only last names), and affiliations with addresses at time of work completion should be listed below the title. The name of the corresponding author should be marked with an asterisk (*). E-mail belonging to the corresponding author is mandatory. The affiliations must be written in this order: Name of the University, Faculty, Department, City, Country. The ORCID numbers must be hyperlinked in title page for each author.

2.2.2 Abstract and Keywords

Articles of all types must have an abstract following the title. The maximum length of the Abstract should be 200 words, organized in a findings-oriented format in which the most important results and conclusions are summarized. Abstracts should not be separated into categories; it should be written in a paragraph format. After the abstract, a section of Keywords not more than five has to be given. Be aware that the keywords, chosen according to the general concept, are very significant during the searching and indexing of the manuscripts. The 'keywords' must be given as below.

Keywords: instructions for authors, template, journal

2.2.3 Introduction

The Introduction should argue the case for the study, outlining only essential background, and should not include the findings or the conclusions. It should not be a review of the subject area but should finish with a clear statement of the question being addressed. Authors should use this template when preparing a manuscript for submission to *Acta Pharmaceutica Sciencia*.

2.2.4 Methodology

Materials, synthetic, biological, demographic, statistical or experimental methods of the research should be given detailed in this section. The authors are free to subdivide this section in the logical flow of the study. For the experimental sections, authors should be as concise as possible in experimental descriptions. General reaction, isolation, preparation conditions should be given only once. The title of an experiment should include the chemical name and a bold Arabic identifier number; subsequently, only the bold Arabic number should be used. Experiments should be listed in numerical order. Molar equivalents of all reactants and percentage yields of products should be included. A general intro-

ductory section should include general procedures, standard techniques, and instruments employed (e.g., determination of purity, chromatography, NMR spectra, mass spectra, names of equipment) in the synthesis and characterization of compounds, isolates and preparations described subsequently in this section. Special attention should be called to hazardous reactions or toxic compounds. Provide analysis for known classes of assay interference compounds.

Latin names of the plants and names of the microorganisms must be written in italic form.

The preferred forms for some of the more commonly used abbrevations are mp, bp, ^{o}C, K, min, h, mL, μL, g, mg, μg, cm, mm, nm, mol, mmol, μmol, ppm, TLC, GC, NMR, UV, and IR. Units are abbreviated in table column heads and when used with numbers, not otherwise.

2.2.5 Results and Discussion

This section could include synthetic schemes and tables of biological, demographic, and statistical data. The discussions should be descriptive. Authors should discuss the analysis of the data together with the significance of results and conclusions.

2.2.6 Ancillary Information

Include pertinent information in the order listed immediately before the references.

PDB ID Codes: Include the PDB ID codes with assigned compound Arabic number. Include the statement "Authors will release the atomic coordinates and experimental data upon article publication."

Homology Models: Include the PDB ID codes with assigned compound Arabic number. Include the statement "Authors will release the atomic coordinates upon article publication."

Corresponding Author Information: Provide telephone numbers and e-mail addresses for each of the designated corresponding authors.

Present/Current Author Addresses: Provide information for authors whose affiliations or addresses have changed.

2.2.7 Statement of Ethics: Authors are requested to declare the identification or case number of institution approval as well as the name of the licensing committee in a statement placed in the section of 'Statement of Ethics'. If the study does not require any ethical approval, it could be stated as follows 'No need for ethical approval for this study.'.

2.2.8 Conflict of Interest Statement: Any conflict should be stated. If there is none, it could be stated as follows 'There is no conlict of interest.'.

2.2.9 Author Contributions: Include statement such as "These authors contributed equally."

2.2.10 Funding Sources: Provide the information of the financial support received for conducting the research, including grants, donations, or sponsorships from institutions, organizations, or agencies.

2.2.11 Acknowledgments: Authors may acknowledge people, organizations, and financial supporters in this section.

2.2.12 References and Notes

Vancouver style is used in the reference list and citations. Manuscripts available on Web with a DOI number are considered published. In-text citations should be given superscript numbers according to the order in the manuscript. Ensure that references that are included in the text in the correct numerical order, corresponding to the sequence of references list. Footnotes are not used. Begin your reference list on a new page and title it 'REFERENCES'. Use Arabic numerals (1, 2, 3, 4, 5, 6, 7, 8, 9) as superscripts in the text. Abbreviate journal titles in the style used in the NLM Catalog. Check the reference details against the actual source – you are indicating that you have read a source when you cite it. Years of the references should not be written boldly. More than one reference from the same author(s) in the same year must be identified by the letters "a", "b", "c", etc., placed after the year of publication. *The use of a DOI URL at the end of the reference is strongly recommended and should be embedded as a hyperlink.*

2.2.12.1 For printed articles

• Article with 1-6 authors:

Author AA, Author BB, Author CC, Author DD. Title of the article. Abbreviated title of journal, Year;volume number(issue number):page numbers.

Sahin Z, Ertas M, Berk B, Biltekin SN, Yurttas L, Demirayak S. Studies on non-steroidal inhibitors of aromatase enzyme; 4-(aryl/heteroaryl)-2-(pyrimidin-2-yl)thiazole derivatives. Bioorg Med Chem, 2018;26(8):1986-1995. Doi:10.1016/j.bmc.2018.02.048

** It is recommended to hyperlink the DOI in the reference section by embedding the link in the DOI number provided.*

• Article with more than 6 authors:

Author AA, Author BB, Author CC, Author DD, Author EE, Author FF, et al. Title of the article. Abbreviated title of journal, Date of publication YYYY;volume number(issue number):page numbers.

2.2.12.2 For electronic journal articles

Author AA, Author BB, Author CC, Author DD, Author EE, Author FF. Title of article. Abbreviated title of Journal [Internet], Year of publication;volume number(issue number):page numbers. Available from: URL DOI

2.2.12.3 For books and book chapters

Books: a) Print book or b) Electronic book

a) Author AA. Title of book. Edition. Place of Publication: Publisher; Date

b) Author AA, Author BB. Name of the book [Internet]. Edition number (if not the first edition). Publication city, publication country: Publisher; year [cited date]. Available from: URL.

Book chapters: a) Print book chapter or b) Electronic book chapter

a) Author AA. Title of the book chapter. In: Editor AA, Editor BB, editors. Title of the book. Publication city, publication country: Publisher; year. p. page numbers.

b) Author AA. Title of the book chapter. In: Editor AA, Editor BB, editors. Title of the book [Internet]. Publisher; year. p. page numbers. Available from: URL. Accessed date: [accessed date].

2.2.12.4 For theses and dissertations

Author AA. Title of the thesis. [Doctoral Thesis/Master's Thesis]. City: Name of the University; Year.

2.2.12.5 For conference or symposium reports

Name of the Organization. Title of the report. In: Name of the symposium or conference; Year Month Day(s); City, Country. Publisher; Year.

2.2.12.6 For guidelines

Guildelines: a) Print guidelines or b) Electronic guidelines

a) Organization or Author(s). Title of the guideline. Edition (if applicable). Place of publication: Publisher; Year of publication. Total number of pages (if applicable).

b) Organization or Author(s). Title of the guideline [Internet]. Edition (if applicable). Place of publication: Publisher; Year of publication [cited date]. Available from: URL.

2.2.13 Tables

Table titles should not be abbreviated exp. tab. is not acceptable. It should be written as; Table 1. Tables should be centered, while table captions should be justified. When writing the table title, "**Table 1.**" should be in bold, followed by the caption in regular font.

Tabulation of experimental results is encouraged when this leads to more effective presentation or to more economical use of space. Tables should be numbered consecutively in order of citation in the text with Arabic numerals. The font used in tables should be Times New Roman, size 10. Footnotes in tables should be given as lowercase size 9 letter designations and cited in the tables as superscripts. The sequence of letters should proceed by row rather than by column. If a reference is cited in both table and text, insert a lettered footnote in the table to refer to the numbered reference in the text. Each table must be provided with a descriptive title that, together with column headings, should make the table self-explanatory. Titles and footnotes should be on the same page as the table. Table captions should be written on the top. Tables may be created using a word processor's text mode or table format feature. The table format feature is preferred. Ensure each data entry is in its own table cell. If the text mode is used, separate columns with a single tab and use a return at the end of each row. Tables may be inserted in the text where first mentioned or may be grouped after the references.

2.2.14 Figures, Schemes/Structures, and Charts

Figure titles should not be abbreviated exp. fig. is not acceptable. It should be written as; Figure 1. Figures should be centered, while figure captions should be justified. When writing the figure title, "**Figure 1.**" should be in bold, followed by the caption in regular font.

Figure captions: A caption should comprise a brief title (not on the figure itself) and a description of the illustration. Keep text in the illustrations themselves to a minimum but explain all symbols and abbreviations used. Figure captions should be written on the bottom.

The use of illustrations to convey or clarify information is encouraged. Structures should be produced with the use of a drawing program such as ChemDraw. Authors using other drawing packages should, in as far as possible, modify their program's parameters so that they conform to ChemDraw preferences. Remove all color from illustrations, except for those you would like

published in color. Illustrations may be inserted into the text where mentioned or may be consolidated at the end of the manuscript. If consolidated, legends should be grouped on a separate page(s). Include as part of the manuscript file.

To facilitate the publication process, please submit manuscript graphics using the following guidelines:

1. The preferred submission procedure is to embed graphic files in a Word document. It may help to print the manuscript on a laser printer to ensure all artwork is clear and legible.

2. Additional acceptable file formats are: TIFF, PDF, EPS (vector artwork) or CDX (ChemDraw file). When submitting individual graphic files and embedding them in a Word document, make sure to name the files according to their graphic function (e.g., Scheme 1, Figure 2, Chart 3), not the scientific name.

EPS files: Ensure that all fonts are converted to outlines or embedded in the graphic file. The document settings should be in RGB mode. NOTE: While EPS files are accepted, the vector-based graphics will be rasterized for production. Please see below for TIFF file production resolutions.

3. TIFF files (either embedded in a Word doc or submitted as individual files) should have the following resolution requirements:

- Black & White line art: 1200 dpi

- Grayscale art (a monochromatic image containing shades of gray): 600 dpi

- Color art (RGB color mode): 300 dpi

- The RGB and resolution requirements are essential for producing high-quality graphics within the published manuscript. Graphics submitted in CMYK or at lower resolutions may be used; however, the colors may not be consistent and graphics of poor quality may not be able to be improved.

- Most graphic programs provide an option for changing the resolution when you are saving the image. Best practice is to save the graphic file at the final resolution and size using the program used to create the graphic.

4. Graphics should be sized at the final production size when possible. Single column graphics are preferred and can be sized up to 240 points wide (8.38 cm). Double column graphics must be sized between 300 and 504 points (10.584 and 17.78 cm's). All graphics have a maximum depth of 660 points (23.28 cm) including the caption (please allow 12 points for each line of caption text).

Consistently sizing letters and labels in graphics throughout your manuscript will help ensure consistent graphic presentation for publication.

2.2.15 Image Manipulation

Images should be free from misleading manipulation. Images included in an account of research performed or in the data collection as part of the research require an accurate description of how the images were generated and produced. Apply digital processing uniformly to images, with both samples and controls. Cropping must be reported in the figure legend. For gels and blots, use of positive and negative controls is highly recommended. Avoid high contrast settings to avoid overexposure of gels and blots. For microscopy, apply color adjustment to entire image and note in the legend. When necessary, authors should include a section on equipment and settings to describe all image acquisition tools, techniques and settings, and software used. All final images must have resolutions of 300 dpi or higher. Authors should retain unprocessed data in the event that the editors request them.

2.3 Specialized Data

2.3.1 Biological Data

Quantitative biological data are required for all tested compounds. Biological test methods must be referenced or described in sufficient detail to permit the experiments to be repeated by others. Detailed descriptions of biological methods should be placed in the experimental section. Standard compounds or established drugs should be tested in the same system for comparison. Data may be presented as numerical expressions or in graphical form; biological data for extensive series of compounds should be presented in tabular form.

Active compounds obtained from combinatorial syntheses should be resynthesized and retested to verify that the biology conforms to the initial observation. Statistical limits (statistical significance) for the biological data are usually required. If statistical limits cannot be provided, the number of determinations and some indication of the variability and reliability of the results should be given. References to statistical methods of calculation should be included.

Doses and concentrations should be expressed as molar quantities (e.g., mol/kg, μmol/kg, M, mM). The routes of administration of test compounds and vehicles used should be indicated, and any salt forms used (hydrochlorides, sulfates, etc.) should be noted. The physical state of the compound dosed (crystalline, amorphous; solution, suspension) and the formulation for dosing (micronized, jet-milled, nanoparticles) should be indicated. For those compounds found to be inactive, the highest concentration (*in vitro*) or dose level (*in vivo*) tested should be indicated.

If human cell lines are used, authors are strongly encouraged to include the following information in their manuscript:

· the cell line source, including when and from where it was obtained;

· whether the cell line has recently been authenticated and by what method;

· whether the cell line has recently been tested for mycoplasma contamination.

2.3.2 Purity of Tested Compounds

Methods: All scientifically established methods of establishing purity are acceptable. If the target compounds are solvated, the quantity of solvent should be included in the compound formulas. No documentation is required unless asked by the editors.

Purity Percentage: All tested compounds, whether synthesized or purchased, should possess a purity of at least 95%. Target compounds must have a purity of at least 95%. In exceptional cases, authors can request a waiver when compounds are less than 95% pure. For solids, the melting point or melting point range should be reported as an indicator of purity.

Elemental Analysis: Found values for carbon, hydrogen, and nitrogen (if present) should be within 0.4% of the calculated values for the proposed formula.

2.3.3 Confirmation of Structure

Adequate evidence to establish structural identity must accompany all new compounds that appear in the experimental section. Sufficient spectral data should be presented in the experimental section to allow for the identification of the same compound by comparison. Generally, a listing of 1H or 13C NMR peaks is sufficient. However, when the NMR data are used as a basis of structural identification, the peaks must be assigned.

List only infrared absorptions that are diagnostic for key functional groups. If a series contains very closely related compounds, it may be appropriate merely to list the spectral data for a single representative member when they share a common major structural component that has identical or very similar spectral features.

3. Submitting the Manuscript

3.1 Communication and Log in to Author's Module

All submissions to Acta Pharmaceutica Sciencia should be made by using e-Collittera (Online Article Acceptance and Evaluation) system on the journal main page (www. actapharmsci.com).

3.2 Registration to System

It is required to register into the e-Collittera system for the first time while entering by clicking the "Create Account" button on the registration screen and the filling out the opening form with real information. Completing all the required fields in the form is essential for a successful registration. Without providing the necessary information, the registration process will not be able to proceed.

After the registration, a "Welcome" email is sent to the user by the system, reminding your user name and password. Authors are expected to return to the entry screen and log in with their user name and password for the submission. Please use only English characters while determining your username and password.

If you already registered into the e-Collittera system and forget your password, you should click on "Forgot My Password" button and your user name and password will be e-mailed to you in a short while.

3.3 Submitting a New Article

The author module's main page is divided into various sections that display the status of your manuscripts in progress. Authors can initiate a new submission by clicking the "New Manuscript" button, which involves a series of nine consecutive levels. In the first 7 levels, information such as the article's kind, institutions, authors, title, summary, keywords etc. are asked respectively as entered. Authors can move back and forth while the information is saved automatically. If the ~~is~~ transaction is discontinued, the system will move the new submission to the "Partially Submitted Manuscripts" part and the transaction can be continued from there.

3.3.1 Sort of Article Authors should first select the type of article from the drop-down menu.

Warning. If "Return to Main Page" button is clicked after this level, the article will be automatically assigned as "Partially Submitted Manuscripts".

3.3.2 Authors The authors' surnames, names, institutional information appear as entered order in the previous page. Filling all e-mail addresses are required. Institutional information is available in Manuscript Details table at the top of the screen. After filling all required fields, you may click the Continue button.

3.3.3 Title should be English, explaining the significance of the study. If the title includes some special characters such as alpha, beta, pi or gamma, they

can easily be added by using the Title window. You may add the character by clicking the relevant button and the system will automatically add the required character to the text.

Warning. No additions to cornered parenthesis are allowed. Otherwise, the system will not be able to show the special characters.

3.3.4 Abstract The summary of the article should be entered to the Abstract window. There must be an English summary for all articles and the quantity of words must be not more than 200. If special characters such as alpha, beta, pi or gamma are used in summary, they can be added from the Abstract window. You may add the character by clicking the relevant button and the system will automatically add the required character to the text. The abstract of the articles is accessible for the reviewers; so, you should not add any information related to the institutions and authors in this summary part. Otherwise, the article will be returned without evaluation. Authors will be required to comply with the rules.

Warning. No additions to cornered parenthesis are allowed. Otherwise, the system will not be able to show the special characters.

3.3.5 Keywords There must be five words to define the article at the keywords window, which will be diverged with commas. Authors should pay attention to use words, which are appropriate for "Medical Subjects Headings" list by National Library of Medicine (NLM).

3.3.6 Cover Letter If the submitting article was published as a thesis and/or presented in a congress (or elsewhere); all information about the thesis, presented congress (or elsewhere) should be delivered to the editor and must be mentioned in the "Cover Letter" section.

3.3.7 Adding Article This process consists of four different steps, beginning with the uploading of the article into the system. The "Browse" button under the "Choose a file to upload" tab is used to reach the article file. After finding and selecting the article file, you may click "Choose File" and the file will be uploaded.

Second step is to select a file category. Options are: Main Document, Black and White Figure, Color Figure and Video.

The explanation of the files (e.g., Figure 1, Full Text Word File, supplements etc.) should be added on the third step. The last step is submitting the prepared article into the system. Then, click the "Download" button.

Reminder: If the prepared article includes more than one file (such as main document, black and white figure, video), the transaction will be continued by starting from the first step. The image files must be in the previously defined format. After all required files are added, "Continue" button should be clicked. All details and features of the article can be reached from the Article Information page.

This page is the last step of the transaction which ensures that the entered information is controlled.

3.3.8 Your Files After submitting the article you may find all information related to the article under "Your Files" window.

File Information: This window includes file names, sizes, forming dates, categories, order numbers and explanations of files. The details about the files can be reached by clicking on "Information" button.

If you click on "Name of File", the file download window will be opened to reach the copy of the file in system.

File Download: This window submits two alternatives; one of them is to ensure that the file can be opened on a valid site and the second is to ensure that the submitted file can be downloaded to the computer.

Opening the Category part on the fourth column can change the category of the file.

Opening the Order column on the fifth column can change the order of the file.

The file can be deleted by clicking on Delete button on the last column. Before deleting, system will ask the user again if it is appropriate or not.

3.3.9 Completing the Submission Last level is submitting the article and the files into the system. Before continuing the transaction; it is important to control the Article Information window so that you can easily go back and make any necessary corrections using the "Previous" button. Otherwise, by clicking the Send the Article button, you will successfully finalize the transaction.

3.3.10 Page to Follow the Article The Main Page tab of the author ensures possibility to follow the article. This page consists of three different parts; some information and bridges related to the sent articles, revision required articles and the articles that are not completed to be sent.

3.3.11 Articles Not Yet Completed for Submission After the sending transaction was started, if article is not able to continue until the ninth step or could not be sent due to technical problems shown at this part, you may find

the information such as the article's number which is assigned by system, title and formation date. You may delete the articles by using Delete button on the right column.

3.3.12 Articles that Require Revision Articles, which were evaluated by the reviewer and accepted by the editor with revision, passes to Waiting for Revision tab.

The required revisions can be seen in "Notes" part by clicking the articles title.

In order to send any revision, Submit Revision button on the last column should be clicked. This connection will take the author to the first level of Adding Article and the author can complete the revision transaction by carrying out the steps. All changes must be made in the registered file, and this changed file must be resent. In addition to the revised manuscript, Author's most efficacious replies relating to the changes must be submitted in "Cover Letter" part.

If the is transaction is discontinued, the system moves the revised article to Submitted Manuscripts tab and the transaction can be continued from there.

After the transaction was completed, the system moves the revised article to "Submitted Manuscripts" part.

3.3.13 Submitted Manuscripts Information related to articles can be followed through the Submitted Manuscripts tab. Here you can find the information such as the article's number assigned by system, title, sending date and transaction situation. The Manuscript Details and summary files can be reached by clicking the title of the article and the Processing Status part makes it possible to follow the evaluation process of the article.

Article Review Process

Articles uploaded to the Manuscript submission system are checked by the journal administration for format consistency and similarity rate which is required to be less than 20%. Then sent to the chief editor if found appropriate.

Articles that are not suitable are sent back to the author for correction and resubmission (sent back to the author). Studies that have not been prepared using the draft for submitting to Acta Pharmaceutica Sciencia "acta_msc_tmp" and that have not been adapted in terms of format, will be directed to the editor-in-chief, after the 3rd time, by giving the information that "the consistency requirements have not been met".

The manuscripts sent to the chief editor will be evaluated and sent to the "language and statistics editor" if deemed necessary.

Studies found appropriate after language and statistics editor will be sent to field editors. If the field editor does not deem it appropriate after evaluating the article scientifically, he/she will inform the editor-in-chief of its negative comments, otherwise, at least two independent reviewers' comments will be asked.

Authors should consider that this process may take time because of the reviewer assignments and acceptance for review may take time for some cases.

Our review system is double-blind. The editor, who evaluates according to the comments of the reviewers, submits his/her comment and suggestion to the editor-in-chief. In this way, the article receives a decision of either acceptance, rejection, or revision. After all the revision process, the editor submits his/her final opinion to the editor-in-chief. The editor-in-chief conveys his or her final decision to the author. After the accepted articles are subjected to the final control by the journal and the corresponding author, the article starts to be included in the "accepted papers" section by giving the inactive DOI number. When the article is placed in one of the following issues, the DOI number will be activated and displayed in the "current issue" section on the homepage of the journal.

EDITORIAL

The rising value of IoT in pharmacy operations: The future starts today

Editorial Article

Oğuz ÖZYARAL*

Antalya Belek University, Vice Rector, Antalya, Türkiye

Advancing technology is leading to profound changes in the healthcare sector. In the world of pharmacy, the Internet of Things (IoT) offers innovative solutions across a wide range of applications, from inventory management to patient monitoring systems. With smart sensors, automated processes, and real-time data analytics, pharmacy operations are becoming faster, more reliable, and more efficient. This rising value of IoT not only transforms pharmacy services but also lays the foundation for the future healthcare ecosystem. The future is no longer distant; it's happening today.

1. Digital transformation of pharmacy operations with IoT: IoT has become the cornerstone of digital transformation in pharmacy operations. By integrating physical processes with digital monitoring and control systems, IoT reduces manual workloads, enhances efficiency, and minimizes errors. For instance, instead of manually tracking medication inventory, IoT sensors automate this process, allowing pharmacists to focus on more critical tasks such as patient care.

2. Smart inventory management: IoT-powered smart inventory management enables the automatic monitoring of pharmacy stock. Sensors identify which medications are running low or nearing expiration, preventing stockouts or waste. For example, IoT devices placed on pharmacy shelves continuously track inventory levels. When a medication is low, the system automatically generates a purchase order or alerts the pharmacist, ensuring uninterrupted availability.

3. Temperature and humidity control: IoT devices monitor temperature and humidity levels to ensure that medications are stored under the right conditions. These systems alert pharmacists in case of any anomalies, preventing

*Corresponding author: Oğuz ÖZYARAL
E-mail: oguzozyaral@gmail.com
ORCID: 0000-0001-5105-8008

the degradation or loss of medication efficacy. For instance, vaccines requiring cold storage are maintained at optimal temperatures through IoT sensors, which immediately send an alarm if the temperature deviates, enabling prompt action.

4. Patient medication tracking and reminders: IoT devices simplify medication adherence by ensuring patients take their medicines on time and in the correct dosage. Smart pillboxes or mobile applications provide reminders and automatically track doses. This improves the effectiveness and consistency of treatment. For example, a patient using a smart pillbox receives alerts via light or sound to take their medicine. The system logs when the box is opened, and if the dose isn't taken, a notification is sent to the patient or their caregiver.

5. Enhancing customer experience: IoT technology improves customer experience in pharmacies through personalized services. Smart kiosks, mobile applications, and connected devices guide customers with medication information, potential side effects, and usage recommendations. For example, an IoT-enabled kiosk in a pharmacy provides detailed information about medications based on scanned prescriptions. It also displays alternative medications or promotions, boosting customer satisfaction.

6. Supply chain traceability: IoT allows real-time tracking of medications throughout the supply chain, from production to the pharmacy. This enhances drug safety, reduces counterfeiting risks, and ensures timely deliveries. For instance, a pharmacy using an IoT-based supply chain system can monitor the location and condition of medications, such as checking whether cold chain vaccines are stored under the correct temperature during transportation.

7. The future of IoT in pharmacies: The development of IoT promises faster, more reliable, and more personalized services in pharmacy operations. Combined with artificial intelligence and big data analytics, IoT enables the analysis of medication consumption habits, paving the way for more proactive healthcare services. In the future, IoT devices won't just manage stock but also analyze patients' health data to offer personalized health recommendations. For instance, a smart prescription system could optimize treatment plans based on a patient's past health records.

8. Conclusion: Smart transformation in pharmacies – the power of IoT: IoT plays a key role in the digital transformation of pharmacy operations. Smart technologies not only enhance operational efficiency but also deliver safer and more personalized services to customers. These innovations position pharmacies as a critical component of future healthcare services. For example, investing in IoT solutions doesn't just streamline processes but also improves customer satisfaction, contributing to long-term success.

Recent epidemiological reports indicate that nearly 80% of the global population incorporates complementary and alternative medicine into their healthcare practices. Herbs are frequently self-administered concurrently with therapeutic drugs. Consequently, clinicians are advised to proactively gather information regarding herb-drug combination in their patients and establish monitoring protocols, particularly for individuals with habitual and concurrent herbal consumption. Herbal products can competitively inhibit cytochrome P450 (CYP) isoenzymes, potentially elevating blood levels of prescription medications and exposing patients to the risk of adverse effects. Studies by Bailey et al. revealed the modification of felodipine biotransformation in the presence of grapefruit juice. Recent investigations further suggest that herbal products may induce both pharmacodynamic and pharmacokinetics interactions of pharmaceuticals.

The majority of drugs, herbal products, and food constituent undergo are metabolism mediated by CYP enzymes. Interactions between herbal product and prescription drugs, manifested as co-medication, encompass the inhibition or induction of metabolizing enzymes and drug efflux proteins, such as P-glicoprotein (P-gp) and multiple resistance proteins (MRPs). The chemical structure of active herbal ingredient significantly modulates drug efflux and metabolism. Adverse effects may arise from the concominant use of herbal products with therapeutic drugs, owing to the alteration of drug metabolism and efflux pathways. Numerous herbal products demonstrate the capacity to induce or inhibit CYP isoenzyme, thereby influencing the metabolism of a broad spectrum of drugs. Predominant among the isoenzymes responsible for the biotransformation of herbal products are CYP3A4/5 and CYP2D6. CYP3A4 metabolizes more than 50% of presently administered therapeutic drugs.

In the recent years, extensive investigation into herb-drug interaction have primarily concentrated on elucidating the pharmacokinetic and pharmacodynamic effects associated with anticancer, anti-HIV, cardiovascular, antidiabetic, antihypertensive, and neuropsychiatric medicines. However, there remains a substantial need for augmented data derived from comprehensive case reports, *in vitro* and *in vivo* studies as well as clinical trials, focusing on the coadministration of naturel products alongside conventional drugs. Moreover, the establishment of a phytovigilance database stands as a prospective initiative for systematically cataloging herb-drug interactions. Notably, the U.S. Federal Adverse Event Reporting System (FAERS) and the Center Adverse Event Reporting System (CAERS) emerge as pivotal conduits for sourcing critical information pertaining to herb-drug interactions.

ORIGINAL ARTICLES

Acta Pharm. Sci. Vol 63:(2), 2025
Original article
DOI: 10.23893/1307-2080.APS6316

Development and *in vitro* characterization studies of novel chitosan nanoparticles for the treatment of Huntington's disease

Emre Şefik ÇAĞLAR[1], Emine Büşra EKER FIDAN[2], Mehmet Koray GÖK[2]
Neslihan ÜSTÜNDAĞ OKUR[3], Saadet Kevser PABUCCUOĞLU[2], Erdal CEVHER[4*]

1 University of Health Sciences, Faculty of Pharmacy, Department of Pharmaceutical Biotechnology, Istanbul, Türkiye
2 Istanbul University-Cerrahpasa, Faculty of Engineering, Department of Chemical Engineering, Istanbul, Türkiye
3 University of Health Sciences, Faculty of Pharmacy, Department of Pharmaceutical Technology, Istanbul, Türkiye
4 Istanbul University, Faculty of Pharmacy, Department of Pharmaceutical Technology, Istanbul, Türkiye

ABSTRACT

Huntington's disease is a fatal disease that occurs when the number of CAG trinucleotides in the IT-15 gene repeats itself more than 35 times. In this study, modified chitosan polymers were synthesized and characterized. siRNA loaded nanoparticles were prepared and characterized. The results showed that the modified chitosan was successfully synthesized and targeted. As a result of the characterization studies, the particle size, polydispersity index and zeta potential of the siRNA-loaded nanoparticle were found to be 99.0 ± 5.1 nm, 0.3190 ± 0.004, and 14.9 ± 3.04 mV, respectively. Lyophilization was successfully achieved with a trehalose rate of 20%. As a result of 12 months of stability, the particle size of the formulations was found to be the highest 273.766 ± 8.957 nm, the highest polydispersity index was 0.324 ± 0.016, and the highest zeta potential was 45.35 ± 1.79 mV. In agarose gel electrophoresis studies, the siRNA:modified chitosan ratio was found to be 5:1. siRNA-loaded nanoparticles maintain the integrity of siRNA for 24h.

Keywords: Huntington's disease, siRNA, chitosan, nanoparticle

*Corresponding author: Erdal Cevher
E-mail: ecevher@istanbul.edu.tr
ORCIDs:
Emre Şefik ÇAĞLAR: 0000-0003-2010-4918
Emine Büşra EKER FIDAN: 0000-0002-6340-5107
Mehmet Koray GÖK: 0000-0003-2497-9359
Neslihan ÜSTÜNDAĞ OKUR: 0000-0002-3210-3747
Saadet Kevser PABUCCUOĞLU: 0000-0002-1793-0859
Erdal CEVHER: 0000-0002-0486-2252
(Received 12 Jan 2025, Accepted 10 Feb 2025)

INTRODUCTION

Huntington's disease (HD) is a progressive neurological condition resulting from the expansion of CAG repeats that encode polyglutamine at the N-terminus of the huntingtin protein. The HD gene (IT-15) spans 180 kb and is classified into four categories according to the quantity of CAG repeats. Individuals possessing 26 or fewer repeats are considered healthy, whereas those with 27 to 35 repeats exhibit intergenerational instability. Those who are more than 35 synthesize the disease protein. The striatum is the predominant brain area associated with instability, experiencing particular deterioration[1,2].

HD induces involuntary movements, motor coordination impairments, cognitive decline, and psychiatric issues. The pathogenic characteristic is the selective death of neurons in the basal ganglia of the brain. Symptoms encompass weight reduction, muscular debilitation, metabolic irregularities, and endocrine abnormalities. Atrophy is evident in multiple brain regions, particularly in severe instances[3].

HD, which is autosomal dominant; In American, European, and Australian societies, it affects about 5-10 out of every 100,000 people in the white race[4,5]. The age of onset of the disease may vary from childhood to the end of eighty years of age[6]. However, the most common age range of the disease is between 30-50[5]. The average time between the occurrence of the disease and death is between 17-20 years[5,6].

Treatment is carried out by symptomatic treatment of motor, behavioral, and psychiatric disorders. There is still no drug that modifies the disease[5,6]. Unfortunately, current pharmacotherapy in HD does not offer anything beyond temporary relief of symptoms and fails to stop both the underlying cause and progression of the disease. Therefore, it is very important to better provide standard care for Huntington's patients and to develop a new treatment strategy that will stop the progression of the disease.

RNA interference (RNAi) is a rapidly evolving field in biological research, potentially treating certain diseases by blocking protein production by inhibiting or degrading mRNA translation or degrading mRNA. This intracellular pathway allows cells to regulate gene expression through microRNAs, playing a crucial role in development[7,8]. siRNAs are loaded on RNA-based silencing complex (RISC), activated by thermodynamic selection or siRNA expansion. RISC targets specific complementary mRNA transcriptions, preventing protein production, and catalyzing numerous chain reactions, increasing the potency of gene silencing compared to ASOs[9,10].

The main pathways for transport from the nose to the brain are olfactory epithelium, olfactory nerve, and blood circulation. The olfactory nerve pathway is formed by fusion of olfactory sensory nerve axons. It travels from the ethmoid bone to the cranial cavity, where it makes synoptical unions with *epiplexus* and mitral cells in the olfactory bulb. Drug molecules remain in the olfactory mucosa after intranasal administration, passing through olfactory epithelial cells and accumulating in Bowman's gland and Sertoli cells in the brain. They also pass through intercellular gap junctions and accumulate in brain tissues. Chitosan, which is a semi- natural cationic biopolymer, offers advantages like biocompatibility, biodegradability, low toxicity, easy preparation, and high loading capacity for hydrophilic drugs, making it a useful carrier for plasmid DNA, siRNA, and cancer drugs[11]. PEGylation is a recognized method for circumventing the elimination of nanoparticles by macrophages. This technique involves coating nanoparticle surfaces with an anti-fouling polymer, such as polyethylene glycol, which is non-toxic and non-immunogenic; this process is referred to as "PEGylation." PEGylation also entails the alteration of the dimensions and morphology of nanoparticles. PEGylation of nanoparticles has been identified as an effective strategy for prolonging nanoparticle circulation time while evading liver macrophages. PEGylation forms a hydrophilic barrier surrounding nanoparticles, safeguarding connections between complement proteins and immunoglobulins (opsonin proteins) through steric repulsion forces, therefore obstructing and postponing the early phase of the opsonization process. Consequently, PEGylation has demonstrated a significant enhancement in the circulatory half-life of nanoparticles by multiple orders of magnitude[12]. For this reason, nanoparticles were PEGylated. In addition, since the number of N-methyl-D-aspartic acid (NMDA) receptors in HD is increasing, the developed nanoparticles have been targeted with NMDA[13].

For instance, Sava et al. found the particle size and zeta potential of siRNA-loaded chitosan nanoparticle formulations developed for use in the treatment of HD between 103.7-205 nm and 42.5-54.7 mV, respectively. As a result of the study, when intranasally administered siRNA-loaded chitosan nanoparticles were compared with intranasally administered siRNA, they found that siRNA-loaded chitosan nanoparticles inhibited the synthesis of mutant huntingtin protein at a rate of 77% compared to siRNA[14].

This study aims to demonstrate the effectiveness of siRNA-loaded modified chitosan nanoparticles in treating HD, as a new treatment and to enhance the effectiveness and reduce side effects of current treatments.

METHODOLOGY

Materials

Human siRNA Oligo Duplex (siRNA), trilencer-27 fluorescent-labeled trans, siTran 2.0 siRNA transfection reagent were purchased from Oligogene (USA). Low molecular weight chitosan (Chi) (75-85% deacetylated), gallic acid (GA), 3-dimethylamino-1-propylchloride hydrochloride (DAPC), N-(3-dimethylaminopropyl)-N'-ethylcarboimide hydrochloride (EDAC), acetic acid, sodium hydroxide (NaOH), methoxy-PEG 2000 (MPEG), isopropanol, sodium acetate, phosphate buffer solution (PBS) tablets, tris base, EDTA, agarose, ethidium bromide (EtBr), and bromophenol blue, in tris-acetate-EDTA buffer (TAE), tris-borate-EDTA (TBE), N-methyl-D-aspartic acid (NMDA) were purchased from Sigma Aldrich (Germany). Sodiumtripolyphosphate (TPP), ethanol, fetal bovine serum (FBS), were purchased from Merck (Germany).

Methods

Synthesis of PEGylated and targeted of chitosan polymers

Firstly, Chi-GA was synthesized by the reaction between Chi and GA, then Chi-GA product was reacted with DAPC for the preparation of the Chi-GA-DAPC product. Afterwards, Chi-GA-DAPC product was pegylated using MPEG and Chi-GA-DAPC-MPEG product was obtained. Finally, Chi-GA-DAPC-MPEG product was targeted with NMDA for the preparation of the targeted product Chi-GA-DAPC-MPEG-NMDA.

Chi was dissolved in 4% acetic acid solution as 1% (w/v). GA (1 mole of GA per 1 mole of glucosamine unit) was dissolved in 10 mL of ethanol and EDAC was used to activate the carboxylic acid groups of GA. Since the concentration of Chi to be used in the synthesis is very high and the high solubility of Chi is desired, the acetic acid concentration has been determined as 4% to obtain high solubility of Chi. The mixture was stirred at room temperature for 24 hours, and the pH was adjusted to 8.5-9.0 with 1 N NaOH for the precipitation of Chi-GA product. To purify the Chi-GA, the precipitated product was centrifugated and washed. Synthesis of the Chi-GA-DAPC product was realized by the reaction of Chi-GA with DAPC in alkaline pH 8.5-9. In addition, DAPC (0.5 moles of DAPC per 1 mole of GA modified glucosamine unit) was dissolved in 1.176 mL of isopropanol and this solution was added to the Chi-GA solution at a rate of 168 µL every 5 minutes and mixed for a period of 30 minutes. The mixture was stirred at 500 rpm for 4 h, and at the end of the incubation period, 60 mL of technical ethanol was added to stop the reaction.

Pegilation of the Chi-GA-DAPC, this product was dissolved in 1% acetic acid, and MPEG was added to the solution. The mixture was stirred 50°C for 48 hours, dialyzed against deionized water for 24 hours, and lyophilized at -50 ± 1°C at a pressure of 0.01 mBar. The purified Chi-GA-DAPC-MPEG product was stored at +4°C. To obtain the targeted polymer Chi-GA-DAPC-MPEG-NMDA, Chi-GA-DAPC-MPEG was dissolved in 4% acetic acid, and NMDA (0.02 mol NMDA per 1 mole of glucosamine unit) was dissolved in ethanol, then this solution was activated with EDAC. EDAC-activated NDMA solution was added to the Chi-GA-DAPC-MPEG solution, mixed under the N_2 gas for 24 hours, and the pH adjusted to 8.5-9 for the precipitation of the product. The Chi-GA-DAPC-MPEG-NMDA product was purified by centrifuging at 6000 rpm for 5 minutes, washed with deionized water, and lyophilized at -50 ± 1°C[15].

Characterization of synthesized polymers

Determination of molecular weight of polymers

The study aimed to determine the molecular weight and molecular weight distributions of suitable polymers for nanoparticle preparation using the Gel Permeation Chromatography (GPC) method. The TOSOH EcoSEC branded GPC/SEC system was used to determine the average molecular weights and molecular weight distributions of modified polymers. The study used chitosan and modified chitosan products, which were dissolved overnight in a 1% acetic acid solution, diluted twice with sodium acetate, filtered through a 0.22 µm membrane, and transferred to vials[16].

Determination of structural properties of polymers

The structural properties of the synthesized polymers were investigated by Fourier Transform Infrared (FT-IR) Spectroscopy, ^{1}H NMR and ^{13}C NMR analyzes.

Fourier Transform Infrared Spectrophotometry (FT-IR)

The structures of all synthesized products were illuminated by Fourier Transform Infrared Spectrophotometer technique. FT-IR analyses showed that the Cary 630 model (Agilent; USA) on the FT-IR device. Using tablets diluted with a product/KBr ratio of 1/200 mg, the spectra was recorded in the wavenumber range of 650-4000 cm^{-1}.

Nuclear Magnetic Resonance (^{1}H-NMR and ^{13}C-NMR)

In addition to the FT-IR method, the UNITY INOVA nuclear magnetic resonance spectrophotometer (Varian, Canada) was used to elucidate the structures of their products. Analyses were performed using MSO - d6:D2O solvents and 500 MHz and 25°C parameters.

Thermal analysis

Thermogravimetric analysis (TGA) was performed to determine the thermal degradation properties of the synthesized polymers. For this purpose, TGA analysis of the samples (15 mg) placed in aluminum crucible was carried out with a thermogravimetric analyzer (Linseis, STA PT 1750 model, USA) with a heating rate of 10°C/minute up to 1000°C by sending air into the system at a speed of 0.4 L/min.

Preparation and characterization of siRNA-loaded chitosan nanoparticles

Positively charged modified chitosan nanoparticles were prepared by ionic gelation technique using tripolyphosphate[17]. Stock chitosan solutions of 0.3% were prepared for the preparation of nanoparticles obtained from modified Chi polymers. Nanoparticles were obtained using a 0.1% TPP solution. The final concentration of 0.025% with the synthesized polymers was studied as shown in Table 1 with a Chi:TPP ratio of 6:1 for 5 mL Chi nanoparticles. TPP was added drop by drop to the Chi solution stirring at 300 rpm, with 3 seconds between each drop.

Table 1. Preparation of modified Chi nanoparticles

Formulation Codes	Modified Chi solution (mL)	Modifed Chi TPP Ratio	TPP solution (mL)	Water (mL)
Chi-GA-DAPC Chi-GA-DAPC-MPEG Chi-GA-DAPC-MPEG-NMDA	0.417	6:1	0.208	4.375

The procedure applied for all modified Chi polymers.

The siRNA added to the nanoparticle by ionic interaction method. For this, the first nanoparticles were prepared as mentioned. Afterwards, for 30 min, nanoparticle and siRNA together stirred at 50 rpm.

Particle size, PDI and surface charges of nanoparticles

The particle size and poly dispersity index (PDI) of the nanoparticles were determined using the photon correlation spectroscopy method (Malvern Zetasizer, Nano-ZS). The zeta potential of the formulations was investigated with a Malvern Zetasizer at 25°C, 78.5 dielectric constant, 5 mS/cm conductivity, using DTS 1060C zeta cuvette, and 40 V/cm field power[18].

Lyophilization of formulations and moisture determination

After the addition of cryoprotectant (trehalose) at different ratios (5%, 10%, 20%, 40%), 5 mL of formulations were frozen in 10 mL glass vials in the freezer at -20°C for 2 hours. Then, it was lyophilized with a VirTis AdvancePlus brand lyophilizer device under 17 mTorr pressure at -45°C for 48 hours.

The lyophilized samples were re-dispersed and analyzed by measuring particle size, particle distribution and zeta potential at certain time intervals for 4 hours. All measurements are the result of at least 3 parallel studies and the measurement has been repeated at least 5 times.

For moisture determination studies, lyophilized formulations were carefully weighed to determine the initial weight (IA). They were then heated in an oven from 30°C to 100°C. They were immediately weighed, and their final weight (FA) was found[19]. The % moisture content is calculated according to the following formula:

Equation 1. % moisture content determination

$$\text{Moisture (\%)} = \frac{\text{IA-FA}}{\text{IA}} \text{ X 100}$$

Agarose gel electrophoresis studies

The study investigated the stability of siRNA loaded on nanoparticles in a formulation using agarose gel electrophoresis. The agarose was dissolved in tris-acetate-EDTA buffer (TAE), then EtBr was added. The gel was then placed in a tank with pH 8.0 TAE buffer and optionally mixed with 6x agarose gel loading dye. The electrophoresis process was completed in 1 hour at 100 V. The gels were then examined on a UV transilluminator[16].

Evaluation of serum stability of nanoparticles

The study demonstrates the integrity of siRNA nanoparticles at different time intervals using polyacrylamide gel electrophoresis. The nanoparticle formulation was enriched with 5% FBS, and 30 µL samples were taken at different times and stored at -20°C. Heparin was added to the formulations and waited for 1 hour for siRNA separation. The integrity of the siRNA was analyzed using 20% polyacrylamide gel electrophoresis stained with 1% EtBr. The gel was prepared by mixing 40% acrylamide with 10X TBE buffer and distilled water, adding ammonium persulfate and tetramethylenediamine, and applying electrophoresis loading buffer with 6x agarose gel loading dye. Samples were conducted for 30 minutes at 200V amperes, and the gel was kept in TBE buffer

containing 1% EtBr for 30 minutes. The gels were then examined on a UV transilluminator for polyacrylamide gel[20,21].

Stability studies

Lyophilized Chi-GA-DAPC-MPEG-NMDA formulations were stored in a stability cabinet at 0, 3, 6, 9, and 12 months at 4 ± 2°C (in the refrigerator), 25 ± 2°C and 60 ± 5% relative humidity and 40 ± 2°C and 75 ± 5% relative humidity to measure particle size, polydispersity index, and zeta potentials. Stability studies were carried out in accordance with the ICH Guidelines[22].

RESULTS and DISCUSSION

Molecular weight determination studies of synthesized polymers

The results of the determination of molecular weights of Chi-GA-DAPC-MPEG, Chi-GS-DAPC-MPEG-NMDA polymers are shown in Table 2. When the molecular weights of Chi-GA-DAPC-MPEG polymer and the related PDI results were examined, it was seen that the Chi-GA-DAPC-MPEG obtained as a result of this study were in appropriate weights and showed a very good distribution (monodisperse). The average molecular weight of the Chi, which is commercially sold as "low molecular weight" by Sigma, which was obtained in previous studies, is 284.0 ± 2.9 kDa and the PDI is 2.62 ± 0.05, which confirms our result[15]. However, the reason why the molecular weight of Chi-GA-DAPC-MPEG polymers is lower than the molecular weight of commercially sold Chi is thought to be that the chains of Chi are broken due to temperature and environmental factors during the modifications made, and then purification and removal processes are applied[15].

Table 2. Average molecular weight determination results of modified Chi polymers

Formulation	M_n (kDa)	M_w (kDa)	PDI (M_w/M_n)
Chi-GA-DAPC-MPEG	92.00 ± 0.53	99.00 ± 0.66	1.079 ± 0.01
Chi-GA-DAPC-MPEG-NMDA	31.84 ± 0.25	40.79 ± 0.27	1.281 ± 0.370

Determination of structural properties of polymers

FT-IR spectra

A careful comparison of the Chi-GA-DAPC-MPEG and the Chi-GA-DAPC-MPEG-NMDA FTIR spectra presented in Figure 1 indicates definite differences about some absorption bands related to the reactions.

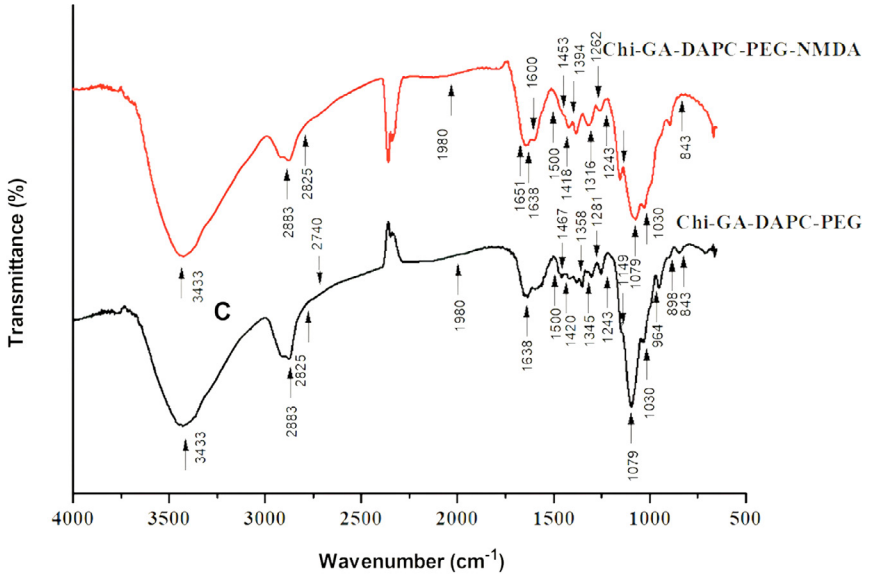

Figure 1. FT-IR spectra of Chi-GA-DAPC-MPEG and Chi-GA-DAPC-MPEG-NMDA

When the FT-IR spectra (Figure 1) were evaluated, new secondary amide structure formation by the reaction between the primary amine (NH_2) group of Chi-GA-DAPC-MPEG and the carboxyl (COOH) group in NDMA molecule was observed at about max. 1651 cm^{-1} corresponding to the stretching vibrations of the Amide I C=O bonds. It has also been observed that formation of the new ester structures (at about max. 1600, 1418, 1394, and 1316 cm^{-1} corresponding to the stretching vibrations of the C-O/C=O bonds in the ester structure) by the reaction between the COOH groups of NMDA molecule and the unreacted methylol groups on the Chi skeletal structure or the free OH group in the MPEG structure.

The data obtained according to the FTIR spectra results show that the Chi-GA-DAPC-MPEG-NMDA product were successfully synthesized as expected.

Nuclear Magnetic Resonance (^{1}H-NMR and ^{13}C-NMR)

As a result of the structural characterization of Chi, Chi-GA-DAPC-MPEG and Chi-GA-DAPC-MPEG-NMDA polymers with ^{1}H-NMR and ^{13}CNMR spectroscopy of selected polymer Chi-GA-DAPC-MPEG-NMDA by performing the reactions with MPEG and NMDA, it was seen that the reactions took place as expected (Figure 2). Accordingly, the intense observance of the peaks of protons belonging to the (-O-CH_2-CH_2) groups around 3.5 ppm in the Chi-GA-DAPC-M-PEG graph showed that PEGylation reactions took place suc-

cessfully. However, in these spectra, it was observed that the peaks of protons belonging to the groups around 3.2 ppm and 1.9 ppm ($NH\text{-}CH_2\text{-}CH_2\text{-}NH\text{-}$,$CH_2\text{-}CH_2\text{-}CH_2\text{-}N\text{-}CH_3\text{-}CH_3\text{-}CH_3$) originating from DAPC compounds disappeared in the Chi-GA-DAPC-MPEG-NMDA graphs and/or interfered with other peaks , and a reaction took place between the unreacted methylol groups of Chi skeletal structure and NMDA.

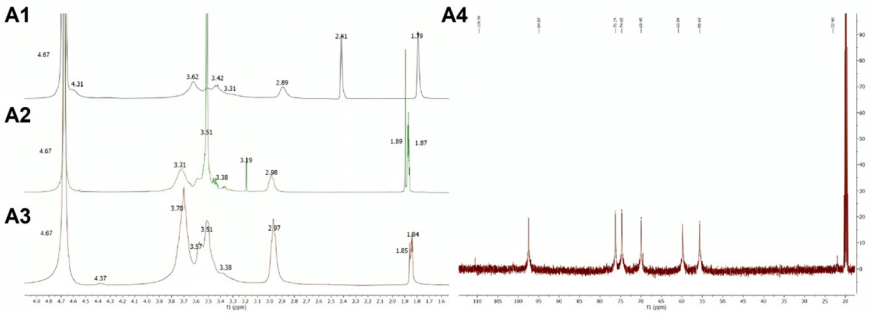

Figure 2. A1) Chi; A2) Chi-GA-DAPC-MPEG, A3) 1H-NMR Spectrum of Chi-GA-DAPC-MPEG-NMDA polymers, A4) ^{13}C-NMR Spectrum of Chi-GA-DAPC-MPEG-NMDA polymer, Chi-GA-DAPC-MPEG-NMDA polymer, ^{13}CNMR (125 MHz, Acetic acid-d_4; δ =19.99) [ppm]: δ = 22.03; 55.62; 55.66; 59.79; 69.47; 69.95; 74.65; 76.24; 97.47; 110.53.

The results were found to be consistent with the results of FT-IR analysis.

Thermal analysis

The data obtained from the TGA curves of Chi-GA-DAPC-MPEG and Chi-GA-DAPC-MPEG-NMDA polymers obtained by this study are given in Table 3. First, the TGA curves of Chi-GA-DAPC-MPEG polymer and the weight losses and final degradation temperatures obtained from these curves are given. In the range of approximately 115 to 208°C, corresponding to the initial degradation stage, a significant weight loss of 10% was observed for Chi-GA-DAPC-MPEG-NMDA and Chi-GA-DAPC-MPEG, respectively. The middle stage took place in the temperature range of approximately 328-415°C with a weight loss of approximately 60-80% depending on the modified polymer structures and the main weight losses were observed at this stage. The final oxidative degradation was completed at approximately 589-760°C due to modified products structures.

Table 3. The weight losses (%) and the final degradation temperatures obtained from TGA data curves of Chi-GA-DAPC-MPEG, Chi-GA-DAPC-MPEG-NMDA polymers

	Temperature (°C)	
Weight Loss* (%)	**Chi-GA-DAPC-MPEG**	**Chi-GA-DAPC-MPEG-NMDA**
5	113	86
10	208	115
20	248	267
50	313	338
100	589	760

*Values calculated from TGA curves

As shown in Table 4, the thermal oxidative degradation properties of Chi-GA-DAPC-MPEG-NMDA exhibit the same behavior. The decomposition of the polymer in air occurs in 4 stages, at temperature ranges very close to each other. Table 3 shows the degradation stages, temperature ranges, corresponding maximum weight loss % amounts and final degradation temperatures of polymer. The polymer showed a weight loss of approximately 5-15% in the initial degradation interval due to the removal of the trapped water in their molecules. Subsequently, until the end of stage 2, the rate of degradation is very slow, and no significant weight loss is observed up to 200-270°C and maintains values of 10-15%. Stage 3 is the fastest step in degradation and a weight loss ranging from 47-65% is achieved in this region. Subsequently, the rate slows down in the final degradation zone and the degradation ends at 650°C for the last two products and at 760°C, which is the higher temperature for the other product, with the formation of CO, CO_2, and similar gases. As a result, it is clearly seen that the attachment of NMDA ligand to chitosan-based modified products does not adversely affect its thermal oxidative resistance[23].

Table 4. Degradation stages of Chi-GA-DAPC-MPEG-NMDA

Polymer	Chi-GA-DAPC-MPEG-NMDA	
Degradation stage	**Temperature range (°C)**	**Weight loss* (%)**
1	25-120	10
2	120-270	15
3	270-300	47
4	300-760	100
Final degradation temperature (°C)	760	

* Values calculated from TGA curves

Preparation of nanoparticles and results of characterization

The particle size and size distribution PDI of the nanoparticles were determined using the photon correlation spectroscopy method. Nanoparticle formulations are ideally selected based on their particle size, size distribution, and zeta potential. Of the ideally selected nanoparticle formulations, the smallest ones were determined as those with a particle distribution of 0.5 and below, and those with a zeta potential of +30mV and above. Table 5 shows the particle size, PDI, and zeta potential results of the formulations determined as ideal. As a result of these evaluations, it is aimed to obtain nanoparticle formulations that cross the blood brain barrier (BBB) without being attached to the reticuloendothelial system, show homogeneous distribution, can be loaded with all siRNA and have no toxic effects[24-26].

Table 5. Particle size, PDI, zeta potential results of blank, and siRNA loaded formulations

Formulation Code	Particle Size (nm) ± SD	PDI ± SD	Zeta Potential (mV) ± SD
Chi-GA-DAPC	165.5 ± 2.6	0.343 ± 0.036	38.8 ± 1.4
Chi-GA-DAPC-MPEG	131.8 ± 9.0	0.311 ± 0.010	29.8 ± 1.0
Chi-GA-DAPC-MPEG-NMDA	146.8 ± 1.1	0.236 ± 0.011	45.3 ± 0.1
Chi-GA-DAPC-MPEG-NMDA-siRNA	99.0 ± 5.1	0.319 ± 0.004	14.9 ± 3.0

The PDI value of null and siRNA-loaded nanoparticle formulations was found to be substantially less than 0.5.

The surface composition of nanoparticles is essential for identifying cell entry mechanisms. It is explained that a highly positive surface charge shows a different bio-dispersion than a slightly negative nanoparticle surface charge. Small particle size and positive surface charge are physicochemical properties that aid cellular uptake by facilitating interactions with the negatively charged cellular membrane[27,28].

For nasal to brain drug administration, the size of the ideally sized nanoparticles should be smaller than 200 nm. The particle size of the prepared delivery systems plays an important role in the formulation development and characterization phase as it affects activities such as drug release, biodistribution, cell uptake, etc. Accordingly, Mantimadugu et al. prepared polymeric nanoparticles with a particle size of ≈200 nm (139.52 ± 5.35 nm) and provided direct passage to the brain by transcellular transport along olfactory axons[29].

Several studies have shown a clear inverse correlation between nanoparticle size and BBB penetration[30,31]. Most of the studies in animal models of stroke and Parkinson's so far have used nanoparticles with sizes between 50 nm and 100 nm. Godinho et al. revealed that the low size (a hydrodynamic diameter between 100 nm and 350 nm) and positive surface charge of β-Cyclodextrin siRNA nano transporter formulations make them ideal for targeting to the brain[32].

The fact that the PDI value was less than 0.5 showed that the particle size distribution of the prepared formulations was homogeneous[18]. Van Woensel et al. prepared siRNA-loaded chitosan nanoparticles for the treatment of glioblastoma. Particle sizes, particle distribution, and zeta potential were found to be 141 ± 5 nm, 0.3, and + 32mV, respectively. As a result of the study, it has been shown that chitosan nanoparticle formulations administered intranasal route carry siRNA to the central nervous system in a short time[33].

Furthermore, the positive zeta potential can improve the stability of nanoparticles intended to be used for siRNA administration. Nanoparticles with medium (up to 15 mV) or high positive zeta potential (above 15 mV) can cross the BBB and have been found to be effective as drug-delivery systems to the brain. For example, Jalluli et al. identified cationic nanoparticles prepared with maltodextrin, which has a high positive zeta potential, as effective in brain transport. In addition, high negative/positive (15 to 30 mV) values of the zeta potential prevent coalescence between particles, stabilizing nanoparticle dispersion due to electrostatic repulsions[34]. When the studies were evaluated, the particle size, particle distribution, and zeta potential of our chitosan nanoparticle formulations were suitable for intranasal application.

Lyophilization studies

Freeze drying is a good technique to improve the long-term stability of colloidal nanoparticles. The poor stability of nanoparticles in an aqueous medium is a major obstacle to their clinical use[35,36]. The use of trehalose, mannitol or sorbitol as a cryoprotectant is an effective way to maintain the physical properties of nanoparticles during freeze-drying[37,38]. Among these cryoprotectants, one of the most preferred is trehalose[39-41]. The non-toxicity of trehalose increases its preferability[42]. Almalik et al. prepared chitosan nanoparticles by ionic gelation method. They investigated the stability of these systems in terms of particle size using six different cryoprotectant species (sucrose, glucose, trehalose, mannitol, polyethylene glycol-2000, and polyethylene glycol-10.000) at concentrations of 5%, 10%, 20%, and 50%. They found that the cryoprotectants of sucrose and trehalose had the highest protective effect in chitosan nanoparticles[43]. As a result of all the optimization studies, the lyophilization of nanoparticle formulations has been successful (Table 6). When the formulations were evaluated, the ideal cryoprotectant ratio was found to be 20%. However, lyophilized formulations were deposited in stability cabinets for 12 months to evaluate their stability.

Table 6. Particle size, polydispersity index and zeta potential values obtained as a result of redispersing formulations containing 20% D-(+)-trehalose

Time (min)	Particle Size (nm) ± SD	PDI ± SD	Zeta Potential (mV) ± SD
Chi-GA-DAPC-MPEG-NMDA			
0	188.1 ± 9.5	0.290 ± 0.010	48.9 ± 0.7
5	203.1 ± 7.7	0.329 ± 0.066	55.3 ± 0.4
15	208.1 ± 0.0	0.338 ± 0.027	53.2 ± 1.5
30	222.6 ± 11.4	0.268 ± 0.044	52.5 ± 1.2
60	207.5 ± 0.0	0.275 ± 0.027	49.1 ± 0.2
120	229.9 ± 4.4	0.216 ± 0.182	51.0 ± 0.1
180	201.0 ± 10.1	0.247 ± 0.002	53.8 ± 2.4
240	200.5 ± 2.7	0.283 ± 0.033	52.5 ± 0.9

Moisture determination of Chi-GA-DAPC-MPEG-NMDA formulation was performed. Determination of moisture content in lyophilized formulations is essential for predicting the quality and stability of freeze-dried products[44]. In the determination of moisture amount of lyophilised Chi-GA-DAPC-MPEG-NMDA, moisture (%) was determined as 0.558%. For this reason, they found that the lyophilization technique used was a suitable and sufficient method to obtain dry powder.

Stability studies

When the twelve-month stability study was evaluated, it was observed that there were no major changes in particle size, polydispersity index and zeta potential of Chi-GA-DAPC-MPEG-NMDA formulation. For this reason, it is predicted that the prepared chitosan nanoparticles can be stored in a lyophilized manner. The improved stability provided by the removal of water is used extensively by the pharmaceutical industry[44]. Üstündağ Okur et al. prepared nebivolol-loaded solid lipid nanoparticles and modified the nanoparticles with chitosan and PEG. They lyophilized the prepared nanoparticle dispersions by adding 11% trehalose. Then, they examined the effects of lyophilization on particle size, PDI, and zeta potential and determined the amount of moisture in nanoparticles after lyophilization. Particle size growth was seen in unmodified nanoparticles, but not specifically in chitosan and PEG-modified nanoparticles[45].

Table 7. Evaluation of the 12-month stability study of formulations in terms of particle size, polydispersity index and zeta potential

	Chi-GA-DAPC -MPEG-NMDA-4°C			Chi-GA-DAPC -MPEG-NMDA-25°C			Chi-GA-DAPC -MPEG-NMDA-40°C		
Time (month)	Particle Size (nm) ± SD	PDI ± SD	Zeta Potential (mv) ± SD	Particle Size (nm) ± SD	PDI ± SD	Zeta Potential (mv) ± SD	Particle Size (nm) ± SD	PDI ± SD	Zeta Potential (mv) ± SD
0	243.8 ± 17.1	0.322 ± 0.054	49.5 ± 1.4	243.8 ± 17.1	0.322 ± 0.054	49.5 ± 1.4	243.8 ± 17.1	0.322 ± 0.054	49.5 ± 1.4
3	247.6 ± 5.2	0.333 ± 0.005	48.0 ± 3.6	241.9 ± 0.2	0.266 ± 0.035	45.0 ± 2.6	243.1 ± 1.6	0.393 ± 0.001	45.4 ± 3.3
6	239.2 ± 5.1	0.291 ± 0.013	40.9 ± 0.7	220.3 ± 1.6	0.382 ± 0.140	43.3 ± 1.3	196.6 ± 7.6	0.347 ± 0.042	34.6 ± 1.0
9	241.4 ± 11.9	0.333 ± 0.024	45.0 ± 0.6	252.2 ± 4.4	0.344 ± 0.087	44.8 ± 2.6	259.5 ± 7.9	0.303 ± 0.022	41.8 ± 2.4
12	273.8 ± 8.9	0.287 ± 0.024	43.63 ± 1.1	263.3 ± 3.1	0.309 ± 0.035	45.35 ± 1.8	270.8 ± 7.9	0.324 ± 0.016	45.3 ± 1.0

The evolution of size during storage is ascribed to multiple factors, such as particle aggregation that promotes effective rearrangement, the interaction of free polymer chains with the particle network leading to the reorganization of intermolecular entanglements, syneresis, and swelling induced by TPP, which causes water influx via osmosis. The identical condition has been noted in the developed formulations. Consequently, as the nanoparticles underwent reorganization over time, the particle size initially diminished and subsequently rose, exhibiting no substantial variation, as illustrated in Table 7.

Agarose gel electrophoresis studies

The polymer:siRNA ratio was determined by calculating milligrams of polymer and gene per microliter. The results of agarose gel electrophoresis are shown in Figure 3. As a result of the study, it was found that the polymer: siRNA retention ratio was 5:1 for for Chi-GA-DAPC-MPEG-NMDA. In this study, the desire is that the siRNA does not emit any radiation during imaging. In this way, it is proven that siRNA is retained by the prepared formulations. The results of the study are consistent with the literature[46].

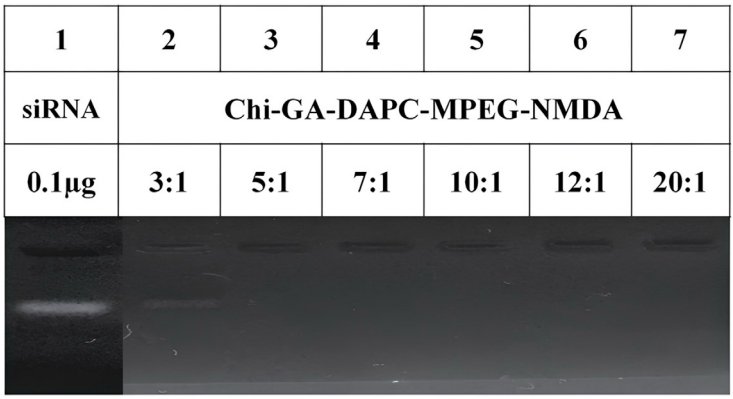

Figure 3. Gel electrophoresis images of nanoparticle formulations derived from Chi-GA-DAPC-MPEG-NMDA

Serum stability results of siRNA-loaded nanoparticles

Nanoparticles interact with various biological environments, including proteins and ions, affecting their physicochemical properties. These interactions can significantly alter colloidal stability and physicochemical properties. However, these interactions can sometimes be overlooked, making it crucial to understand their impact on drug transport, as they can significantly alter the physicochemical properties, colloidal stability, and nanoparticle-cell interactions[47]. The study examined the stability of nanoparticles in serum, predicting

they might enter the bloodstream through intranasal administration. Table 8 shows the changes in particle size, PDI value, and zeta potential, and siRNA integrity was examined over time by using polyacrylamide gel electrophoresis.

Table 8. Particle size, size distribution and zeta potential values of nanoparticles in the presence of 5% FBS

Chi-GA-DAPC -MPEG-NMDA			
Time (h)	**Particle Size (nm) ± SD**	**PDI ± SD**	**Zeta Potential (mv) ± SD**
0	235.3 ± 8.4	0.349 ± 0.049	53.6 ± 2.9
0.5	586.8 ± 36.4	0.812 ± 0.032	12.8 ± 0.1
2	733.7 ± 20.1	0.695 ± 0.180	10.3 ± 0.2
4	770.2 ± 53.0	0.275 ± 0.054	9.85 ± 0.4
24	785.5 ± 11.8	0.263 ± 0.028	10.3 ± 0.2

The size, PDI value and zeta potential of the Chi-GA-DAPC -MPEG-NMDA nanoparticle were found to be 235.3 ± 8.4 nm, 0.349 ± 0.049, and 53.6 ± 2.9 mV, respectively. As the process progressed, the zeta potential of the nanoparticles decreased due to the presence of proteins in the environment, while its size increased. After a while, when the zeta potential was fixed, the nanoparticle regenerated and remained at a constant particle size as specified in the stability study. As a result of this study, it was observed that the particle size and polydispersity indices of the formulations increased as they approached 24 hours.

Figure 4 shows examples of polyacrylamide gels. Polyacrylamide gel electrophoresis studies were also conducted in polyacrylamide gel, as it is a more sensitive system to small particles of siRNA.

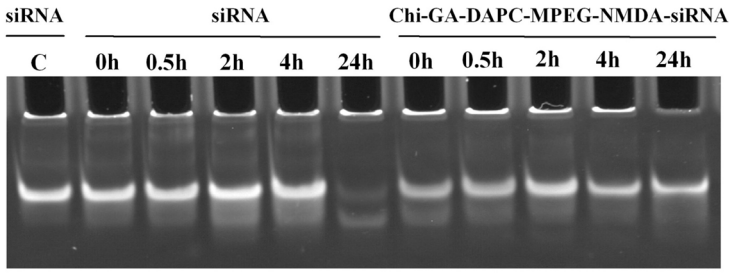

C: Control

Figure 4. Electrophoretic action of siRNA loaded with ionic interaction to Chi-GA-DAPC-MPEG-NMDA in 5% FBS in polyacrylamide gel

Malcolm et al.'s study found an increase in particle size and polydispersity index of nanoparticle-siRNA complexes in serum and nanoparticle-siRNA aggregation. The study found similar results in environments with 0.5% and 1% FBS. The zeta potential of the nanoparticles also changed, but it was not of high value that affected stability[48]. However, in the medium containing 5% FBS, the nanoparticles showed relatively different properties due to increased protein concentration. The study found that formulations with larger particle sizes and polydispersity indices increased over 24 hours. Polyacrylamide gel electrophoresis studies showed that all formulations maintained siRNA integrity for 24 hours. Katas et al. developed chitosan nanoparticle formulations with smaller sizes to eliminate siRNA properties, which are rapidly metabolized and taken into cells. These formulations were completely broken down after 72 hours of application in serum[21]. In our studies with Chi-GA-DAPC-MPEG-NMDA nanoparticle formulation, we found that siRNA integrity was maintained for 24 hours.

As a result, nanoparticle formulations prepared from modified chitosan polymers were successfully developed in this study, in which nanoparticle systems containing siRNA were prepared and evaluated. As a result of the characterization studies, it has been determined that the ideal formulations obtained can be used in the treatment of HD intranasal route and as gene therapy due to its gene silencing effect. It has been determined that the obtained formulations have the desired particle size, zeta potential and particle size distribution and maintain their stability for a long time. The formulation showed a high rate of siRNA loading capacity. At the same time, it maintained siRNA integrity for 24 hours. The developed formulation is promising in the treatment of HD.

STATEMENT OF ETHICS

Ethics approval is not required in this study, as no human and experimental animal samples are involved.

CONFLICT OF INTEREST STATEMENT

The authors declare no conflict of interest.

AUTHOR CONTRIBUTIONS

Emre Şefik ÇAĞLAR, Emine Büşra EKER FİDAN, Mehmet Koray GÖK collected data, analyzed and interpreted results, and prepared the initial manuscript. Emre Şefik ÇAĞLAR, Mehmet Koray GÖK, Neslihan ÜSTÜNDAĞ OKUR, Saadet Kevser PABUCCUOĞLU, and Erdal CEVHER participated in the final version of the text. Erdal CEVHER supervised the project.

FUNDING SOURCES

This project was supported by TUBITAK Project No: 218S628.

ACKNOWLEDGMENTS

This study was generated from the PhD thesis of Emre Şefik Çağlar.

REFERENCES

1. Ross CA, Poirier MA. Protein aggregation and neurodegenerative disease. Nat Med, 2004;10 (7):10-17. Doi: 10.1038/nm1066

2. Richards RI. Dynamic mutations: a decade of unstable expanded repeats in human genetic disease. Hum Mo Genet, 2001;10(20):2187-2194. Doi: 10.1093/hmg/10.20.2187

3. Ross CA, Tabrizi SJ. Huntington's disease: from molecular pathogenesis to clinical treatment. Lancet Neuro, 2011;10(1):83-98. Doi: 10.1016/S1474-4422(10)70245-3

4. Godinho BMDC, Ogier JR, Darcy R, O'Driscoll CM, Cryan FJ. Self-assembling modified β- cyclodextrin nanoparticles as neuronal siRNA delivery vectors: focus on Huntington's disease. Mol Pharm, 2013;10(2):640-649. Doi: 10.1021/mp3003946

5. Roos RAC. Huntington's disease: a clinical review. Orphanet J Dis, 2010;20(5):40. Doi: 10.1186/1750-1172-5-40

6. Videnovic A. Treatment of Huntington disease. Curr Treat Options Neurol, 2013;15(4):424-438. Doi: 10.1007/s11940-013-0219-8

7. Stefani G, Slack FJ. Small non-coding RNAs in animal development. Nat Rev Mol Cell Biol, 2008;9:219-230. Doi: https://doi.org/10.1038/nrm2347

8. He L, Hannon GJ. MicroRNAs: small RNAs with a big role in gene regulation. Nat Rev Genet, 2004;5:522-531. Doi: 10.1038/nrg1379

9. Zamore PD, Tuschl T, Sharp PA, Bartel DP. RNAi: double-stranded RNA directs the ATP-dependent cleavage of mRNA at 21 to 23 nucleotide intervals. Cell, 2000;101(1):25-33. Doi: 10.1016/S0092-8674(00)80620-0

10. Martinez J, Patkaniowska A, Urlaub H, Lührmann R, Tuschl T. Single-stranded antisense siRNAs guide target RNA cleavage in RNAi. Cell, 2002;110(5):563-574. Doi: 10.1016/S0092-8674(02)00908-X

11. Bernkop-Schnürch A, Dünnhaupt S. Chitosan-based drug delivery systems. Eur J Pharm Biopharm, 2012;81(3):463-469. Doi: 10.1016/j.ejpb.2012.04.007

12. Ezhilarasan D, Shree Harini K. Nanodrug delivery: strategies to circumvent nanoparticle trafficking by Kupffer cells in the liver. J Drug Deliv Sci Technol, 2023;86:104731. Doi: 10.1016/j.jddst.2023.104731

13. Fan MMY, Raymond LA. *N*-methyl-D-aspartate (NMDA) receptor function and excitotoxicity in Huntington's disease. Prog Neurobiol, 2007;81(5-6):272-293. Doi: 10.1016/j.pneurobio.2006.11.003

14. Sava V, Fihurka O, Khvorova A, Sanchez-Ramos J. Enriched chitosan nanoparticles loaded with siRNA are effective in lowering Huntington's disease gene expression following intranasal administration. Nanomed, 2020;24102119. Doi: 10.1016/j.nano.2019.102119

15. Eker Fidan EB, Bal K, Şentürk S, Kaplan Ö, Demir K, Gök MK. Enhancing gene delivery efficiency with amphiphilic chitosan modified by myristic acid and tertiary amino groups. Int J Biol Macromol, 2024;282(1):136775. Doi: 10.1016/j.ijbiomac.2024.136775

16. Gök MK, Demir K, Cevher E, Özgümüş S, Pabuccuoğlu S. Effect of the linear aliphatic amine functionalization on *in vitro* transfection efficiency of chitosan nanoparticles. Carbohydr Polym, 2019;207:580-587. Doi: 10.1016/j.carbpol.2018.12.013

17. Ahmed T, Aljaeid B. Preparation, characterization, and potential application of chitosan, chitosan derivatives, and chitosan metal nanoparticles in pharmaceutical drug delivery. Drug Des Devel Ther, 2016;2016(10):483. Doi: 10.2147/DDDT.S99651

18. Üstündağ-Okur N, Gökçe EH, Bozbıyık Dİ, Eğrilmez S, Özer Ö, Ertan G. Preparation and *in vitro–in vivo* evaluation of ofloxacin loaded ophthalmic nano structured lipid carriers modified with chitosan oligosaccharide lactate for the treatment of bacterial keratitis. Eur J Pharm Sci, 2014;63:204-215. Doi: 10.1016/j.ejps.2014.07.013

19. Hazzah HA, Farid RM, Nasra MMA, EL-Massik MA, Abdallah OY. Lyophilized sponges loaded with curcumin solid lipid nanoparticles for buccal delivery: development and characterization. Int J Pharm, 2015;492(1-2):248-257. Doi: 10.1016/j.ijpharm.2015.06.022

20. Abdul M, Raja G, Katas H. Stability, intracellular delivery, and release of siRNA from chitosan nanoparticles using different cross-linkers. Plos One, 2015;10(6):1-19. Doi: 10.1371/journal.pone.0128963

21. Katas H, Alpar HO. Development and characterisation of chitosan nanoparticles for siRNA delivery. J Control Release, 2006;115(2):216-225. Doi: 10.1016/j.jconrel.2006.07.021

22. Muthu MS, Feng S-S. Pharmaceutical stability aspects of nanomedicines. Nanomed, 2009; 4(8):857-860. Doi: 10.2217/nnm.09.75

23. Gedde UW. Thermal analysis of polymers. In: Polymer physics. Springer, Dordrecht: Netherlands. 1999. pp. 217-237. Doi: 10.1007/3-540-06552-0_2

24. Gao K, Jiang X. Influence of particle size on transport of methotrexate across blood brain barrier by polysorbate 80-coated polybutylcyanoacrylate nanoparticles. Int J Pharm, 2006;310(1-2):213-219. Doi: 10.1016/j.ijpharm.2005.11.040

25. Olivier JC. Drug transport to brain with targeted nanoparticles. NeuroRx, 2005;2:108-119. Doi: 10.1602/neurorx.2.1.108

26. Patel S, Chavhan S, Soni H, Babbar AK, Mathur R, Mishra AK, et al. Brain targeting of risperidone-loaded solid lipid nanoparticles by intranasal route. J Drug Target, 2011;19(6):468-474. Doi: 10.3109/1061186X.2010.523787

27. Gratton SEA, Ropp PA, Pohlhaus PD, Luft JC, Madden VJ, Napier ME, DeSimone JM. The effect of particle design on cellular internalization pathways. Proc Natl Acad Sci USA, 2008;105(33):11613-11618. Doi: 10.1073/pnas.0801763105

28. Hillaireau H, Couvreur P. Nanocarriers' entry into the cell: relevance to drug delivery. Cell Mol Life Sci, 2009;66:2873-2896. Doi: 10.1007/s00018-009-0053-z

29. Muntimadugu E, Dhommati R, Jain A, Challa VGS, Shaheen M, Khan W. Intranasal delivery of nanoparticle encapsulated tarenflurbil: a potential brain targeting strategy for Alzheimer's disease. Eur J Pharm Sci, 2016;92:224-234. Doi: 10.1016/j.ejps.2016.05.012

30. Etame AB, Smith CA, Chan WCW, Rutka MD JT. Design and potential application of PE-Gylated gold nanoparticles with size-dependent permeation through brain microvasculature. Nanomed, 2011;7(6):992-1000. Doi: 10.1016/j.nano.2011.04.004

31. Hanada S, Fujioka K, Inoue Y, Kanaya F, Manome Y, Yamamoto K. Cell-based *in vitro* blood-brain barrier model can rapidly evaluate nanoparticles' brain permeability in association with particle size and surface modification. Int J Mol Sci, 2014;15(2):1812-1825. Doi: 10.3390/ijms15021812

32. Godinho BMDC, Ogier JR, Darcy R, O'Driscoll CM, Cryan JF. Self-assembling modified β-cyclodextrin nanoparticles as neuronal siRNA delivery vectors: focus on Huntington's disease. Mol Pharm, 2013;10(2):640-649. Doi: 10.1021/mp3003946

33. Van Woensel M, Wauthoz N, Rosière R, Mathieu V, Kiss R, Lefranc F, et al. Development of siRNA-loaded chitosan nanoparticles targeting Galectin-1 for the treatment of glioblastoma multiforme via intranasal administration. J Control Release, 2016;227:71-81. Doi: 0.1016/j.jconrel.2016.02.032

34. Jallouli Y, Paillard A, Chang J, Sevin E, Betbeder D. Influence of surface charge and inner composition of porous nanoparticles to cross blood-brain barrier *in vitro*. Int J Pharm, 2007;344(1-2):103-109. Doi: 10.1016/j.ijpharm.2007.06.023

35. Alihosseini F, Ghaffari S, Dabirsiaghi AR, Haghighat, S. Freeze-drying of ampicillin solid lipid nanoparticles using mannitol as cryoprotectant. Braz J Pharm Sci, 2015;51:797-802. Doi: 10.1590/S1984-82502015000400005

36. Abdelwahed W, Degobert G, Stainmesse S, Fessi, H. Freeze-drying of nanoparticles: formulation, process and storage considerations. Adv Drug Deliv Rev, 2006;58(15):1688-1713. Doi: 10.1016/j.addr.2006.09.017

37. Almalik A, Alradwan I, Kalam MA, Alshamsan A. Effect of cryoprotection on particle size stability and preservation of chitosan nanoparticles with and without hyaluronate or alginate coating. Saudi Pharm J, 2017;25(6):861-867. Doi: 10.1016/j.jsps.2016.12.008

38. Gokce Y, Cengiz B, Yildiz N, Calimli A, Aktas Z. Ultrasonication of chitosan nanoparticle suspension: influence on particle size. Colloids Surf A Physicochem Eng Asp, 2014;462:75-81. Doi: 10.1016/j.colsurfa.2014.08.028

39. Fonte P, Soares S, Costa A, Andrade JC, Seabra V, Reis S, Sarmento B. Effect of cryoprotectants on the porosity and stability of insulin-loaded PLGA nanoparticles after freeze-drying. Biomatter, 2012;2(4):329-339. Doi: 10.4161/biom.23246

40. Akbaba H, Demir Dora D, Kantarci AG. The effects of lyophilization and cryoprotectants on solid lipid nanoparticle-DNA systems. Rom Biotechnol Lett, 2017;22(6):13186-13195. Doi: 10.26327/RBL2017.05

41. Ball R, Bajaj P, Whitehead K. Achieving long-term stability of lipid nanoparticles: examining the effect of pH, temperature, and lyophilization. Int J Nanomedicine, 2016;2017(12):305-315. Doi: 10.2147/IJN.S123062

42. Zhang Y, Wang H, Stewart S, Jiang B, Ou W, Zhao G, He X. Cold-responsive nanoparticle enables intracellular delivery and rapid release of trehalose for organic-solvent-free cryopreservation. Nano Lett, 2019;19(12):9051-9061. Doi: 10.1021/acs.nanolett.9b04109

43. Almalik A, Alradwan I, Kalam MA, Alshamsan A. Effect of cryoprotection on particle size stability and preservation of chitosan nanoparticles with and without hyaluronate or alginate coating. Saudi Pharm J, 2017;25(6):861-867. Doi: 10.1016/j.jsps.2016.12.008

44. Anchordoquy TJ, Jinxiang Y. Effects of moisture content on the storage stability of dried lipoplex formulations. J Pharm Sci, 2009;98(9):3278-3289. Doi: 10.1002/jps.21846

45. Üstündağ-Okur N, Yurdasiper A, Gündoğdu E, Gökçe Homan E. Modification of solid lipid nanoparticles loaded with nebivolol hydrochloride for improvement of oral bioavailability in treatment of hypertension: polyethylene glycol versus chitosan oligosaccharide lactate. J Microencapsul, 2016;33(1):30-42. Doi: 10.3109/02652048.2015.1094532

46. Carrillo C, Suñé JM, Pérez-Lozano P, García-Montoya E, Sarrate R, Fàbregas A, Ticó JR. Chitosan nanoparticles as non-viral gene delivery systems: determination of loading efficiency. Biomed Pharmacother, 2014;68(6):775-783. Doi: 10.1016/j.biopha.2014.07.009

47. Raval N, Jogi H, Gondaliya P, Kalia K, Tekade RK. Method and its composition for encapsulation, stabilization, and delivery of siRNA in Anionic polymeric nanoplex: an *in vitro- in vivo* assessment. Sci Rep, 2019;9:1-18. Doi: 10.1038/s41598-019-52390-4

48. Malcolm DW, Varghese JJ, Sorrells JE, Ovitt CE, Benoit DS. The effects of biological fluids on colloidal stability and siRNA delivery of a pH-responsive micellar nanoparticle delivery system. ACS Nano, 2018;12(1):187-197. Doi: 10.1021/acsnano.7b05528

Acta Pharm. Sci. Vol 63:(2), 2025
Original article
DOI: 10.23893/1307-2080.APS6317

Preparation and evaluation of sodium alginate hydrogel sheet loaded with *Carica papaya* L. seed extract for wound healing

Ishan DURVASHA[1], Anil KUMAR[1], Shweta AGARWAL[1,2*]

1 LR Institute of Pharmacy, Department of Pharmaceutics, Solan, India
2 ICFAI University, Faculty of Pharmaceutical Sciences, Baddi, India

ABSTRACT

In this study, an innovation in the form of a hydrogel sheet containing *Carica papaya* seed extract was developed and assessed for wound healing activity. The hydrogel sheet was prepared by using sodium alginate, guar gum, glycerol, methyl, and propyl paraben as excipients. Ninehydrogel formulations were prepared by varying the amount of sodium alginate (1.5%, 2.5%, and 3.5%), extract (8%, 10%, and 12%), and guar gum (0.8%, 1.2%, and 1.5%). The formulations prepared were evaluated for physicochemical characteristics like colour, pH, weight variations, folding endurance, tensile strength. Surface characteristics were studied by scanning electron microscopy. Wound healing potential was studied on wistar rats with hydrogel sheet (12%) showing 97.5% wound closure. All hydrogels containing seed extracts showed superior healing performance vis-a-vis control hydrogel. It can be deduced from the *in vivo* evaluation that the *Carica papaya* seed extract hydrogel sheet has wound healing properties comparable to the marketed hydrogel sheet.

Keywords: sodium alginate, innovation, *Carica papaya* extract, hydrogel, wound healing

*Corresponding author: Shweta AGARWAL
E-mail: shweta_ag26@rediffmail.com
ORCIDs:
Ishan DURVASHA: 0000-0002-2784-1243
Anil KUMAR: 0000-0002-2742-0705
Shweta AGARWAL: 0000-0002-9412-0788
(Received 9 Nov 2023, Accepted 28 Mar 2024)

INTRODUCTION

The dynamic process of wound healing involves inflammation, epithelisation, collagen synthesis, and remodelling of tissue[1]. The process of wound healing starts from the moment the tissue injury occurs. The contact of platelets with the exposed collagen initiates the healing cascade. Clotting factors are released as platelets aggregate, emanating in the formation of a clot of fibrin at the injury site. This clot acts as a temporary matrix and paves the way for further healing events[2].

Inflammatory cells appear at the site of injury along with platelets and provide key signals in the form of cytokines[3]. Fibroblasts, the connective-tissue cells leading to collagen deposition, are required for tissue restoration. Collagen imparts structural integrity and strength to normal tissues. When tissues are damaged as a result of an injury, collagen is required to rebuild the damaged anatomic structure and restore its function. A therapeutic system could alter the wound healing process by interfering with any of the stages of wound healing[4].

Carica papaya L. (Caricaceae) is widely used in conventional medicine as papain, a proteolytic enzyme, the active principal provides protection against ulcers[5]. The *C. papaya* seed extract has been reported to possess high phenolic and flavonoid content having free radical scavenging property which helps in reducing wound inflammation. The papain and chymopapain present in *Carica papaya* seed extract cause proteolytic wound debridement, facilitating wound healing[6,7]. The presence of these phytoconstituents enables *C. papaya* to possess antimicrobial, antioxidant, and anti-inflammatory activities[8] that may be valuable in the treatment of chronic skin ulcers[9]. It is extensively used as an efficacious and easily accessible substance for wounds, especially burns, in developing countries. Care of wounds and maintenance entails a variety of procedures, including dressing.

Alginate is a biopolymer with numerous biomedical uses owing to its bio compatibility, nontoxic nature, and ease of availability. These attributes are also favourable for wound healing application[10]. By virtue of hydrophilic nature of alginate polymer, alginate-based hydrogel dressing have the potential to soak up unnecessary wound fluid, maintain an optimum hydration level at the wound site and reduce bacterial load at wound bed. Maintenance of moist milieu reduces the risk of scar formation, facilitates epithelisation of tissue and cell migration for wound healing. Also, moist conditions allow for effective debridement by clearing away of necrotic tissue, and foreign elements like microbes because of the sorption potential of hydrogel. Their mechanical strength enables them to act as a barrier to entry of microbes and foreign

bodies. The porous polymeric network permits exchange of gases allowing the tissue to breathe as elaborated by Kohler et al. in their comprehensive review on Hydrogel based wound dressings[11].

The present study was undertaken with the aim of developing a hydrogel sheet of sodium alginate loaded with bioactives of seed extract of *C. papaya* to expedite the wound healing process. Sodium alginate was chosen as the polymer as sodium alginate itself has been shown to possess wound healing properties and the hydrogel sheet would further aid in wound healing by absorption of exudates, allowing oxygen permeability, providing a protective covering over the wound and providing an optimum moist environment for better healing. Several studies have reported the use of sodium alginate either alone or in combination with antibiotics[12] inorganic substances[13] and plant extracts[14] for wound healing dressing. In fact, some alginate-based dressings have been commercialized like Nu-Gel (Systanix), Tegagel (3M GmBh)[11]. The novelty of the study lies in the fact that although alginate wound dressings have been developed earlier but none of the studies used a combination of papaya seed extract and sodium alginate as wound dressing, both being components aiding in expediting wound healing.

Several studies have been carried out on therapeutic effects of seed, pulp, peel extracts either in crude form or the form of dosage form. For example, seed extract has been investigated for contraception, antiulcerogenic activity in crude form and in the form of jelly for anthelminthic activity. Ethanolic seed extract of papaya has been studied for excision wound healing in rats by[15]. The results demonstrated hastened wound healing in comparison to the standard taken. Papain, an enzyme from the *Carica papaya* extract, added to sodium alginate membrane improved the healing wounds by improving debridement of necrotic tissue[16]. Papaya leaf extract formulated in the form of tablets and syrup form have been studied and used for treatment of dengue. Spray gel of papaya leaf extract was investigated for wound healing by Wijaya et al. and it showed accelerated wound healing as compared to placebo[17]. The novelty of the work lies in the fact that no work has been reported on the wound healing potential of seed extract of papaya along with sodium alginate in a dosage form. It was hypothesized that papaya seed extract along with sodium alginate in the form of hydrogel sheet will promote healing of wounds as sodium alginate alone has been shown to assist wound healing.

Sodium alginate hydrogel sheets loaded with papaya seed extract were formulated and evaluated for physicochemical characteristics like appearance, thickness, pH, moisture content, gelation time, weight variation, tensile strength,

water vapour transmission rate, folding endurance and swelling capacity. Animal studies were also carried out on rat model to study the effectiveness of the formulated hydrogel sheet in wound healing against the commercially available sodium alginate based wound dressings.

It was envisaged that the seed extract loaded hydrogel sheet would be an effective alternative to the usually used synthetic wound healing formulations as it would have the advantage of presence of sodium alginate, *C. papaya* seed extract and hydrogel sheet formulation.

METHODOLOGY

Chemicals and reagents

Glycerol was obtained from Fisher Scientific Pvt Ltd. Sodium alginate methylparaben, propylparaben and calcium chloride were procured from SD Fine Chem LTD. Ethanol and guar gum was procured from Loba Chemie Pvt Ltd.

Collection of seeds

The seeds of *Carica papaya* were collected from the local vendor, Solan.

Preparation of seed extract:

For the extraction of seed extract, the method given by Nayak et al. was employed with some modifications[15]. The seeds of *Carica papaya* were collected, washed thoroughly under running water to remove dirt and finally washed with distilled water. Seeds were shade dried for 15 days at room temperature. Then the seeds were dried at 40°C to get a constant weight and were powdered. The dry powder (25 g) was exhaustively macerated with water and alcohol (1:1) as the solvent. The extract obtained was filtered using Whatman filter paper and then, the extract was partially concentrated at 60 ± 2°C in vacuum oven to obtain the semi dried form.

Phytochemical screening

Preliminary qualitative phytochemical screening of the hydroalcoholic extract was conducted to ascertain the presence of secondary metabolites like alkaloids, glycosides, saponins, tannins and phenolic compounds, carbohydrates, terpenoids, and amino acids by using standard phytochemical screening and identification tests. Variation in color and form or formation of characteristic precipitate was noted to determine the presence of these secondary metabolites[18-23]. Hager's test, Wagner's test, and Mayer's test were used to check for the presence of alkaloids. The presence of Saponin glycosides was checked for by the foam test and cardiac glycosides were determined by Keller Killiani

test and Legal test. Lead acetate and Ferric chloride test were utilized to establish the presence of tannins and phenolic compounds. Carbohydrates were checked by Molisch, Benedict and Fehling's test and amino acids by Ninhydrin test. Salkowski and lead acetate tests were used to establish the existence of Terpenoids and Flavonoids respectively in the extract.

Physicochemical characterization of extract

Extract was characterized for pH, density and percentage yield. pH meter was calibrated at pH 4, 7, 9.2, and then pH was determined by directly dipping the electrode into the semi-dried extract till a constant pH was obtained. Density was measured by pycnometer/specific gravity bottle. The percentage yield of the extract was determined as percentage of the weight of the extract to the original weight of the dried powdered sample used.

Fourier Transform Infra-Red spectroscopy (FTIR):

The FTIR spectra were obtained by using ATR FTIR Spectrophotometer (Agilent technologies; Model: CARY 630). FTIR spectra were recorded for hydroalcoholic seed extract of *Carica papaya* and optimized formulation. The spectra were recorded in the range of 4000-650 cm^{-1} and were used to study extract-excipient interactions by checking for major alterations in peaks.

Preparation of hydrogel sheet

Hydrogel sheet was prepared by ionotropic gelation method. Hydrogel sheets were prepared by using the composition as given in Table 1. The required quantity of sodium alginate was dissolved in 15ml of distilled water. The solution was then continuously stirred for 30 min using a magnetic stirrer set at 300 rpm. The guar gum mixture was prepared in 5ml distilled water with specified amount of glycerol, propyl paraben, methyl paraben, and seed extract. Guar gum mixture was then added into the sodium alginate solution and stirred continuously. All weight calculations were done considering 30g as the final weight of hydrogel. For removal of air bubbles, the solution was placed in a bath sonicator for 10 min and then was poured into the petri dishes with 19 cm^2 surface area. Then 30 ml of 0.5% calcium chloride solution was prepared and poured over the petri dish containing extract-excipient mixture for the crosslinking of the sodium alginate polymer. The petri dishes were left undisturbed at room temperature for 12 h. Then the hydrogel sheet was removed from the petri dish. Finally, the hydrogel sheet was placed in the desiccator for drying and a clear thin hydrogel sheet was obtained[24].

Table 1. Composition of the hydrogel sheets

Ingredients	F1	F2	F3	F4	F5	F6	F7	F8	F9
Plant extract (w/w)	10%	10%	10%	10%	10%	10%	10%	10%	10%
Glycerol (w/w)	21%	21%	21%	21%	21%	21%	21%	21 %	21%
Methyl paraben (w/w)	0.06%	0.06%	0.06%	0.06%	0.06%	0.06%	0.06%	0.06%	0.06%
Propyl paraben (w/w)	0.02%	0.02%	0.02%	0.02%	0.02%	0.02%	0.02%	0.02%	0.02%
Sodium Alginate (w/w)	2.5%	1.5%	3.5%	2.5%	1.5%	3.5%	2.5%	1.5%	3.5%
Guar Gum (w/w)	1.2%	1.5%	0.8%	1.5%	0.8%	1.2%	0.8%	1.2%	1.5%
Distilled water (q.s)	30 g	30 g	30 g	30 g	30 g	30 g	30 g	30 g	30g

Physico-chemical characterization of hydrogel sheets

The hydrogel sheets were characterized as the following parameters:

Physical appearance: Physical parameters like color and appearance were determined visually.

pH: pH of the sheet was checked after adding 1-2ml of distilled water to a small area of sheet to wet and swell the hydrogel. The pH was then determined by using digital pH meter after calibrating it with buffer pH 4, 7, 9.2.

Homogeneity: All the prepared hydrogel sheets were checked for homogeneity by visual inspection.

Gelation time: The gelation time of the hydrogel was observed by tilting the petri dish containing the formulation at an angle of 45° periodically. The time at which the hydrogel did not flow at the tilted angle for at least 30s was taken as the gelation time[25].

Weight Variations: Analytical weighing balance was used for the study of weight variation of the formulated sheets. The data obtained was averaged for obtaining weight variation values. Three patches from each batch were taken for weight variation and result reported as (mean ± SD)[26].

Thickness: Vernier caliper was used for the evaluation of thickness of sheets. Sheet thickness uniformity was ensured by measuring its thickness at 6 different places. The values obtained were averaged and reported (mean ± SD)[27].

Folding Endurance: This test is conducted to ensure mechanical strength and plasticizer efficacy in hydrogel sheet. The folding of formulated hydrogel sheets at same place was carried out until breaking and cracking in the sheet

was observed and the number of folds till the sheet broke gave the folding endurance (n=3)[28].

Swelling Index Evaluation: The individual weights of prepared hydrogel sheets were taken and then sheets were dipped in water until they started to almost disintegrate. The initial and final weight of formulated sheets was used for the calculation of swelling index for the formulated sheets. The following equation was used for calculating % swelling index:

$$SI = (w2 - w1)/w1 \times 100$$

Where w1 is the sheets initial weight, w2 is final weight. The result obtained were averaged and reported (mean ± SD, n=3).

Tensile Strength: The tensile strength was measured for formulated sheets using the tensiometer (UTM (servo & Vector Model). It consists of two load grips; the lower one being fixed and the upper one being mobile. Film strips 2*2cm were fixed between these grips, and force was gradually increased till the film broke. The tensile strength was read from the dial in kg (n=3)[29].

Water Vapor Transmission Rate: Oven-dried bottles and individually weighed formulated sheets were used in this study to make transmission cells. Saturated solution of potassium chloride was kept in desiccator to maintain an approximate humidity of 85%, and 1 g of anhydrous calcium chloride was put in each bottle. The transmission cells with their mouth covered with hydrogel sheet were weighed and kept in the desiccator. These were removed from the desiccator after specified intervals of time, i.e., 6, 12, 24, 36, 48, and 72 h. The transmission cells were reweighed at the end of the study to get the result as mean ± SD (n=3)[30].

$$Water\ vapor\ transmission\ rate = W/ST$$

W = Final weight- initial weight

W is the increase in weight in 24 h; S is area of film exposed (m^2); T is exposure time.

Percentage Moisture Content: Formulated sheets were weighed initially and then kept in desiccator. Silica was also placed in desiccator for 24 h. The patches were kept in the desiccator till they attained a constant weight. The % moisture content value was estimated from the difference in the initial and final weights of sheets. The following equation was used to calculate the value of % moisture content. (n=3)

$$\%\text{Moisture Content} = \frac{wi - wf}{wi}\ x\ 100 \quad (5)$$

Where wi represents the initial weights, and wf represents the final weight[31].

Study of surface morphology

The surface morphological study of the optimized sheet was carried out by scanning electron microscopy (SEM). The mesh structures of the sample were observed using field-emission SEM (S-3000 N, Hitachi, Japan).

Accelerated stability study

Accelerated stability study for the optimized formulation was performed at a temperature of 40 ± 2°C and relative humidity of 75 ± 5% RH for 3 months. The hydrogel sheet was stored for the stability study for 3 months and was checked for physical appearance, physicochemical properties like swelling index, tensile strength by the methods used for the evaluation of formulated sheets stated above at 0, 1, and 3 months.

Incision wound model

In vivo protocol bearing number (LRIP/IAEC/2022/PH-03) for carrying out wound healing study was passed by IAEC of the institute. CPCSEA guidelines were followed for carrying out animal studies. Wistar rats (RattusNorvegicus) were purchased from National Institute of Pharmaceutical Education and Research (NIPER) Mohali. The animals were anesthetized with Ketamine and Xylazine. The animals were kept on the operating table in the common position. One paravertebral strength incision of six cm was made on either side of the vertebral segment with the help of the scalpel blade. The wound was cleaned with methylated spirit. The animals were kept in independent cages. The rats were divided into six groups and each group contained 6 rats. The experimental design of *in vivo* study is given in Table 2. The first group was normal control group on which 0.9% normal saline was applied, second group was the blank hydrogel group in which blank sodium alginate hydrogel sheet was applied, third group was standard control group on which a commercially available hydrogel (Tegaderm) was applied, and the fourth group was experimental group on which formulated hydrogel sheet (8% extract) was applied. Two more groups for hydrogel sheets having 10% (fifth group) and 12% (sixth group) extract concentration were used. The wounds were created by following the method of incision wound model. Wounds of normal control group were covered with a simple gauze dipped in normal saline; wounds of the standard control group were treated with Tegaderm hydrogel (commercially available alginate dressing), and the wounds of experimental group were covered with formulated hydrogel sheets. Dressings were changed every day. Progressive changes in the wound length at the 0th, 3rd, 7th, and 11th days of the treatment were photographed with camera and measured with help of graph paper[32-33].

Table 2. *In vivo* experimental design

S. No	Group	Drug	Route	No. of animals
1	Control group	Normal Saline	Topical	6
2	Blank Hydrogel	Sodium Alginate Hydrogel	Topical	6
3	Marketed formulation	Tegaderm Hydrogel	Topical	6
4	Test group 1st	8% Ext Hydrogel sheet	Topical	6
5	Test group 2nd	10% Ext hydrogel sheet	Topical	6
6	Test group 3rd	12% Ext hydrogel sheet	Topical	6

RESULTS and DISCUSSION

Preparation of seed extract

Fresh seeds of the papaya fruit were collected, washed and sorted. The seeds were shade dried for approximately 15 days, to prevent the loss of active constituents and further dried in an oven at 40°C to get a constant weight and then powdered coarsely. The powder was sieved through sieve No. 40 and stored in an airtight container till used for extraction. The dry powder (25g) was exhaustively macerated with water and alcohol (1:1) and extract obtained was filtered using Whatman filter paper. The extract was then partially concentrated at 60 ± 2°C in vacuum oven to obtain the semi dried form.

Phytochemical screening

Phytochemical screening of the extract obtained was carried out to check for the presence of alkaloids, glycosides, saponin glycosides, tannins, phenolic compounds, carbohydrates, flavonoids, cardiac glycosides, amino acids, and terpenoids. It was established that alkaloids, tannins, phenolic compounds, carbohydrates, and flavonoids were present while saponins, amino acids, and terpenoids gave negative results as shown in Table 3[15].

Table 3. Phytochemical screening of the extract

S. No.	Phytochemical tests	Result
1	Alkaloids	
1.1	Hagers test	+
1.2	Wagners test	+
1.3	Mayers test	-
2	Saponin glycosides	
2.1	Foam test	_
3	Cardiac glycosides	
3.1	Killer killani test	-
3.2	Legal test	+
3.3	Kedde test	-
4	Tannins and phenolic compounds	
4.1	Lead acetate test	+
4.2	Ferric chloride test	+
5	Carbohydrates	
5.1	Molish test	-
5.2	Benedict test	+
5.3	Felhing test	+
6	Amino acids	
6.1	Ninhydrin test	-
7	Terpenoids	
7.1	Salkowski test	-
8	Flavonoids	
8.1	Lead acetate test	+

Physiochemical evaluation of the extract

Results of physicochemical evaluation have been illustrated in Table 4. The extract after partial dehydration, gave a semi-solid product with a yield of 5.1 ± 0.25%, pH 5.8 ± 0.31, and density 1.2 ± 0.13 g/ml. The extract appeared to be brownish in colour.

Table 4. Results of physiochemical evaluation of the *C. papaya* seed extract

S. No.	Parameter	Observations (Mean ± SD*)
1	Percent yield	5.1 ± 0.25
2	Density	1.2 ± 0.13
3	pH	5.8 ± 0.31

*n=3

Preparation of hydrogel sheet

Hydrogel sheet was prepared by ionotropic gelation method by using a solution of calcium chloride. It was method of choice because the calcium ions absorbed during the process are exchanged for the sodium ions from the wound exudate and promote hemostasis by platelet activation. Also, this method is economical, simple and requires less equipment and time. Sodium alginate was selected because it was a bio compatible, non-toxic, non-immunogenic, biodegradable polymer and has an antimicrobial property with the advantage of gelation in presence of divalent cation[34]. Guar gum is a natural polysaccharide that had the ability to form hydrogen bonds with water. It is also used as a thickener and a stabilizer. Glycerol was used as a humectant, plasticizer, and bacteriostatic agent that allows the exudate to dry out and keeps hydrogel hydrated overlong periods of time. The combination of methylparaben and propylparaben was used as preservative, and it is commonly employed to increase the shelf life. Using the mentioned excipients and method, hydrogel sheet loaded with *Carica papaya* seed extract was successfully prepared.

Physicochemical evaluation of hydrogel sheets

The outcomes of physicochemical characterization of hydrogel sheet are revealed in Table 5. During the evaluation of the hydrogel sheet for different parameters, it was observed that the formulation F2, F5, and F8 were not suitable because minimal crosslinking has taken place in hydrogel due to the low concentration of polymer resulting in cracks and low mechanical strength[35]. Moreover, their gelation time was very long (48-49 h). It depends on the so-

dium alginate concentration and the concentration of divalent cations used for cross linking. When the sodium alginate solution is brought in contact with calcium chloride (or any other divalent cation), the calcium ions diffuse into the solution and crosslink the alginate. Gelation time varied from 12 h to 49 h. It was found to be longer in formulations composed of low concentration of sodium alginate[35].The thickness of the remaining hydrogel sheets was in the range of 2.1 0 ±.3 to 4.1 ± 0.15 mm[36]. Tensile strength indicates the strength and mechanical property of the sheet. The results for tensile strength were between 0.81 ± 0.18 to 1.82 ± 0.13 kg/cm^2 and the results of weight variation indicated uniformity of weight. The results revealed that change in the polymer concentration has effect on thickness and tensile strength[37]. With elevation in polymer concentration, thickness, and tensile strength were found to increase. The moisture content studies, showed less than 2.5% moisture in all formulations except F3, F6, and F9. Low moisture content is desirable as this results in stable formulation, reduced bulkiness and minimized microbial contamination during long term storage. The pH of all formulations was less than 7 (6.5-6.9) making them non-irritant to skin[22]. The folding endurance indicates mechanical strength of the formulations, and it varied from 162 ± 1.7 to 310 ± 1.8 for the various batches. These results indicate direct proportionality of folding endurance to polymer concentration[14]. F9 batch which has the highest polymer concentration (Sodium alginate + guar gum) has the maximum value of 310 while F5 batch having lowest concentration of polymers developed cracks at initial stages only. WVTR results (912-2110) show that it is inversely proportional to the polymer concentration in the formulation. The desirable range for WVTR is taken as 2000-2500 g/m^2/day as values within this range prevent maceration of wound by collection of exudates and also prevent excessive drying up of wound, thus providing an optimum hydration level for healing[38-39].

Table 5. Evaluation of hydrogel sheet formulations

Testing Parameter	F1	F2	F3	F4	F5	F6	F7	F8	F9
Physical Appearance	Translucent	Translucent	Translucent	Translucent	Translucent	Translucent	Translucent	Translucent	Translucent
Color	Brown	Brown	Brown	Light brown	Dark brown	Light brown	Light brown	Dark brown	Light brown
pH	6.9 ± 0.2	6.5 ± 0.12	6.8 ± 0.2	6.7 ± 0.12	6.8 ± 0.2	6.5 ± 0.3	6.9 ± 0.3	6.8 ± 0.2	6.9 ± 0.12
Thickness** (mm)	2.4 ± 0.1	ND	3.5 ± 0.2	2.8 ± 0.3	ND	4.1 ± 0.15	2.2 ± 0.2	ND	4.5 ± 0.1
Weight uniformity*(g)	4.5 ± 0.02	ND	5.9 ± 0.25	5.5 ± 0.17	ND	6.1 ± 0.3	4.3 ± 0.3	ND	6.3 ± 0.2
Folding Endurance	215.67 ± 1.7	ND	254.33 ± 1.0	225 ± 1.89	ND	301 ± 1.7	192.67 ± 4.1	ND	310 ± 1.89
Swelling Index*(%)	79 ± 0.1	ND	71 ± 0.3	69 ± 0.2	ND	49 ± 0.12	33 ± 2.34	ND	60 ± 2.12
Moisture Content*(%)	1.7 ± 1.2	ND	3.2 ± 0.2	1.9 ± 2.1	ND	3.8 ± 0.2	2.1 ± 2.2	ND	4.5 ± 0.1
Tensile strength (kg/cm^2)	1.05 ± 0.20	ND	1.4 ± 0.02	1.21 ± 0.06	ND	1.54 ± 0.04	0.81 ± 0.18	ND	1.8 ± 0.13
Water vapor transmission* rate ($g/m^2/day$)	2110 ± 0.2	ND	1200 ± 1.2	2025 ± 2.2	ND	990 ± 1.2	1080 ± 1.1	ND	912 ± 2.2
Gelationtime* (h)	12	48	10	12	49	10	12	48	10

ND=Not Determined, *n=3, **n=6

Selection of optimized formulation

Selection of optimized batch of hydrogel sheet was done on the basis of results of physiochemical characterization. Folding endurance, tensile strength, swelling index, WVTR were considered as important parameters during selection as they influence the performance of the sheet. The selected batch was subjected to stability study, surface morphological study by SEM and would further be formulated at 2 more extract levels (8%, 12%) for *in vivo* study. F2, F5, and F8 were not evaluated further after initial characterization as they exhibited poor mechanical integrity and had developed surface cracks during the gelation process. This could be due to the improper crosslinking because of low sodium alginate concentration[35].

F1 was selected as the final formulation for further stability, SEM and *in vivo* studies as it had optimum thickness (2.4 ± 0.1 mm) for the ease of application, retention on skin and acceptability. It had adequate mechanical integrity exhibited by the results of tensile strength (1.05 ± 0.20 kg/cm^2) and folding endurance (215.67 ± 1.7)[14]. It had excellent swelling and absorption capacity of 79% for absorption of wound exudates and for providing a moist physiological environment for wound healing. Its water vapour transmission rate was also optimum between 2000-2500 to prevent maceration of wounds and for oxygen exchange for rapid healing[40]. Its gelation time of 12 h was also optimum. F3, F6, and F9 had high alginate concentration and were thick with low WVTR and were therefore not considered appropriate. F1 was further formulated at 2 more extract levels for *in vivo* studies.

Fourier Transform Infra-red (FTIR) study of extract and optimized formulation

FTIR spectra of the extract Figure 1(a) showed a broad peak on 3337 cm^{-1} due to presence of hydroxyl group, 1637 cm^{-1} due to presence of C=C stretching, 1044 cm^{-1} manifested the presence of C-O stretching[41]. The spectrum obtained corroborated well with the spectrum obtained by Prasetya et al.[31]. In FTIR spectrum of optimized formulation, Figure 1(b), the characteristics peaks of seed extract were retained with only minor shifts and changes in intensity indicating compatibility with excipients.

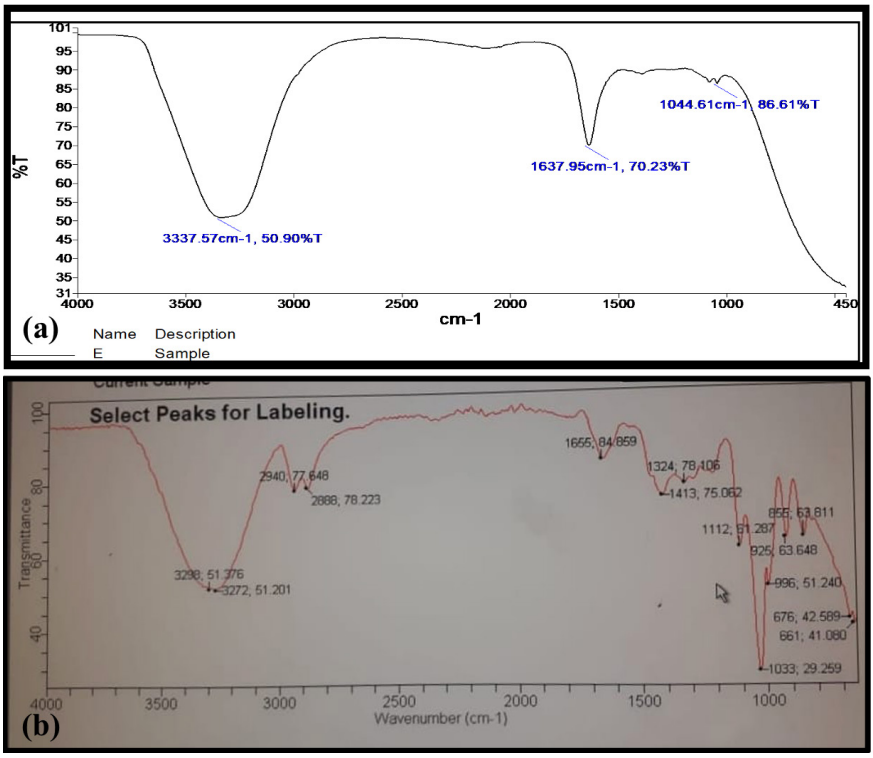

Figure 1. FTIR spectrum of (a) extract (b) optimized formulation

Scanning electron microscopy

Scanning electron microscopy was performed for F1. It revealed the surface morphology of the hydrogel sheet to be porous, rough and irregular (Figure 2[a] and [b]). These characteristics corroborate with the shrinkage occurring during the drying process. Based on SEM, formulation F1 was observed to possess optimum porosity, which would help prevent accumulation of exudates at the wound site and aid in exchange of gases[42].

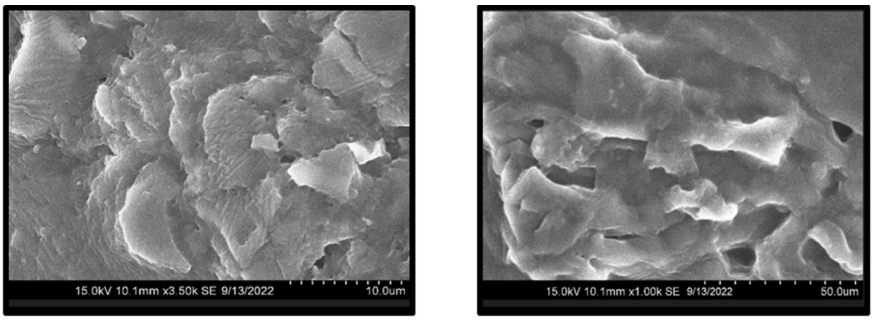

(a) (b)

Figure 2. SEM of optimized (F1) formulation at (a) 2500X (b) 700X magnification

Accelerated stability study for physical properties of hydrogel sheet

Stability study is performed to predict the shelf life of a product by hastening the rate of decomposition, ideally by increasing the temperature and relative humidity. The optimized formulation (F1) was put through stability study as per ICH guidelines by storing at 40°C/75% RH for 3 months and samples were analysed for changes in physiochemical properties at regular intervals. The results are shown in Table 6.

No major changes were found on the tested hydrogel sheet during stability study. The tested formulation was observed to be stable after exposure to accelerated humidity and temperature environment for a period of 3 months confirming the stability of the formulation.

Table 6. Results of accelerated stability study

Stability Conditions	Sampling interval (month)	Color	Thickness (mm)	pH	Moisture content (%)	Tensile strength (kg/cm²)	Swelling index (%)	Water vapour transmission rate (g/m²/day)
40 ± 2°C / 75 ± 5 % RH	0	No change	2.4 ± 0.1	6.5 ± 0.12	2.5 ± 1.2	1.05 ± 0.20	79 ± 0.1	2110 ± 0.2
	1	No change	2.3 ± 0.1	6.6 ± 0.23	2.5 ± 3.2	1.07 ± 0.20	77 ± 1.1	2107 ± 0.2
	3	No change	2.1 ± 0.1	6.6 ± 0.12	2.4 ± 0.2	1.09 ± 0.20	78 ± 1.2	2105 ± 0.2

In vivo evaluation (incision wound model)

The wound contraction rate was measured at every time interval. It is the percentage reduction of wound size. It can also be treated as a percentage of wound protection. By using a transparency paper and a suitable marker, progress of wound healing was assessed on 1st, 3rd,7th, and 11th day post wound creation. Length of the wound was traced by a placing a transparent tracing

paper over the wound and then this was placed on a sheet of graph paper (2 mm) to count the number of squares within the wound length.

$$\textit{Wound closure \%} = \frac{\text{(Wound length on day O – wound length on day N}}{\text{Wound length on day O}} \text{ X 100}$$

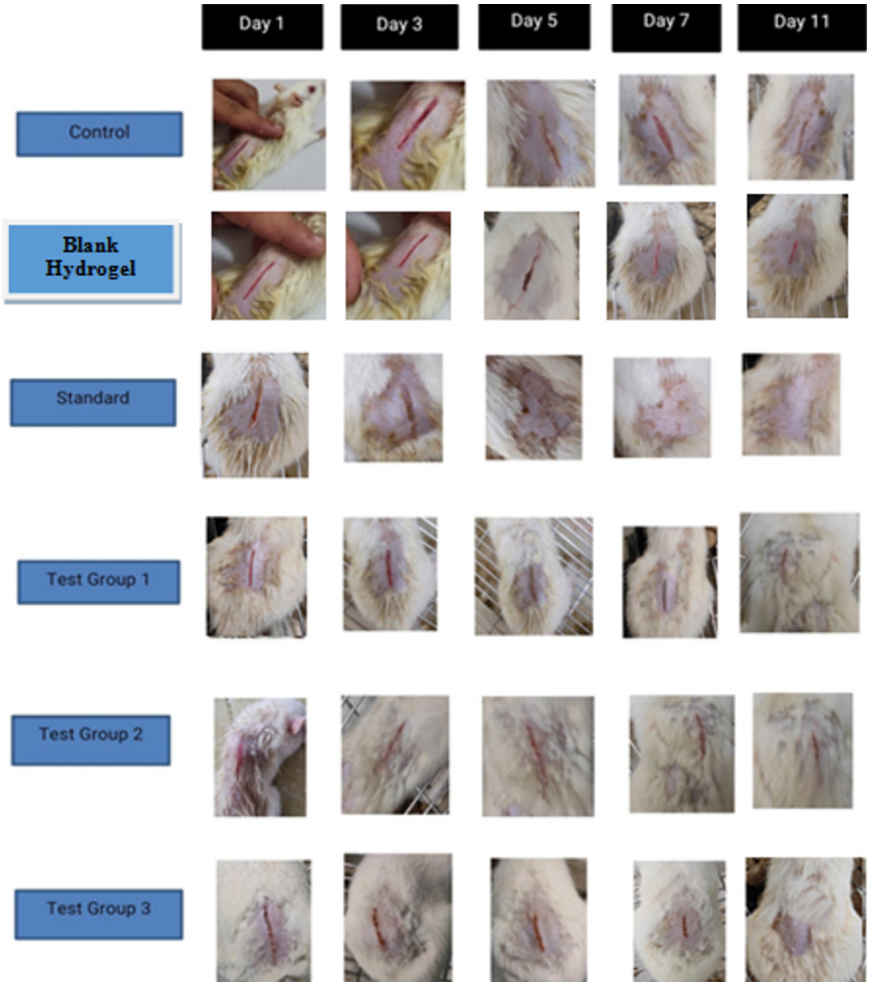

Figure 3. Progress of wound healing in different groups

Perusal of the data in Table 7 reveals that the rats treated with hydrogel sheet (12%) were found to possess accelerated wound recovery as compared to control, blank, test group 1 and test group 2 animals. The wound length of different groups was observed on 1st, 3rd, 5th ,7th, and 11th day for incision wound model and percentage wound contraction was calculated accordingly. The

standard group was treated with the commercially available Tegaderm™. The control group, blank hydrogel group, test group 1 and test group 2 rats showed lesser wound contraction while faster wound contraction was observed in the animals in test group 3 (12%) (Figure 3). The shorter epithelization period in test group 3 (12%) as compared to control and test group 1, 2, and blank hydrogel group might be due to rapid regeneration of epithelial cells. Therefore we can conclude that the *Carica papaya* hydrogel sheet with 12% extract accelerates wound healing more as compared to the control group, blank hydrogel, test group 1 and 2, and its wound healing potential was found to be insignificantly different from the standard group (Tegaderm) at 95% confidence interval (calculated p=0.9984) making it comparable or similar to the commercially available formulation Tegaderm™.

Table 7. Assessment of wound healing (Wound length in mm)

Groups	Day 1	Day 3	Day 5	Day 7	Day 11
Control Group (mm)	60 ± 0.2 (0%)	55 ± 1.1 (8.3%)	47 ± 1.2 (21.6%)	38 ± 0.2 (36.6%)	31 ± 0.1 (48.3%)
Blank Hydrogel	60 ± 0.2 (0%)	52 ± 1.8 (13.3%)	43 ± 0.2 (28.3%)	35 ± 0.2 (41.6%)	28 ± 0.1 (53.3%)
Standard (marketed) Group (mm)	60 ± 0.3 (0%)	50 ± 1.2 (16%)	41 ± 1.1 (31%)	20 ± 0.3 (66%)	1 ± 0.2 (98.3%)
Test group 1 (mm)	60 ± 0.1 (0%)	54 ± 0.2 (10%)	45 ± 1.4 (25%)	26 ± 1.1 (56%)	11 ± 0.2 (81.6%)
Test group 2 (mm)	60 ± 0.1 (0%)	53 ± 0.3 (11%)	44 ± 2.1 (26%)	25 ± 0.2 (58%)	8 ± 0.1 (86.6%)
Test group 3 (mm)	60 ± 0.2 (0%)	51 ± 0.2 (15%)	42 ± 0.1 (30%)	21 ± 0.2 (65%)	1.5 ± 0.1 (97.5%)

n=6 for each group

STATEMENT OF ETHICS

In vivo studies were approved by IAEC of L.R Institute of Pharmacy, Solan vide protocol number LRIP/IAEC/2022/PH-03.

CONFLICT OF INTEREST STATEMENT

The authors declare no conflict of interest.

AUTHOR CONTRIBUTIONS

Concept – I.D., S.A.; Design – İ.D., S.A.; Supervision – S.A., A.K.; Resource – S.A.; Materials – I.D., S.A.; Data Collection and/or Processing – I.D., S.A.,

A.K.; Analysis and/or Interpretation - I.D., S.A., A.K.; Literature Search – I.D., S.A.; Writing - I.D., S.A., A.K; Critical Reviews – S.A., A.K.

FUNDING SOURCES

The authors did not receive any funding for the study**.**

ACKNOWLEDGMENTS

The authors acknowledge the support received from L.R Institute of Pharmacy, Solan during the study.

REFERENCES

1. Reddy GK, Stehno-Bittel L, Enwemeka CS. Laser photostimulation accelerates wound healing in diabetic rats. Wound Repair Regen, 2001;9(3):248-255. Doi: 10.1046/j.1524-475x.2001.00248.x

2. Clark RAF. Fibrin and wound healing. Annals New York Academy Sci, 2006;936(1):355-367. Doi: 10.1111/j.1749-6632.2001.tb03522.x

3. Thomas LW, Diegelmann RF. Growth factors in wound healing. Clinics Dermatol, 1994;12(1):157-169. Doi: 10.1016/0738-081X(94)90266-6

4. Prockop DJ, Kari KI. Collagens: molecular biology, diseases, and potentials for therapy. Annual Rev Biochem, 1995;64(7):403-434. Doi: 10.1146/annurev.bi.64.070195.002155

5. Emeruwa AC. Antibacterial substance from *Carica papaya* fruit extract. J Natural Products, 1982;45(2):123-127. Doi: 10.1021/np50020a002

6. Singh SP, Kumar S, Mathan SV, Tomar MS, Singh RK, Verma PK, et al. Therapeutic application of *Carica papaya* leaf extract in the management of human diseases. Daru, 2020;28(2):735-744. Doi: 10.1007/s40199-020-00348-7

7. Ahmad N, Fazal H, Ayaz M, Abbasi BH, Mohammad I, Fazal L. Dengue fever treatment with *Carica papaya* leaves extracts. Asian Pac J Trop Bomed, 2011;4(1):330-333. Doi: 10.1016/S2221-1691(11)60055-5

8. Dawkins G, Hewitt H, Wint Y, Obiefuna PC, Wint B. Antibacterial effects of *Carica papaya* fruit on common wound organisms. West Indian Med J, 2003;52(4):290-292.

9. Gupta OP, Sing S, Bani S, Sharma N, Malhotra S, Gupta BD, et al. Anti-inflammatory and anti-arthritic activities of silymarin acting through inhibition of 5-lipoxygenease. Phytomedicine, 2000;7:21-24. Doi: 10.1016/S0944-7113(00)80017-3

10. Lee KY, Mooney DJ. Alginate: properties and biomedical applications. Prog Polym Sci, 2012;37(1):106-126. Doi: 10.1016/j.progpolymsci.2011.06.003

11. Koehler J, Brandl FP, Goepferich AM. Hydrogel wound dressings for bioactive treatment of acute and chronic wounds. Eur Polym J, 2018;100(3):1-11. Doi: 10.1016/j.eurpolymj.2017.12.046

12. Froelich A, Jakubowska E, Wojtyłko M, Jadach B, Gackowski M, Gadziński P, et al. Alginate-based materials loaded with nanoparticles in wound healing. Pharmaceutics, 2023;15(4):1142. Doi: 10.3390/pharmaceutics15041142

13. Lu W, Bao D, Ta F, Liu D, Zhang D, Zhang Z, et al. Multifunctional alginate hydrogel protects and heals skin defects in complex clinical situations. ACS Omega, 2020;5(28):16986-17849. Doi: 10.1021/acsomega.0c01108

14. Ishfaq B, Khan IU, Khalid SH, Asghar S. Design and evaluation of sodium alginate-based hydrogel dressings containing *Betula utilis* extract for cutaneous wound healing. Front Bioeng Biotechnol, 2023;11(1):1042077. Doi: 10.3389/fbioe.2023.1042077

15. Nayak BS, Ramdeen R, Adogwa A, Ramsubhag A, Marshall JR. Wound-healing potential of an ethanol extract of *Carica papaya* (Caricaceae) seeds. Int Wound J, 2012;9:650-655. Doi:10.1111/j.1742-481X.2011.00933.x

16. Moreira Filho RNF, Vasconcelos NF, Andrade FK, Rosa MF, Vieira RS. Papain immobilized on alginate membrane for wound dressing application. Colloids Surf B Biointerfaces, 2020;194(10):111222. Doi: 10.1016/j.colsurfb.2020.111222

17. Wijaya DP, Herlina H, Fitri NA, Mardiyanto M, Musktisusanti M, Firnando F. Preparation, characterization and wound healing activity of papaya leaves extract on spray gel. Trad Med J, 2020;25(2):105-109. Doi: 10.22146/mot.53690

18. Gul R, Jan SU, Faridullah S, Sherani S, Jahan N. Preliminary phytochemical screening, quantitative analysis of alkaloids, and antioxidant activity of crude plant extracts from *Ephedra intermedia* indigenous to Balochistan. Sci World J, 2017;5873648. Doi: 10.1155/2017/5873648

19. Madike LN, Takaidza S, Pillay M. Preliminary phytochemical screening of crude extracts from the leaves, stems, and roots of *Tulbaghia violacea*. Int J Pharmacog Phytochem Res, 2017;9(10):1300-1308. Doi: 10.25258/PHYTO.V9I10.10453

20. Harborne AJ. Phytochemical methods: a guide to modern techniques of plant analysis. London: Chapman and Hall; 1998.

21. Subashini K, Sivakami R, Jeyasankar A. Phytochemical screening and ovicidal activity of *Scutellaria violacea* (Lamiaceae) leaf extract against vector mosquitoes (Diptera: Culicidae). Int J Adv Res Biol Sci, 2017;4(3):152-158. Doi: 10.22192/ijarbs.2017.04.03.017

22. Kaushik K, Sharma RB, Sharma A, Agarwal S. formulation and evaluation of anti-fungal activity of gel of crude methanolic extract of leaves of *Ipomoea carnea* Jacq. J Res in Pharm, 2020;24(3):368-379. Doi: 10.35333/jrp.2020.159

23. Obonga WO, Omeje EO, Nnadi CO, Ocheme WG. Phytochemical evaluation of extracts and GC-MS analysis of oil from *Monodora myristica* seed. Dhaka Univers J Pharm Sci, 2019;18(1):69-73. Doi: 10.3329/dujps.v18i1.41893

24. Latif MS, Al-Harbi FF, Nawaz A, Rashid SA, Farid A, Mohaini MA, et al. Formulation and evaluation of hydrophilic polymer based methotrexate patches: *in vitro* and *in vivo* characterization. Polymers, 2022;14(7):1310. Doi: 10.3390/polym14071310

25. Gajic IMS, Savic IM, Svircev Z. Preparation and characterization of alginate hydrogels with high water-retaining capacity. Polymers, 2023;15(12):2592. Doi: 10.3390/polym15122592

26. Rhee YS, Nguyen T, Park ES, Chi SC. Formulation and biopharmaceutical evaluation of transdermal patches containing aceclofenac. Arch Pharm Res, 2013;36(5):602-607. Doi: 10.1007/s12272-013-0073-y

27. Patel R, Patel G, Baria A. Formulation and evaluation of transdermal patch of aceclofenac. Int J Drug Deliv, 2009;1(1):41-52. Doi: 10.5138/IJDD.2009.0975.0215.01005

28. Gowda DV, Rajesh N. Development and evaluation of aceclofenac loaded transdermal film. Int J Pharmatech Res, 2010;2(4):2224-2233.

29. Atta AM, El-Ghazawy RAM. Effect of chemical crosslinking on swelling parameters of modified PVA hydrogel. Int J Polymeric Mater and Biomat, 2003;52;623-636. Doi: 10.1080/00914030304905

30. Dey S, Malgope A. Preparation of carvedilol transdermal patch and the effect of propylene glycol on permeation. Int J Pharm Pharmaceutical Sci, 2010;2(1):137-143.

31. Prasetya AT, Mursiti S, Maryan S, Jati NK. Isolation and identification of active compound of papaya plants and activities as antimicrobial. IOP Conf Ser: Mater Sci Eng, 2018;349:012007. Doi: 10.1088/1757-899X/349/1/012007

32. Gong C, Wu Q, Wang Y, Zhang D, Luo F, Zhao X, et al. A biodegradable hydrogel system containing curcumin encapsulated in micelles for cutaneous wound healing. Biomaterials, 2013;34(27):6377-6387. Doi: 10.1016/j.biomaterials.2013.05.005

33. Sabat PK, Pradhan SP, Patro R. Evaluation of excisional and incisional wound healing activity of electrohomeopathic drug (spagyric essence) green electricity in rats. Int J Pharm Pharm Sci, 2020;12(10):72-75. Doi: 10.22159/ijpps.2020v12i10.38674

34. H Zhang, Cheng Zhungiu, Ao Quang. Preparation of alginate-based biomaterials and their applications in biomedicine. Mar Drugs, 2021;19(5):264. Doi: 10.3390/md19050264

35. Saarai VK, Sedlacek T, Saha P. On the development and characterisation of crosslinked sodium alginate/gelatine hydrogels. J Mech Behav Biomed Mater, 2013;18(2):152-166. Doi: 10.1016/j.jmbbm.2012.11.010

36. Aderibigbe BA, Buyana B. Alginate in wound dressings. Pharmaceutics, 2018;10(2);42. Doi: 10.3390/pharmaceutics10020042

37. Racmayani N, Husni A. Effect of different formulations on characteristics of biobased alginate edible films as biodegradable packaging. E3S Web Conf, 2020;147:03003. Doi: 10.1051/e3sconf/202014703003

38. Peppas NA, Bures P, Leobandung W, Ichikawa H. Hydrogels in pharmaceutical formulations. Eur J Pharma Biopharm, 2000;50:27-46. Doi: 10.1016/S0939-6411(00)00090-4

39. Park H. Superporous hydrogels for pharmaceutical and other applications. Drug Deliv Technol, 2002;2:38-39.

40. Nuutila K, Eriksson E. Moist wound healing with commonly available dressings. Adv Wound Care, 2021;10(12):685-698. Doi: 10.1089/wound.2020.1232

41. Kong YR, Jong YX, Balakrishnan M, Bok ZK, Weng JKK, Tay KC, et al. Beneficial role of *Carica papaya* extracts and phytochemicals on oxidative stress and related diseases: a mini review. Biology, 2021;10(4):287. Doi: 10.3390/biology10040287

42. Shafique M, Sohail M, Minhas MU, Khaliq T, Kousar M, Khan S, et al. Bio-functional hydrogel membranes loaded with chitosan nanoparticles for accelerated wound healing. Int J Biol Macromol, 2021;170(2):207-221. Doi: 10.1016/j.ijbiomac.2020.12.157

Acta Pharm. Sci. Vol 63:(2), 2025
Original article
DOI: 10.23893/1307-2080.APS6318

Neuroprotective effects of aminophylline in LPS-induced Alzheimer's disease in rat model

Hebah Majed HAMOOD[1*], Adeeb A. AL-ZUBAIDY[2]

1 Al-Nahrain University, College of Pharmacy, Department of Pharmacology, Baghdad, Iraq
2 University of Warith Al-Anbiyaa, College of Medicine, Department of Pharmacology, Karbala, Iraq

ABSTRACT

This research aimed to evaluate the aminophylline neuroprotective benefits against Alzheimer's Disease -like characteristics caused by lipopolysaccharide (LPS) in forty rats divided into four groups: control group, induction group received lipopolysaccharide single dose once a day for seven days, third group received donepezil orally once daily for 21 days and fourth groups received aminophylline once daily for 21 days, and both third and fourth group received LPS once. The Barnes Maze behavioral parameters evaluated, inflammatory cytokines, and oxidative stress indicators were measured in brain tissue samples and the results showed that primary latency and primary error for the three phases of Barnes Maze behavioral test and the levels of studied inflammatory cytokines (IL-1b, IL-6, and TNFa) in addition to malondialdehyde (MDA) were reduced significantly in aminophylline group comparing with induction group while SOD1 levels increased significantly in aminophylline group comparing with induction group which indicate that aminophylline has neuroprotective effects via antioxidant and anti-inflammatory properties.

Keywords: neuroprotective effects, aminophylline, LPS-induced Alzheimer's disease

*Corresponding author: Hebah Majed HAMOOD
E-mail: hebarafal@yahoo.com
ORCIDs:
Hebah Majed HAMOOD: 0000-0001-6210-9595
Adeeb A. AL-ZUBAIDY: 0000-0002-5207-383X
(Received 12 Dec 2023, Accepted 7 May 2024)

INTRODUCTION

Alzheimer's disease (AD) is one of the most typical degenerative neurological conditions in the world, with symptoms including decreased cognitive function, abnormal behaviour, psychiatric difficulties, and memory loss[1]. The etiology of AD is unknown, but it is linked to several pathological manifestations, including accumulation of microtubule tau protein, cholinergic neuron death, abnormal amyloid beta (Aβ), oxidative stress caused by metals, and irregular acetylcholinesterase (AChE) activity[2]. Previous research demonstrated that Neurodegeneration considered one several pathological conditions that include also inflammation and cancer that related to lipid peroxides which are highly reactive elements, that participated in accelerating the chain reaction of reactive oxygen species (ROS) formation[3]. The degradation of lipid peroxide leads to producing 4-hydroxynonenal and malondialdehyde (MDA) which are commonly used for the quantification of lipid peroxidation in the obtained tissue samples[3,4]. Catalase and Superoxide dismutase (SOD) enzymes provide the first line protection against the tissue injury which is caused by the ROSs as they have the ability to scavenge free radical along with the other nutritional antioxidants[5]. SOD protects the cell from the oxidative damage by catalyzing the conversion of superoxide into oxygen and hydrogen peroxide[6]. In the cases of SOD activity elevation, the possibility of lipid peroxidation become reduced[5] and the estimation of SOD's activity and its relation with the lipid peroxidation could help in understanding the prognosis of the neuronal damage and to provide an optimum treatment regimen[7].

Microglial cells in the brain of patients with AD showed an enhanced Inflammatory process as they become activated and produce high levels of cytokines. In early stages, microglia cells when activated become able to phagocytize Aβ, but if the activation persist for an extended period, they loss this ability and the pro inflammatory cytokines they release such as are interleukin (IL)-1, IL-1, IL-6, and tumour necrosis factor (TNF) participate in propagation of pathological tau proteins and neuron damage[8].

The current treatment for AD involves usage of cholinesterase inhibitor (rivastigmine, galantamine, and donepezil) and memantine which is considered as N-methyl-D-aspartate (NMDA) antagonists[9]. Aminophylline which is a methylxanthine derivative is considered as a competitive non-selective phosphodiesterase inhibitor that inhibits several types of the phosphodiesterase (PDE) enzyme family, mostly the PDE4 isoforms, and activates protein kinase. Also, it increases intracellular concentrations of cAMP and cGMP, inhibits the synthesis of TNF-alpha and leukotriene, and decreases inflammation and innate immunity[10].

The present research was aimed at investigating and evaluating the potential neuroprotective ability of aminophylline against AD-like characteristics caused by lipopolysaccharide in rats.

METHODOLOGY

Experimental groupings and treatments

A case-control study was conducted in the department of Pharmacology in the College of medicine, Al Nahrain University between June and December 2022 that include forty male rats (250 to 500 g in weight) of 3 to 4 months old were accommodated under standard laboratory conditions at a temperature of 20-22°C. Aminophylline vial (Radiant Pharma), lipopolysaccharide powder (LPS) (Sigma-Aldrich, USA), and donepezil (Pfizer) were dissolved in normal saline. The rats were split into four treatment groups and each group consist of ten rats as the following:

Group 1: which is consist of the control group.

Group 2 (induction group): received a dose of 250 g/kg of LPS i.p. once a day for 7 days, to induce AD-like characteristics[11].

Group 3: in this group the animals received a prophylactic oral treatment with donepezil in a dose of 0.5 mg/kg once a day[12], for 21 days, followed by LPS (250 g/kg i.p. once a day) and the same dosages of donepezil for another 7 days.

Group 4: administered prophylactic treatment with aminophylline (20 mg/kg i.p. once a day)[13], for 21 days, followed by LPS (250 g/kg i.p. once a day) and the same dosages of aminophylline for another 7 days.

After three days of treatment, a behavioural test, including cognitive testing utilizing the Barnes Maze, was performed.

Behavioural test using the Barnes Maze procedure

Barnes Maze was manufactured in Baghdad. The Barnes Maze was made up of a wood circular platform (122 cm diameter) with 21 similar and evenly spaced holes (10 cm wide) around it, one of which was connected to an escape box (35 cm x 12 cm x 12 cm), and the Maze was elevated 100 cm above the ground. Because all of the holes looked the same, the rats couldn't tell the escape hole apart from the others until they were right next to it. The buzzer positioned in the center of the Maze was to give sounds that encouraged the escape from the platform to stimulate an effective escape response. The Barnes Maze procedure was conducted in line with the method of Kuzmin et al.[14], with slight adjustments. The Barnes Maze procedure includes the following phases:

Habituation phase: To lessen anxiety, the animals had become accustomed to the platform and the escape box a day prior to the acquisition phase. This familiarization procedure was conducted without the use of a buzzer.

The acquisition phase: This phase started 24 hours following the Maze habituation phase. Three training sessions each day were included in the acquisition. Each training session lasted 180 seconds, with a 10-minute break after that, the animals were put back in the cage from which they came. Throughout the acquisition trials, the escape box and platform position were still fixed. In each experiment, the rats were placed in the platform middle, the buzzer was activated, and they were free to roam around the facility. The experiment ended 180 seconds once the animal had gotten to the escape box. Then, the hole was immediately closed for 30 seconds, and the animal was brought back to its initial cage. The animal was led there slowly and given 30 seconds to explore it if it failed to reach the escape box within 180 seconds. After each session, the outer layer of the facility and the escape box were sanitized by employing a 100% (w/v) solution of ethanol for removing smell cues. Primary errors and primary latency were captured as parameters. Primary latency was defined as the time it took the rat to make first contact with the escape box. The primary error was the number of holes that were explored before coming into contact with the escape box[14].

Probe trial: After 24 hours of acquisition, a probe trial commenced. This phase was distinguished by a duration of 90 seconds to assess spatial memory, and in this trial, the escape box was shut[15]. Therefore, the animals were permitted to look around the Maze and the escape box, and neighbouring holes. The primary errors and primary latency also were recorded.

Reversal learning: Three reversal trials were held an hour following the conclusion of the probe experiment (180 seconds for each trial). Except for the escape hole being rotated 180°, the reversal learning experiment was similar to the acquisition experiment. As a result, despite the acquired spatial clues, the animal was unable to escape the Maze and was forced to remember the new position of the hole. The primary errors and primary latency required to get to the escape box were then calculated. The animals were anesthetized by inhaling diethyl ether after completing all phases of the behavioural test[14].

Sample collection and biochemical analysis

The animals were killed, and their brains were promptly rinsed in cold phosphate-buffered saline (0.02 mol/L, pH 7.2-7.4)[16]. The right hemisphere of the brain was washed with BSP and homogenized. The homogenized tissue was

utilized to evaluate oxidative stress indices which include malondialdehyde (MDA) and superoxide dismutase 1 (SOD1) and cytokines of inflammation that include tumour necrosis factor-α (TNF-α), interleukin-1β (IL-1β), and interleukin-6 (IL-6) that estimated by using ELISA according to the manufacturer's (Elabscience) recommendations.

Statistical analysis

The data of the study are presented as mean ± standard deviation. To compare the means of two groups, the unpaired t-test was utilized, and analysis of variance (ANOVA) with a post-hoc Tukey test was employed to compare the means of three or more groups. The data were analyzed employing the Statistical Package for Social Sciences (SPSS) version 23. ($p<0.05$) or ($p\leq0.001$) were regarded as significant or highly significant, respectively[17].

RESULTS and DISCUSSION

Behavioural pattern of the experimental rats

In the results obtained in the current work, the averages for primary latency and primary error for the three phases (acquisition, probe, and reversal) were increased significantly ($p<0.001$) in the induction group in relation to the control group. On the other hand, the parameters evaluated showed to be decreased significantly ($p<0.001$) in rats receiving either donepezil or aminophylline in contrast to the induction group and these averages demonstrated values comparable to that of control group which indicated by the non-significant ($p>0.05$) different in these parameters between groups receiving either donepezil or aminophylline and those of controls as illustrated in Table 1.

Table 1. Effects of aminophylline on rats in the Barnes maze test

Group		Control	Induction (LPS)	Donepezil	Aminophylline
Acquisition Phase	Primary Latency	99.14 ± 23.86	155.72 ± 13.99##	99.33 ± 24.0**	109.48 ± 17.94**
	Primary Error	18.76 ± 4.85	28.43 ± 3.55##	18.76 ± 4.85**	17.57 ± 3.74**
Probe Phase	Primary Latency	27.0 ± 11.62	69.29 ± 23.01##	28.57 ± 11.1**	44.14 ± 18.56**
	Primary Error	7.43 ± 5.13	31.29 ± 7.87##	7.43 ± 5.13**	9.29 ± 2.69**
Reversal Phase	Primary Latency	80.05 ± 29.39	159.76 ± 10.77##	80.19 ± 29.52**	135.33 ± 12.93**
	Primary Error	10.14 ± 3.17	27.62 ± 7.56##	10.19 ± 3.18**	16.33 ± 7.27**

##: Highly statistically significant ($p\leq0.001$) compared to control group; **: Highly statistically significant ($p\leq0.001$) compared to induction LPS group.

Inflammatory cytokine levels in the experimental rats

In the induction group, TNFa, IL-6, and IL-1b levels showed to be increased significantly ($p<0.05$) in a comparison with those levels in the control group. Meanwhile, the TNFa, IL-6, and IL-1b levels were significantly ($p<0.05$) reduced in rats receiving donepezil or aminophylline when compared to the induction group. The levels of these pro-inflammatory markers in groups administered donepezil or aminophylline were non-significantly differ from those of controls as illustrated in Table 2.

Table 2. Effects of aminophylline on inflammatory cytokines

Group	Control	Induction (LPS)	Donepezil	Aminophylline
IL-1b (pg/ml)	78.26 ± 32.95	177.51 ± 64.02##	91.57 ± 36.19**	98.83 ± 22.73**
IL-6 (pg/ml)	52.47 ± 9.5	144. 23 ± 64.09##	57.02 ± 9.82**	69.27 ± 12.53**
TNF-a (pg/ml)	110.92 ± 5.71	316.10 ± 30.178##	123.75 ± 6.88**	134.44 ± 7.83**

##: Highly statistically significant ($p\leq0.001$) compared to control group; **: Highly statistically significant ($p\leq0.001$) compared to induction LPS group.

Levels of oxidative stress in experimental rats

In relation to the control group, the induction group revealed a significant increase ($p\leq0.001$) in MDA levels and a significant decrease ($p\leq0.001$) in SOD1 activity, whereas the levels of these oxidative stress markers in donepezil or aminophylline groups showed a significant decrease ($p\leq0.001$) in MDA levels with a significant increase ($p\leq0.05$) in SOD1 activity compared to the induction group as demonstrated in Table 3. It was also noticed that the levels of MDA and the activity of SOD1 in rats received donepezil or aminophylline were achieved levels somehow comparable to that of controls.

Table 3. Effects of aminophylline on oxidative stress parameters

Groups	Control	Induction (LPS)	Donepezil	Aminophylline
SOD1(ng/ml)	0.97 ± 0.13	0.70 ± 0.06##	0.83 ± 1.36**	0.81 ± 0.05**
MDA (ng/ml)	115.279 ± 83.9	241.37 ± 29##	122.17 ± 3.03**	131.96 ± 4.35**

##: Highly statistically significant ($p\leq0.001$) compared to control group; **: Highly statistically significant ($p\leq0.001$) compared to induction LPS group.

The pathogenesis of AD is complex, involving the accumulation of cerebral (beta-amyloid and hyperphosphorylated tau proteins), an inflammatory re-

sponse, and an increase in oxidative stress[18]. LPS was used to induce cognitive impairment in rats in this study because it induced memory loss and amyloidogenesis *in vivo* and *in vitro* due to systemic inflammation, by stimulating the generation and release of pro-inflammatory cytokines including TNFa, IL-6, and IL-1b[19]. Peripheral systemic infusion of LPS has been proven to cause oxidative stress as well as neuro-inflammation in the brain due to a rise in the Aβ level[20]. LPS treatment impaired both cognitive flexibility and spatial memory in the Barnes Maze test. Pre-treatment with cholinesterase inhibitors (donepezil) and aminophylline inhibited these LPS effects. Aminophylline has been demonstrated to have anti-inflammatory, anti-lipid peroxidation, and free radical scavenging characteristics[21]. Aminophylline has been reported to decrease levels of inflammatory cytokine's MDA and increase SOD in homogenized rat brains, an observation similar to the results of this study.

Many studies have shown that methyl-xanthine drugs have anti-inflammatory properties that act systemically as well as locally on airway inflammation[22,23]. By harvesting peripheral blood monocytes over 4 days, methyl-xanthine caused a progressive decrease in pro-inflammatory cytokine (TNFa, IL-8, IL-6, and IL-1) production (20% to 80%). This feature appears to be mediated by an epigenetic process that activates histone deacetylase-dependent gene switches, causing them to flip to a more anti-inflammatory phenotype. Thus, these impacts appear to be due to theophylline-induced macrophage re-direction, and other immune cells toward an anti-inflammatory state, which has been demonstrated to have a plethora of dose-dependent gene switches that regulate several cytokines[24]. As a non-selective adenosine receptor antagonist, aminophylline can antagonize adenosine receptors and inhibit the release and production of inflammatory factors by inhibiting phosphodiesterase activity[25]. Results obtained in the current study revealed that Aminophylline have a clear anti-inflammatory effect against a lipopolysaccharide (LPS)-induced inflammatory model which is consistent with recent study which demonstrated that aminophylline have reduced the permeability of the endothelial cell by down-regulating the related protein level in a lipopolysaccharide (LPS)-induced inflammatory model[26]. Aminophylline was discovered to effectively reduce lipid peroxidation in the rat brain, as evidenced by a considerable drop in MDA and pro-inflammatory cytokines generation as well as an increase in SOD activity in several parts of the rat brain, such as (cortex, cerebellum, midbrain, and basal ganglia). Aminophylline is a salt made up of two molecules of theophylline and one of ethylenediamine. Because of the ethylene diamine component, aminophylline at therapeutic concentrations is capable of antagonizing hypochlorous acid (HOCl). Some studies have found that low concentrations

of aminophylline are capable of effectively scavenging hydroxide radicals[27,28] because the anti-inflammatory and antioxidant activities of aminophylline improve cognitive flexibility spatial memory in the Barnes Maze task.

In conclusion, the findings in this study demonstrate that aminophylline enhances learning and memory in LPS-induced AD-like rats, implying that aminophylline has neuroprotective benefits via antioxidant and anti-inflammatory mechanisms.

STATEMENT OF ETHICS

The study received approval from the "Institute Review Board (IRB) of Al-Nahrain University" in October, 2022 (142/2022).

CONFLICT OF INTEREST STATEMENT

Authors declared no conflict of interest.

AUTHOR CONTRIBUTIONS

Design – AL-Zubaidy AA; Acquisition of data – Hamood HM; Analysis of data – Hamood HM; Drafting of the manuscript – Hamood HM; Critical revision of the manuscript – AL-Zubaidy AA; Statistical analysis – Hamood HM, AL-Zubaidy AA; Technical or financial support – Hamood HM, AL-Zubaidy AA; Supervision – AL-Zubaidy AA.

FUNDING SOURCES

This work was not supported or funded by any drug company.

ACKNOWLEDGMENTS

Special appreciation to College of Pharmacy Al-Nahrain University for providing services and facilities for this research.

REFERENCES

1. Knopman DS, Amieva H, Petersen RC, Chételat G, Holtzman DM, Hyman BT, et al. Alzheimer disease. Nat Rev Dis Primers, 2021;7(1):33. Doi: 10.1038/s41572-021-00269-y

2. Morroni F, Sita G, Graziosi A, Ravegnini G, Molteni R, Paladini MS, et al. PQM130, a novel feruloyl-donepezil hybrid compound, effectively ameliorates the cognitive impairments and pathology in a mouse model of Alzheimer's disease. Front Pharmacol, 2019;10:658. Doi: 10.3389/fphar.2019.00658

3. Gaschler MM, Stockwell B. Lipid peroxidation in cell death. Biochem Biophys Res Commun, 2017;482(3):419-425. Doi: 10.1016/j.bbrc.2016.10.086

4. Ayala A, Muñoz MF, Argüelles S. Lipid peroxidation: production, metabolism, and signalling mechanisms of malondialdehyde and 4-hydroxy-2-nonenal. Oxid Med Cell Longev, 2014;2014:360438. Doi: 10.1155/2014/360438

5. Abdel-Hafez HZ, Mohamed EE, Abd-Elghany AA. Tissue and blood superoxide dismutase activity and malondialdehyde level in leprosy. J Eur Acad Dermatol Venereol, 2010;24(6):704-708. Doi: 10.1111/j.1468-3083.2009.03496.x

6. Coimbra-Costa D, Alva N, Duran M, Carbonell T, Rama R. Oxidative stress and apoptosis after acute respiratory hypoxia and reoxygenation in rat brain. Redox Biol, 2017;12:216-225. Doi: 10.1016/j.redox.2017.02.014

7. Mohan S, Gobinath T, Salomy A, Nisha M, Kandasamy M, Essa MM, et al. Biophysical interaction of resveratrol with sirtuin pathway: significance in Alzheimer's disease. Front Biosci (Landmark Ed), 2018;23:1380-1390. Doi: 10.2741/4650

8. Babić Leko M, Nikolac Perković M, Klepac N, Štrac DŠ, Borovečki F, et al. IL-1β, IL-6, IL-10, and TNFα single nucleotide polymorphisms in human influence the susceptibility to Alzheimer's disease pathology. J Alzheimers Dis, 2020;75(3):1029-1047. Doi: 10.3233/JAD-200056

9. Ghumatkar PJ, Patil SP, Jain PD, Tambe RM, Sathaye S. Nootropic, neuroprotective and neurotrophic effects of phloretin in scopolamine induced amnesia in mice. Pharmacol Biochem Behav, 2015;135:182-191. Doi: 10.1016/j.pbb.2015.06.005

10. Deree J, Martins JO, Melbostad H, Loomis WH, Coimbra R. Insights into the regulation of TNF-alpha production in human mononuclear cells: the effects of non-specific phosphodiesterase inhibition. Clinics, 2008;63(3):321-328. Doi: 10.1590/s1807-59322008000300006

11. Zhu B, Wang ZG, Ding J, Liu N, Wang DM, Ding LC, et al. Chronic lipopolysaccharide exposure induces cognitive dysfunction without affecting BDNF expression in the rat hippocampus. Exp Ther Med, 2014;7(3):750-754. Doi: 10.3892/etm.2014.1479

12. Zhou Q, Nie S, Liu Z. Effect of Donepezil hydrochloride on cognitive function recovery of rats with Alzheimer's disease. Med One, 2016;1:e160023.

13. Al-Thamir SN, Oubaid EN. Protective effect of aminophylline on doxorubicin-induced cardiotoxicity in rats. Med j Babylon, 2013;10(1):219-228.

14. Kuzmin A, Liljequist S, Meis J, Chefer V, Shippenberg T, Bakalkin G. Repeated moderate-dose ethanol bouts impair cognitive function in Wistar rats. Addict Biol, 2012;17(1):132-140. Doi: 10.1111/j.1369-1600.2010.00224.x

15. Patil SS, Sunyer B, Höger H, Lubec G. Evaluation of spatial memory of C57BL/6J and CD1 mice in the Barnes maze, the Multiple T-maze and in the Morris water maze. Behav Brain Res, 2009;198(1):58-68. Doi: 10.1016/j.bbr.2008.10.029

16. Bhattacharyya D, Pandit S, Mukherjee R, Das N, Sur TK. Hepatoprotective effect of himoliv, a polyherbal formulation in rats. Indian J Physiol Pharmacol, 2003;47(4):435-440.

17. Goodman SN. P values, hypothesis tests, and likelihood: implications for epidemiology of a neglected historical debate. Am J Epidemiol, 1993;137(5):485-496. Doi: 10.1093/oxfordjournals.aje.a116700

18. Mirzaei F, Khazaei M, Komaki A, Amiri I, Jalili C. Multitarget effects of coconut oil (virgin type) on Aβ-induced Alzheimer's disease animal model. Arch Neurosci, 2019;6(2):e85715. Doi: 10.5812/ans.85715

19. Jeong YH, Park JS, Kim DH, Kang JL, Kim HS. Anti-inflammatory mechanism of lonchocarpine in LPS- or poly(I:C)-induced neuroinflammation. Pharmacol Res, 2017;119:431-442. Doi: 10.1016/j.phrs.2017.02.027

20. Ho YH, Lin YT, Wu CW, Chao YM, Chang AY, Chan JY. Peripheral inflammation increases seizure susceptibility via the induction of neuroinflammation and oxidative stress in the hippocampus. J Biomed Sci, 2015;22(1):46. Doi: 10.1186/s12929-015-0157-8

21. Barnes PJ. Theophylline: new perspectives for an old drug. Am J Respir Crit Care Med, 2003;167(6):813-818. Doi: 10.1164/rccm.200210-1142pp

22. Monteiro JP, Alves MG, Oliveira PF, Silva BM. Structure-bioactivity relationships of methylxanthines: trying to make sense of all the promises and the drawbacks. Molecules, 2016;21(8):974. Doi: 10.3390/molecules21080974

23. Janitschke D, Lauer AA, Bachmann CM, Grimm HS, Hartmann T, Grimm MOW. Methylxanthines and neurodegenerative diseases: an update. Nutrients, 2021;13(3):803. Doi: 10.3390/nu13030803

24. Allen SC, Tiwari D. Theophylline as a systemic anti-inflammatory agent: the need for its revival as a possible adjunctive treatment for 'inflammaging'. Biol Eng Med, 2019;4(1):1-3. Doi: 10.15761/BEM.1000162

25. Zhang R, Liu H, Dai D, Ding X, Wang D, Wang Y, et al. Adjunctive sepsis therapy with aminophylline (STAP): a randomized controlled trial. Chin Med J, 2022;135(23):2843-2850. Doi: 10.1097/CM9.0000000000002282

26. Chen Q, Zhou X, Hou R, Zhou Z, Wang Z, Chen Y, et al. Aminophylline modulates the permeability of endothelial cells via the Slit2-Robo4 pathway in lipopolysaccharide-induced inflammation. Exp Ther Med, 2021;22:1042. Doi: 10.3892/etm.2021.10474

27. Pal M, Datta S, Mandol M. Antioxidant property of aminophylline in rat brain. Al Ameen J Med Sci, 2015;8(1):22-27.

28. Aldafaay AAA, Abdulamir HA, Abdulhussain HA, Badry AS, Abdulsada AK. The use of urinary α-amylase level in a diagnosis of chronic renal failure. Res J Pharm Technol, 2021;14(3):1597-1600. Doi: 10.5958/0974-360X.2021.00283.3

Acta Pharm. Sci. Vol 63:(2), 2025
Original article
DOI: 10.23893/1307-2080.APS6319

Serum selenium and manganese levels in obstructive sleep apnea patients and their relationship with GPx and SOD enzyme activities

Gulbin ERDOGAN[1*], Sevda KARADAG[2], Ozlem Unay DEMIREL[3], Zerrin PELIN[4]
Hacer KUZU OKUR[5], Meral YUKSEL[6]

1 Marmara University, Faculty of Pharmacy, Analytical Chemistry Department, Istanbul, Türkiye
2 Marmara University, Institute of Health Sciences, Istanbul, Türkiye
3 Bahçeşehir University, School of Medicine, Department of Biochemistry, Istanbul, Türkiye
4 Hasan Kalyoncu University, Faculty of Health Sciences, Department of Physiotherapy and Rehabilitation, Gaziantep, Türkiye
5 Acibadem Altunizade Hospital, Chest Disease Unit, Istanbul, Türkiye
6 Marmara University, Vocational School of Health Services, Department of Medical Laboratory Techniques, Istanbul, Türkiye

ABSTRACT

Selenium and manganese are antioxidant elements, are cofactors in the functioning of enzymes. Obstructive sleep apnea (OSA) is the inability to breathe during sleep and may develop due to changes in oxidative stress, antioxidant defense system, and serum trace element levels. Therefore, we aimed to determine the antioxidant enzyme activities glutathione peroxidase (GPx), superoxide dismutase (SOD), as well as Se, Mn levels, in OSA patients (n=38) and healthy controls (n=27). Se and Mn were determined by Graphite Furnace Atomic Absorption Spectrometry (GFAAS), and GPx, SOD enzyme activities were determined by ELISA method in samples taken after polysomnography (PSG). Our results showed that Se, Mn levels in patients were significantly lower than in controls ($p<0.0001$). GPx activity in patients was lower than in controls ($p<0.01$), but serum SOD activity was lower than in healthy individuals but not significant ($p>0.05$). The results showed that the patients' Se, Mn

*Corresponding author: Gulbin ERDOGAN
E-mail: gerdogan@marmara.edu.tr
ORCIDs:
Gulbin ERDOGAN: 0000-0002-6428-5899
Ozlem Unay DEMIREL: 0000-0002-3059-9398
Zerrin PELİN: 0000-0002-8841-0068
Hacer KUZU OKUR: 0000-0002-0814-3634
Meral YUKSEL: 0000-0002-4760-3306
(Received 13 Mar 2024, Accepted 10 May 2024)

levels, as well as GPx, SOD enzyme activities, were lower than the controls. In conclusion, our study showed that low levels of Se and Mn trace elements in OSA patients are associated with decreased antioxidant enzyme activities and increased oxidative stress. These findings suggest that trace elements affect the antioxidant enzyme activities in which they act as cofactors and that their deficiencies should be eliminated with supportive treatments in OSA patients.

Keywords: selenium, manganese, glutathione peroxidase, superoxide dismutase, obstructive sleep apnea

INTRODUCTION

Trace elements, which are essential minerals at the micro and macro levels, have very important functions in the body and play a part in the synthesis and structural stabilization of nucleic acids and proteins[1]. Hence, imbalances in the optimal levels of trace elements may adversely impress biological processes and are associated with many diseases[2].

Selenium (Se) is known as an important trace element for the body; however, its high concentrations have a toxic effect on the body. Low Se concentrations in the blood can lead to heart diseases[3-4]. Epidemiological studies have shown that Se has anti-inflammatory and antioxidant effects that can protect against cardiovascular diseases and reduce cardiovascular mortality and certain types of cancer[5-6]. Se is a microelement and cofactor for many enzymes and is also a component of the glutathione peroxidase (GPx) enzyme structure, which protects the organism from oxidative damage[7]. Se protects cells by the catalytic activity of GPx from the damage caused by free radicals that formed from molecular oxygen and disrupts hydrogen peroxide (H_2O_2), and fatty acid peroxidases formed in the cells. Moreover, Se is present in kidney and liver more than in another tissues[8-9]. Se, manganese (Mn), copper, and zinc are essential trace elements in the activation of antioxidant enzymes, such as GPx and superoxide dismutase (SOD) enzymes[10]. GPx contains a Se atom in its structure. The concentration of Se in the blood is 60–100 μg L^{-1} has been reported[11].

The other microelement we studied, Mn is essential for the activity of many enzymes (hydrazines, kinases, decarboxylases, and transferases) and metalloenzymes (arginase, pyruvate carboxylase, and manganese superoxide dismutase [MnSOD]) in the body involved in normal growth, reproduction, and skeletal development through nutrients, and plays an important role in carbohydrate, amino acid, and cholesterol metabolism. Mn is present in the mitochondrial MnSOD composition, which exhibits antioxidant activity against

oxidative production. Mn has a toxic effect at high doses. It participates in lipid and carbohydrate metabolism, cell function, and the construction of cell membranes[10,12]. In people who are exposed to high levels of this metal, it can accumulate in different parts of the brain, causing neurotoxicity[13]. In an experimental study, brain cortical neurons, which are an important component of obstructive sleep apnea syndrome (OSA), were subjected to chronic intermittent hypoxia. It was determined that the cells produced excessive amounts of reactive oxygen species (ROS), whereas the antioxidant defense system, especially MnSOD, was found to elicit them. These studies demonstrate that Mn acts as a cofactor of the MnSOD enzyme. There is a linear relationship between serum Mn and SOD activity[14-16]. Among the adverse health effects that results from increased Mn absorption are central nervous system effects. Symptoms that have been observed include dyspnea, tachycardia, fever, rigidity, and Parkinsonian muscle weakness. Conversely, Mn deficiency has been suggested to be associated with osteoporosis-like decalcification in bones[17]. Normal ranges of Mn levels in body fluids are 4.0–15.0 μg L^{-1} in blood[18].

OSA is known for recurrent attacks of the upper airways and is associated with respiratory depression, repetitive sleep-stimulating outcomes, and episodic oxyhemoglobin desaturation. Sleep apnea syndrome is a risk factor for cardiovascular and cerebrovascular morbidity and mortality, as well as daytime sleepiness and loss of cognitive performance[19]. The most common complaint of this syndrome is excessive daytime sleepiness and/or snoring. These attacks, especially with the temporary cessation of breathing during sleep, have been observed to increase oxidative stress and inflammation in OSA patients[20-21]. Oxidative stress can cause lipid peroxidation, including low-density lipoprotein (LDL) oxidation[22]. Major cardiovascular diseases results accompanying OSA are hypertension, coronary artery disease, metabolic syndrome, cardiac arrhythmia, left or right-sided heart failure, pulmonary hypertension, stroke, and sudden death[19,23]. The severity of obstructive sleep apnea is indicated by the apnea–hypopnea index (AHI) and divided into certain segments. The AHI is the sum of apnea and hypopnea in a 1-h sleep and has tensile polysomnography as its gold standard. The severity of the syndrome of the AHI is as follows: AHI < 5, normal; AHI = 5–15, mild; AHI = 15–30, moderate; and AHI > 30, severe OSA[19].

Free radicals that also cause oxidative stress are high-energy, unstable compounds that contain one or more pairs of electrons in their outer atomic orbital. Organic free radicals formed during metabolic events can also be caused by external factors. They are very active and can interact with all cell components.

The organism has defensive systems that will neutralize the harmful effects of free radicals. This defense system protects the organism from the harmful effects of free radicals by keeping the rate of physiological activity neutralized by the formation of free radicals. The oxidant–antioxidant balance is provided to protect the organism from damage. Degradation of this balance leads to oxidative stress[24].

GPx, SOD, glutathione reductase, and catalase enzymes are the principal endogenous enzymatic defensive systems of whole aerobic cells. They work in this system, with some microelements acting as cofactors of these enzymes[25]. SOD enzymes are the first and most important line of antioxidant enzyme defense systems against ROS and particularly superoxide anion radicals[10]. Three distinct isoforms of SOD have been identified in mammals, two of them have copper and zinc as cofactors and are localized in the intracellular compartment. The third SOD has Mn as cofactor and is localized in the mitochondria. SOD enzymes transform superoxide into oxygen and hydrogen peroxide[12]. GPx is a selenoenzyme that converts hydrogen peroxide into the water with the element Se. Additionally, it can transform other ROS into water. The effects of the elements associated with these enzymes and acting as cofactors are shown in Figure 1.

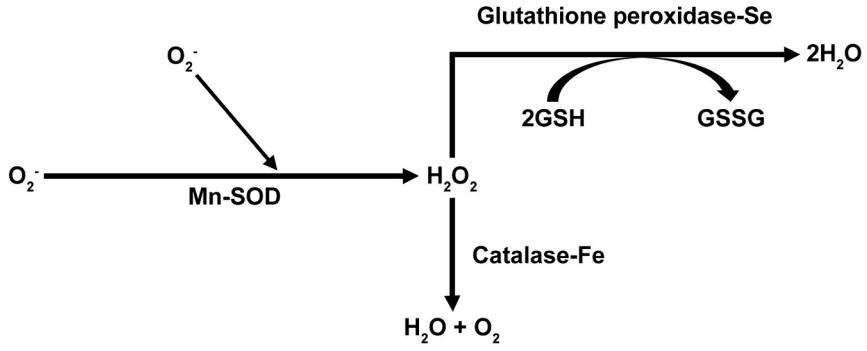

Figure 1. The kinetic mechanism of manganese superoxide dismutase (Mn-SOD) and glutathione peroxidase-Se (GPx-Se) as antioxidants

In this study we want to determine the levels of serum Se and Mn elements in OSA patients and also quantify the amounts of the antioxidant enzymes GPx and SOD, which are related to these elements. All results were detected in OSA patients, and these levels were compared with control groups.

METHODOLOGY

Study population and data collection

The present study was approved by the Marmara University, Institute of Health Sciences, Ethics Committee of Clinical Research. Blood samples were collected from OSA (n=38) patients and AHI index>5 patients who applied to the Somnus Sleep Disorders Center, Istanbul for routine examination. And healthy volunteers (n=27) were taken as controls with an AHI < 5. All people who want to take part in the study gave written inform consent to participate in the study. Subjects participating in the study underwent a polysomnography (PSG) test19-20. Overnight PSG (Somnologica, Flaga, Iceland) was performed between 11 PM and 7 AM. PSG consisted of simultaneous recordings of two channels EEG (C3 A2 and C4 A1), left and right electro-oculography, and chin electromyography from surface leads for sleep staging. In addition, air flow from a nasal cannula, thoracic and abdominal strain gauges for respiratory effort, tracheal microphone for snoring, pulse oximetry for oxyhemoglobin level, and sensor for body position during sleep were used. Respiratory data including AHI, minimum and mean oxyhemoglobin desaturations, were produced automatically by a computer program (Somnologica version 2.0.1, Flaga, Iceland). In the first hour, the blood samples were centrifuged at 3500 rpm for 10 min to separate the serum. They were aliquoted into Eppendorf tubes and stored at –80°C until analysis.

Exclusion criteria

People with Diabetes Mellitus, any kind of neurodegenerative diseases, endocrinological diseases, cancer and acute or chronic infection were excluded from the study groups.

Measurement of trace elements

To measure these concentrations of Se and Mn were measured in a graphite furnace atomic absorption spectrometer (Shimadzu, AA-6800, Japan) with an autosampler (Shimadzu, ASC-6100, Japan) and refrigerated circulator (EYELA CA1115A-1). Pyrolytic graphite platforms and furnaces were used. A background corrector (Zeeman) was used to prevent interference. Argon (99.996%) was applied as a protective gas. All reagents and standards were the analytical grades, and 0.5% (v/v) HNO_3 was used in the dilutions of standard solutions and blank.

For sample preparation, 70% nitric acid (99.999% trace metals basis) (Merck) and Triton X-100 (Merck) were used. Because of the low sample sizes and high

protein structure, the samples were studied using a palladium matrix modifier Pd $(NO_3)_2$ (10.0 g L^{-1}) in HNO_3 0.1% and TritonX-100 0.1%). Triton acts as a detergent to eliminate carbonaceous residues formed inside the graphite tube and helps in the cleaning of the autosampler capillary between sampling[25]. Standard solutions were prepared the 1000 mg L^{-1} selenium titrisol (SeO_2 in 6.3% HNO_3) and manganese titrisol standard ($MnCl_2$ in H_2O). The calibration curves were plotted at Se 196.0 nm and Mn 279.5 nm with a graphite furnace atomic absorption spectrophotometer (GFAAS) using an autosampler. GFAAS and furnace conditions are given in Table 1 and Table 2.

Table 1. Graphite furnace atomic absorption spectrophotometer instrumental parameters for Mn and Se analysis in serum samples

Parameters	Mn (II)	Se (IV)
Wavelength	279.5 nm	196.0 nm
Slit	0.2 nm	1.0 nm
Lamp current	10.0 mA	23.0 mA
Calibration mode	Absorbance, peak high	Absorbance, peak high
Background correction	Zeeman effect	Zeeman effect
Light Mode	BGC-D2	BGC-D2
Injection volume	20.0 µL	20.0 µL

Table 2. Graphite furnace atomic absorption spectrophotometer furnace conditions for Mn and Se determination in OSA patients and healthy control groups

Step	Temp°C Mn	Temp°C Se	Ramp (s)	Hold (s)	Flow (mL min^{-1})
1	150	120	5	20	1.0
2	250	250	5	10	1.0
3	600	600	5	10	1.0
4	600	600	2	3	0
5	2300	2200	1	3	0

The slope values and R values of the curves were calculated as for Se: R = 0.9990; for Mn: R = 0.9948.

Recovery and accuracy studies of trace element measurement

A recovery study was performed for these metals to better evaluate the accuracy and reliability of the results of the Se and Mn concentrations obtained from the analysis. In the absence of a reliable comparison method, recovery studies should be important[26]. Reference serum material Seronorm Serum level 1 (lot JL 4409) used for the accuracy of the developed analytical method was used. To determine the accuracy of the method for GFAAS, Se, and Mn were evaluated in a serum sample using a spike recovery test. According to the accuracy studies, it was determined whether the results met the AOAC (2002) criteria[27].

Biochemical analysis

Total lipid, total cholesterol, low-density lipoprotein (LDL) cholesterol, triglyceride, and high-density lipoprotein (HDL) cholesterol levels were determined by Abbott Architect ci8200 auto-analyzer (Abbott Park, IL, USA). GPx and SOD enzyme activities were evaluated by using enzyme-linked immunosorbent assay (ELISA) according to the manufacturer's instructions (Cayman Chemical, Ann Arbor, USA).

Statistical analysis

Statistical analysis was carried out using GraphPad InStat Software Inc. All data are expressed as the means ± SD. The student's t-test was used to evaluate the group's results; comparisons of more than two independent groups were undertaken by analysis of variance with Tukey's post hoc test. Values of $p<0.05$ were regarded as significant.

RESULTS and DISCUSSION

OSA has been increasing in the middle-aged population in recent years and is associated with obesity and heart diseases. It is known as a recurrent upper respiratory tract barrier and is a disease often accompanied by oxygen desaturations during sleep[28].

In our study we included 65 patients and 38 of them were OSA (AHI ≥ 5) whereas 27 were in the control group (AHI < 5). The age distribution was found to be in a similar range between the OSA group (41.8 ± 9.1 years) and the control group (41.0 ± 8.9 years). The AHI of OSA patients was 15.0 ± 8.0 while the oxygen desaturation index was 79.5 ± 21.2%. Patients with these findings are classified as mild to moderate OSA group. Because the healthy control group has an AHI level of 3.0 ± 2.0 and an oxygen saturation index 95.4 ± 11.2%, which were significantly different to the OSA group. The general anthropometric, PSG and biochemical results of the OSA and healthy control group are

shown in Table 3.

Table 3. Anthropometric, polysomnographic, and biochemical results in OSA and healthy control subjects

Anthropometric results	OSA group (n=38)	Control group (n=27)	P value
Age (years)	41.8 ± 9.0	41.0 ± 8.9	0.7210
Weight (kg)	91.4 ± 13.3	79.7 ± 16.6	0.0030
Size (m)	1.75 ± 7.0	1.71 ± 10.0	0.0659
BMI (kg m^{-2})	30.1 ± 4.3	27.3 ± 4.3	0.0137
Polysomnographic results			
AHI	15.0 ± 8.0	3.0 ± 2.0	<0.0001
Oxygen saturation (%)	79.5 ± 21.2	95.4 ± 11.2	<0.0001
Biochemical results			
Total lipid (mg dL^{-1})	570.2 ± 207.6	534.3 ± 126.9	0.4143
Triglycerides (mg dL^{-1})	219.3 ± 177.3	141.6 ± 74.3	0.0304
Total cholesterol (mg dL^{-1})	217.7 ± 41.8	210.0 ± 45.8	0.4765
LDL cholesterol (mg dL^{-1})	97.4 ± 23.2	137.3 ± 41.9	<0.0001
HDL cholesterol (mg dL^{-1})	35.8 ± 5.5	44.6 ± 11.0	<0.0001

BMI: Body mass index; AHI: apnea–hypopnea index; LDL: low-density lipoprotein; HDL: high-density lipoprotein.

According to the biochemical results in Table 3, when the cholesterol levels of the samples were examined, it was found that weight, total lipid, triglycerides, and total cholesterol levels were higher in OSA patients compared to the control group. LDL and high-density lipoprotein (HDL) cholesterol were found to be significantly lower than the control groups. According to the polysomnographic results, the AHI index was found to be significantly higher than the results obtained in patients with OSA, and the oxygen saturation (%) was lower compared to the control group. Abnormalities in lipid metabolism are very commonly observed in patients who are obese. As shown on Table 3 BMI and weight of the OSA patients are significantly higher than the control group, which confirms the data. A reduction in LDL-cholesterol level and a higher HDL-cholesterol level in OSA patients with respect to the control group show

that these patients use medications against hypercholesterolemia[19].

The serum Se concentration in OSA patients were 35.06 ± 10.12 μg L^{-1} and in control subjects 59.73 ± 8.98 μg L^{-1}, $p<0.0001$. Additionally, the Mn levels in serum samples of OSA patients were 7.09 ± 2.33 μg L^{-1} and 19.85 ± 9.14 μg L^{-1} in control, $p<0.0001$ (Figure 2).

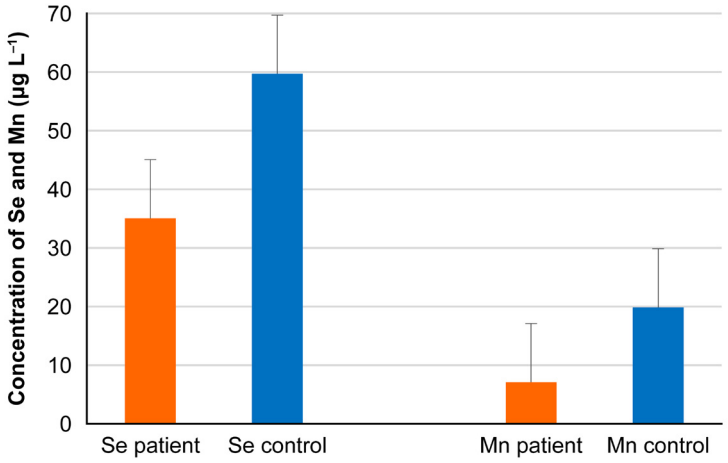

Figure 2. Serum Se and Mn values in OSA and control groups. The significance between OSA patients and control groups were $p<0.0001$ for both parameters.

The recovery results obtained in the serum sample for 13.00 mg L^{-1} Se, 24.00 mg L^{-1} Se, 1.00 mg L^{-1} Mn, and 2.00 mg L^{-1} Mn were 91.30%, 98.10%, 95.38%, and 101.5%, respectively. According to the accuracy studies, the results were found to be appropriate because recoveries were within the range proposed by AOAC (2002) (70%–125%) upon the concentration series studied[27]. These findings demonstrate that the Se and Mn levels measured in our study are accurate and valid.

The major antioxidant enzymes -GPx and SOD- found in mammalian cells are thought to be essential for life in all cells that metabolize oxygen. As shown in Table 4 the GPx activity in OSA patients and healthy control groups were 27.30 ± 11.70 U mL^{-1} vs. 34.90 ± 13.70 U mL^{-1}, respectively. The minimum and maximum levels were 5.09 U mL^{-1} and 71.30 U mL^{-1} in OSA patients and 15.28 U mL^{-1} and 81.49 U mL^{-1} in control subjects. There was a significant change between the groups ($p<0.01$). The mean serum SOD activity in patients with OSA were found to be 2.62 ± 1.83 U mL^{-1} and 3.03 ± 1.71 U mL^{-1} in the control group. The minimum and maximum levels were changed between 0.30 U mL^{-1} and 9.00 U mL^{-1} in OSA patients and 1.00 U mL^{-1} and 7.60 U mL^{-1} in control

subjects. The meaningfulness between the groups was not significant (p>0.10)

Table 4. Statistical evaluation of serum GPx and SOD activities in OSA patients and healthy control subjects

Statistical data	GPx Activity		SOD Activity	
	OSA group (n=38)	Control group (n=27)	OSA group (n=38)	Control group (n=27)
Mean (U mL^{-1})	27.30	34.90	2.62	3.03
Standard deviation (SD)	± 11.70	± 13.70	± 1.83	± 1.71
Standard error the mean (SEM)	1.90	2.50	0.30	0.32
Minimum (U mL^{-1})	5.09	15.28	0.30	1.00
Medium (U mL^{-1})	25.47	30.59	2.35	2.30
Maximum (U mL^{-1})	71.30	81.49	9.00	7.60
P value	p<0.01		p>0.10	

Se is one of the most important elements of our study and the GPx enzyme is an important part of our body and shows an antioxidant property. The low level of Se paralleled with decreased activity of GPx enzyme. In a study of moderate and severe OSA patients, GPx and SOD activities were found to be in parallel with our study. In this study serum zinc and erythrocyte Se levels were low, and serum Cu and Fe levels were high determined in OSA patients[29]. These studies strengthen our hypothesis and demonstrate that serum or erythrocyte trace element levels can alter antioxidant enzyme activities[29-30].

Studies have reported that Se detoxifies heavy metal ions such as mercury and Mn in the human body and protects the nervous system by reducing ROS production. OSA causes sleep hypoxia and low GPx and SOD activities in humans. The apnea/apnea index of OSA is negatively correlated with the amount of Se in red blood cells, suggesting that low Se levels increase OSA severity[29]. Se has different roles in different diseases[6,8-9]. Studies show that evaluation of Se levels in humans, low levels of Se can significantly trigger the disease, and the addition of Se to daily diet helps prevent and to treat the disease[31].

Compared with the literature, the results were found to be compatible. According to the data obtained from our experimental studies GPx and SOD enzyme activities were also found to be decreased in the OSA patients, related to the low levels of Se and Mn levels,

which act as cofactors in enzyme systems in the participants. This can be considered one of the reasons for the emergence of OSA. Here in, it can be said that the possibility of low activities of enzymes is expected due to low Se and Mn amounts. In a study with cell culture and transgenic mice, overexpression of MnSOD was shown to reduce chronic intermittent hypoxia (CIH)-mediated cortical neuronal apoptosis. Together, data from in-vitro and in-vivo experiments have shown that CIH-mediated mitochondrial oxidative stress can play an important role in neuronal cell loss and neurocognitive dysfunction in OSA. Therefore, therapeutic strategies aimed at reducing ROS from mitochondria may increase neurobehavioral morbidity in OSA[14].

Research has revealed the role of trace elements, particularly Se and Mn, and the antioxidant defense system in combating OSA. Se and Mn trace elements have a fundamental importance for human life[1]. Recent studies show that essential elements may be associated with various diseases and immune system diseases[2].

Acute decompensated heart failure is a common cause of acute respiratory failure. When the studies conducted were examined, it was found in the articles that there was a relationship between acute decompensated heart failure and antioxidant enzyme levels. It has been observed that oxidative stress increases heart failure and is closely related to mortality[32]. Studies conducted to elucidate the effects of Se, and the antioxidant system have reported that Se decreases ROS production and increases the level and activity of antioxidant enzymes, such as GPx and thioredoxin reductase[30]. GPx, which contains four Se atoms in its structure, and is responsible for the removal of hydroperoxides formed in cells, is known as a selenoenzyme that protects cells against damage. Se deficiency causes a decrease in GPx activity[6]. The inverse correlation between serum Se and C-reactive protein (CRP) suggests that low amounts of Se may be associated with oxidative stress leading to lipid peroxidation. The existing literature has a few studies investigating the pathophysiological role of Se and selenoenzymes in OSA. The inverse correlation between serum Se and CRP suggests that low amounts of Se may be associated with oxidative stress leading to lipid peroxidation[33]. It has been demonstrated that serum GPx concentrations are lower in individuals with OSA and are inversely correlated with average oxygen saturation and directly correlated with AHI[20,22,34]. A study by Chen and colleagues with OSA patients showed lower levels of antioxidant enzyme activity and lower erythrocyte Se concentrations in erythrocyte GPx levels compared with OSA patients and control groups. Erythrocyte Se levels showed a large reverse correlation with the AHI ratio. In other words, when the AHI is high, the Se concentration was found to be low[29].

Vitamins A, C, and E and minerals are essential microelements that act as antioxidants to protect lipids, proteins, nucleic acids, and other important biomolecules against oxidative stress damage[24]. Their antioxidant properties

are related to their ability to donate electrons. Se is present as selenoproteins, which are important in many reactions, such as the formation of thyroid hormones and antioxidant defense[8]. In particular, the slow metabolism in the elderly slows the transition to blood in essential elements such as vitamins and minerals[2]. Additionally, respiratory events are slowing due to various diseases, such as heart diseases, lung diseases, and deformation in the upper respiratory tract. This prevents the passage of oxygen from the lungs to the blood, thereby reducing the enzymes and activities involved in the blood composition. As seen from the studies done, air, water, nutrient support, and balanced nutrition are needed for human metabolism to work properly and healthy[35]. Mineral entry into the human body should be achieved through the regular and balanced feeding of the people. Furthermore, activities such as sports and hiking, which are necessary for regular metabolism, are diminished in elderly individuals. Moreover, with the development of technology, people are constantly being in a still position for a long time[35]. Consequently, various illnesses arise at early ages with various side effects. Considering that OSA is not treated and followed correctly for human life, it is very important, and its treatment is necessary. Therefore, although the roles of Se and Mn in different diseases are still different, low levels of these elements significantly induce disease and may help prevent and treat disease when supplemented. Considering that OSA is not treated and followed correctly for human life, it should be considered that it is very important, and its treatment should be done. Although ventilators are provided in hospitals, it should be considered that the application of supportive treatment containing Se and Mn under the control of a doctor may contribute to recovery. It has been suggested that an increase in the intake of antioxidant-rich foods and supplements may lead to less exposure to free radicals, thereby minimizing health problems[35].

In conclusion, we found that Se and Mn levels in OSA patients decreased in parallel with GPx and SOD activities compared to the control group, the antioxidant defense systems of the patients were weakened, and oxidative stress became clear. These results show that patients with OSA have a weakened antioxidant defense system due to increased oxidative stress due to decreased SOD and GPx enzyme activities synthesized due to Se and Mn. Se and Mn, which are essential elements, play an important role in the synthesis of ROS by binding to the structures of SOD and GPx, which act as antioxidant enzymes in our body. Since ROS are harmful species that should not be produced in our body, in the management of patients with OSA, Se and Mn containing antioxidant food or antioxidant food supplements can be used as complementary treatments to prevent complications and other serious diseases. There have not been illuminating

studies on the roles of Se and Mn in the progression of OSA and various related cardiovascular comorbidities, and more research is needed on this subject.

STATEMENT OF ETHICS

This study was approved by the Marmara University, Institute of Health Sciences, Ethics Committee of Clinical Research (Project No:16.11.2012-16).

CONFLICT OF INTEREST STATEMENT

The authors declare that they have no conflict of interest.

AUTHOR CONTRIBUTIONS

Concept – G.E., S.K.; Design – G.E., S.K., M.Y.; Supervision – G.E., M.Y.; Resources G.E., S.K., M.Y.; Materials – G.E., M.Y., O.U.D., Z.P., H.K.O.; Data Collection and/or Processing – S.K., G.E., M.Y.; Analysis and/or Interpretation – G.E., S.K., M.Y.; Literature Search – S.K.; Technical or Financial Support– Marmara University BAPKO; Writing – S.K.; Critical Reviews and Supervisions – G.E., M.Y.

FUNDING SOURCES

This study was supported by the Marmara University, Scientific Research Projects Commission (Project No: SAG-C-YLP-100413-0113).

ACKNOWLEDGMENTS

We would like to thank the Marmara University Scientific Research Projects Commission Chair for their support for the thesis.

REFERENCES

1. Quintaes KD, Diez-Garcia RW. The importance of minerals in the human diet. In: de la Guardia M, Garrigues S, editors. Handbook of mineral elements in food. [Internet]. Wiley-Blackwell; 2015. Available from: https://doi.org/10.1002/9781118654316.ch1 [Accessed Date: 2024 Mar 13].

2. Prashanth L, Kattapagari KK, Chitturi RT, Baddam VRR, Prasad LK. Review on role of essential trace elements in health and disease. J NTR Univ Health Sci, 2015;4:75-85. Doi: 10.4103/2277-8632.158577

3. Wojewoda M, Duszyński J, Szczepanowska J. Antioxidant defence systems and generation of reactive oxygen species in osteosarcoma cells with defective mitochondria: effect of selenium, Biochim Biophys Act, 2010;1797:890-896. Doi: 10.1016/j.bbabio.2010.01.035

4. Nève, J. Selenium as a risk factor for cardiovascular diseases. J Cardiovasc Risk, 1996;3:42-47. Doi: 10.1097/00043798-199602000-00006

5. Beaglehole R, Jackson R, Watkinson J, Scragg R, Yee RL. Decreased blood selenium and risk of myocardial infarction. Int J Epidemiol, 1990;19:918-922 Doi: 10.1093/ije/19.4.918

6. Steinbrenner H, Sies H. Protection against reactive oxygen species by selenoproteins. Biochim Biophys Acta, 2009;1790(11):1478-1485. Doi: 10.1016/j.bbagen.2009.02.014

7. Reunanen A, Knekt P, Marniemi J. Serum calcium, magnesium, copper and zinc and risk of cardiovascular death. Eur J Clin Nutr, 1996;50:431-437.

8. Avery JC, Hoffmann PR. Selenium, selenoproteins, and immunity. Nutrients, 2018;10:1-20. Doi: 10.3390/nu10091203

9. Barrett CW, Short SP, Williams CS. Selenoproteins and oxidative stress-induced inflammatory tumorigenesis in the gut. Cell Mol Life Sci, 2017;74:607-616. Doi: 10.1007/s00018-016-2339-2

10. Zelko IN, Mariani TJ, Folz RJ. Superoxide dismutase multigene family: a comparison of the CuZn-SOD (SOD1), Mn-SOD (SOD2), and EC-SOD (SOD3) gene structures, evolution, and expression. Free Radic Biol Med, 2002;33(3):337-349. Doi: 10.1016/s0891-5849(02)00905-x

11. Dennouni-Medjati ND, Harek Y, Tarik A, Lahcene L. Whole blood selenium levels in healthy adults from the west of Algeria. Biol Trace Elem Res, 2012;147:44-48. Doi: 10.1007/s12011-011-9287-3

12. Islam MN, Rauf A, Fahad FI, Emran TB, Mitra S, Olatunde A, et al. Superoxide dismutase: an updated review on its health benefits and industrial applications. Crit Rev Food Sci Nutr, 2022;62(26):7282-7300. Doi: 10.1080/10408398.2021.1913400

13. Taylor MD, Erikson KM, Dobson AW, Fitsanakis VA, Dorman D, Aschner M. Effects of inhaled manganese on biomarkers of oxidative stress in the rat brain. Neuro Toxicology, 2006;27:788-797. Doi: 10.1016/j.neuro.2006.05.006

14. Shan X, Chi L, Ke Y. Manganese superoxide dismutase protects mouse cortical neurons from chronic intermittent hypoxia-mediated oxidative damage. Neurobiol Dis, 2007;28:206-215. Doi: 10.1016/j.nbd.2007.07.013

15. Farina M, Avila DS, da Rocha JBT, Aschner, M. Metals, oxidative stress and neurodegeneration: a focus on iron, manganese and mercury. Neurochem Int, 2013;62:575-594. Doi: 10.1016/j.neuint.2012.12.006

16. Smith MR, Fernandes J, Go YM, Jones DP. Redox dynamics of manganese as a mitochondrial life-death switch. Biochem Biophys Res Commun, 2017;482:388-398. Doi: 10.1016/j.bbrc.2016.10.126

17. O'Neal SL, Zheng W. Manganese toxicity upon overexposure: a decade in review. Curr Environ Health Rep, 2015;2:315-328. Doi: 10.1007/s40572-015-0056-x

18. Agency for Toxic Substances and Disease Registry (ATSDR). Toxicological profile for manganese. Atlanta (GA): U.S. Department of Health and Human Services, Public Health Service; 2012. Accessed July 12, 2022. Available from: https://www.atsdr.cdc.gov/toxprofiles/tp151.pdf

19. Andrisani G, Andrisani G. Sleep apnea pathophysiology. Sleep Breath, 2023;27(6):2111-2122. Doi: 10.1007/s11325-023-02783-7

20. Yüksel M, Okur HK, Pelin Z, Ogunc, AV, Ozturk L. Arginase activity and nitric oxide levels in patients with obstructive sleep apnea syndrome. Clinics, 2014;69:247-252. Doi: 10.6061/clinics/2014(04)05

21. Mancuso M, Bonanni E, LoGerfo A, Orsucci D, Maestri M, Chico L, et al. Oxidative stress biomarkers in patients with untreated obstructive sleep apnea syndrome. Sleep Med, 2012;13:632-636. Doi: 10.1016/j.sleep.2011.10.030

22. Okur HK, Pelin Z, Yuksel M, Yosunkaya, S. Lipid peroxidation and paraoxonase activity in nocturnal cyclic and sustained intermittent hypoxia. Sleep and Breath, 2013;17:365-371. Doi: 10.1007/s11325-012-0703-5

23. Atılgan ZA, Abakay A, Ülgen S. Obstructive sleep apnea syndrome and cardiovascular problems. Dicle Med J, 2011;38(2):253-256. Doi: 10.5798/diclemedj.0921.2011.02. 007

24. Meliante PG, Zoccali F, Cascone F, Di Stefano V, Greco A, de Vincentiis M, et al. Molecular pathology, oxidative stress, and biomarkers in obstructive sleep apnea. Int J Mol Sci, 2023; 13;24(6):5478. Doi: 10.3390/ijms24065478

25. Kuppusamy UR, Dharmani M, Kanthimathi MS. Antioxidant enzyme activities of human peripheral blood mononuclear cells exposed to trace elements. Biol Trace Elem Res, 2005; 106:29-40. Doi: 10.1385/BTER:106:1:029

26. Westgard JO. Basic method validation: training in analytical quality management for healthcare laboratories. 3rd ed. Madison: Westgard Quality Corporation; 2008.

27. AOAC (Association of Official Analytical Chemists). Guidelines for single laboratory validation of chemical methods for dietary supplements and botanicals. 1st ed. Gaithersburg (MD): AOAC International; 2002 [cited 2024 Mar 13]. Available from: [https://s27415.pcdn.co/wp-content/uploads/2020/01/64ER20-7/Validation_Methods/d-AOAC_Guidelines_For_Single_Laboratory_Validation_Dietary_Supplements_and_Botanicals.pdf]

28. Hopps E, Caimi G. Obstructive sleep apnea syndrome: links between pathophysiology and cardiovascular complications. Clin Invest Med, 2015;38:362. Doi: 10.25011/cim.v38i6.26199

29. Chen PC, Guo CH, Tseng CJ, Wang KC, Liu PJ. Blood trace minerals concentrations and oxidative stress in patients with obstructive sleep apnea. J Nutr Health Aging, 2013;17:639-644. Doi: 10.1007/s12603-013-0023-x

30. Guo Q, Wang Y, Li QY. Levels of thioredoxin are related to the severity of obstructive sleep apnea: based on oxidative stress concept. Sleep Breath, 2013;17:311–316. Doi: 10.1007/s11325-012-0692-4

31. Albuquerque R G, Hirotsu C, Tufik S. Why Should we care about selenium in obstructive sleep apnea? J Clin Sleep Med, 2017;13:931-932. Doi: 10.5664/jcsm.6674

32. Ulaş T, Büyükhatipoğlu H, Sezen Y. The effect of acute decompansated hearth failure treatment on oxidative stress. J Clin Exp Investig, 2011;2:267-272. Doi: 10.5799/ahinjs.01.2011.03.0052

33. Molnar J, Garamvolgyi Z, Herold M. Serum selenium concentrations correlate significantly with inflammatory biomarker high-sensitive crp levels in hungarian gestational diabetic and healthy pregnant women at mid-pregnancy. Biol Trace Elem Res, 2008;121:16-22. Doi: 10.1007/s12011-007-8018-2

34. Asker S, Asker M, Sarikaya E. Oxidative stress parameters and their correlation with clinical, metabolic and polysomnographic parameters in severe obstructive sleep apnea syndrome. Int J Clin Exp Med, 2015;8:11449-11455.

35. Mehri A. Trace elements in human nutrition (II) - an update. Int J Prev Med, 2020;11:2. Doi: 10.4103/ijpvm.IJPVM_48_19

Acta Pharm. Sci. Vol 63:(2), 2025
Original article
DOI: 10.23893/1307-2080.APS6320

DFT, molecular docking, and ADMET prediction of compounds from *Cinnamomum zeylanicum* for dengue inhibitor DEN2 NS2B/NS3 serine protease

Neni FRIMAYANTI*, Mustika FURI, Indriani SYAFITRI

University of Malaya, Department of Pharmacy, Pekanbaru, Indonesia

ABSTRACT

Dengue, an infectious disease transmitted by *Aedes aegypti* and *Aedes albopictus* mosquitoes, is caused by a virus. This study aimed to assess whether compounds isolated from cinnamon (*Cinnamomum zeylanicum*) possess antidengue properties and whether the bonds formed after docking these compounds are stable. Three compounds from the NADI database were chosen as samples, with panduratin A serving as the positive control. Molecular docking simulations were conducted alongside density functional theory (DFT) studies using Gauss View 5. The docking results indicated that delta-Cadinene (compound **3**) exhibited the lowest binding free energy of -4.93 kcal/mol, with a binding factor of 9. According to density functional theory (DFT) calculations, panduratin A, and compound **3** displayed gap values of -0.26 and -0.24, respectively. Thus, compound **3** demonstrates potential as a highly stable inhibitor of dengue DEN2 NS2B/NS3 serine protease.

Keywords: *Cinnamomum zeylanicum,* dengue, DFT, docking, ADMET

*Corresponding author: Neni FRIMAYANTI
Email: nenifrimayanti@gmail.com
ORCIDs:
Neni FRIMAYANTI: 0000-0003-2369-6787
Mustika FURI: 0000-0002-4065-2068
Indriani SYAFITRI: 0009-0001-6415-4346
(Received 14 Nov 2023, Accepted 28 May 2024)

INTRODUCTION

Dengue virus is a positive single-stranded RNA virus transmitted through mosquito bites from the Flaviviridae family of the genus Flavivirus[1]. Dengue virus is transmitted through the saliva of infected mosquitoes[2]. Viruses use host cell ribosomes for the translation of genomic RNA into polyproteins. The translation of genomic RNA into polyproteins forms structural and non-structural proteins[3]. NS2B and NS3 proteins are attractive targets for new antiviral therapies. The N-terminal NS3 with its cofactor NS2B is a protease that can cleave the polyprotein in the virus. NS2B/NS3 functions as a link to the flavivirus replication complex and modulates viral pathogenesis and the host immune response[4]. NS3 activity depends on its cofactor NS2B (47 amino acids) in forming the NS2B/NS3 complex[5]. Disturbances in NS2B and NS3 inhibit viral replication[6].

Drug discovery is a time-consuming and expensive process. Molecular docking is a computational procedure used to predict the chemical bonding between a protein (receptor) and small molecule (ligand) in order to form a stable complex. it aims to predict the complex intermolecular structures formed between two or more molecular constituents, which can ultimately be used to predict the binding affinities of two molecules[7,8]. Another computational method that can be employed is the density functional theory (DFT) method. DFT is a useful approach for solving the Schrödinger equation in systems with multiple particles. The underlying principle of this method is that the energy of a molecule can be determined based on its electron density. Unlike traditional methods, DFT does not treat electrons as discrete entities. But rather calculates results based on the electron density. This method is convenient because it can produce results that are comparable to experimental data without requiring a significant amount of time.

Cinnamon (*Cinnamomum zeylanicum*), a tropical plant, is renowned for its culinary use and associated health benefits[9]. Its leaves and bark are commonly used as flavourings and cooking seasonings. Notably, cinnamon essential oil, derived from this plant, contains key compounds such as cinnamaldehyde (60.72%), eugenol (17.62%), and coumarin (13.39%)[10]. Research suggests that cinnamon essential oil can serve as an effective repellent against *Aedes aegypti* mosquitoes, which transmit diseases such as dengue fever. The strong aroma of essential oils is unappealing to mosquitoes, prompting them to avoid areas where such scents are present, thereby reducing the risk of mosquito-borne illnesses.

This study involved acquiring compounds from the NADI database which is a repository of natural products. Three similar compounds (cadalene, cadina-1(2), 4-diene, and delta cadinene) sourced from *Cinnamomum zeylanicum* were selected for computational analysis. Similar compounds in this context are chemical compounds with comparable structural or functional characteristics that potentially influence their biological activities or chemical behaviors[10]. These compounds were chosen for their similarity in terms of chemical composition or properties, facilitating comparative analysis in this study. These compounds were subjected to docking simulations to assess their potential bioactivity. In addition, their drug-likeness was evaluated to predict their pharmacokinetic properties as potential drugs. Furthermore, density functional theory (DFT) calculations were performed on these compounds to ascertain their efficacy as inhibitors against dengue DEN2 NS2B/NS3 viruses. To date, although there has been research on the discovery of new dengue inhibitors using *in silico* tools, it has not been extensively studied. Thus, the primary aim of this research was to identify novel inhibitors derived from *Cinnamomum zeylanicum* that target the NS2B/NS3 serine protease against the dengue virus.

METHODOLOGY

Molecular docking

The structure of the isolated compound from *Cinnamomum zeylanicum* is accessible through http://www.nadi-discovery.com. Three similar compounds were selected as the ligands. Chemdraw Professional 15.0, was used to sketch the molecular structures of the ligands, and Panduratin A was used as a positive control. The 3D structure was then prepared using the Molecular Operating Environment (MOE) 2022.0901 software package with an MMFF94x force field and 0.0001 gradient. Figure 1 shows the molecular structure of the ligands.

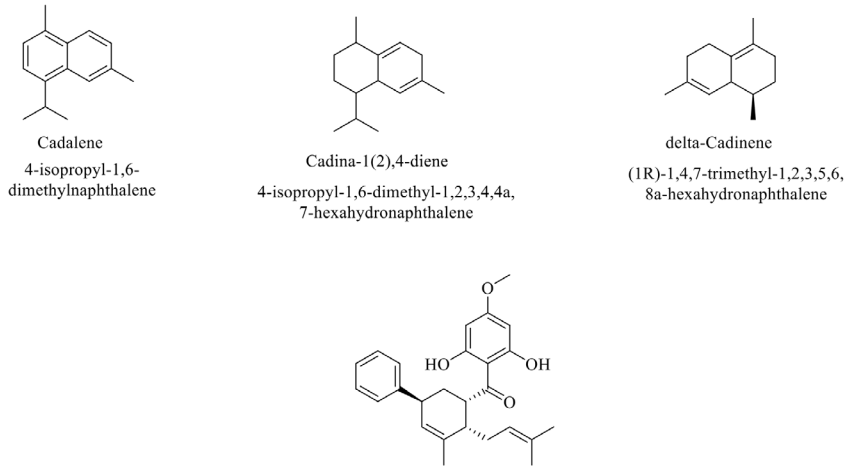

Figure 1. Molecular structure of ligands

The protein structure was obtained from the https://www.rcsb.org/ website, identified by the PDB code 2FOM. The crystallographic representation of this protein was generated using MOE 2022.0901 and DSV 2020 (Biovia). Chains A and B constitute two chains that form the 2FOM protein. Water molecules, natural ligands, and Cl^- ions associated with the protein were excluded. The molecular arrangement of the protein was established using the MOE 2022.0901 software package. The construction of the protein involved setting the parameter, specifically the root mean square (RMS) gradient, to 0.01 kcal/mol/A, employing CHARMM27 as the force field. Energy minimization was applied to alpha the carbon, H, and backbone atoms[11]. Following this, the constructed structure was saved in the PDB format to facilitate its later use as a docking receptor.

A site finder was used to identify the protein's active site prior to docking. Leu128, Asp129, Phe130, Ser131, Pro132, Ser135, Tyr150, Gly151, and Gly153 composed site whereas His51, Lys74, Asp75, Gly151, Asn152, Gly153, and Val154 composed site 13. Site 13 was established as a dummy atom to serve as the docking target site. Subsequently, the ligand structure, contained within an MDB file, was selected as the ligand, and the site was configured in the docking menu to function as a dummy atom. Following this, the refinement parameters were adjusted to rigid, the posture to 50 and 10, and the placement set to triangle visualization. Optimal docking sites, demonstrating similar binding interactions to the positive control, were identified based on several criteria, including binding free energy, root mean square deviation (RMSD), and binding factor.

Density functional theory

The Gaussian software was employed for molecular simulations. Density functional theory (DFT) was utilized to optimize the molecular geometry of each molecule in the gas phase. All quantum chemical calculations were conducted at the B3LYP level using the 6-31G basis set.

Drug-likeness and ADMET properties

SwissADME, an online tool developed by the Swiss Institute of Bioinformatics and accessible at http://www.swissadme.ch, was used for *in silico* ADME screening and drug-likeness assessment[12]. This screening process targeted compounds with high binding free energy scores. Various physical and chemical parameters such as atom counts, polar surface area (PSA), molecular weight (MW) and molecular refractivity (MR), were calculated. The drug-likeness of candidates was evaluated using the Rules of 5 (RO5) criteria established by many scientists. Abbot Bioavailability scores, based on the total charge, TPSA, and compliance with Lipinski's filter, were computed to predict the likelihood of at least 10% oral bioavailability for a given chemical. Lipophilicity was assessed using the iLOGP, XLOGP3, WLOGP, MLOGP, and SILICOS-IT models, and a consensus log Po/w[12] was derived. The solubility (log S) of the selected ligands was determined using three alternative models: ESOL[13], Ali[14], and SILICOS-IT[12].

RESULTS and DISCUSSION

Molecular docking

Molecular docking is a computational method employed to predict the interaction between a macromolecule (receptor) and small molecule (ligand) by simulating their chemical bonding based on their structures[15]. This technique is crucial in drug design as it enables the prediction of how small drug molecules bind to target proteins and facilitates the estimation of free binding energy and molecular activity[16].

Through molecular docking, various parameters were derived, including root mean square deviation (RMSD) and binding free energy (ΔG) measured in kcal/mol. The binding free energy signifies the energy required for a ligand to bind to a protein, where smaller values indicate a more stable association between the ligand and the protein[17]. RMSD values, on the other hand, indicate discrepancies or errors in docking. Lower RMSD values suggest smaller deviations or errors during the docking process. The selection of the best ligand-protein complex poses was based on the combination of the lowest binding free energy and RMSD values. Additionally, Van der Waals interactions and

hydrogen bonding were considered as supportive parameters to evaluate the stability of the ligand in relation to the receptor[16].

Based on the docking results presented in Table 1, panduratin A was used as a positive control, it showed a binding free energy of -6.8354 kcal/mol and an RMSD of 0.8704. Panduratin A forms Van der Waals interactions with the amino acid residue Asp75, which facilitates its binding to other amino acids. Moreover, panduratin A interacts with amino acid residues including Tyr161, Gly 53, His51, Pro132, Asn152, Ser131, Leu128, Tyr150, Phe130, Ser135, and Gly151. The spatial arrangement of panduratin A the protein can be seen in Figure 2.

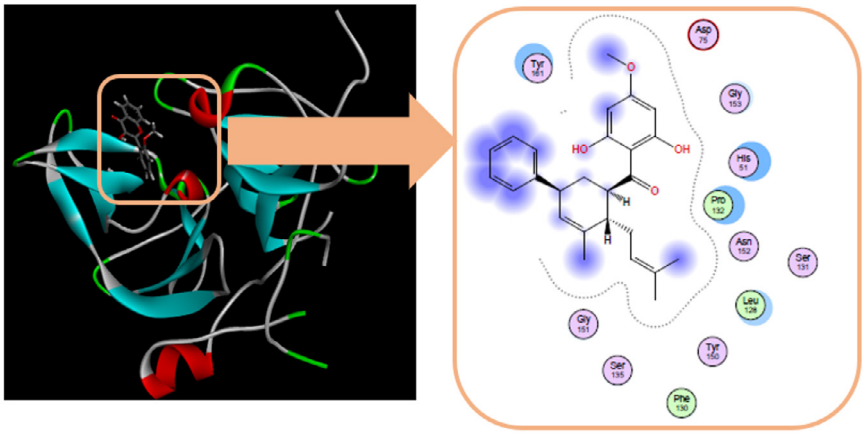

Figure 2. Spatial arrangement of the binding site for panduratin A as positive control

Table 1. Docking results

Compounds	Binding free energy (kcal/mol)	RMSD	Hydrogen bond	Hydrophobic interaction	Van der Waals interaction	Another interaction	Binding factor
Panduratin A	-6.83	0.87	-	-	Asp75	Tyr161, Gly153, His51, Pro132, Asn152, Ser131, Leu128, Tyr150, Phe130, Ser135, Gly151	12
1	-4.62	0.79	-	Arg54	**Asp75**	Trp50, Val72, **His51, Gly151, Asn152, Gly153, Tyr161**	6
2	-4.34	0.58	Tyr161	Arg54	**Asp75**	Val72, Trp50, **His51, Gly153**	3
3	-4.93	1.29	Tyr161, His51	-	-	**Ser135, Ser131, Gly153, Gly151, Pro132, Asn152, Tyr150, Phe130, Leu128**	9

Based on the docking data for compound **1**, an RMSD value of 0.79 and a binding free energy of -4.62 kcal/mol bind through Arg54, Asp75, Trp50, Val72, His51, Gly151, As152, Gly153, and Tyr161. Upon visualization, interactions were observed between compound **1** and the amino acid residues Arg54 and Asp75 through hydrophobic and Van der Waals bonds, respectively. Additionally, other interactions were observed between compound 1 and the amino acid residues Trp50, Val72, His51, Gly151, Asn152, Gly153, and Tyr161.

Superimposition analysis of compound 1 with a positive control (panduratin A) showed that compound **1** did not bind to the active site. The size of compound **1** is not able to penetrate deeply into the cavity of the NS2B/NS3 serine protease active site. Therefore, compound **1** cannot be classified as a potential inhibitor of NS2B or NS3. The spatial arrangement of compound **1** and its superimposition with panduratin A is shown in Figure 3.

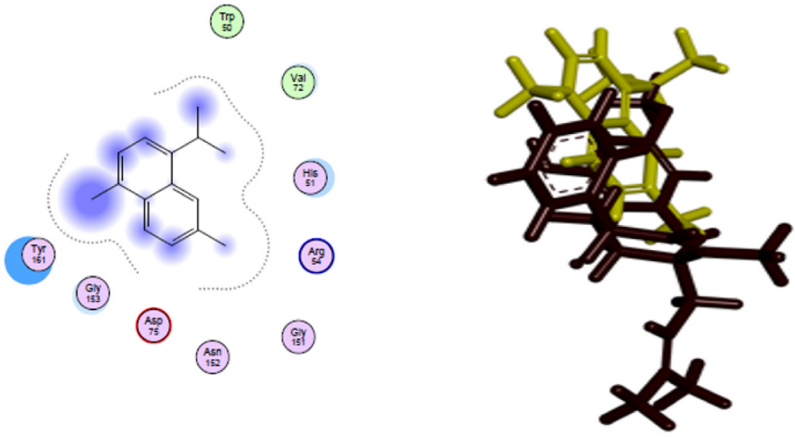

Figure 3. Visualization of (a) spatial arrangement of compound **1** (b) superimposition of compound **1** (yellow) and panduratin A (brown)

Based on the docking analysis, compound **2** exhibited a binding free energy value of -4.34 kcal/mol, with an RMSD value of 0.5809. Comparatively, panduratin A (used as the positive control) had a lower negative binding free energy than compound **2**. It is important to note that no hydrogen bonding was observed between compound **2** and the amino acid residues surrounding its binding site. However, the compound did engage in hydrophobic interactions with the amino acid residue Arg54 and interacted with the catalytic triad Asp75 through Van der Waals interactions. Despite these interactions, compound **2** only demonstrated three binding factors with the positive control, suggesting that it may not penetrate deeply into the active site cavity of NS2B/NS3 serine protease. Consequently, compound **2** may not be a potential inhibitor of dengue virus DEN2 NS2B/NS3 serine protease. The spatial arrangement of compound **2** with the protein and superimposition is depicted in Figure 4.

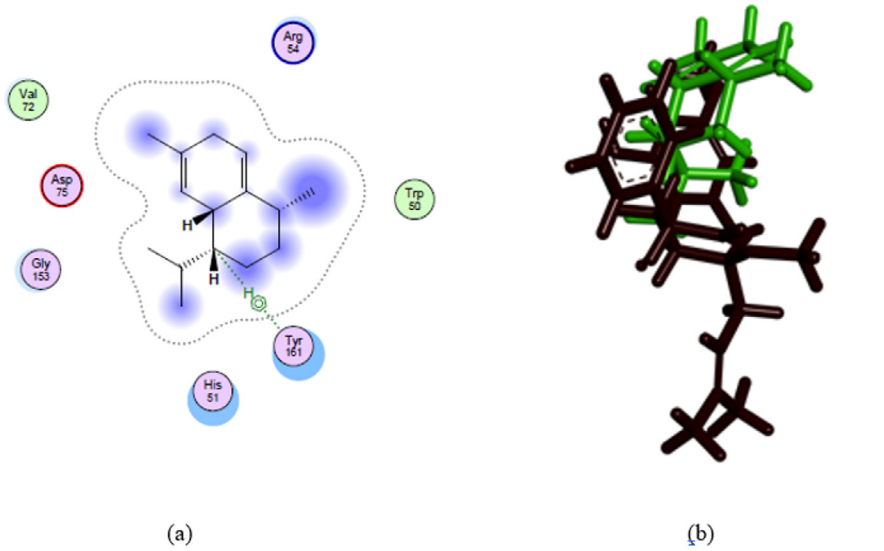

Figure 4. Spatial arrangement of compound **2** (a) and (b) superimposition of compound **2** (green) and positive control (brown)

The docking method was verified by superimposing the ligand and the positive control. This demonstrated how several significant residues could effectively bind to the ligands during the binding process. Superimposition was also utilized[18-20] to determine the properties of the active components that can stabilize the interaction between the ligand and the protein target. Additionally, superimposition was used to simultaneously evaluate the orientation of the ligands and the receptor simultaneously[20].

Based on the docking results in Table 1, compound **3** was found to have a binding free energy value of -4.93 kcal/mol and an RMSD of 1.62. Panduratin A had a more negative value than compound **3**, indicating that it was more challenging for compound 3 to bind to the active site of the NS2B/NS3 serine protease. Based on visualization of the docking results, it was observed that compound **3** interacted through hydrogen bonding with the amino acid residues Tyr161 and His51. In addition, compound **3** was able to interact with other amino acids (Ser135, Ser131, Gly153, Gly151, Pro132, Asn152, Tyr150, Phe130, and Leu128 through different interactions). The presence of hydrogen bonding with one of the catalytic triads (His51) may potentially explain why compound **3** had a better binding free energy compared to compounds **1** and **2**. The spatial arrangement of compound **3** and its superimposition with panduratin A are shown in Figure 5.

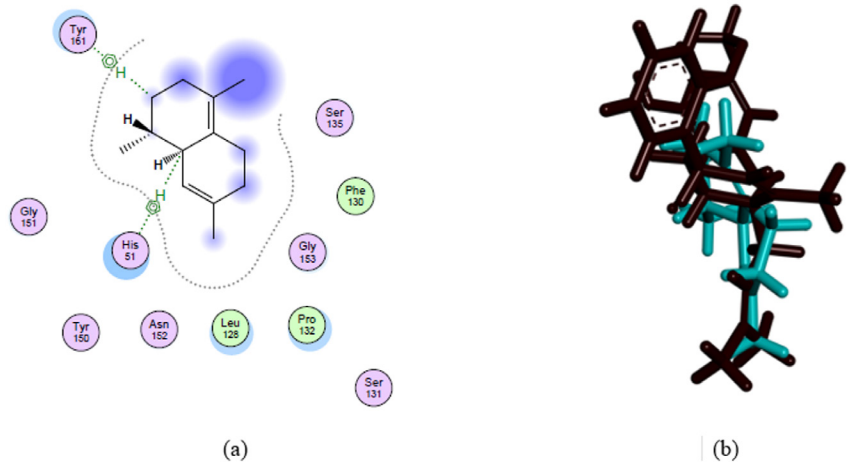

Figure 5. Visualization of (a) spatial arrangement of compound **3** (b) superimposition of compound **1** (blue) and panduratin A (brown)

DFT calculation

The gas-phase structures of compound **3** and panduratin A were optimized using Density Functional Theory (DFT) with the B3LYP approach and the 6-31 G basis set[19], implemented through the Gaussian program. The chemical stabilities of these compounds were assessed using the highest occupied molecular orbital (HOMO) and lowest unoccupied molecular orbital (LUMO)[21,22]. Energy gap and chemical reactivity descriptors were determined using the DFT/B3LYP/6-31G method, and the results are presented in Table 2. Figure 6 illustrates the HOMO and LUMO of compound **3** and panduratin A.

Table 2. DFT calculation

Compound	Energy (au)	Structure Electronic		Energy gap
		HOMO	LUMO	
Senyawa 3	-507.44	-0.21	-0.02	-0.24
Panduratin A	-130.97	-0.22	-0.04	-0.26

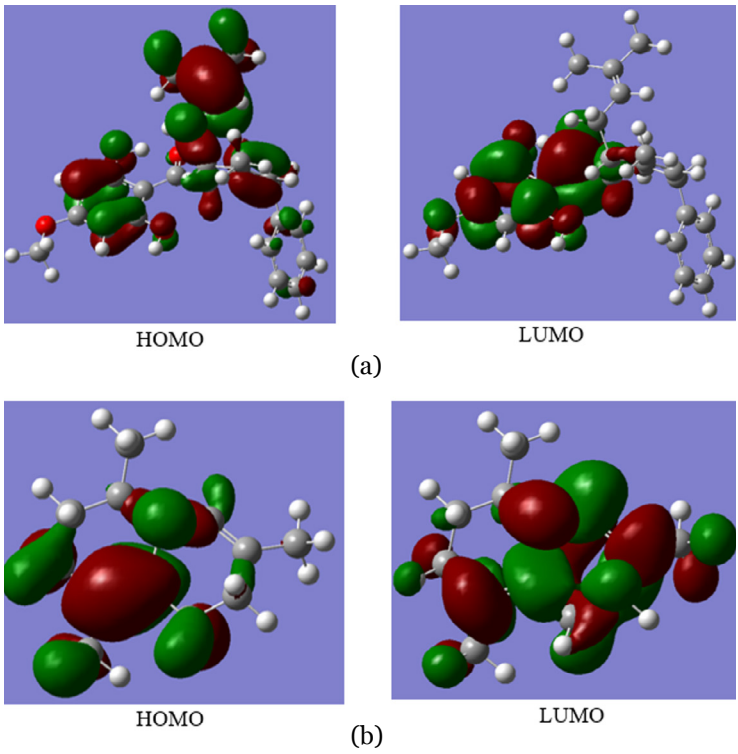

Figure 6. HOMO and LUMO for (a) compound **3** and (b) panduratin

Drug-likeness and ADMET properties

In order for a molecule to be considered a potential drug candidate, it must possess appropriate pharmacokinetics and safety properties[23]. Additionally, it should exhibit the necessary biological action. Compound **3** as determined by ADME analysis has a molecular weight of 176.30 kcal/mol, but it has no hydrogen bond donors or acceptors. This compound has a lipophilicity value of 3.57, which indicates optimal lipophilicity and enables to achieve good bioavailability when administered orally. Table 3 depicts the ADME analysis for compound **3**.

Table 3. ADME analysis

Compound	Cpd 3
Physicochemical properties	
Number of H-bond acceptors	0
Number of H-bond donors	0
Molecular weight (g/mol)	176.30
Number of heavy atoms	13
Number of aromatic Heavy atoms	0
Fraction Csp3	0.69
Number of rotable bonds	0
Molar refractivity	59.43
TPSA ($Å^2$)	0.00
Lipophilicity	
iLOGP	3.06
XLOGP3	3.01
WLOGP	4.09
MLOGP	4.11
SILICOS-IT	3.58
Consensus Log $P_{o/w}$	3.57
Water solubility	
ESOL	-2.83
Ali	-2.67
SILICOS-IT	-3.08
Pharmacokinetics	
GI absorption	Low
BBB permeation	Yes
Skin permeation Log K_p (cm/s)	-5.24

Veber and Muegge rules state that the maximum number of rotatable bonds in a molecule is 10 and 15, respectively. Compound **3** was examined using the Veber and Muegge criteria and was found to have a maximum of seven rotatable linkages. The aliphatic degree of a molecule is determined by the fraction of sp3 carbon atoms, which is also used to predict solubility. It is hypothesized that increasing saturation increases the clinical success rate 24, 25. In this study, Compound **3** had substantially higher degrees of saturation compared to the majority of other compounds studied, with a proportion of C sp3 of 0.69, which is higher than 0.25. Compound **3** had an XLOGP3 value of 3.01. PAIN analysis showed no alerts; in the Brenk analysis, only one alert was found, and no violations were observed in the lead-likeness analysis. The results indicated that the synthetic accessibility scores ranged from 1.60–4.55. The drug-like properties are presented in Table 4.

Table 4. Drug-likeness

Compound	Cpd 3
Drug-likeness	
Lipinski	Yes
Ghose	Yes
Veber	Yes
Egan	Yes
Muegge	No
ABS	0.55
Medicinal chemistry	
PAINS (Alerts)	0
Brenk (alerts)	1
Leadlikeness	No (1)
Synthetic accessibility	3.94

Based on Pro-Tox II calculations, it appears that compound **3** falls into the five parameters used for predicting toxicity: size, lipophilicity, insolubility, insaturation, and flexibility. Furthermore, compound **3** was predicted to be an inhibitor of nuclear receptors, family A G protein-coupled receptors, and transcription factors with probabilities of 33.3%, 26.7%, and 13.3%, respectively. The toxicity model report in Figure 7 demonstrates that compound **3** affects only the aromatase target.

The BOILED-Egg method proved effective in predicting the permeability of the human blood-brain barrier (BBB) and gastrointestinal absorption based on polarity (topological polar surface area, TPSA) and lipophilicity (WLOGP).

In this study, compound **3** exhibited a WLOGP value of 4. Molecules were depicted as points in the yolk of boiled eggs. Molecules positioned in the white region (BOILED Egg's white) were expected to passively absorption through the gastrointestinal system, while points situated in the black region (BOILED Egg's black) were predicted to actively penetrate the BBB. P-glycoprotein is presumed to expel certain chemicals from the central nervous system, as indicated by the blue (PGP+) and red (PGP-) dots.

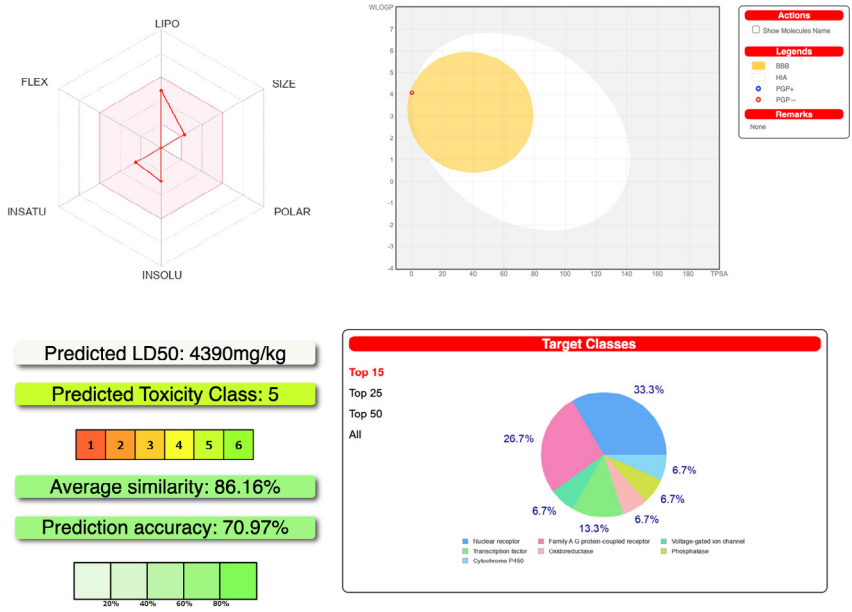

Classification	Target	Shorthand	Prediction	Probability
Organ toxicity	Hepatotoxicity	dili	Inactive	0.78
Toxicity end points	Carcinogenicity	carcino	Inactive	0.68
Toxicity end points	Immunotoxicity	immuno	Inactive	0.58
Toxicity end points	Mutagenicity	mutagen	Inactive	0.65
Toxicity end points	Cytotoxicity	cyto	Inactive	0.72
Tox21-Nuclear receptor signalling pathways	Aryl hydrocarbon Receptor (AhR)	nr_ahr	Inactive	0.91
Tox21-Nuclear receptor signalling pathways	Androgen Receptor (AR)	nr_ar	Inactive	0.99
Tox21-Nuclear receptor signalling pathways	Androgen Receptor Ligand Binding Domain (AR-LBD)	nr_ar_lbd	Inactive	0.99
Tox21-Nuclear receptor signalling pathways	Aromatase	nr_aromatase	Active	0.56
Tox21-Nuclear receptor signalling pathways	Estrogen Receptor Alpha (ER)	nr_er	Inactive	0.81
Tox21-Nuclear receptor signalling pathways	Estrogen Receptor Ligand Binding Domain (ER-LBD)	nr_er_lbd	Inactive	0.97
Tox21-Nuclear receptor signalling pathways	Peroxisome Proliferator Activated Receptor Gamma (PPAR-Gamma)	nr_ppar_gamma	Inactive	0.99
Tox21-Stress response pathways	Nuclear factor (erythroid-derived 2)-like 2/antioxidant responsive element (nrf2/ARE)	sr_are	Inactive	0.90
Tox21-Stress response pathways	Heat shock factor response element (HSE)	sr_hse	Inactive	0.90
Tox21-Stress response pathways	Mitochondrial Membrane Potential (MMP)	sr_mmp	Inactive	0.88
Tox21-Stress response pathways	Phosphoprotein (Tumor Supressor) p53	sr_p53	Inactive	0.99
Tox21-Stress response pathways	ATPase family AAA domain-containing protein 5 (ATAD5)	sr_atad5	Inactive	0.99

Figure 7. Toxicity results (middle left and bottom), prediction of drug (middle-right), BOILED-Egg model (top-right) together with the bioavailability radar

STATEMENT OF ETHICS

All the necessary ethical rules were followed while performing research.

CONFLICT OF INTEREST STATEMENTS

The authors report no conflict of interest.

AUTHOR CONTRIBUTIONS

IS: Literature search, designing the study, data analysis and interpretation, manuscript drafting. MF: Designing the study, data analysis and interpretation, and manuscript editing. NF: Ideas and concept, data analysis and manuscript editing, review of manuscript.

FUNDING SOURCES

None.

ACKNOWLEDGEMENT

None.

REFERENCES

1. Rodenhuis-Zybert IA, Wilschut J, Smit JM. Dengue virus life cycle: viral and host factors modulating infectivity. Cell Mol Life Sci, 2010;67(1):2773-2786. Doi: 10.1007/s00018-010-0357-z

2. Carrington BL, Simmons PC. Human to mosquito transmission of dengue viruses. USA. Front Immunol, 2014;5(1):1-8. Doi: 10.3389/fimmu.2014.00290

3. Stadler K, Allison SL, Schalich J, Heinz FX. Proteolytic activation of tick-borne encephalitis virus by furin. Virol J, 1997;71(11):8475-8481. Doi: 10.1128/jvi.71.11.8475-8481.1997

4. Luo D, Vasudevan SG, Lescar J. The flavivirus NS2B-NS3 protease-helicase as a target for antiviral drug development. Journal Elsevier, 2015;118(5):148-158. Doi: 10.1016/j.antiviral.2015.03.014

5. Yusof R, Clum S, Wetzel M, Murthy HMK, Padmanabhan R. Purified NS2B/NS3 serine protease of dengue virus type 2 exhibits cofaktor NS2B dependence for cleavage of substrates with dibasic amino acids *in vitro*. J Biol Chem, 2000;276(14):9963-9969. Doi: 10.1074/jbc.275.14.9963

6. Geiss BJ, Stahla H, Hannah AM, Gari HH, Keenan SM. Focus on flaviviruses: current and future drug targets. Future Med Chem, 2009;1(2):327-344. Doi: 10.4155/fmc.09.27

7. Frimayanti N, Ikhtiarudin I, Teruna HY, Jasri J. Search for new potential breast cancer inhibitors (mcf-7) based on molekular docking and biological assay of pyrazoline analogue compounds. ASTESJ, 2020;5(5):121-126. Doi: 10.25046/aj050517

8. Zamri A, Frimayanti N, Teruna HY. Docking and molecular dynamic simulations: study of 1, 3, 4-oxadiazolechalcone hybrid derivatives to search new active anticancer agent. Thai J Pharm Sci, 2016;40(4):179-184. Doi: 10.56808/3027-7922.1911

9. Rao PV, Gan SH. Cinnamon: a multifaceted medicinal plant. Evid Based Complement Alternat Med, 2014;642942. Doi: 10.1155/2014/642942

10. Wu W, Yang Y, Feng Y, Ren X, Li Y, Li W, et al. Study of the repellent activity of 60 essential oils and their main constituents against *Aedes albopictus* and nano-formulation development. Insects, 2022;13(12):1077. Doi: 10.3390/insects13121077

11. Frimayanti N, Chee CF, Zain SM, Rahman NA. Design of new competitive dengue Ns2b/Ns3 protease inhibitors-a computational approach. Int J Mol Sci, 2011;12(2):1089-1100. Doi: 10.3390/ijms12021089

12. Daina A, Michielin O, Zoete V. SwissADME: a free web tool to evaluate pharmacokinetics, drug-likeness and medicinal chemistry friendliness of small molecules. Sci Rep, 2017;3;7:42717. Doi: 10.1038/srep42717

13. Delaney JS. ESOL: estimating aqueous solubility directly from molecular structure. J Chem Inf, Model. 2004;44(3):1000-1005. Doi: 10.1021/ci034243x

14. Ali J, Camilleri P, Brown MB, Hutt AJ. Kirton SB. Revisiting the general solubility equation: *in silico* prediction of aqueous solubility incorporating the effect of topographical polar surface area. J Chem Inf Model, 2012;52:420-428. Doi: 10.1021/ci200387c

15. Frimayanti N, Yaeghoobi M, Namavar H, Utari MC, Djohari M, Laia CO. *In silico* analysis approach for screening new agents for breast cancer inhibitors based on 1,5-benzothiazepine. Pharm Sci Asia, 2022;49(5):446-453. Doi: 10.29090/psa.2022.05.22.001

16. Prieto-Martínez FD, Arciniega M, Medina-Franco JL. Molecular docking: current advance and challanges. TIP Revista Especializa da En Ciencias Químico-Biológicas, 2018;21:65-87. Doi: 10.22201/fesz.23958723e.2018.0.143

17. Du X, Li Y, Xia Y, Ai S, Liang J, Sang P, et al. Insights into protein–ligand interactions: mechanisms, models and methods. Int J Mol Sci, 2016;17(22):144. Doi: 10.3390/ijms17020144

18. Frimayanti N, Yaeghoobi M, Namavar H, Ikhtiarudin I, Meysam A. *In silico* studies and biological evaluation of chalcone-based 1,5-benzothiazepines as new potential H1N1 neuraminidase inhibitors. J Appl Pharm Sci, 2020;10(10):86-94. Doi: 10.7324/JAPS.2020.1010010

19. Baroroh U, Setiani NA, Mardiah I, Astriany D, Yusuf M. Computational design of nanobody binding to cortisol to improve their binding affinity using molecular docking and molecular dynamics simulations. J Chem, 2022;22(2):515-525. Doi: 10.22146/ijc.71480

20. Shivanika C, Deepak Kumar S, Ragunathan V, Tiwari P, Sumitha A, Brindha Devi P. Molecular docking, validation, dynamics simulations, and pharmacokinetic prediction of natural compounds against the SARS-CoV-2 main-protease. J Biomol Struct Dyn, 2022;40(2):585-611. Doi: 10.1080/07391102.2020.1815584

21. Becke AD. Becke's three parameter hybrid method using the LYP correlation functional. J Chem Phys, 1993;98(7):5648-5652. Doi: 10.1063/1.464913

22. Ramalingam A, Gurunathan RK, Nagarajan PC. Investigation of potential azeotrope breakers using DFT and COSMO approach. ACS Omega, 2020;5(27):16885-16900. Doi: 10. 1021/acsomega.0c02086

23. Hu Q, Feng ML, Lai LM, Pei J. Prediction of drug-likeness using deep autoencoder neural networks. Front Genet, 2018;9(585):1-8. Doi:10.3389/fgene.2018.00585

24. Liangzhen Z, Jintao M, Kai J, Haidong L, Zechen W, Mingzhi L, et al. Improving protein–ligand docking and screening accuracies by incorporating a scoring function correction term. Brief Bioinform, 2022;23(3). Doi: 10.1093/bib/bbac051

25. Lee C, Yang W, Parr RG. Development of the Colle-Salvetti correlation energy formula into a functional of the electron density. Phys Rev B, 1988;37:785-789. Doi: 10.1103/physrevb.37.785

Acta Pharm. Sci. Vol 63:(2), 2025
Original article
DOI: 10.23893/1307-2080.APS6321

Cardioprotective potential of *Cucurbita maxima* seeds and its active fractions

Pallavi Abhijit PATIL*, Sayali Rajendra KALE

Bharati Vidyapeeth's College of Pharmacy, Department of Pharmacology, C.B.D. Belapur, Navi Mumbai, India

ABSTRACT

The current study's goal was to assess the cardiovascular impact of *Cucurbita maxima* (CM) seed's hydroalcoholic extract and, its ethyl acetate and *n*-butanol fractions, for potential usage in myocardial infarction. All of the resulting extracts underwent qualitative screening using techniques like High Performance Thin Layer Chromatography (HPTLC), Fourier Transform Infrared Spectroscopy (FTIR), and UV Visible Spectroscopy. *In vitro* studies revealed that the crude extract and fractions of *Cucurbita maxima* seeds have total antioxidant and free radical scavenging properties. The Chick Chorioallantoic Membrane Assay (CAM), an *in ovo* assay, was used to assess the cardiovascular activity of the crude extract and its fractions. The study illustrated the findings by demonstrating the angiogenic impact, which indicated desired cardiovascular activity in the CAM Assay.

Keywords: *Cucurbita maxima,* HPTLC, antioxidant activity, fractionation, chick chorioallantoic membrane assay

INTRODUCTION

Cardiotoxicity is the term used to describe conditions when the electrophysiology of the heart is compromised, or its muscles are harmed. Some cancer treatments have the potential to cause cardiotoxicity. The most used chemotherapeutic medications are cytostatic anthracycline-class antibiotics. Utilizing a substance like perfluorooctanoic acid allows for the induction of cardiotoxicity in laboratory studies[1].

*Corresponding author: Pallavi A. PATIL
E-mail: sbvp2023@gmail.com
ORCIDs:
Pallavi Abhijit PATIL: 0009-0003-7217-128X
Sayali Rajendra KALE: 0009-0001-5037-9309
(Received 28 Jul 2023, Accepted 25 May 2024)

Angiogenesis, which is defined as the growth of new blood vessels from pre-existing blood vessel networks, is crucial for extending the vascular bed that was first generated during vasculogenesis. For cardiovascular disorders to be successfully treated, blood flow must be restored. Therapeutic angiogenesis, which promotes the development of new blood vessels from pre-existing vessels, is a useful approach for treating cardiovascular problems[2-3].

The chorioallantoic membrane (CAM) assay, which involves the implantation of a substance or compound on the extra embryonic membrane of the developing chick egg, is one prospective method for improving animal experiments. Importantly, the CAM is not innervated; as a result, the chick feels no pain. One of the most effective and well-liked methods for evaluating the angiogenic potential of whole cells and purified components is the CAM model. The mesodermal layers of two embryonic structures—the Allantois and the Chorion of the avian embryo combine to produce the CAM[4-7].

In the current investigation, the cardiovascular activity was measured using *Cucurbita maxima* seeds, also referred to as pumpkin seeds, a plant in the Cucurbitaceae family. Various names for this squash include pumpkin, buttercup, autumn squash, etc. It is widely grown in India and most other warm countries for usage as both a vegetable and a medicinal[8]. Pumpkin seeds are a rich natural source of phytosterols, antioxidant vitamins including tocopherols and carotenoids, and unsaturated fatty acids like oleic and linoleic. The high quantity of fatty acids and proteins in *Cucurbita maxima* seeds nutritional composition is its primary distinguishing feature. In addition to tyros (phenylethanoid), vanillic acid, vanillin, luteolin, and sinapic acid, pumpkin seed oil also contains other phenolic compounds. Lipid-lowering, hypertension, hypoglycemic, anthelmintic, and wound-healing effects are included in pumpkin seed oil supplements[9-11].

METHODOLOGY

Preparation of extract and fractions

Dried CM seeds were procured from S.V. Bhandar, Vashi, Navi Mumbai and the same were sent for authentication. The same seeds were grinded to coarse powder. The powdered materials were extracted using soxhlet apparatus using hydroalcohol as the extraction solvent. The hydroalcoholic extract of CM (HECM) seeds was further fractionated using ethyl acetate (EACM) and *n*-butanol (NBCM) as the fractionation solvent. Fractionation procedure was carried out using separating funnel.

Phytochemical screening

Extract was subjected to preliminary phytochemical screening in order to identify the nature of constituents present in it i.e. flavonoids, tannins, phenols, alkaloids, glycosides, carbohydrates etc.

Qualitative phytochemical screening

UV-Vis Spectroscopy is advantageous in qualitative analysis. It is one of the greatest techniques for figuring out what impurities there are in organic compounds. The Shimadzu 1800 UV spectrophotometer was used to obtain the maximum wavelength of the crude extract and the fractions. The concentration used for the analysis was 100ppm solution of crude extract and fractions. The HECM, EACM, and NBCM samples were subjected to find out maximum wavelength[14].

The analytical technique known as Fourier transform infrared spectroscopy (FTIR) is quick and non-destructive. It is an effective approach for identifying functional groups and is connected to chemometrics. It is evolving into an effective method for studying herbal medicine. The primary chemical components of the extracts were analyzed using FTIR, as well as the compounds' structures. The Shimadzu FTIR spectrometer was used to record the herbal drug's FTIR spectra. For FTIR spectra analysis, about 1 mg of the herbal medication is employed. The HECM, EACM, and NBCM samples were subjected to find out functional groups present in extract[15].

The HECM extract and its fractions (EACM, NBCM) were subjected for fingerprinting using HPTLC. These studies were performed on pretreated silica gel 60 F_{254}, 50X50 mm HPTLC plates (Merck, Germany), with toluene: methanol: *n*-butanol 9:0.5:0.5 (v/v) as a mobile phase at 264 nm. Spotting of sample of concentration 500 µg/ml were applied to the plates as 5 mm bands, sample application with CAMAG-Linomat 5 automated spray on band applicator equipped with a 100 µL syringe and operated with following settings: band length 5 mm, application rate 150 nL/sec, distance between 6.2 mm, distance from the plate side edge 9 mm and solvent front of the plate 40 mm. CAMAG TLC Scanner 4 was used to densitometrically to quantify the bands using vision CATS software. The scanner operating parameters were: (Mode: absorbance / reflection; Slit dimension; 4 x 0.45 mm; scanning rate: 20 mm/s and at an optimized wavelength 264 nm in visible range)[16].

In vitro antioxidant assays

This study examined the antioxidant activity of CM seeds using three distinct scavenging assays. With the same seeds' crude extract and its derived fractions, DPPH, H_2O_2, and Reducing Power assays were conducted.

2,2-Diphenyl-1-picrylhydrazyl (DPPH) radical scavenging activity were determined by measuring the capacity to bleach purple colored ethanol solution of DPPH. 2 mL of varying concentrations (10-100 µg/mL) of the samples in ethanol were added to 2 mL of a 0.2 mM DPPH in ethanol. After a 30 min incubation period at room temperature, the absorbance was read against blank at 517 nm. The blank solution was containing 0.2mM DPPH in ethanol[17].

$$\text{Percentage DPPH Inhibition (\%I)} = \frac{\text{Ao-As}}{\text{Ao}} \text{ X 100}$$

Hydrogen peroxide (H_2O_2) scavenging activity was determined according to the procedure described further. Briefly, 3.4 mL of varying concentration (10-100 µg/mL) of fractions in phosphate buffer saline (pH 7.4) were mixed with 0.6 mL of 40 mM H_2O_2. The absorbance was read at 230 nm after 10 min of incubation at room temperature. Blank readings were taken containing phosphate buffer without H_2O_2[17].

$$H_2O_2 \text{ Scavenging Activity (\% } H_2O_2\text{)} = \frac{\text{Ao-As}}{\text{Ao}} \text{ X 100}$$

1 ml standard and fractions of different concentrations (10-100 µg/ml) were mixed with 2.5 ml of (pH 6.6) phosphate buffer and 2.5 ml of (1%) potassium ferricyanide. Further this mixture was incubated at 50°C in water bath for 20 min. After cooling, Aliquots of 2.5ml (10%) trichloroacetic acid were added to the mixture, which were then centrifuged at 3000 rpm for 10 min. The upper layer of solution 2.5 ml was mixed with 2.5 ml distilled water and a freshly prepared 0.5 ml of (0.1%) ferric chloride solution. The absorbance was measured at 700 nm in Shimadzu UV-visible spectrometer. A blank was prepared without adding extract. Ascorbic acid at various concentrations (10 to 100 µg/ml) was used as standard[18].

In ovo evaluation of cardioprotective activity

Embryonic Development Day (EDD-9) chick embryos were frequently used for testing irritants and medication compositions. The eight healthy, fully formed embryos (n=8) were divided into groups at random and intravenously injected into the CAM's main blood vessels (CAM allantoic arteries). Using microliter

capillary syringes with 33-gauge needles and the necessary medication doses (Hamilton). After that, eggs were parafilm-sealed and kept in an incubator at 37°C for additional monitoring at 24 hours, during which the mortality rate was reported[19].

The experimental design for *in ovo* evaluation of cardioprotective activity by CAM Assay consists of nine different groups. Each group consists of 8 eggs. Group I (Vehicle Control) received 1% CMC as the treatment. The Group II (Disease Control) received Perfluorooctanoic acid (PFOA 2mg/kg)[19]. Group III (Standard Treatment) received Pyruvic acid (300 µg)[20]. Group IV and Group V the low and high dose of HECM respectively. Group VI and Group VII were treated as the low and high dose of EACM fraction respectively. Group VIII and Group IX were treated as the low and high dose of NBCM fraction respectively.

Eggs from fertilized chickens were purchased and inspected for damage from Central Poultry development org. (WR), Aarey milk colony, Mumbai, 400065. Eggs were washed with 70% ethanol before being incubated at 37°C with continuous humidity. On the third day of incubation, an 18 gauge hypodermic needle was used to remove 2-3 ml of albumin by piercing a tiny hole. The eggs were taped shut with adhesive / clear tape. A window was opened on the 8th day of incubation, and medication was given on top of the membrane[20]. PFOA was administered intravenously on Day 12 to all treatment groups, including the disease group. After injection, the window was once again taped shut and placed in an incubator set at 37°C. After 24 hours, the window was unsealed, and observations were made[21].

Morphometric evaluation of CAM assay

The CAM area was calculated as;

$$\text{Area} = \left(\frac{1}{2}\text{A}\right) \times \left(\frac{1}{2}\text{B}\right) \times \pi$$

Where A= longest length, B= is longest width. Image J- WIN R Fiji software was used to evaluate the length and breadth for the morphometric evaluation of CAM assay. Region of Interest (ROI) was selected in order to measure the length and breadth. Morphometric study of the number of secondary and tertiary blood vessels were counted manually on computer image by counting branching points[22].

Angiogenesis index

After the 14th day the eggs were removed from the incubator. Adhesive tape was removed completely, and CAM area was captured. The number of vessel branch points contained region equal to the area was counted using Image J-WIN R Fiji software and findings from 8 CAM preparations were analyzed for each group. The resulting angiogenesis index is the mean ± SEM of new branch point in each set of samples[23].

The results of angiogenesis by *Cucurbita maxima* crude extracts & active fractions were subjected to statistical analysis. Graph Pad Prism version 9.0 was used to analyze the data with one-way ANOVA and evaluate the results using the Dunnett test.

RESULTS and DISCUSSION

Phytochemical screening

The results indicate the presence of flavonoids, tannins, phenols, alkaloids, glycosides and carbohydrates (Table 1).

Table 1. The results showing the presence of flavonoids, tannins, phenols, alkaloids, glycosides, and carbohydrates

Sr. No.	Phytochemical Test	Test Methods/ Reagents	Results
1	Alkaloids	Mayer's Reagent	**Present**
		Hager's Reagent	**Present**
		Wagner's Reagent	**Present**
2	Carbohydrates	Molisch's	**Present**
3	Tannins & Phenols	Lead Acetate	**Present**
		Ferric Chloride Test	**Absent**
4	Flavonoids	Alkaline Reagent	**Present**
		Sulphuric Acid	**Present**
5	Glycosides	Keller-Killani	**Present**
		Baljet's Test	**Absent**

Qualitative characterization

Figure 1(a), (b), and (c) shows the characteristic FTIR spectra of the HECM and its EACM and NBCM fractions.

Peaks at 3303.29 cm^{-1}, 2921.04 cm^{-1}, 2852.58 cm^{-1}, 2361.94 cm^{-1}, 1591.74 cm^{-1}, and 1044.04 cm^{-1} showed the presence of O-H, N-H/C-H stretching, C-H stretching, O=C=O, N-H bending, and CO-O-CO which signifies the presence of hydroxyl group, primary amine or alkane, alkane, carbon dioxide, amine group, and anhydride groups respectively.

Peaks at 2921.04 cm^{-1}, 2852.58 cm^{-1}, 2361.94 cm^{-1}, 1740.07 cm^{-1}, 1460.52 cm^{-1}, 1158.15 cm^{-1}, and 718.85 cm^{-1} showed the presence of N-H/C-H stretching, C-H stretching, O=C=O bond, C=O stretching, C-H bond, C-O stretching, and C=C bond which signifies the presence of primary amine, alkane, carbon dioxide, carboxylic acids, alkane, tertiary alcohol, and alkene group respectively.

Peaks at 3337.52 cm^{-1}, 1038.34 cm^{-1}, 2926.75 cm^{-1}, 2361.94 cm^{-1}, 1648.79 cm^{-1}, and 1454.82 cm^{-1} showed the presence of O-H stretching, S=O stretching, C-H bond, O=C=O bond, C=O stretching, and CH2 bending which signifies the presence of alcohol, sulfoxide group, alkane, carbon dioxide, alkene and methylene group respectively.

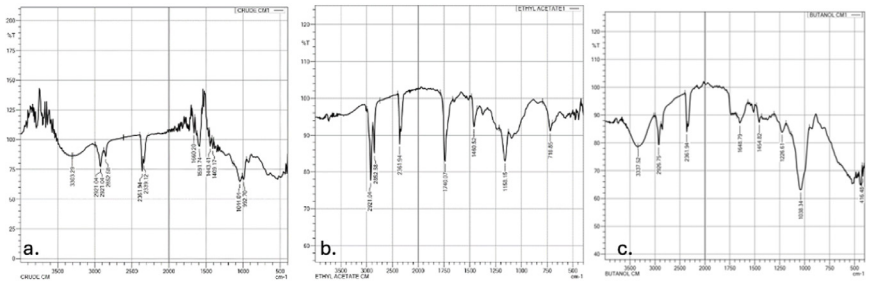

Figure 1. a: FTIR Spectroscopy of HECM; b: FTIR Spectroscopy of EACM; c: FTIR Spectroscopy of NBCMr

A variety of mobile phases were tested, namely methanol: water (9:1 v/v), butanol: acetic acid: water (4:1:1), butanol: acetic acid: water (6:1:1 v/v), chloroform: methanol (8:2 v/v), *n*-hexane: ethyl acetate: glacial acetic acid (7.5:2:0.5 v/v)[12]. The mobile chosen was Toluene: Methanol: *n*-butanol (9:0.5:0.5 v/v). Three peaks of Rf value 0.080, 0.513, 0.900 were seen in the crude extract. The ethyl acetate fraction showed three peaks of Rf value 0.230, 0.587, 0.800. The *n*-butanol fraction showed three peaks of Rf value 0.823, 0.933, 0.980 (Figure 2).

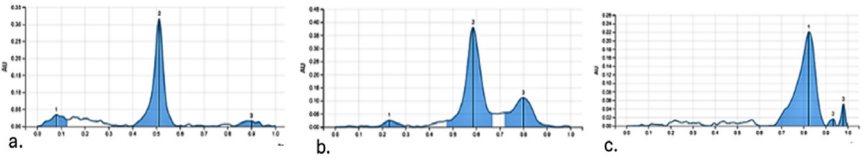

Figure 2. The results showing a: HPTLC Chromatogram of HECM; b: HPTLC Chromatogram of EACM; c: HPTLC Chromatogram of NBCM.

Maximum antioxidant activity of DPPH, H_2O_2 scavenging, and reducing power assay was shown by EACM, at the highest concentration of 100 µg/ml. The scavenging activity of EACM was equivalent to ascorbic acid which was used as the standard (Figure 3).

The percent inhibition of DPPH radical scavenging activity was maximum with EACM i.e. 84.96% ± 0.010 at the highest concentration (100 µg/ml) which was comparable to ascorbic acid i.e. 91.88% ± 0.107.

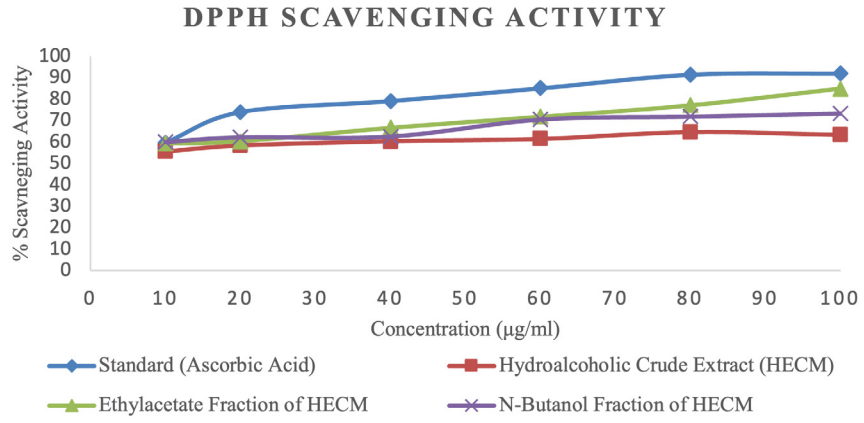

Values are expressed as mean ± SEM (n=3).

Figure 3. The results showing the presence of DPPH radical scavenging assay of hydroalcoholic extract and ethyl acetate and n-butanol fractions of *Cucurbita maxima*.

The percent inhibition of H_2O_2 scavenging activity was maximum with EACM i.e. 87.5% ± 0.008 at the highest concentration (100 µg/ml) which was comparable to ascorbic acid i.e. 93.22% ± 0.036 (Figure 4).

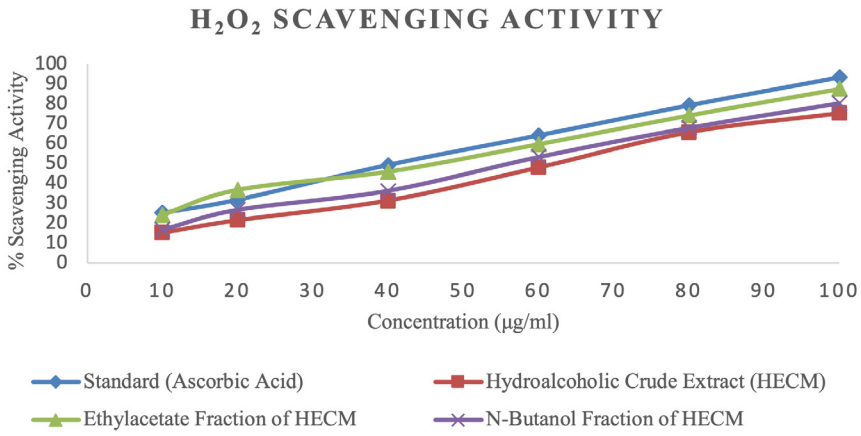

Values are expressed as mean ± SEM (n=3).

Figure 4. The results showing the presence of H2O2 scavenging assay of hydroalcoholic extract and ethyl acetate and n-butanol fractions of *Cucurbita maxima.*

The percent inhibition of reducing power assay was maximum in EACM i.e. 0.889 ± 0.041 at the highest concentration (100 µg/ml) which was comparable to ascorbic acid i.e. 0.91 ± 0.011 (Figure 5).

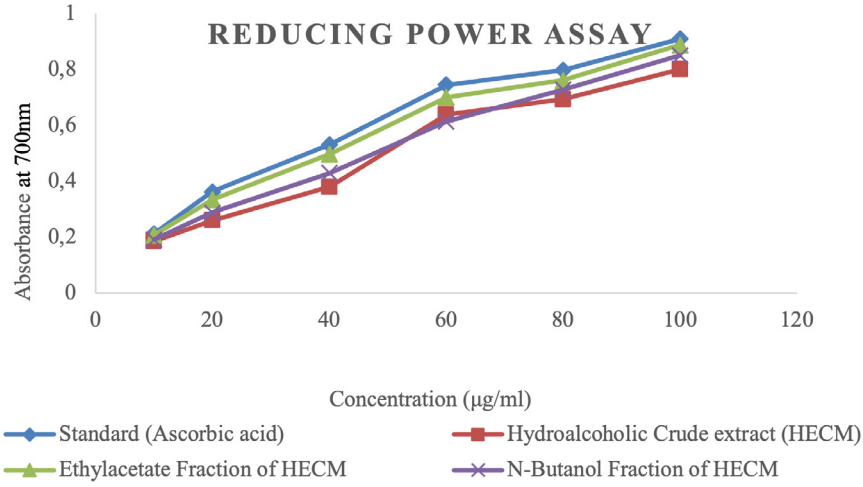

Values are expressed as mean ± SEM (n=3).

Figure 5. The results showing the presence of Reducing power assay of hydroalcoholic extract and ethyl acetate and n-butanol fractions of *Cucurbita maxima.*

In ovo evaluation of cardioprotective activity of active fractions of hydroalcoholic extract of *Cucurbita maxima* seed powder

Toxicity study of active fractions of hydroalcoholic extract of *Cucurbita maxima* seeds powder. The HECM, EACM, and NBCM samples were evaluated for its Maximum Tolerated Dose (MTD). The toxicity study was carried out using six different concentrations of doses such as 10 µg/mL, 20 µg/mL, 40 µg/mL, 60 µg/mL, 80 µg/mL, and 100 µg/mL; eight eggs were administered with each of the doses. After the administration of the drugs observation was made after 24 h. After all the observations made 10 µg/mL was used as the low dose and 60 µg/mL was used as the high dose. This was observed based on number of dead embryos and number of surviving embryos. According to the data obtained the % survival for the low dose was 83.33% for HECM & NBCM and % survival for high dose was 50.00% in HECM & NBCM. Whereas the % survival for low dose of EACM is 100% and for high dose it is 66.66%.

The disease group showed a significant decrease ($p<0.001$) in the CAM area and vascularization. All the treatment groups i.e. Group III, IV, V, VI, VII, VIII, and IX showed significant increase ($p<0.001$) in CAM area and vascularization when compared to disease control group (Table 2, Figure 6, Figure 7). Group VII (60 µg/ml) showed significant angiogenic response when compared to disease group where the results were comparable to the standard group.

Table 2. The results showing the Morphometric Evaluation & Angiogenesis activity of active fractions of hydroalcoholic extract of *Cucurbita maxima* seeds on the CAM assay after treatment

Group No.	Groups	Dose	CAM area (cm^2)	Eggs showing angiogenic response	Total eggs	% activation	Angiogenesis index
I	Vehicle Control	1% CMC	8.908 ± 0.3721	8	8	100%	95.65 ± 4.246
II	Disease Control	2 mg/kg	1.915 ± 0.291 #	6	8	75%	23.1 ± 1.736 #
III	Standard Treatment	300 µg/egg	6.804 ± 0.2948 ****	7	8	87.50%	66.2 ± 3.397 *****
IV	HECM LD	10 µg/egg	3.947 ± 0.198 *	5	8	62.50%	39.21 ± 4.054 **
V	HECM HD	60 µg/egg	4.132 ± 0.4404 **	6	8	75%	43.44 ± 2.641 **
VI	EACM LD	10 µg/egg	4.385 ± 0.4487 **	6	8	75.00%	45.15 ± 2.835 **
VII	EACM HD	60 µg/egg	5.04 ± 0.8752 ***	7	8	87.50%	55.1 ± 4.561 ***
VIII	NBCM LD	10 µg/egg	3.837 ± 0.2221 **	5	8	62.50%	38.09 ± 3.736 **
IX	NBCM HD	60 µg/egg	4.103 ± 0.4357 **	6	8	75%	41.36 ± 4.902 **

Values was expressed as mean ± SEM (n=8). #p<0.0001 when compared to vehicle control, *****p<0.000001, ****p<0.00001, ***p<0.0001, **p<0.001, *p<0.05 when compared with disease control. Data was analyzed by one way ANOVA followed by Dunnett's test.

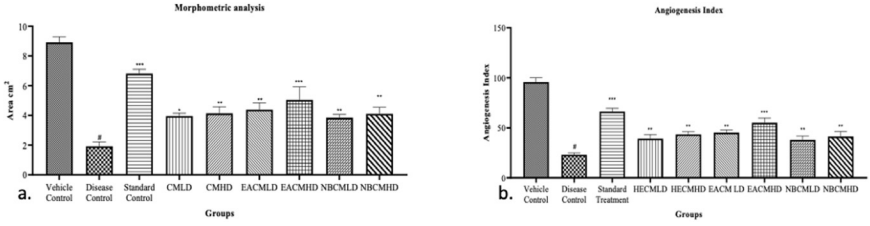

Figure 6. The results showing the a: Morphometric Evaluation and b: Angiogenesis activity of active fractions of hydroalcoholic extract of *Cucurbita maxima* seeds on the CAM assay after treatment.

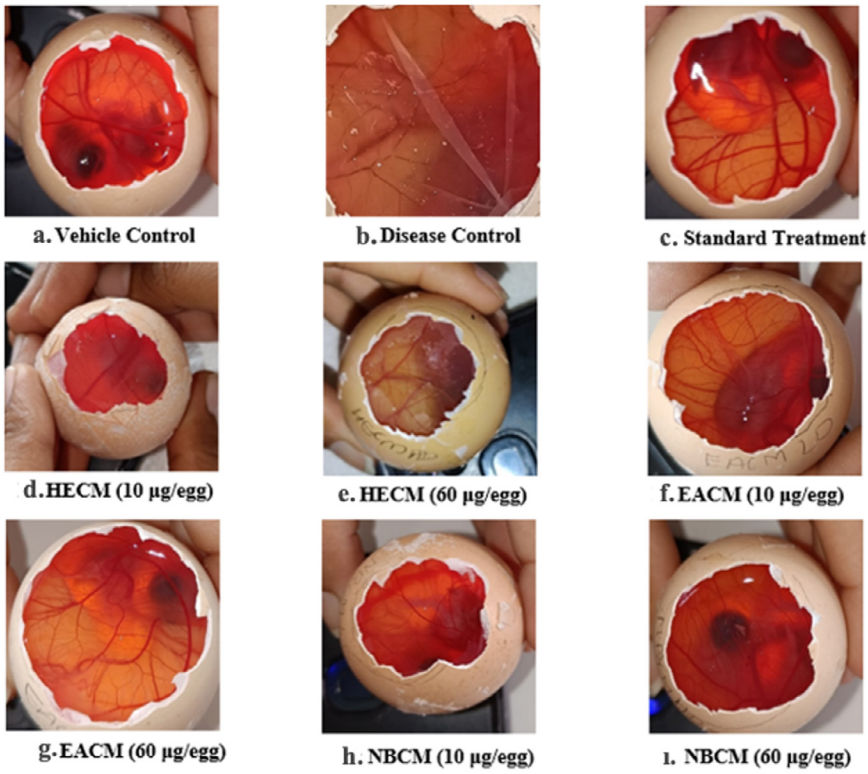

Figure 7. Cardioprotective effect of *Cucurbita maxima* seeds and its fractions by evaluating its angiogenesis potential on (AMOT) (a: Vehicle control; b: Disease Control; c: Standard treatment; d: HECM 10 µg/egg; e: HECM 60 µg/egg; f: EACM 10 µg/egg; g: EACM 60 µg/egg; h: NBCM 10 µg/egg and ı: NBCM 60 µg/egg).

Cucurbita maxima seeds are proven to have anti-diabetic, anti-obesity, hepatoprotective, and anti- hyperlipidemic properties. In the present study hydroalcoholic extract of *Cucurbita maxima* seeds, its fractions cardiovascular activity was tested in CAM assay by inducing cardiotoxicity with Perfluorooctanoic acid (PFOA).

The yield obtained from hydroalcoholic extract was 3.34% w/w. The phytochemical analysis showed the presence of alkaloids, carbohydrates, tannins & phenols, flavonoids, and glycosides.

The UV and FTIR spectra of all the extracts and fractions were collected in order to ascertain the absorption at the maximum wavelength and the presence of a functional group, respectively. The maximum wavelength which was obtained was 270 nm for HECM and 264.22 nm for EACM and NBCM. HPTLC fingerprinting was used to assess the separation of compounds from extracts

and fractions. Three peaks of Rf value 0.080, 0.513, 0.900 were seen in HECM. The ethylacetate fraction showed three peaks of Rf value 0.230, 0.587, 0.800. The *n*-butanol fraction showed three peaks of Rf value 0.823, 0.933, 0.980.

The *in vitro* antioxidant assays proved the free radical scavenging activity of the crude extract and its fractions. The *in vitro* assays assessed were DPPH radical scavenging assay, H_2O_2 scavenging assay and reducing power assay. The *in vitro* assays showed better free radical scavenging activity with ethylacetate fraction followed by *n*-butanol fraction and lastly the crude extract.

Organogenesis and advanced embryonic and foetal development depend greatly on angiogenesis. Angiogenesis includes the formation of new blood vessels from the existing one which helps in the preparation of oxygen and nutrients for the cells, as well as the removal of waste materials. An important therapeutic goal has been to use angiogenic cytokines like VEGF or members of the fibroblast growth factor (FGF) family to promote collateral blood vessel formation in the ischemic heart and limb, a method known as therapeutic angiogenesis. This has given rise to a particularly active pathogenic role for angiogenesis in atherosclerosis[24]. In the present study the angiogenic activity of hydroalcoholic extract and its ethylacetate and *n*-butanol fractions was evaluated using CAM assay. PFOA was used as the inducing agent which showed anti-angiogenic property. As a result, the angiogenic activity of the crude extract and the fractions was assessed. This was evaluated based on the efficiency of the new blood vessels formation which were most prominent in the vehicle control. The disease control showed a poor growth of blood vessels. Among the treatment groups the high dose of ethylacetate fraction (60 µg/egg) showed a greater angiogenesis response. The study depicted better effect of the fractions as compared to the hydroalcoholic extract of *Cucurbita maxima* seeds.

The ethyl acetate fraction of CM seeds proved to have maximum cardioprotective activity with all the evaluation parameters. As the CAM assay cannot be the most reliable model to assess the cardioprotective activity the results obtained may serve to evaluate the same in *in vivo* models.

STATEMENT OF ETHICS

Not applicable.

CONFLICT OF INTEREST STATEMENT

The author(s) declare that they have no conflicts of interest regarding this work.

AUTHOR CONBTRIBUTIONS

The authors confirm contribution to the paper as follows:

Study conception and design: Sayali Kale and Dr. Pallavi Patil

Data collection: Sayali Kale

Analysis and interpretation of results: Sayali Kale and Dr. Pallavi Patil

Draft manuscript preparation: Sayali Kale.

All authors reviewed the results and approved the final version of the manuscript.

FUNDING SOURCES

Bharati Vidyapeeth's College of Pharmacy, Navi Mumbai.

ACKNOWLEDGMENT

I would like to thank my guide, Dr. Pallavi Patil ma'am, Assistant Professor Department of Pharmacology, for her supervision, advice, and guidance from the very early stage of this research. I would like to show my greatest appreciation for her immense support and guidance throughout the journey. Thank you, ma'am, for believing in me and making this possible. I am grateful to our Principal Sir Dr. Vilasrao J Kadam, Bharati Vidyapeeth's College of Pharmacy, Navi Mumbai for providing me the institutional facilities during the project work.

REFERENCES

1. Lanier GM, Garg J, Shah N. Cardiotoxicity of chemotherapeutic agents: incidence, treatment and prevention. Drug Saf, 2000;22(4):263-302. Doi: 10.2165/00002018-200022040-00002

2. Deveza L, Choi J, Yang F. Therapeutic angiogenesis for treating cardiovascular diseases. Theranostics, 2012;2(8):801-814. Doi: 10.7150/thno.4419

3. Chu H, Wang Y. Therapeutic angiogenesis: controlled delivery of angiogenic factors. Ther Deliv, 2012;3(6):693-714. Doi: 10.4155/TDE.12.50

4. Moreno-Jiménez I, Hulsart-Billström G, Lanham S. The chorioallantoic membrane (CAM) assay for the study of human bone regeneration: a refinement animal model for tissue engineering. Sci Rep, 2016;6:32168. Doi: 10.1038/srep32168

5. Naik M, Brahma P, Dixit M. A cost-effective and efficient chick ex-ovo CAM assay protocol to assess angiogenesis. Methods Protoc, 2018;1(2):19. Doi: 10.3390/mps1020019

6. Nowak-Sliwinska P, Segura T, Iruela-Arispe ML. The chicken chorioallantoic membrane model in biology, medicine, and bioengineering. Angiogenesis, 2014;17(4):779-804. Doi: 10.1007/s10456-014-9440-7

7. Romanoff AL. The avian embryo: structural and functional development. New York, NY: Macmillan; 1960.

8. North Carolina Extension Gardener Plant Toolbox. *Cucurbita maxima* (Autumn squash, buttercup squash, Hubbard squash, marrow, pumpkin, squash, turban gourd, winter squash) [Internet]. 2022 [cited 28 Jul 2023]. Available from: https://plants.ces.ncsu.edu/plants/cucurbita-maxima/

9. Lemus-Mondaca R, Marin J, Rivas J, Sanhueza L, Soto Y, Vera N, et al. Pumpkin seeds (*Cucurbita maxima*): a review of functional attributes and by-products. Rev Chil Nutr, 2019;46(6):783-791.

10. Stevenson DK, Eller FJ, Wang L, Jane J, Wang T, Inglett GE. Oil and tocopherol content and composition of pumpkin seed oil in 12 cultivars. J Agric Food Chem, 2007;55(10):4005-4013. Doi: 10.1021/jf0706979

11. Lazos ES. Nutritional, fatty acid, and oil characteristics of pumpkin and melon seeds. J Food Sci, 1986;51(5):1382-1383. Doi: 10.1111/j.1365-2621.1986.tb13133.x

12. Bajpai R, Jain N, Pathak AK. Standardization of ethanolic extract of *Cucurbita Maxima* seed. J Appl Pharm Sci. 2012;2(8):92-95. Doi: 10.7324/JAPS.2012.2814

13. Tahergorabi Z, Khazaei M. A review on angiogenesis and its assays. Iran J Basic Med Sci, 2012;15(6):1110-1126.

14. Gunti L, Dass RS, Kalagatur NK. Phytofabrication of selenium nanoparticles from *Emblica officinalis* fruit extract and exploring its biopotential applications: antioxidant, antimicrobial, and biocompatibility. Front Microbiol, 2019;10:931. Doi: 10.3389/fmicb.2019.00931

15. Bunaciu AA, Aboul-Enein HY, Fleschin S. Recent applications of Fourier transform infrared spectrophotometry in herbal medicine analysis. Appl Spectrosc Rev, 2011;46(4):251-260. Doi: 10.1080/05704928.2011.565532

16. Nile SH, Park SW. HPTLC analysis, antioxidant and antigout activity of Indian plants. Iran J Pharm Res, 2014;13(2):531-539.

17. Adigun N, Oladiji A, Ajiboye T. Antioxidant and anti-hyperlipidemic activity of hydroethanolic seed extract of *Aframomum melegueta* K. Schum in Triton X-100 induced hyperlipidemic rats. S Afr J Bot, 2016;105:324-332. Doi: 10.1016/j.sajb.2016.03.015

18. Bhalodia N, Nariya P, Shukla V, Acharya R. *In vitro* antioxidant activity of hydro alcoholic extract from the fruit pulp of *Cassia fistula* Linn. AYU, 2013;34(2):209-214. Doi: 10.4103/0974-8520.119684

19. Kue CS, Tan KY, Lam ML, Lee HB. Chick embryo chorioallantoic membrane (CAM): an alternative predictive model in acute toxicological studies for anti-cancer drugs. Exp Anim, 2014;64(2):129-138. Doi: 10.1538/expanim.14-0059

20. Vinoth Prabhu V, Gopal V. Evaluation of Angiogenesis potential of *Terminalia bellirica* Roxb. by chick chorioallantoic membrane (CAM) assay. Int J Drug Dev Res, 2021;3(2):256-264.

21. Jiang Q, Lust RM, Strynar MJ, Dagnino S, DeWitt JC. Perfluorooctanoic acid induces developmental cardiotoxicity in chicken embryos and hatchlings. Toxicology, 2012;293(1-3):97-106. Doi: 10.1016/J.TOX.2012.01.005

22. Padmanaban P, Chizari A, Knop T, Zhang J, Trikalitis VD. Assessment of flow within developing chicken vasculature and biofabricated vascularized tissues using multimodal imaging techniques. Sci Rep, 2021;11:18251. Doi: 10.1038/s41598-021-97008-w

23. Prabhu V, Chidambaranathan N, Gopal V. Evaluation and quantification of angiogenesis activity of *Terminalia bellirica* Roxb. by mice sponge implantation method. J Young Pharm, 2012;4(1):22-27. Doi: 10.4103/0975-1483.93577

24. Tahergorabi Z, Khazaei M. A review on Angiogenesis and its assays. Iran J Basic Med Sci, 2012;15(6):1110-1126.

Acta Pharm. Sci. Vol 63:(2), 2025
Original article
DOI: 10.23893/1307-2080.APS6322

Healthcare professionals' familiarity, perceptions, attitudes, and obstacles towards the use of prebiotics and probiotics

Zahraa Amer HASHIM[1*], Marwa H. MOHAMMED[1], Radhwan Nidal Al-ZIDAN[2]
Hiba Radhwan TAWFEEQ[3]

1 Mosul University, College of Pharmacy, Department of Clinical Laboratory Sciences, Mosul, Iraq
2 Mosul University, College of Pharmacy, Department of Pharmaceutics, Mosul, Iraq
3 Rutgers University, Faculty of Pharmacy, Department of Nutritional Sciences, New Jersey, USA

ABSTRACT

Objective: This study aimed to investigate healthcare providers' (HCPs) knowledge and practice toward probiotics. Method: This cross-sectional study involved 294 randomly targeted pharmacists, physicians, and dentists in different health care settings (Mosul/Iraq) using an online questionnaire forum from April 2023 to July 2023. The questionnaire was divided into four main branches; demographic characteristics, familiarity, and experience, probiotic use perception and barriers against prescribing probiotics. Results: The majority (92.9%) of participants were aware of the definition of probiotics, over 77% were mindful of probiotics gastrointestinal health-effectiveness while 33.3% were aware of their dental usefulness. Around 26.8% indicated they would recommend probiotics to their patients, 4.0% refused to advise patients of using probiotics and 7.8% preferred to prescribe antibiotics over probiotics. The main reason of not prescribing probiotics was unfamiliarity with the availability of probiotics products (22.1%). The majority of HCPs (72.4%) showed their interest in broadening their knowledge about pre- and probiotics. Conclusion: This study showed that participants have insufficient knowledge to make them confident of prescribing probiotics. Tutoring HCPs regarding the use of probiotics is substantial to boost patients' wellbeing.

*Corresponding author: Zahraa Amer HASHIM
E-mail: hashimz@uomosul.edu.iq
ORCIDs:
Zahraa Amer HASHIM: 0000-0002-0635-5772
Marwa H. MOHAMMED: 0000-0003-3597-0851
Radhwan Nidal Al-ZIDAN: 0000-0003-2067-4531
Hiba Radhwan TAWFEEQ: 0000-0003-4855-8516
(Received 11 Feb 2024, Accepted 03 Jun 2024)

Keywords: probiotics, prebiotics, healthcare, prescriptions

INTRODUCTION

As it has been defined by the Food and Agriculture Organization (FAO) of the United Nations and World Health Organization, probiotics are "live microorganisms that, when administered in adequate amounts, confer a health benefit on the host"[1]. The general concept of using probiotics has been increasing recently owing to their health-beneficial effects. These effects involve alleviating a number of gastrointestinal problems such as lactose intolerance, traveler's diarrhea, gastritis, and enteritis[2]. Probiotics have also been shown effective in some oral health issues such as mal-odor, periodontitis, gingivitis, and dental caries[3]. In addition, probiotics have been investigated and demonstrated activity in a number of different diseases such as autoimmune diseases (allergy and type 2 diabetes mellitus) and chronic diseases such as chronic urogenital infections, skin infections, chronic liver diseases, over-weight, and hypercholesterinemia[4-11].

The global sales of probiotic products have been expected to grow by 48% (approximately from $2.7 billion in 2011 to $4 billion in 2016) and by 66% in 2020[12]. In spite of this global sale expansion, marketing of probiotics is poorly evaluated by the food and drug administration (FDA)[13]. Since healthcare providers (HCPs) have a substantial role in patients' health-education, their knowledge and attitudes regarding probiotics as therapy or co-therapy is vital. Additionally, exploring HCPs clinical practice trend of probiotics can aid in spotting the main obstacles preventing them from prescribing probiotics alongside prebiotics and help in addressing these barriers. HCPs knowledge, attitudes, and practice towards prescribing probiotics to their patients have been investigated in a number of studies all over the world[14-18]. However, no satisfactory data regarding HCPs of Iraq is available. Herein, the main aim of this survey-based study was to assess HCPs knowledge and attitudes toward probiotic use and to determine the potential barricades averting their clinical use in health settings.

METHODOLOGY

Participants and questionnaire

The study was a network sampling cross-sectional study directed to the HCPs in Mosul/Iraq, including pharmacists, physicians, and dentists working in academia, hospitals, private health sectors or even retirees who were working in the medical field. The study was conducted using an online questionnaire forum[19,20] from April 2023 to July 2023, starting with a pilot testing for content validity and rest-rest reliability (for memory and testing effect). The

questionnaire was delivered first to a small number of participants and adjusted gradually benefiting from the previous literature review and related investigations[21,22] to chive a reliability and content validity indices (CVI) of 0.7 for both. Basically, the questionnaire was divided into four main branches. The first one (demographic characteristics) was subdivided into further five questions about participants age, gender, profession, practice setting, and years in practice. Familiarity and experience was the second branch and this branch included questions regarding the participants' general knowledge and background about probiotics and prebiotics definition and effectiveness. The third and fourth branches were about probiotic use perception and barriers against prescribing probiotics from the participants' perspective. All questions were answered anonymously, and participants had the freedom to skip questions they did not want to answer. Ethical approval was obtained by the Ethical Approval Committee of the University of Mosul (EACUM) prior to performing the study, and all participants signed an online informed consent.

Statistical analysis

Microsoft Excel (2010) was used to tabulate the data. Percentage (%) and mean were used to express the result for categorical variables and continuous variables, respectively. Data analysis was performed using Jeffrey's Amazing Statistics Program (JASP) version 0.18.3. Chi-square test and fisher exact test were used to express statistical significance and a p value of <0.05 was considered significant.

RESULTS and DISCUSSION

Demographic characteristics

Table 1 demonstrates the demographic characteristics of the study sample. The total number of distributed surveys was 294 (considering an error rate of 5% and a confidence level of 95%), however different numbers of responses were obtained for individual questions (20% of non-respondents was taken into account). The maximum number of participants were in the age range of 24-34 years (53.4%) followed by participants of the age group 35-45 years (34.6%) while only 35 (12.0%) participants were aged>45 years. The majority of study sample was females (68.4%). Pharmacists were the main contributors to the study (62.8%) while physicians and dentist accounted for 22.8% and 14.5% of the participants, respectively. One hundred fifty-nine (55.8%) participants were hospital-based health-care providers, 81 (28.4%) were academics, 41 (14.4%) worked in private sector and only 4 (1.4%) were retirees. Considering the duration that was spent by the contributors in the medical field, 108 (37.9%) were newly graduated with an experience duration between 1-5 years. Around 20% of the participants had 6-10 and 11-15 year-experience in practice

and 13.7% had been in practice for more than 20 years.

This is a survey-based study aimed to assess the Iraqi HCPs knowledge towards the use of probiotics and the main obstacles stand against their prescription in Mosul city. Considering the study limitation, we experienced the inadequate number of HCPs who actively participated and that the study was run in one city which may affect its generalizability. Similarly, researchers who conducted an international survey study in 2019 faced the same issue[19] and justified this outcome by the poor probiotics' knowledge of some HCPs or that the questioning style of the survey did not get much agreement by some of the participants causing them to be uncomfortable to fulfill the survey entirely. Male to female ratio was unequal (1:2) which additionally contributed to the inability to statistically evaluate the finding[19]. The higher percentage of female participation may be attributed to their general interest in dietary and nutritional supplementation.

Table 1. Demographic features of study population

Characteristics	N (%)
Age range (mean, range)	
24-34	156 (53.4)
35-45	101 (34.6)
>45	35 (12.0)
Gender	
Male	93 (31.6)
Female	201 (68.4)
Profession	
Pharmacist	182 (62.8)
Physician	66 (22.8)
Dentist	42 (14.5)
Practice Setting	
Academic	81 (28.4)
Hospital	159 (55.8)
Private sector	41 (14.4)
Retired	4 (1.4)
Duration in Practice (year)	
1-5	108 (37.9)
6-10	55 (19.3)
11-15	59 (20.7)
16-20	24 (8.4)
>20	39 (13.7)

Familiarity and experiences

By assessing the participants' general knowledge and background information (Table 2), the majority (92.9%) rated themselves as being acquainted with the definition of the probiotics (160 pharmacists, 40 physicians and 21 dentists; p value=0.0001). The highest percentage (84.4%) of the study subjects were aware that probiotics are consumed as supplements or probiotics-fortified food products (156 pharmacists, 18 physicians, and 15 dentists; p value=0.0001), while around 8% of them did not know that. A minority of the participants (n=13, 5.9% and n=32, 15.0%) were unmindful that probiotics have proven clinical health beneficial effects on diarrhea and inflammatory bowel diseases, respectively while most of them (n=200, 91.3%, and n=165, 77.5%) admitted their knowledge of such effectiveness (168 pharmacists, 28 physicians, and 4 dentists; p value=0.0001). Despite that, only 33.3% of the study population were familiar with the dental application of probiotics, however, more than half of them were not (24 pharmacists, 19 physicians, and 23 dentists; p value=0.268). Around 61% assumed that there are no high risks associated with the clinical use of probiotics for the patients (83 pharmacists, 15 physicians, and 21 dentists; p value=0.00001). Considering prebiotics, 69.4% of the participants were aware of the definition of prebiotics (76 pharmacists, 41 physicians, and 10 dentists; p value=0.00001) and 35.8% were confused between pre- and probiotics definition (10 pharmacists, 32 physicians, and 22 dentists; p value=0.00029).

Though the majority of the participants rated themselves as familiar with the gastrointestinal effect of probiotics, more than half of them were unaware of the dental effectiveness of the probiotics. In a recent study, the majority of the participated dentists was found to be aware of the general probiotic term but when it comes to the in-depth knowledge of the dosing and uses they were found to be less knowledgeable[23]. This lack of confidence in prescribing probiotics to oral/dental health issues might be due to the fact that most studies approved the clinical effectiveness of probiotics for gastrointestinal problems while assessment of their use for dental problems is still in its infancy.

Table 2. Questions assessing participants' probiotics knowledge and background information

Questions	Total number of responses	N (%)	Pharmacist	Physician	Dentist	P value
Probiotics are live microorganisms that provide a health benefit when taken in adequate amounts	238					
True		221 (92.9)	160	40	21	0.0001*
False		9 (3.8)	1	4	4	
Do not know		8 (3.4)	1	3	4	
Probiotics are consumed as supplements or in probiotic-fortified foods	224					
True		189 (84.4)	156	18	15	0.0001*
False		18 (8.0)	3	7	8	
Do not know		17 (7.6)	1	8	8	
Some probiotic products have clinically proven beneficial effects on diarrhea	219					
True		200 (91.3)	168	28	4	0.0001*
False		6 (2.7)	2	1	3	
Do not know		13 (5.9)	2	6	5	
Some probiotic products are effective for inflammatory bowel disease and irritable bowel syndrome	213					
True		165 (77.5)	160	4	1	0.0001*
False		16 (7.5)	3	5	8	
Do not know		32 (15.0)	7	10	15	
Probiotics along with prebiotics could be useful for periodontal diseases and oral malodor	198					
True		66 (33.3)	24	19	23	0.268
False		30 (15.2)	8	15	7	
Do not know		102 (51.5)	35	30	37	
There are high risks associated with the clinical use of probiotics for most patients	194					
True		30 (15.5)	8	11	11	0.00001*
False		119 (61.3)	83	15	21	
Do not know		45 (23.2)	12	9	24	
Prebiotics are food that you eat that can help the good bacteria in your body	183					
True		127 (69.4)	76	41	10	0.00001*
False		28 (15.3)	5	7	16	
Do not know		28 (15.3)	2	13	13	

Prebiotics are live bacteria that are helpful to your health when you eat them	179					
True		64 (35.8)	10	32	22	0.00029*
False		76 (42.5)	34	18	24	
Do not know		39 (21.8)	6	16	17	
Prebiotics are harmful synthetic chemicals	176					
True		9 (5.1)	1	3	5	0.00001*
False		136 (77.3)	118	6	12	
Do not know		31 (17.6)	1	14	16	
Prebiotics are natural antibiotics	174					
True		50 (28.7)	12	17	21	0.00001*
False		72 (41.4)	53	8	11	
Do not know		52 (29.9)	7	23	22	

Percentage (%): Indicates the percentage of each answer of the total answer obtained for each question.
*: The result is significant at $p<0.05$ using Chi-square test (to compare the answers in-between professions: pharmacist, physician and dentist.

Probiotics uses perception and barriers against prescribing probiotics

When participants were asked about their willingness of prescribing probiotics to their patients, 26.8% indicated they would recommend probiotics to their patients (14 pharmacists, 13 physicians, and 13 dentists; p value=0.99) and that 9.2% have no concerns of such use (p value=0.73 in-between professions). However, 4.0% refused to advise their patients of using probiotics (2 pharmacists, 2 physicians, and 2 dentists; p value=0.99) and 7.8% preferred to prescribe antibiotics over probiotics in conditions treated by the two agents (2 pharmacists, 4 physicians, and 5 dentists; p value=0.56). Regarding prescribing prebiotics, 23.1% didn't mind to prescribe prebiotics to the patients along with probiotics.

The majority of survey participants (72.4%) showed their interest in broadening their knowledge about pre- and probiotics (45 pharmacists, 28 physicians, and 32 dentists; p value=0.52) and 55.9% indicated they would benefit from related workshops (40 pharmacists, 18 physicians, and 22 dentists; p value=0.59). Data are shown in Table 3.

Of the total participants in the current study, more than 90% defined probiotics correctly. In accordance, a previous study conducted in the United State got a near percentage (86.7%)[24], while a lower percentage (65.6%) was reported by Otuto et al.[25] among the HCPs. On the other hand, we found that only 69.4%

of the HCPs defined prebiotics properly. Although that probiotic agents have a beneficial impact on the body health, still there is a need to increase HCPs knowledge about prebiotics.

From the respondents' point of view, when they were asked about the main barriers that stand against probiotic uses, 13.7% justified it to the high cost of the commercial products (24 pharmacists, 15 physicians, and 15 dentists; p value=0.73), 13.0% attributed it to the lack of sufficient data on probiotics' safety (pharmacists, 13 physicians, and 16 dentists) and 12.7% doubted the quality of the available probiotic products (25 pharmacists, 9 physicians, and 16 dentists). The relatively high percentage (22.1%: 15 pharmacists, 33 physicians, and 39 dentists) claimed that the lack of information regarding the availability of probiotic products made them unaware of such medication. Of all respondents, the excuse of 64 participants (16.3%: 9 pharmacists, 24 physicians, and 31 dentists) for not prescribing probiotics was the limited or the non-availability of clinically proven probiotic products and 10.9% blamed themselves for knowing little or nothing about probiotics (10 pharmacists, 17 physicians, and 16 dentists).

When participants were questioned about their attitude of prescribing probiotics to their patients, 26.8% answered positively. In Canada, it has been reported that around 60% of community pharmacists had already recommended probiotics for patients of different ailments[26]. Similarly, but opposite to our finding, prescribing probiotics in UK and India has attained a wider acceptance than in other parts of the world[27-29]. Practically, the relatively low rate of probiotic use that was concluded in our study may be attributed, in part, to the lack of information of the available products in the market as it was justified by the participants (22.1%). Similarly, around 70% of HCPs participated in a survey conducted in more than eight of the Middle Eastern countries (Jordan, Lebanon, Palestine, Syria, Iraq, Egypt, the Gulf, and Morocco) in 2023 stated that "lack of information regarding available probiotics products" was the main barrier to probiotic prescription or use[14]. Here, we can suggest that more efforts should be made by the pharmacists who work as medical representatives to expand the HCPs awareness of these products. Jordanian HCPs were also reported to have the same probiotics marketing issue[20]. Moreover, the same study found that participants insufficient knowledge about probiotics was one of the barriers against using them which comes in accordance with our study. Academic specialists can introduce the concept of pro- and prebiotics to the undergraduate's syllabus and HCPs can benefit from related workshops. Cost is another barrier that was claimed by 13.7% of the participants to stand against

their willingness to prescribe probiotics. Locally produced probiotic products could be a good solution to overcome the importation expenses of probiotics products. A high percentage of the participants showed negative attitudes when it comes to preferring probiotics over traditional antibiotics. This point needs to get much attention since using probiotics as alternative or complementary therapy to antibiotics in certain infectious diseases has been reported to be as effective as antibiotics in addition to reducing the cost implied[30-34]. The study declared a shortage in the general knowledge and in practicing the use of probiotics by HCPs in Mosul/Iraq. The majority of participants showed their intention to learn more about probiotics; academic teachers and medical representatives may play a role in widening the awareness of the general population and HCPs in this regard. However, the small sample size of the current study limits the possibility of generalizing these findings and future studies with a large sample size is essential to make a conclusive statement.

Table 3. Questions assessing participants' probiotics use perception and reasons preventing their use

Questions	Number of responses	N (%)	Pharmacist	Physician	Dentist	P value
Do you believe probiotics are beneficial for health?	164					
Not at all		11 (6.7)	2	4	5	0.0017*[a]
A little		11 (6.7)	1	5	5	
Somewhat		48 (29.3)	7	21	20	
Quite a bit		41 (25.0)	5	16	20	
Very much		53 (32.3)	25	18	10	
If supported by peer-reviewed literature, would you be willing to recommend probiotics to your patients?	149					
Not at all		6 (4.0)	2	2	2	0.99[a]
A little		26 (17.4)	8	9	9	
Somewhat		44 (29.5)	15	14	15	
Quite a bit		33 (22.1)	12	10	11	
Very much		40 (26.8)	14	13	13	
Do you believe prebiotics are beneficial for health?	149					

Not at all		9 (6.0)	1	4	4	0.96[a]
A little		21 (14.1)	8	7	6	
Somewhat		38 (25.5)	12	15	11	
Quite a bit		41 (27.5)	13	15	13	
Very much		40 (26.8)	13	14	13	
Do you think that prebiotics are harmful to the health?	148					
Not at all		87 (58.8)	56	19	12	0.99[b]
A little		40 (27.0)	10	15	15	
Somewhat		17 (11.5)	5	6	6	
Quite a bit		4 (2.7)	1	2	1	
Very much		0 (0.0)	0	0	0	
If supported by peer-reviewed literature, would you be willing to recommend prebiotics to your patients?	147					
Not at all		14 (9.5)	4	5	5	0.98[a]
A little		28 (19.0)	8	9	11	
Somewhat		38 (25.9)	14	12	12	
Quite a bit		33 (22.4)	11	13	9	
Very much		34 (23.1)	12	12	10	
I am interested in learning more about pre- & probiotics	145					
Not at all		4 (2.8)	1	2	1	0.52[a]
A little		12 (8.3)	2	5	5	
Somewhat		11 (7.6)	3	5	3	
Quite a bit		13 (9.0)	7	2	4	
Very much		105 (72.4)	45	28	32	
I would benefit from education or workshops related to the uses o pre- & probiotics	143					
Not at all		4 (2.8)	1	1	2	0.59[a]
A little		17 (11.9)	5	7	5	
Somewhat		16 (11.2)	6	5	5	
Quite a bit		26 (18.2)	8	8	10	
Very much		80 (55.9)	40	18	22	
I accept using pre- & probiotics in the management of medical conditions	142					

Not at all		5 (3.5)	1	3	1	
A little		15 (10.6)	5	5	5	
Somewhat		35 (24.6)	12	11	12	0.79[a]
Quite a bit		38 (26.8)	17	11	10	
Very much		49 (34.5)	20	19	10	
I recommend pre- & probiotics without any concerns	141					
Not at all		42 (29.8)	16	12	14	
A little		40 (28.4)	16	8	16	
Somewhat		30 (21.3)	7	12	11	0.73[a]
Quite a bit		16 (11.3)	6	5	5	
Very much		13 (9.2)	3	4	6	
I prefer prescribing antibiotics more than probiotics in conditions which could be treated by both antibiotics and probiotics	141					
Not at all		48 (34.0)	20	10	18	
A little		31 (22.0)	7	13	11	
Somewhat		32 (22.7)	11	10	11	0.56[a]
Quite a bit		19 (13.5)	4	7	8	
Very much		11 (7.8)	2	4	5	
From your point of view, what are the most important barriers against probiotic use? (Please select all that apply)	393					
I have little or no idea about probiotics		43 (10.9)	10	17	16	
Lack of information regarding available probiotic products		87 (22.1)	15	33	39	
Limited or non-availability of clinically proven probiotic products		64 (16.3)	9	24	31	
Clinical use of probiotics is controversial		44 (11.2)	11	16	17	0.73[a]
I do not trust the quality of the available probiotic products		50 (12.7)	25	9	16	
There is limited data on the safety of probiotics		51 (13.0)	22	13	16	
The high cost of the available probiotic products		54 (13.7)	24	15	15	

Percentage (%): Indicates the percentage of each answer of the total answer obtained for each question.

*: The result is significant at $p<0.05$ using a: Chi-square test and b: Fischers exact test (to compare the answers in-between professions: pharmacist, physician, and dentist.

STATEMENT OF ETHICS

Ethical approval was obtained via the Ethical Approval Committee of the University of Mosul (ID: 22RCM002).

CONFLICT OF INTEREST STATEMENT

The authors declared no conflict of interest.

AUTHOR CONTRIBUTIONS

Zahraa Amer Hashim: design and planning, data analysis and writing; Radhwan Nidal Al-ZIDAN: questionnaire design and data collection, Marwa H. Mohammed: editing, Hiba Radhwan Tawfeeq: proof reading.

FUNDING SOURCES

The study is self-funded by the authors.

ACKNOWLEDGMENTS

The authors express their gratefulness to the College of Pharmacy/University of Mosul for facilitating the conduct of this research.

REFERENCES

1. Food and Agriculture Organization. Guidelines for the evaluation of probiotics in food [Internet]. Rome (Italy): Food and Agriculture Organization; 2002 [cited 11 Feb 2024].

2. Shaukat A, Levitt MD, Taylor BC, MacDonald R, Shamliyan TA, Kane RL, et al. Systematic review: effective management strategies for lactose intolerance. Ann Intern Med, 2010;152: 797-803. Doi: 10.7326/0003-4819-152-12-201006150-00241

3. Haukioja A. Probiotics and oral health. Eur J Dent, 2010;4(3):348-355. Doi: 10.1055/s-0039-1697851

4. Cuello-Garcia CA, Brożek JL, Fiocchi A, Pawankar R, Yepes-Nuñez JJ, Terracciano L, et al. Probiotics for the prevention of allergy: a systematic review and meta-analysis of randomized controlled trials. JACI, 2015;136(4):952-961. Doi: 10.1016/j.jaci.2015.04.031

5. Cesaro C, Tiso A, Del Prete A, Cariello R, Tuccillo C, Cotticelli G, et al. Gut microbiota and probiotics in chronic liver diseases. Dig Liver Dis, 2011;43(6):431-438. Doi: 10.1016/j.dld.2010.10.015

6. Hanson L, VandeVusse L, Jerme M, Abad CL, Safdar N. Probiotics for treatment and prevention of urogenital infections in women: a systematic review. JMWH, 2016;61(3):339-355. Doi: 10.1111/jmwh.12472

7. Zhang Q, Wu Y, Fei X. Effect of probiotics on glucose metabolism in patients with type 2 diabetes mellitus: a meta-analysis of randomized controlled trials. Med, 2016;52(1):28-34. Doi: 10.1016/j.medici.2015.11.008.

8. Shimizu M, Hashiguchi M, Shiga T, Tamura HO, Mochizuki M. Meta-analysis: effects of probiotic supplementation on lipid profiles in normal to mildly hypercholesterolemic individuals. PLoS One, 2015;10(10):e0139795. Doi: 10.1371/journal.pone.0139795

9. Huang R, Wang K, Hu J. Effect of probiotics on depression: a systematic review and meta-analysis of randomized controlled trials. Nutr, 2016;8(8):483-495. Doi: 10.3390/nu8080483

10. Hashim ZA, Qasim ZS. Assessment of *Saccharomyces boulardii* effect on rats *Staphylococcus aureus* induced skin infection: an *in-vivo* study. J Res Pharm, 2022;26(5). Doi: 10.29228/jrp.226

11. Hashim ZA, Maillard JY, Wilson MJ, Waddington RJ. Determining the potential use of biosurfactants in preventing endodontic infections. Eur J Oral Sci, 2022;130(6):e12900. Doi: 10.1111/eos.12900

12. International Probiotics Association. Global analysis of probiotic data [Internet]. 2024 [cited 11 Feb 2024]. Available from: https://internationalprobiotics.org/wp-content/uploads/Global-Analysis-of-Probiotic-Data-2024.pdf

13. de Simone C. The unregulated probiotic market. Clin Gastroenterol Hepatol, 2019;17(5): 809-817. Doi: 10.1016/j.cgh.2018.01.018

14. AL-Fawares OA, Rayyan WA, Fararjeh AFS, Seder N. Probiotic therapy: a survey of Middle Eastern healthcare providers' attitudes, beliefs, and practice patterns. J Appl Pharm Sci, 2023;13(10):172-180. Doi: 10.7324/JAPS.2023.143603

15. Ababneh M, Elrashed N, Al-Azayzih A. Evaluation of Jordanian healthcare providers' knowledge, attitudes, and practice patterns towards probiotics. Expert Rev Pharm Out, 2020;20(1):93-97. Doi: 10.1080/14737167.2019.1609354

16. Arshad MS, Saqlain M, Majeed A, Imran I, Saeed H, Saleem MU, et al. Cross-sectional study to assess the healthcare professionals' knowledge, attitude and practices about probiotics use in Pakistan. BMJ Open, 2021;11(7):e047494. Doi: 10.1136/bmjopen-2020-047494

17. Hasosah M, Qurashi M, Balkhair A, Alzahrani Z, Alabbasi A, Alzahrani M, et al. Knowledge, attitudes, and understanding of probiotics among pediatricians in different regions of Saudi Arabia. BMC Med Educ, 2021;21(1):1-7. Doi: 10.1186/s12909-021-02499-w

18. Khalesi S, Vandelanotte C, Thwaite T, Russell AM, Dawson D, Williams SL. Awareness and attitudes of gut health, probiotics and prebiotics in Australian adults. J Diet Suppl, 2021;18(4):418-432. Doi: 10.1080/19390211.2020.1783420

19. Fijan S, Frauwallner A, Varga L, Langerholc T, Rogelj I, Lorber M, et al. Health professionals' knowledge of probiotics: an international survey. IJERPH, 2019;16(17):3128. Doi: 10.3390/ijerph16173128

20. Qasim ZS, Hashim ZA. Activity of *Silybum marianum* in oral candidiasis of Albino rats. J Med Chem Sci, 2023;6(5):976-985. Doi: 10.26655/JMCHEMSCI.2023.5.5

21. Williams MD, Ha CY, Ciorba MA. Probiotics as therapy in gastroenterology: a study of physician opinions and recommendations. J Clin Gastroenterol, 2010;44(9):631-636. Doi: 10.1097/MCG.0b013e3181d47f5b

22. Ensminger A. Clinical use of probiotics: a survey of physicians' beliefs and practice patterns. [Master's Thesis]. Ypsilanti: Eastern Michigan University; 2011.

23. Krishnan L, Poorni S, Nivedhitha MS, Srinivasan MR. Knowledge, attitude, and practice of probiotics for oral health among dental students: a cross-sectional study. JIAPHD, 2022;20(3):230-233. Doi: 10.4103/jiaphd.jiaphd_23_22

24. Oliver L, Rasmussen H, Gregoire MB, Chen Y. Health care provider's knowledge, perceptions, and use of probiotics and prebiotics. Top Clin Nutr, 2014;29(2):139-149. Doi: 10.1097/01.TIN.0000445898.98017.eb

25. Amarauche CO. Assessing the awareness and knowledge on the use of probiotics by healthcare professionals in Nigeria. JYP, 2015;8(1):53-55. Doi: 10.5530/JYP.2016.1.12

26. Wheeler KE, Cook DJ, Mehta S, Calce A, Guenette M, Perreault MM, et al. Use of probiotics to prevent ventilator-associated pneumonia: a survey of pharmacists' attitudes. J Crit Care, 2016;31(1):221-226. Doi: 10.1016/j.jcrc.2015.10.016

27. Khaleel SM, Shanshal SA, Khalaf MM. The role of probiotics in colorectal cancer: a review. J Gastroint Cancer, 2023;54:1202-1211. Doi: 10.1007/s12029-022-00903-2

28. Manipal S, Kota A, Adusummili P, Satisch K, Prabu D. Awareness about probiotics in dental, medical professionals and health care providers. Unique J Med Dent Sci, 2013;1:36-40.

29. Shanshal SA, Alsaaty MH, Al-Qazaz H, Al-Zidan RN. Two *Lactobacilli* strains as adjuvant therapy in the management of irritable bowel syndrome: a randomized control trial. Ceska Slov Farm, 2024;72(5):233-241.

30. Aldabbagh, KA., Hashim, ZA., Qasim, ZS. TAS2R38 gene in relation to *Helicobacter pylori* infection and blood groups in different age groups. Pharmacia, 2023;70(1):197-202. Doi: 10.3897/pharmacia.70.e97329

31. Shen NT, Leff JA, Schneider Y, Crawford CV, Maw A, Bosworth B, et al. Cost-effectiveness analysis of probiotic use to prevent *Clostridium difficile* infection in hospitalized adults receiving antibiotics. Open Forum Infect Dis, 2017;4(3):ofx148. Doi: 10.1093/ofid/ofx148

32. Li N, Zheng B, Cai HF, Chen YH, Qiu MQ, Liu MB. Cost-effectiveness analysis of oral probiotics for the prevention of *Clostridium difficile*-associated diarrhoea in children and adolescents. JHI, 2018;99(4):469-474. Doi: 10.1016/j.jhin.2018.04.013

33. Hashim ZA. Evaluation of bacterial contents, package labelling and antimicrobial activity of some commercial probiotic products available in local market. J Res Pharm, 2022;26(3): 502-509. Doi: 10.29228/jrp.147

34. Hashim ZA. Bacteriotherapy. J Res Pharm, 2023;27(Suppl.):001-003. Doi: http://dx.doi.org/10.29228/jrp.384

Acta Pharm. Sci. Vol 63:(2), 2025
Original article
DOI: 10.23893/1307-2080.APS6323

Cisplatin treatment in EMT6 murine breast cancer cells: Impact on cell viability and molecular pathways

Tuba OĞUZ[1,2*], Arda KEBAPCI[1,2], Neşe AYŞİT[1,2,3]

1 Istanbul Medipol University, Regenerative and Restorative Medicine Research Center (REMER), Research Institute for Health Sciences and Technologies (SABITA), Istanbul, Türkiye

2 Istanbul Medipol University, Graduate School of Health Sciences, Department of Neuroscience, Istanbul, Türkiye

3 Istanbul Medipol University, School of Medicine, Department of Medical Biology and Genetics, Istanbul, Türkiye

ABSTRACT

Breast cancer is a prevalent malignancy that requires tailored treatments. Cisplatin, a platinum-based chemotherapy agent, is widely used for its anti-proliferative and pro-apoptotic properties. Understanding its molecular mechanisms is crucial for optimizing its efficacy. We investigated cisplatin's effect on the EMT6 breast cancer cell line across various doses and durations. Using MTT assay and qPCR, we examined cell survival and gene expressions of *PTEN, MAPK, NFEL2L2*, and *Survivin* after 24 h and 48 h of cisplatin treatments. The highest viability was at 5 µM after 24 h and at 1 and 5 µM after 48 h, with significant decreases at higher concentrations. Significant changes were observed in *MAPK, NFEL2L2* and *Survivin,* while *PTEN* remained unaffected. Notably, *Survivin* was upregulated at lower doses, while *NFEL2L2* and *MAPK* showed no significant changes. Our findings indicate that cisplatin induces apoptosis and alters gene expression in a dose-dependent manner, providing insights into its molecular mechanisms in EMT6 cells.

Keywords: breast cancer, ROS, gene expression, cisplatin, cell survival

*Corresponding author: Tuba OĞUZ
E-mail: oguz.tuba@gmail.com
ORCIDs:
Tuba OĞUZ: 0000-0002-7852-0394
Arda KEBAPCI: 0000-0003-0556-8247
Neşe AYŞİT: 0000-0002-4243-9092
(Received 23 Apr 2024, Accepted 15 Jun 2024)

INTRODUCTION

Breast cancer is one of the most frequently diagnosed cancers and is the second-highest ranked cancer type causing death in women[1]. Breast cancer occurs in different forms, including estrogen receptor-positive (ER-positive) breast cancer, progesterone receptor positive (PR-positive) breast cancer, HER-positive (HER2+) breast cancer, triple-negative breast cancer (TNBC), and advanced breast cancer. Different treatments are preferred according to the specific subtype of breast cancer: hormone therapy is often used for hormone-based breast cancers, while chemotherapeutic drugs are preferred for TNBC and advanced breast cancer[2]. Combining these treatments can increase efficiency of the chemotherapeutic drugs by targeting different pathways and/or reduce serious side effects by lowering the drug doses.

Cisplatin is a platinum-based and one of the commonly used chemotherapy drugs[2,3]. It functions by forming DNA adducts that create crosslinks between DNA strands[4]. These crosslinks can lead to DNA replication errors and subsequent DNA damage, which, if not repaired, results in cell death due to apoptosis[3,5]. Therefore, cisplatin exhibits anti-proliferative properties and induces apoptosis. Cisplatin has been used to treat several cancer types including breast[2], ovarian[6], lung[7], head, and neck cancer[8]. It is a cost effective, and easily accessible chemotherapy drug, making its application preferrable for different cancer types. However, it also causes serious side effects, limiting its application[9]. It has been shown that cisplatin treatment effects the levels of reactive oxygen species (ROS), the activity of mitogen-activated protein kinase (MAPK) and the phosphatidylinositol-3-kinase (PI3K)/Akt signalling pathways in various cancer cells types[2,9-13]. These pathways are believed to contribute to cisplatin-induced cytotoxicity[14,15].

In this article, we aimed to investigate the cytotoxic effects of cisplatin on the EMT6 murine breast cancer cell line across a range of doses, from low to high. We also sought to analyze cisplatin resistance and cisplatin-induced cytotoxicity in these cells, utilizing EMT6 as a model which is well-suited for such investigations, given that it is an ER-negative and triple negative breast cancer cell line. To gain insights into the molecular mechanisms underlying cisplatin response, starting from very low concentrations, we analyzed the expression profiles of key genes involved in cell survival, drug resistance and cytotoxicity—namely phosphatase and tensin homolog (*PTEN)*, mitogen-activated protein kinase (*MAPK)*, nuclear factor-erythroid 2-related factor 2 (*NFEL2L2*), and *Survivin*—following cisplatin treatment for 24 and 48 hours.

METHODOLOGY

Cell culture

EMT6 cells[16] (ATCC, CRL-2755) were cultured in RPMI-1640 (Invitrogen) medium supplemented with 10% fetal bovine serum (FBS) and 1% penicillin/streptomycin. Cells were maintained at 37°C, with 5% CO_2 and subcultured at 80-90% confluency.

Evaluation of cell viability by MTT Test

The MTT colorimetric assay was used to assess cell viability[17]. EMT6 cells were seeded into 96-well plates, at a density of 1.0 x 10^4 cells/ml in 0.1 ml complete medium. 24 hours (h) after seeding, the cells were treated with different concentrations of cisplatin. After incubation for 24h or 48h, 100 µl of MTT solution [0.5 mg/ml in DMEM w/o phenol red] was added to each well and cells were incubated for 4h at 37°C. After removal of MTT solution, the purple-blue MTT formazan precipitates were dissolved in 100 µl DMSO. The absorbance was measured at 540 nm using absorbance microplate reader. The relative cell viability was expressed as the ratio (%) of the absorbance in the cisplatin treated wells to that of non-treated control wells. The IC_{50} values for 24h and 48h cisplatin treatments were determined from the dose-response curves.

Cisplatin treatment

1.0 x 10^5 cells/ml were seeded to six-well plates. 24h after seeding, cells were treated with cisplatin with various concentrations in addition to non-treated control cells: 0.1 µM, 1 µM, 5 µM, 10 µM, and 50 µM. Cells were incubated for 24h and 48h before being collected for gene expression analysis.

qRT-PCR analysis

EMT6 cells were collected, total RNA was extracted and synthesized into cDNA. qPCR reaction was performed according to the following protocol: (a) for preincubation: 95°C for 10 minutes (min), (b) for amplification: 95°C for 10 seconds (sec), 57°C for 20 sec and 72°C for 30 sec, for 45 cycles. Samples were assayed in BioRad CFX Connect Real-Time System. $^{\Delta\Delta C}$t value was then calculated by subtracting the average Ct from the corresponding average Ct. Relative expression levels were analyzed by calculating $2^{-\Delta\Delta Ct}$. GAPDH was used as an internal control.

Statistical analysis

Data were analyzed using GraphPad Prism 8 software (GraphPad Software Inc., La Jolla, California). Statistical analysis of the data was performed with two-tailed unpaired student's t-test. For multiple comparisons, one-way anal-

ysis of variance (ANOVA) followed by Dunnett's multiple comparison. Data were normalized to GAPDH expression levels. P-values less than 0.05 were considered statistically significant.

RESULTS and DISCUSSION

Elevated cell viability at lower doses of cisplatin treatment

To assess the cytotoxic effects of cisplatin on EMT6 cancer cells at different concentrations and treatment durations, we treated the cells with varying concentrations of cisplatin and measured cell viability using MTT assay after 24 h and 48 h (Figure 1). In both 24 h and 48 h treatment groups, we observed highly significant change in cell viability in almost all concentrations of cisplatin, except 10 μM in 24 h, and 5 μM in 48 h treatment groups. The highest cell viabilities were recorded at 5 μM after 24 h treatment (Figure 1[a]), and at 1 μM and 5 μM after 48 h treatment (Figure 1[b]). In 24 h and 48 h treatment groups, cell viability dramatically decreases after 10 μM and 5 μM; respectively (Figure 1[a] and [b]). Thus, similar levels of cell survival are observed at higher doses (Figure 1[a] and [b]).

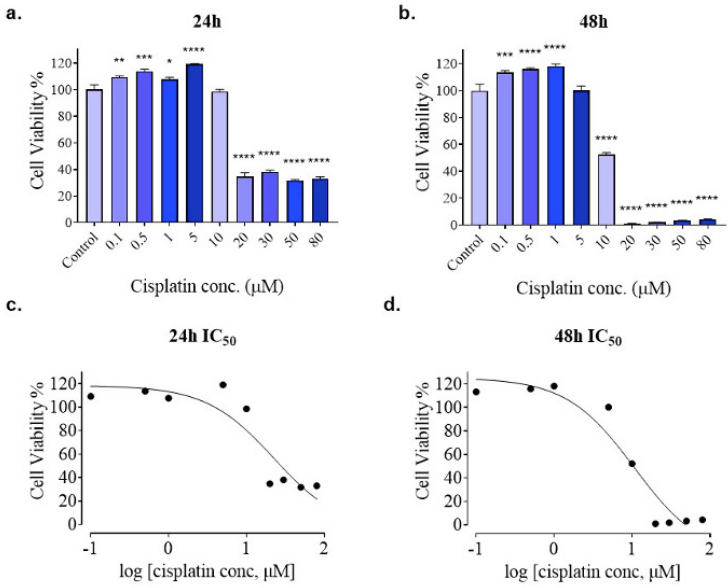

(*: p<0.05; **: p<0.01; ***: p<0.001; ****: p<0.0001)

Figure 1. Cisplatin's effect on EMT6 cell survival. Cells were incubated with different doses of cisplatin for 24h (a, c) and 48h (b, d). Cisplatin significantly improved cell viability in all concentrations below 10 μM after 24h (a) and below 5 μM after 48h treatments (b). Cisplatin significantly decreased cell viability in all concentrations above 10 μM after 24h (a) and above 5 μM after 48h treatments (b). The data were normalized to the control and presented as mean ± SEM. (n=3). Asterisks indicate statistical significance compared with the corresponding control.

Next, we calculated the IC_{50} values for cisplatin in EMT6 cells after 24 h and 48 h treatments (Figure 1[c] and- [d]). IC_{50} value for cisplatin in EMT6 cells after 24 h treatment was determined to be 22.5 μM (Figure 1[c]), and after 48 h treatment was determined to be as 10.7 μM (Figure 1[d]) (n=3).

Based on these cell viability results and calculated IC_{50} values for both treatment durations, we selected five different cisplatin concentrations to perform gene expression analysis to understand the proliferative activity at lower concentrations and cell death at higher concentrations. Next, we analyzed the gene expression levels of *PTEN*, *MAPK*, *NFEL2L2*, and *Survivin* in both treatment groups.

Cisplatin treatment shows no effect on *PTEN* expression in EMT6 cells

PTEN gene encodes for a lipid and protein phosphatase, that acts on phosphatidylinositol-3-kinase (PI3K)/Akt signaling pathway[12,13]. PTEN acts as a tumor suppressor and has an important role in controlling cell survival, proliferation and migration[12,18,19]. In healthy cells, PTEN activity inhibits the PI3K signalling pathway, thereby supressing cell survival, proliferation and migration. Mutations in the *PTEN* gene or reduced PTEN activity have been observed in various types of cancer[12,18,20].

Here, we analyzed *PTEN* expression levels in EMT6 cells with increasing concentrations of cisplatin at 24 h and 48 h treatment durations. At both time points, we did not observe any significant decrease in *PTEN* expression compared to the control (Figure 2). This observation supports the idea that cisplatin may promote cell survival and proliferation in EMT6 cells, as shown in Figure 1 (a) and (b). This could be due to an indirect effect of cisplatin on cell proliferation pathways, or suggest that EMT6 cells begin to exhibit resistance to cisplatin within 24 hours. Considering that many studies prefer a 24 h drug treatment to study drug resistance in cancer cells[21,22], it is possible that we are observing the development of cisplatin resistance in EMT6 cells.

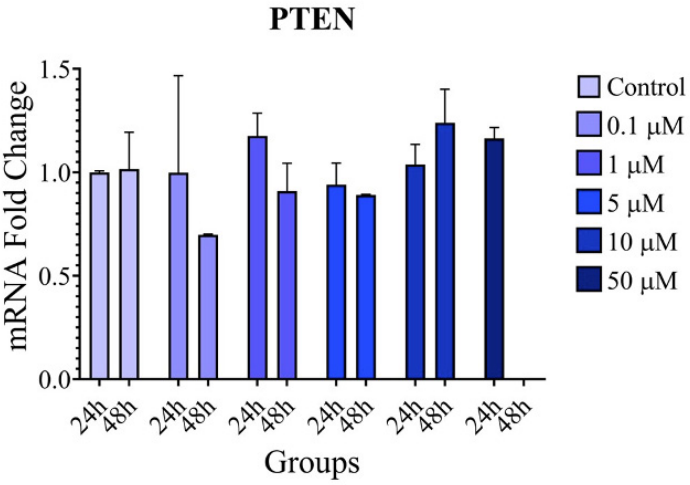

Figure 2. Relative mRNA expression levels of PTEN after 24h and 48h treatment with various cisplatin concentrations. No significant changes were observed in PTEN expression across all the tested concentrations in both treatment groups. Statistical analysis was performed using one-way ANOVA followed by Dunnett's multiple comparison test relative to the control. $p<0.05$ were considered statistically significant.

MAPK expression in EMT6 cells is elevated at higher doses of cisplatin

The MAPK signaling pathway is another important intracellular pathway which plays a crucial role in regulating survival, differentiation, cell growth and apoptosis. The activation of the MAPK pathway in response to cisplatin treatment has been extensively studied in various cancer cells, and its activation has been documented in several studies[10,11,23]. Cisplatin is known to activate the MAPK pathway, increase MAPK protein levels, and induce apoptosis[23]. Conversely, some studies have suggested that cisplatin treatment leads to MAPK activation and associated autophagy, which may counteract the apoptotic effects of cisplatin[11,24].

In our study we observed a significant increase in *MAPK* levels in the 48h treatment group at concentrations of 5 μM and a notably strong expression at 10 μM (Figure 3). When we correlate this observation with the cell viability results shown in Figure 1(b), we notice an association between increased *MAPK* expression and elevated cell death at these concentrations, likely due to apoptosis induction. Although we observed minor changes in *MAPK* levels at other concentrations in both the 48h and 24h treatment groups, these changes were not statistically significant.

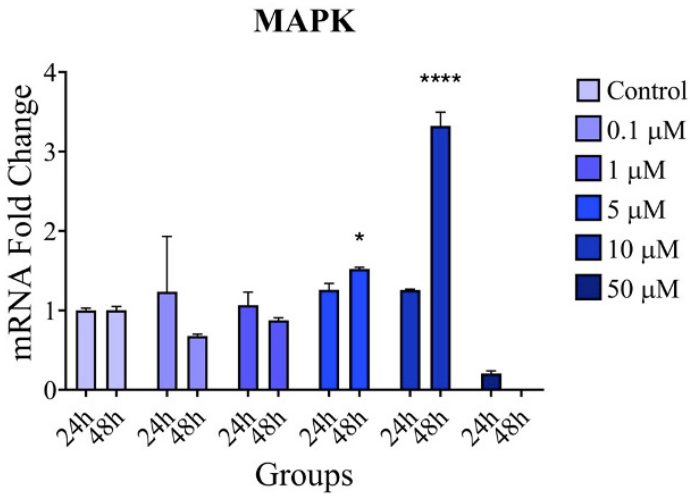

(*: p<0.05; ****: p<0.0001)

Figure 3. Relative mRNA expression levels of MAPK after 24h and 48h treatments with various cisplatin concentrations. A significant elevation in MAPK expression was observed at 5 μM, with a notably strong expression at 10 μM after 48h treatment. Statistical analysis was performed using one-way ANOVA followed by Dunnett's multiple comparison test relative to the control.

Cisplatin treatment causes dose-dependent increase in *NRF2* expression

The NRF2 transcription factor, encoded by the *NFEL2L2* gene, acts on Antioxidant Response Elements (ARE) located in the promoters of several antioxidant genes and regulates transcription of many antioxidant and detoxifying genes in different cell types[22,25]. It is an important transcription factor overseeing the maintenance of the correct oxidative balance and regulating the expression of antioxidant genes in varying oxidative stress conditions[25]. As mitochondria being the main site of energy production of the cells, free radicals are constantly generated in mitochondria[26]. If these NRF2 mediated antioxidative gene machinery will not work properly, oxidation inside the cell due to ROS production leads to several diseases, like cancer[27]. In the basal condition of normal cells, *NRF2* is expressed at lower levels. Elevated *NRF2* expression in the cancer cells decreases the efficiency and toxicity of the chemotherapeutic drug, provides cyto-protection and potentiates cancer metastasis[28,29].

In our study, we observed a dose-dependent increase in *NRF2* expression levels following cisplatin treatment. After 24h of treatment, a nearly three-fold

increase in *NRF2* expression was observed at a concentration of 10 μM of compared to the control. Moreover, overexpression of *NRF2* is at the highest level after 48h treatment with 10 μM cisplatin (Figure 4).

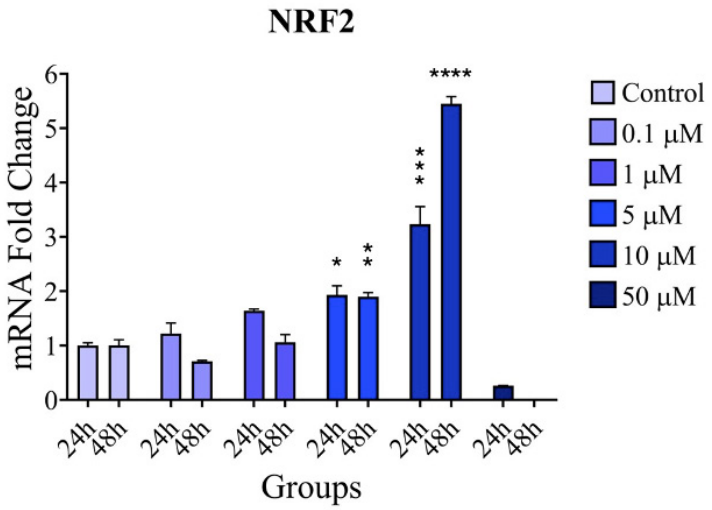

(*: p<0.05; **: p<0.01; ***: p<0.001; ****: p<0.0001)

Figure 4. Relative mRNA expression levels of NRF2 after 24h and 48h treatment with various cisplatin concentrations. At the higher doses of cisplatin, that are 5 μM and 10 μM, strong increases in gene expressions were observed in both treatment groups. Statistical analysis was performed using one-way ANOVA followed by Dunnett's multiple comparison test relative to the control.

It has been shown that cisplatin induces mitochondrial-ROS production in cancer cells at 24h treatment[5]. Thus, this has been proposed as a mechanism behind cisplatin-induced cytotoxicity observed in non-cancerous cells during chemotherapy with cisplatin[5]. Additionally, elevated ROS levels trigger the upregulation of *NRF2* gene, through NF-κB pathway[30]. Here, in our results, higher levels of *NRF2* expression are correlated with higher doses of cisplatin and supporting cisplatin-induced oxidative stress and cisplatin-induced cytotoxicity. In the 24h treatment group, there were tendencies for increased *NRF2* expression at lower cisplatin concentrations, but these changes were not statistically significant. At the lower doses of cisplatin in 48h treatment group, lower expression of *NRF2* is observed, although slightly higher expressions are observed at the same doses of 24h treatment group. This suggests that at these lower concentrations, cisplatin may not induce oxidative stress to the same extent and may instead promote cell survival and proliferation.

Moreover, observation of low ROS levels and oxidative stress adaptation of cancer cells in case of prolonged exposure to chemotherapeutic drugs, and subsequent occurrence of drug resistance have been suggested in the literature[31-34]. At 50 μM dose in 24h treatment of cisplatin, we surprisingly observed extreme and significant decrease in the ROS levels compared to 10 μM dose. Considering that a 24h exposure can be sufficient to induce drug resistance and that a 50 μM dose is relatively high, the result suggests that the observed low ROS levels at this concentration may indeed be indicative of cancer cells adapting to oxidative stress.

Cisplatin treatment at low doses increases *Survivin* expression in EMT6 cells

Survivin is a key member of the inhibitor of apoptosis protein (IAP) family, along with X-linked IAP (XIAP)[35,36]. These proteins play crucial roles in tumorigenesis, influencing various biological functions in cancer cells, and their expressions are found to be higher in some cancer types[35-37].

One of the significant functions of these proteins is their contribution to chemotherapeutic resistance by promoting cell proliferation, migration, and metastasis[35,36,38-41]. In the cancerous state, the interaction of XIAP and Survivin prevents XIAP from polyubiquitination and proteasomal degradation, and therefore inhibition of caspases and activation of NF-κB pathway occur[42]. These result in the occurrence of cancer cell metastasis and evasion from apoptosis[35].

In our study, we observed an increase in *Survivin* expression in almost all low doses of cisplatin in both 24h and 48h treatment groups (Figure 5). Statistically significant increases in *Survivin* expression were observed at concentrations of 0.1 μM and 1 μM in the 24h treatment group (Figure 5). Higher expression of *Survivin* correlates with increased cell viability observed in these concentrations shown in Figure 1(a), supporting the literature.

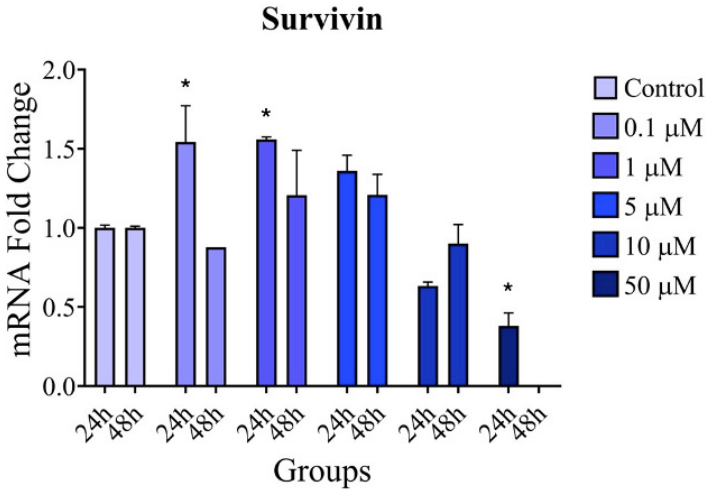

(*: p<0.05)

Figure 5. Relative mRNA expression levels of Survivin after 24h and 48h treatment with various cisplatin concentrations. A decreasing trend in gene expression levels was observed in a dose-dependent manner in both treatment groups. Statistical analysis was performed using one-way ANOVA followed by Dunnett's multiple comparison test relative to the control.

Moreover, higher doses of cisplatin led to decreased *Survivin* expression after 24 h treatment, potentially inhibiting cell proliferation (Figure 5). Similar trends, although not statistically significant, were observed in the 48 h treatment group (Figure 5). We observed statistically significant decrease in *Survivin* expression at 50 μM in the 24 h treatment group. Silencing *XIAP* and *Survivin* expression using shRNA has been shown to significantly reduce cell proliferation, increase *caspase-3/7* levels, and enhance the response to chemotherapeutics, consistent with existing literature[36,43,44]. Moreover, it has been shown that partial reversion of epithelial-mesenchymal transition (EMT) to mesenchymal-epithelial transition (MET) occurs when *XIAP* and *Survivin* expressions were inhibited, further confirming their active role in metastasis[36].

Based on these findings, we hypothesize that cisplatin may contribute to cell proliferation by upregulating *Survivin* expression at lower concentrations. These results suggest that *Survivin* plays a role in the cellular response to cisplatin, potentially influencing cell viability and proliferation in a dose-dependent manner.

In conclusion, varying doses and durations of cisplatin treatment result in differential expression of key genes regulating important molecular mechanisms in cancer cells, such as cell survival and apoptosis. Our findings indicate that

cisplatin induces apoptosis and alters gene expression levels in a dose-dependent manner. However, lower doses of cisplatin may not be sufficient to change the cancerous state of EMT6 cells, potentially supporting their survival. Looking forward, additional gene expression analyses could elucidate the molecular alterations induced by lower concentrations of cisplatin. To explore this further, low concentrations of cisplatin can be combined with nanoparticles for enhanced delivery to the cell and effects can be investigated in terms of cell survival and gene expression. Such insights could be pivotal in devising more effective treatment strategies with reduced side effects for breast cancer.

STATEMENTS OF ETHICS

No ethical approvals are required for this study.

CONFLICT OF INTEREST STATEMENT

The authors claim no conflicts of interest.

AUTHOR CONTRIBUTIONS

T.O. and A.K. designed and performed the experiments, analyzed and interpreted the data. T.O. wrote the draft; T.O., A.K., and N.A. revised the manuscript.

FUNDING SOURCES

The authors declare that there are no funding sources.

ACKNOWLEDGMENTS

We thank our colleagues for their fruitful discussions.

REFERENCES

1. Siegel RL, Miller KD, Jemal A. Cancer statistics, 2016. CA: A Cancer J Clin, 2016;66(1):7-30. Doi: 10.3322/caac.21332

2. Weng HC, Sung CJ, Hsu JL, Leu WJ, Guh JH, Kung FL, et al. The combination of a novel GLUT1 inhibitor and cisplatin synergistically inhibits breast cancer cell growth by enhancing the DNA damaging effect and modulating the Akt/mTOR and MAPK signaling pathways. Front Pharmacol, 2022;13:879748. Doi: 10.3389/fphar.2022.879748

3. Kelland L. The resurgence of platinum-based cancer chemotherapy. Nat Rev Cancer, 2007; 7(8):573-584. Doi: 10.1038/nrc2167

4. Jordan P, Carmo-Fonseca M. Molecular mechanisms involved in cisplatin cytotoxicity. Cell Mol Life Sci CMLS, 2000;57(8):1229-1235. Doi: 10.1007/pl00000762

5. Marullo R, Werner E, Degtyareva N, Moore B, Altavilla G, Ramalingam SS, et al. Cisplatin induces a mitochondrial-ROS response that contributes to cytotoxicity depending on mitochondrial redox status and bioenergetic functions. PLoS ONE, 2013;8(11):e81162. Doi: 10.1371/journal.pone.0081162

6. Hedemann N, Herz A, Schiepanski JH, Dittrich J, Sebens S, Dempfle A, et al. ADAM17 inhibition increases the impact of cisplatin treatment in ovarian cancer spheroids. Cancers, 2021;13(9):2039. Doi: 10.3390/cancers13092039

7. Li Y, Chen X, He W, Xia S, Jiang X, Li X, et al. Apigenin enhanced antitumor effect of cisplatin in lung cancer via inhibition of cancer stem cells. Nutr Cancer, 2021;73(8):1489-1497. Doi: 10.1080/01635581.2020.1802494

8. Li X, Guo S, Xiong XK, Peng BY, Huang JM, Chen MF, et al. Combination of quercetin and cisplatin enhances apoptosis in OSCC cells by downregulating xIAP through the NF-κB pathway. J Cancer, 2019;10(19):4509-4521. Doi: 10.7150/jca.31045

9. Liu H, Lee JI, Ahn TG. Effect of quercetin on the anti-tumor activity of cisplatin in EMT6 breast tumor-bearing mice. Obstet Gynecol Sci, 2019;62(4):242-248. Doi: 10.5468/ogs.2019.62.4.242

10. Guégan JP, Ezan F, Théret N, Langouët S, Baffet G. MAPK signaling in cisplatin-induced death: predominant role of ERK1 over ERK2 in human hepatocellular carcinoma cells. Carcinogenesis, 2013;34(1):38-47. Doi: 10.1093/carcin/bgs317

11. Jiang Y, Ji F, Liu Y, He M, Zhang Z, Yang J, et al. Cisplatin-induced autophagy protects breast cancer cells from apoptosis by regulating yes-associated protein. Oncol Rep, 2017;38(6):3668-3676. Doi: 10.3892/or.2017.6035

12. Ciuffreda L, Falcone I, Incani UC, Curatolo AD, Conciatori F, Matteoni S, et al. PTEN expression and function in adult cancer stem cells and prospects for therapeutic targeting. Adv Biol Regul, 2014;56:66-80. Doi: 10.1016/j.jbior.2014.07.002

13. deGraffenried LA, Fulcher L, Friedrichs WE, Grünwald V, Ray RB, Hidalgo M. Reduced PTEN expression in breast cancer cells confers susceptibility to inhibitors of the PI3 kinase/Akt pathway. Ann Oncol, 2004;15(10):1510-1516. Doi: 10.1093/annonc/mdh388

14. Florea AM, Büsselberg D. Cisplatin as an anti-tumor drug: cellular mechanisms of activity, drug resistance and induced side effects. Cancers, 2011;3(1):1351-1371. Doi: 10.3390/cancers3011351

15. Dasari S, Tchounwou PB. Cisplatin in cancer therapy: molecular mechanisms of action. Eur J Pharmacol, 2014;740:364-378. Doi: 10.1016/j.ejphar.2014.07.025

16. Rockwell SC, Kallman RF, Fajardo LF. Characteristics of a serially transplanted mouse mammary tumor and its tissue-culture-adapted derivative. J Natl Cancer Inst, 1972;49(3):735-749. Doi: 10.1093/jnci/49.3.735

17. Ghasemi M, Turnbull T, Sebastian S, Kempson I. The MTT assay: utility, limitations, pitfalls, and interpretation in bulk and single-cell analysis. Int J Mol Sci, 2021;22(23):12827. Doi: 10.3390/ijms222312827

18. Lee JI, Soria JC, Hassan KA, El-Naggar AK, Tang X, Liu DD, et al. Loss of PTEN expression as a prognostic marker for tongue cancer. Arch Otolaryngol Head Neck Surg, 2001;127(12):1441-1445. Doi: 10.1001/archotol.127.12.1441

19. Gil A, Andrés-Pons A, Fernández E, Valiente M, Torres J, Cervera J, et al. Nuclear localization of PTEN by a ran-dependent mechanism enhances apoptosis: involvement of an n-terminal nuclear localization domain and multiple nuclear exclusion motifs. Mol Biol Cell, 2006;17(9):4002-4013. Doi: 10.1091/mbc.e06-05-0380

20. Qi Y, Liu J, Chao J, Scheuerman MP, Rahimi SA, Lee LY, et al. PTEN suppresses epithelial–mesenchymal transition and cancer stem cell activity by downregulating Abi1. Sci Rep, 2020;10(1):12685. Doi: 10.1038/s41598-020-69698-1

21. Singh M, Chaudhry P, Fabi F, Asselin E. Cisplatin-induced caspase activation mediates PTEN cleavage in ovarian cancer cells: a potential mechanism of chemoresistance. BMC Cancer, 2013;13(1):233. Doi: 10.1186/1471-2407-13-233

22. Yamagishi N, Yamamoto Y, Nishi T, Ito T, Kanai Y. Lansoprazole protects hepatic cells against cisplatin-induced oxidative stress through the p38 MAPK/ARE/Nrf2 pathway. PLOS ONE, 2023;18(6):e0287788. Doi: 10.1371/journal.pone.0287788

23. Ramesh G, Reeves WB. p38 MAP kinase inhibition ameliorates cisplatin nephrotoxicity in mice. Am J Physiol-Ren Physiol, 2005;289(1):166-174. Doi: 10.1152/ajprenal.00401.2004

24. Yu L, Gu C, Zhong D, Shi L, Kong Y, Zhou Z, et al. Induction of autophagy counteracts the anticancer effect of cisplatin in human esophageal cancer cells with acquired drug resistance. Cancer Lett, 2014;355(1):34-45. Doi: 10.1016/j.canlet.2014.09.020

25. Forman HJ, Zhang H. Targeting oxidative stress in disease: promise and limitations of antioxidant therapy. Nat Rev Drug Discov, 2021;20(9):689-709. Doi: 10.1038/s41573-021-00233-1

26. Franci L, Vallini G, Bertolino FM, Cicaloni V, Inzalaco G, Cicogni M, et al. MAPK15 controls cellular responses to oxidative stress by regulating NRF2 activity and expression of its downstream target genes. Redox Biol, 2024;72:103131. Doi: 10.1016/j.redox.2024.103131

27. Davalli P, Mitic T, Caporali A, Lauriola A, D'Arca D. ROS, Cell senescence, and novel molecular mechanisms in aging and age-related diseases. Oxidative Med Cell Longev, 2016;3565127. Doi: 10.1155/2016/3565127

28. Kumar H, Kumar RM, Bhattacharjee D, Somanna P, Jain V. Role of Nrf2 signaling cascade in breast cancer: strategies and treatment. Front Pharmacol, 2022;13:720076. Doi: 10.3389/fphar.2022.720076

29. Lamy M, Ferreira A, Dias JS, Braga S, Silva G, Barbas A. Notch-out for breast cancer therapies. N Biotechnol, 2017;39(Pt B):215-221. Doi: 10.1016/j.nbt.2017.08.004

30. Bellezza I, Giambanco I, Minelli A, Donato R. Nrf2-Keap1 signaling in oxidative and reductive stress. Biochim Biophys Acta Mol Cell Res, 2018;1865(5):721-733. Doi: 10.1016/j.bbamcr.2018.02.010

31. Trachootham D, Alexandre J, Huang P. Targeting cancer cells by ROS-mediated mechanisms: a radical therapeutic approach? Nat Rev Drug Discov, 2009;8(7):579-591. Doi: 10.1038/nrd2803

32. Junior PL de S, Câmara DAD, Porcacchia AS, Fonseca PMM, Jorge SD, Araldi RP, et al. The roles of ROS in cancer heterogeneity and therapy. Oxidative Med Cell Longev, 2017;2467940. Doi: 10.1155/2017/2467940

33. Maiti AK. Gene network analysis of oxidative stress-mediated drug sensitivity in resistant ovarian carcinoma cells. Pharmacogenomics J, 2010;10(2):94-104. Doi: 10.1038/tpj.2009.49

34. Yang H, Villani RM, Wang H, Simpson MJ, Roberts MS, Tang M, et al. The role of cellular reactive oxygen species in cancer chemotherapy. J Exp Clin Cancer Res, 2018;37(1):266. Doi: 10.1186/s13046-018-0909-x

35. Dizdar L, Tomczak M, Werner TA, Safi SA, Riemer JC, Verde PE, et al. Survivin and XIAP expression in distinct tumor compartments of surgically resected gastric cancer: XIAP as a prognostic marker in diffuse and mixed type adenocarcinomas. Oncol Lett, 2017;14(6):6847-6856. Doi: 10.3892/ol.2017.6999

36. Yi XP, Han T, Li YX, Long XY, Li WZ. Simultaneous silencing of XIAP and survivin causes partial mesenchymal-epithelial transition of human pancreatic cancer cells via the PTEN/PI3K/Akt pathway. Mol Med Rep 2015;12(1):601-608. Doi: 10.3892/mmr.2015.3380

37. Yang L, Cao Z, Yan H, Wood WC. Coexistence of high levels of apoptotic signaling and inhibitor of apoptosis proteins in human tumor cells: implication for cancer specific therapy. Cancer Res, 2003;63(20):6815-6824.

38. Mita AC, Mita MM, Nawrocki ST, Giles FJ. Survivin: key regulator of mitosis and apoptosis and novel target for cancer therapeutics. Clin Cancer Res, 2008;14(16):5000-5005. Doi: 10.1158/1078-0432.ccr-08-0746

39. Srinivasula SM, Ashwell JD. IAPs: what's in a name? Mol Cell, 2008;30(2):123-135. Doi: 10.1016/j.molcel.2008.03.008

40. Mehrotra S, Languino LR, Raskett CM, Mercurio AM, Dohi T, Altieri DC. IAP regulation of metastasis. Cancer Cell, 2010;17(1):53-64. Doi: 10.1016/j.ccr.2009.11.021

41. Bertrand MJM, Milutinovic S, Dickson KM, Ho WC, Boudreault A, Durkin J, et al. cIAP1 and cIAP2 facilitate cancer cell survival by functioning as E3 ligases that promote RIP1 ubiquitination. Mol Cell, 2008;30(6):689-700. Doi: 10.1016/j.molcel.2008.05.014

42. Lu M, Lin SC, Huang Y, Kang YJ, Rich R, Lo YC, et al. XIAP induces NF-κB activation via the BIR1/TAB1 interaction and BIR1 dimerization. Mol Cell, 2007;26(5):689-702. Doi: 10.1016/j.molcel.2007.05.006

43. Kunze D, Kraemer K, Erdmann K, Froehner M, Wirth MP, Fuessel S. Simultaneous siRNA-mediated knockdown of antiapoptotic BCL2, Bcl-xL, XIAP and Survivin in bladder cancer cells. Int J Oncol, 2012;41(4):1271-1277. Doi: 10.3892/ijo.2012.1549

44. Rückert F, Samm N, Lehner AK, Saeger HD, Grützmann R, Pilarsky C. Simultaneous gene silencing of Bcl-2, XIAP and Survivin re-sensitizes pancreatic cancer cells towards apoptosis. BMC Cancer, 2010;10(1):379. Doi: 10.1186/1471-2407-10-379

Acta Pharm. Sci. Vol 63:(2), 2025
Original article
DOI: 10.23893/1307-2080.APS6324

Investigation the selective anticancer activities of montmorillonite and curcumin on the pancreatic and breast cancer

Metin TURAN[1*], Tugba KIRKIK[2], Mustafa GUZEL[3], Ayten ALTINTAS[4]

1 Istanbul Medipol University, Complemantary and Traditional Medicine, Istanbul, Türkiye
2 Istanbul Medipol University, Molecular Medicine and Biotechnology, Istanbul, Türkiye
3 US Food and Drug Administration, Pharmaceutical Quality, Silver Spring, USA
4 Istanbul Medipol University, Department of Medical History and Deontology, Istanbul, Türkiye

ABSTRACT

Breast and pancreatic cancers are among the leading causes of death worldwide. In this study, the anticancer activities of natural-based montmorillonite and modified curcumin are examined in pancreatic and breast cancer. MRC-5, PANC-1, and MDA-MB-231 cell lines are used as healthy fibroblast cell lines (control), pancreatic and breast cancer respectively. 10-1000 μg/mL doses applied to each cell line. As a result, we obtained that montmorillonite has no significant reducing effects on cell viability in the MRC-5 cell line. IC_{50} values were 1456 μg/mL for MDA-MB-231 and 1166 μg/mL for PANC-1 cells. When modified curcumin therapy doses were applied, IC_{50} values were 215 μg/mL for MRC-5, 56.45 μg/mL for MDA-MB-231, and 72.34 μg/mL for PANC-1 cells. In conclusion, this study demonstrates that these two natural compounds have antitumoral effects on pancreatic and breast cancer. These compounds may be useful in the development of natural-based treatments for breast and pancreatic cancer.

Keywords: Bentonite, montmorillonite, curcumin, pancreatic neoplasms, breast neoplasms

*Corresponding author: Metin TURAN
E-mail: metin.turan@std.medipol.edu.tr
ORCIDs:
Metin TURAN: 0000-0003-0381-8433
Tugba KIRKIK: 0009-0002-4651-1028
Mustafa GUZEL: 0000-0002-1423-0435
Ayten ALTINTAS: 0000-0003-0531-0035
(Received 22 Mar 2024, Accepted 27 Jun 2024)

INTRODUCTION

Breast cancer (BC) and pancreatic cancer (PC) are two of the most lethal cancers worldwide, and effective treatment options for these diseases are urgently needed. Montmorillonite, a natural mineral, and curcumin, a natural compound derived from the spice turmeric, have shown potential anticancer effects *in vitro* and *in vivo*. In this study, we examined the anticancer activities on pancreatic and breast cancer by using natural compounds of montmorillonite and modified curcumin.

Pancreatic cancer

PC ranks 12th among the most common types of cancer worldwide and 7th in terms of cancer-related mortality[1]. Some risk factors for PC can be altered, like smoking, obesity, diabetes, chronic pancreatitis, and exposure to specific workplace chemicals. However, there are immutable risk factors such as age, gender, race, family history, inherited genetic syndromes, and chronic pancreatitis stemming from a gene mutation[2,3]. Surgical removal is a potential treatment option for localized PC tumors, but early detection is challenging due to the lack of accurate and reliable detection methods. As a result, most patients with PC are diagnosed at advanced stages, and only 10-20% of them have tumors that are eligible for surgical removal. Adjuvant therapies, such as chemotherapy and radiotherapy, are commonly used after surgery to improve the survival rate of patients with PC[4]. Unfortunately, PC is known for its aggressive nature and fast spread, which can lead to fatal outcomes. The 5-year survival rate for localized PC tumors is 42%, while for regional metastasized tumors, it is 14%, and for distal metastasized tumors, it is only 3%[5]. Despite advancements in medical technology, there is still no effective medical treatment for metastasized PC.

Breast cancer

BC is the most common cancer and 5th in terms of cancer-related mortality[1]. Several BC risk factors can be changed, including alcohol consumption, being overweight or obese, physical inactivity, nulliparity, not breastfeeding, and the use of birth control or menopausal hormone therapy. Conversely, there are also BC risk factors that cannot be changed, such as being female, increasing age, inheriting specific gene mutations, having a family history of BC, having a personal history of BC, ethnicity, height, dense breast tissue, specific benign breast conditions, early onset of menstruation, late onset of menopause, exposure to radiation to the chest, and exposure to diethylstilboestrol[6]. The 5-year survival rate of BC tumors is 90%[7]. Due to the presence of numerous muta-

tions, the development of resistance to treatments, and individual variations in treatment response in BC, there is a focus on alternative therapies. In addition to traditional treatments such as surgery, chemotherapy, and radiotherapy in BC treatment, receptor inhibitors and nanotechnological approaches are among the current therapies[8-10].

Effects of montmorillonite on breast and pancreatic cancer

Montmorillonite (MMT) is a natural nanomolecular clay[11] that has been used for treatment for over 100 years and has been observed to have no side effects in phase 1 and phase 2 studies[12,13]. According to the WHO, MMT is mainly composed of highly colloidal and plastic clays that belong to the Smectite Group and are predominantly made up of the clay mineral MMT. In the healthcare sector today, 99% of the clays used are from the Smectite Group. The most common subgroup among the Smectite Group is MMT (Bentonite). Its chemical formula is (Na, Ca)(Al, Mg)(Si_4O_{10})(OH)[14]. MMT has a large surface area of 750 m^2/gram, possesses high water absorption and swelling properties (2-20 times its volume). Additionally, in suspension form, it has the ability to release a significant amount of negative (-) ions into the environment[15,16]. Most of the substances that threaten human health, from the air we breathe to the water we drink, such as heavy metals, toxins, viruses, bacteria, and radiation, are positively charged (+) ions. MMT has a nano-particle structure, and its particles are layered. Its particle size ratio is around 1000:1. It is not harmed by stomach acid and can easily pass through the intestines, skin, and blood-brain barrier[17]. It is excreted from the body without being metabolized, through faces, urine, sweat, and tears. MMT is not a chemically synthesized compound, but rather a natural substance that nature has provided us. MMT is classified as SCOGS Type 1 by the FDA, meaning that "there is no evidence to demonstrate or suggest reasonable grounds to suspect, a hazard to the public when they are used at levels that are currently in use or might reasonably be expected in the future"[18]. Due to its properties, MMT can be used in detoxification, immune system disorders, gastrointestinal system disorders, metabolic syndrome, skin diseases, radiation protection, and reducing the adverse effects of chemotherapy and radiation therapy in cancer patients[19-26]. Preclinical and clinical studies on MMT have shown that it is antibacterial, antiviral, antifungal, antitumor, and radioprotective. Additionally, MMT is a good drug carrier. MMT has been modified with drugs used in cancer treatment such as Docetaxel, Irinotecan, 5-fluorouracil, and Tamoxifen, and has been shown to increase their effects and reduce their side effects[27]. Recent studies on MMT have observed that it has antitumor properties[25-28]. A study by Cervini-Silva et al. in 2016 showed

that MMT inhibits the development of high-grade gliomas[28]. MMT has an antiproliferative effect that is affected by both cell type and protein levels. In a 2020 study conducted by Sabzevari et al., MMT was found to induce G0/G1 phase arrest in MRC-5 and HT-29 cell cultures by modulating the expression of the P21, P27, and Cyclin D1 genes. Additionally, MMT induced S phase arrest in HepG2 cell cultures by regulating the expression of the mTOR gene. As a result of this study, it has been demonstrated that MMT induces apoptosis in cells by modulating pro/anti-apoptotic genes[25]. In an *in vitro* study conducted by Abduljauwad et al., MMT exhibited a significant reduction in melanoma cell viability and proliferation in a dose-dependent manner. In the same study's *in vivo* tumor model, treatment with MMT significantly decreased tumor mass and reduced cell mitosis[26]. Based on these studies, it has been proven that MMT has different effects on each tumor. There are no studies on the effect of MMT on pancreatic and breast tumors.

Effects of curcumin on breast and pancreatic cancer

Turmeric's primary active compound, curcumin, has a long history of use in traditional medicine spanning centuries and has recently gained attention for its potential health benefits. The vibrant yellow compound, extracted from the *Curcuma longa* plant, is a member of the ginger family and exhibits powerful anti-cancer, antibacterial, anti-inflammatory, and antioxidant characteristics[29]. Research findings indicate that curcumin exhibits tumor-suppressing properties across a range of cancer types, encompassing breast cancer, leukemia, lymphoma, neurological cancers, gastrointestinal cancers, ovarian cancer, lung cancer, head and neck squamous cell carcinoma, melanoma, and genitourinary cancers[30]. Research has shown that curcumin may be beneficial in the treatment of various conditions, including arthritis, diabetes, Alzheimer's disease, and cancer[31-33]. Studies have demonstrated its ability to inhibit tumor formation in different cancer types by affecting multiple signaling pathways.

In PC cells, curcumin has been shown to inhibit KRAS expression and stabilize p53 to prevent mutations[34]. It also exhibits anti-angiogenic effects by inhibiting the expression of VEGF and VEGFR1 genes and increases apoptosis by inhibiting COX-2 and EGFR[35]. Furthermore, it prevents metastasis by regulating miRNAs and blocking CAF-mediated EMT[36]. Curcumin also affects signaling pathways such as EGF-Akt, EGF-ERK, Hedgehog, Wnt-β-catenin, PI3K-Akt, and ATM-Chk1, thereby demonstrating anti-tumoral effects[37]. Additionally, it regulates pro-inflammatory cytokines (IL-8↓, IL-8R↑) and inhibits transcription factors such as NF-κB, Sp1, Sp3, and Sp4, thereby exerting anti-tumoural effects[38] (Table 1).

Table 1. Effect of curcumin on pancreatic cancer

Prevent mutations	**Inhibit KRAS expression and stabilize p53**
Anti-angiogenic effects	Inhibiting the expression of VEGF and VEGFR1 genes
Increases apoptosis	Inhibiting COX-2 and EGFR
Signaling pathways	EGF/ERK↓, EGF/Akt↓, Hedgehog↓, PI3K/Akt↓, ATM/Chk1↑, and Wnt/b-catenin↓
Pro-inflammatory cytokines	IL-8↓, IL-8R↑
Transcription factors	Inhibits NF-κB and AP-1

In BC, curcumin has been found to inhibit the activity of ornithine decarboxylase, which is an enzyme that plays a role in cell proliferation[39]. Moreover, curcumin has been demonstrated to suppress the expression of various genes and enzymes in breast cancer cells, including the aromatic hydrocarbon receptor, cytochrome P450 1A1, COX-1, and COX-2 enzymes, and VEGF and b-FGF growth factors. Curcumin also induces the expression of p-53-dependent Bax, which can lead to apoptosis (cell death) in cancer cells. Furthermore, curcumin has been found to reduce the expression of MMP-2 and increase the expression of TIMP-1, which can inhibit cancer cell invasion and metastasis. Ultimately, curcumin has demonstrated its ability to inhibit the activation of several transcription factors, including AP-1 and NF-κB, both of which are involved in the proliferation and growth of cancer cells[40].

Unfortunately, due to the breakdown of curcumin in the stomach, low absorption in the intestines, and rapid metabolism in the body, its efficacy in clinical application was limited[41]. As a result, enhancing the drug delivery system becomes a crucial strategy to augment the bioavailability of curcumin and enhance its effectiveness. Several drug delivery systems, including micelles, liposomes, nanoparticles, and cyclodextrins, have been devised to enhance the solubility and stability of curcumin, thus improving its delivery to target tissues[42]. MMT, a type of clay, has a high surface area and adsorption capacity, which allows it to bind to curcumin and protect it from degradation in the gastrointestinal tract. This, in turn, enhances the absorption of curcumin from the gastrointestinal tract into the bloodstream and increases its effectiveness in the body. In a study conducted by Karataş et al., it was shown that modified curcumin with montmorillonite passes through the intestine 2000 times more than PLGA and significantly increases the retention time in the body[43]. In preclinical studies, employing MMT as a carrier for curcumin has yielded promising results. Therefore, the modification of curcumin with MMT has been shown to improve its bioavailability and retention time in the body.

As mentioned above, in the past decade, much research has focused on the effect of curcumin on cancer cells. However, there is no study in the literature about MMT and curcumin with enhanced bioavailability using MMT (as a drug carrier) on pancreatic and breast tumors. Hence, this study endeavors to examine the anticancer effects of modified curcumin with MMT and MMT alone on breast and pancreatic cancer cells, thereby offering novel insights to the existing literature.

METHODOLOGY

Cell culture and cell growth

Human pancreatic cancer cell line (PANC-1, CRL-1469, ATCC, Rockville, MD, USA), human breast cancer cell line (MDA-MB-231, HTB-26, ATCC, Rockville, MD, USA), and healthy human fibroblast lung cells as control (MRC-5, CCL-171, ATCC, Rockville, MD, USA) were utilized in the study. All cells were cultured in high glucose DMEM (Pan Biotech, Aidenbach, Germany) supplemented with 10 % heat-inactivated FBS (Gibco Company, Grand Island, NY, USA), 100 IU/mL of penicillin, and 100 μg/mL of streptomycin (Pan Biotech, Aidenbach, Germany) in a humidified atmosphere at 37°C with 5% CO_2. Upon reaching over 80% confluency, cells were harvested using 0.25% trypsin-EDTA (Gibco Company, Grand Island, NY, USA).

Preparation of montmorillonite and montmorillonite (as a drug carrier) along with modified solutions

MMT (MediClay) and modified curcumin solutions were taken from Alya Mineral Company, Ordu, Türkiye. MMT solution was a liquid form and consisted of water and montmorillonite (5.4 g montmorillonite / 60 mL). Modified curcumin solution consisted of 0.5 mg/ml *Rosa canina* L., 4 mg/ml *Curcuma longa*, 1 mg/ml *Rosmarinus officinalis* extracts, and 70 mg/ml MMT (To enhance the bioavailability of curcumin). Experiments were done for MMT and modified curcumin solutions separately. MMT dilutions were made with sterilized distilled water for 10, 25, 50, and 100 μg/mL doses. Following doses which were 500, 750, and 1000 μg/mL were made with DMEM. Preparing MMT along with modified curcumin solutions was mentioned in Figure 1. All of the modified curcumin testing doses were made in DMEM.

Figure 1. Montmorillonite and montmorillonite along with modified curcumin solutions. The left one is the montmorillonite clay solution which is composed of montmorillonite and water (a). Right one is modified curcumin (Bentonizer) solution which is composed of *Curcuma longa, Rosmarinus officinalis* and *Rosa canina* L. (b). 100 mL of concentrated bentonizer was poured into a 400 mL montmorillonite bottle. It was shaken for 2-3 minutes. After 20 hours in the refrigerator at +4°C, it became ready for use.

Cytotoxicity assay

A cytotoxicity assay was conducted using an MTT solution. PANC-1 and MDA MB-231 cells were seeded in 96-well plates at a density of $8x10^3$ cells per well. MRC-5 cells were seeded at a density of $1x10^4$ cells per well due to their slower doubling time compared to the cancer cell lines. The cell lines were then incubated for 24 hours. After incubation, the medium was removed, and the appropriate doses were applied to each well for an additional 24 hours. Following this incubation period, the supernatant was carefully removed, and MTT solution (5 mg/mL in 100 µL medium) was added to each well. The plates were then incubated for 2.5 hours. Afterward, the supernatant was removed, and 200 µL of DMSO was added to each well. The absorbance was measured at 570 nm using a spectrophotometer (Thermo Scientific, USA). The experiment was performed in triplicate for each condition.

RESULTS and DISCUSSION

The anticancer activities of natural-based MMT and MMT along with modified curcumin were measured depending on cell viability for MRC-5, PANC-1, and MDA-MB 231 cell lines by using an MTT assay. MRC-5 cells, PANC-1 cells, and MDA-MB-231 cells belong to healthy cell control, pancreatic cancer, and breast cancer respectively. The MTT assay is based on the metabolic activity that reduction of tetrazolium salts to formazan crystals. The results of MMT and modified curcumin are presented in concentration-dependent cell viability graphs. The cell viability percentages for 10-1000 µg/mL doses of MRC-5, MDA MB-231, and PANC-1 cells of the MMT. The effect of MMT on MRC-5

cells showed that increased in 10, 50, and 100 µg/mL. The cell viability exhibited a decrease below 100% specifically in response to the administration of doses at 750 and 1000 µg/µl. However, within the given dose ranges, no cytotoxic effect was observed, and the viability did not drop below 90%. In MDA MB-231 (human breast cancer cell line) cells, MMT demonstrated a consistent decrease across the administered doses. A 40% decrease in viability was observed with the application of 1000 µg/µl of MMT. The cell viability decreased to below 80% when the smallest doses of 10 ug/ml were given to the PANC1-1 cell line. MMT has shown a more effective result at lower doses in PANC-1 cells compared to MDA-MB-231 cells. IC_{50} values of MDA MB-231 and PANC-1 cells were approximately 1456 and 1166 µg/mL for MMT (Figure 2).

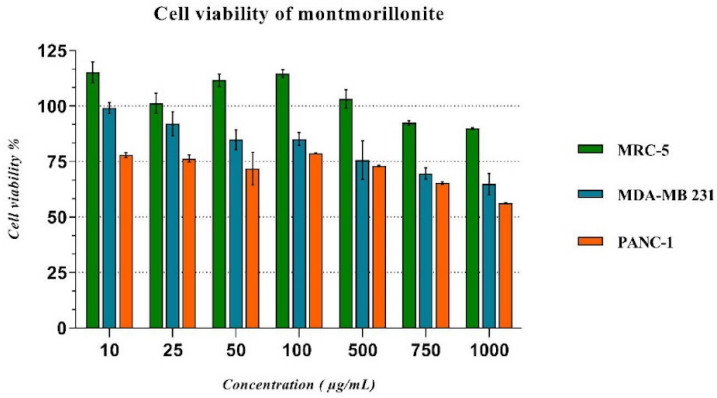

Figure 2. Percentage cell viability graph according to the doses of montmorillonite applied to MRC-5, MDA-MB-231, and PANC-1 cells. 10-1000 µg/mL doses were applied to each cell line. Error bars show SEM.

The anticancer effects of modified curcumin for 10-1000 µg/mL doses of MRC-5, MDA MB-231, and PANC-1 cells. The cell viability of the MRC-5 cell line reduced as of 25 µg/mL and sharply below 30% in 500 µg/mL. However, in MDA-MB-231 cells, a decrease in viability was observed at the lowest dose (10 µg/mL), indicating cell viability decreased to 50% when a 50 µg/mL dose was applied. In PANC-1 cells, similar to MDA-MB-231 cells, a decrease in viability was also observed at the lowest dose of 10 µg/mL, with viability dropping to approximately 75%. Viability dropped below 50% when a dose of 100 µg/mL was applied. IC_{50} values of modified curcumin for MRC-5, MDA-MB-231, and PANC-1 cells were about 215, 56.45, and 72.34 µg/mL respectively (Figure 3). Looking at both graphs, it is evident that when MMT is applied alone, it promotes an increase in viability in healthy cell lines. In cancer cell lines, however, viability decreased by approximately 50% with the application of the highest

dose. However, when MMT (as a drug carrier) is applied in combination with modified curcumin, decreases in viability in cancer cells have been observed even at low doses. Within the dose ranges that kill 50% of cancer cells, viability in healthy cells remains high. These results indicate that modified curcumin has been successful in killing cancer cells and MMT has been found to effectively kill cancer cells without causing harm to healthy cells.

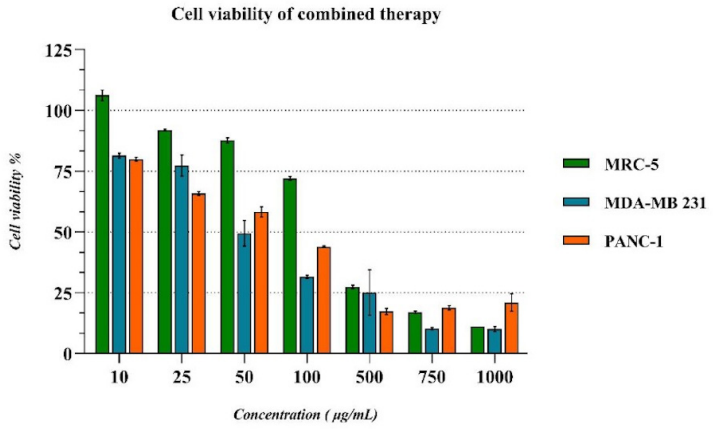

Figure 3. Percentage cell viability graph based on the doses of modified curcumin applied to MRC-5, MDA-MB-231, and PANC-1 cells. 10-1000 µg/mL doses were applied to each cell line. Error bars show SEM.

Based on the results of our study, it is evident that both MMT and combined therapy have cytotoxic effects on breast and pancreatic cell lines. It has been proven that MMT has no cytotoxic effects on healthy fibroblast cells, and in fact, it has been observed to increase cell viability at doses of 10, 50, and 100 µg/mL. However, in the breast cancer cell line, MMT exhibited cytotoxic effects at a dose of 25 µg/mL and above, with an IC_{50} of 1456 µg/mL. Similarly, the pancreatic cancer cell line, exhibited cytotoxic effects at a dose of 10 µg/mL and above, with an IC_{50} of 1166 µg/mL. These findings indicate that the effects of MMT vary in different cell lines, and it even suggests that MMT is capable of distinguishing between healthy and cancer cells.

In a study conducted by Sabzevari et al., MMT was found to have a cytotoxic effect of around 40% on MRC5 healthy lung fibroblast cells at a dose of 1000 µg/mL, whereas, in our study, cell viability was in the range of 98% at the same dose[25]. This study also showed that MMT increased cell viability at low doses, but then decreased it. In this study, it is hypothesized that the low cell growth observed at low doses is attributed to the interactions between MMT and the cell surface. The IC_{50} of MMT for MRC-5, HT-29, and HepG2 cells was approximate-

ly 1000, 880, and 625 μg/mL, respectively. Thus, it can be inferred that cancerous HT-29 and HepG2 cells exhibit greater susceptibility to MMT compared to normal MRC-5 cells. In a study by Javier Cervini-Silva et al., it was observed that low-dose MMT induced growth inhibition in the presence of U251 cells, while promoting growth in the presence of SKLU-1 cells[28]. Hence, it is clear that the interactions between MMT and cell surfaces are highly specific. Similar to our study, these findings also illustrate that MMT exerts varied effects on different cell lines at different dosage levels.

Several studies have explored the efficacy of curcumin against breast cancer using MDA-MB-231 cell lines in the literature. For instance, a study by Bimonte et al. revealed that curcumin, at doses of 50 μM, effectively eliminated half of the breast cancer cells within 48 hours, while enhancing the apoptotic effect at a concentration of 10 μM[44]. In 2018, Li et al. discovered an IC_{50} value of 37 μg/mL for free curcumin in MDA-MB-231 cell lines[45]. Following a 24-hour treatment with 15-100 μM curcumin, the viability of MDA-MB-231 cell cultures decreased by up to 25%[46]. Treatment with 50 μg/mL curcumin resulted in a 55.2% decrease in the viability of MDA-MB-231 colonies. Additionally, other studies have reported apoptosis in MDA-MB-231 cells treated with curcumin concentrations ranging from 10 to 50 μM for durations of 24 and 48 hours[47-49]. It seems that in our study, modified curcumin was also effective in the MDA-MB-231 cell line, exhibiting an IC_{50} value of 56 μg/mL. These findings align with other studies in the literature and endorse the potential utility of modified curcumin as a cytotoxic agent against breast cancer cells.

It was first demonstrated by Li et al., that curcumin exhibits anti-tumour activity in pancreatic tumors[50]. It is known in the literature that curcumin induces apoptosis and significantly reduces proliferation, invasion, metastasis, viability, migration, and colony formation in the PANC-1 cell line[51]. Guo et al. showed that the IC_{50} of curcumin in the PANC-1 cell line is 68 μM[52]. Another study found the IC_{50} of curcumin in the same cell line to be 73 μM[53]. Consistent with the literature, our study found the IC_{50} of curcumin in the PANC-1 cell line to be 72 μg/mL.

It is known that curcumin exhibits antitumor effects when used alone or in combination with other treatment methods *in vitro* studies of breast and pancreatic tumors[54]. However, due to its low bioavailability, curcumin is broken down and does not show these effects in *in vitro* and clinical studies. Therefore, studies to increase the bioavailability of curcumin are ongoing. In this study, modified curcumin with increased bioavailability was used, and its effect on breast and pancreatic tumors was proven *in vitro*. Our study is the first in the literature to show the anti-tumor effect of MMT in pancreatic tumors. Further *in vivo* and clinical studies should be conducted to investigate the effectiveness of MMT and modified curcumin.

In this study, we aimed to study the anticancer activity of MMT and MMT (as a drug carrier) along with modified curcumin in MDA MB-231 and PANC-1 cancer cells and MRC-5 healthy cells. MDA MB-231 cell line was used for breast cancer studies, the PANC-1 cell line was used for pancreatic cancer studies and the MRC-5 cell line was used for healthy control fibroblastic cells. In conclusion, the findings of this study clearly show that MMT supports cell viability in MRC-5 healthy cell lines and has a dose-dependent reduction effect on MDA-MB-231 and PANC-1 cancer cell lines. In addition, IC_{50} values of MMT for MDA-MB-231 cell was 1456 μg/mL and for PANC-1 cell was 1166 μg/mL. Whereas modified curcumin showed a reducing effect on cell viability depending on the given doses for MDA MB-231 and PANC-1 cancer cell lines. Our data showed that after the modified curcumin was applied, the intervals in which the viability of the cancerous cells began to decrease, and the viability of the MRC-5 cell line used as the control did not affect the viability in the same way. For the MRC-5 cells, the viability remained high. In addition, IC_{50} values of modified curcumin for the MRC-5 cell were 215 μg/mL, for the MDA MB-231 cell was 56.45 μg/mL, and for the PANC-1 cell was 72.34 μg/mL. Contrary to heavy drugs and chemotherapies in cancer treatments, it is necessary to discover methods that use chemicals as little as possible and adverse cause side effects in the human body. Therefore, regarding all data, our study presents that the MMT and modified curcumin have the potential to reduce pancreatic and breast cancer cells, which could be studied for future alternative therapies to treat other tumor cells using natural substances. Furthermore, the effects of MMT vary in different cell lines, and it even suggests that MMT is capable of distinguishing between healthy and cancer cells.

STATEMENT OF ETHICS

Ethical approval was not required to perform this study.

CONFLICT OF INTEREST STATEMENT

The author declares that there is no conflict of interest.

AUTHOR CONTRIBUTIONS

All authors contributed equally to the work.

FUNDING SOURCES

This research received no external funding.

ACKNOWLEDGMENTS

Not applicable.

REFERENCES

1. Sung H, Ferlay J, Siegel RL, Laversanne M, Soerjomataram I, Jemal A, et al. Global cancer statistics 2020: GLOBOCAN estimates of incidence and mortality worldwide for 36 cancers in 185 countries. CA: Cancer J Clin, 2021;71(3):209-249. Doi: 10.3322/caac.21660

2. Canto MI. Familial risk factors for pancreatic cancer and screening of high-risk patients [Internet]. UpToDate Inc; 2024 [cited 22 Mar 2024]. Available from: https://www.uptodate.com/contents/familial-risk-factors-for-pancreatic-cancer-and-screening-of-high-risk-patients

3. Rock CL, Thomson C, Gansler T, Gapstur SM, McCullough ML, Patel AV, et al. American Cancer Society guideline for diet and physical activity for cancer prevention. CA: Cancer J Clin, 2020;70(4):245-271. Doi: 10.3322/caac.21591

4. McGuigan A, Kelly P, Turkington RC, Jones C, Coleman HG, McCain RS. Pancreatic cancer: a review of clinical diagnosis, epidemiology, treatment and outcomes. World J Gastroenterol, 2018;24(43):4846. Doi: 10.3748/wjg.v24.i43.4846

5. American Cancer Society. Survival rates for pancreatic cancer [Internet], 2024 [cited 2025 Jan 6]. Available from: https://www.cancer.org/cancer/pancreatic-cancer/detection-diagnosis-staging/survival-rates.html

6. Chlebowski RT, Hayes DF. Factors that modify breast cancer risk in women [Internet]. In: Post TW, editor. UpToDate. Waltham, MA: UpToDate Inc.; 2023 [cited 22 Mar 2024]. Available from: https://www.uptodate.com/contents/factors-that-modify-breast-cancer-risk-in-women?search=Chlebowski%20RT,%20Hayes%20DF.%20Factors%20that%20modify%20breast%20cancer%20risk%20in%20women.%20&source=search_result&selectedTitle=1~150&usage_type=default&display_rank=1

7. Zhai J, Wu Y, Ma F, Kaklamani V, Xu B. Advances in medical treatment of breast cancer in 2022. Cancer Innov, 2023;2:1-17. Doi: 10.1002/cai2.46

8. Dickler MN, Saura C, Richards DA, Krop IE, Cervantes A, Bedard PL, et al. Phase II Study of Taselisib (GDC-0032) in combination with fulvestrant in patients with HER2-negative, hormone receptor-positive advanced breast cancer. Clin Cancer Res, 2018;24(18):4380-4387. Doi: 10.1158/1078-0432.CCR-18-0613

9. O'Shaughnessy J, DeMichele A, Ma CX, Richards P, Yardley DA, Wright GS, et al. A randomized, double-blind, phase 2 study of ruxolitinib or placebo in combination with capecitabine in patients with advanced HER2-negative breast cancer and elevated C-reactive protein, a marker of systemic inflammation. Breast Cancer Res Treat, 2018;170(3):547-557. Doi: 10.1007/s10549-018-4770-6

10. Godone RLN, Leitão GM, Araújo NB, Castelletti CHM, Lima-Filho JL, Martins DBG. Clinical and molecular aspects of breast cancer: targets and therapies. Biomed Pharmacother, 2018;106:14-34. Doi: 10.1016/j.biopha.2018.06.066

11. Zhu TT, Zhou CH, Kabwe FB, Wu QQ, Li CS, Zhang JR. Exfoliation of montmorillonite and related properties of clay/polymer nanocomposites. Appl Clay Sci, 2019;169:48-66. Doi: 10.1016/j.clay.2018.12.006

12. Nazir MS, Mohamad Kassim MH, Mohapatra L, Gilani MA, Raza MR, Majeed K. Characteristic properties of nano clays and characterization of nanoparticles and nanocomposites. In: Nanoclay reinforced polymer composites. Springer; 2016. p. 35-55. Doi: 10.1007/978-981-10-1953-1_2

13. Wang J-S, Luo H, Billam M, Wang Z, Guan H, Tang L, et al. Short-term safety evaluation of processed calcium montmorillonite clay (NovaSil) in humans. Food Addit Contam, 2005;22(3):270-279. Doi: 10.1080/02652030500111129

14. Jiraskova Y, Bursik J, Seidlerova J, Kutlakova KM, Safarik I, Safarikova M, et al. Microstructural analysis and magnetic characterization of native and magnetically modified montmorillonite and vermiculite. J Nanotechnol, 2018;1:3738106. Doi: 10.1155/2018/3738106

15. Hojiyev R, Ulcay Y, Çelik MS, Carty WM. Effect of CEC coverage of hexadecyltributylphosphonium modified montmorillonite on polymer compatibility. Appl Clay Sci, 2017;141:204-211. Doi: 10.1016/j.clay.2017.02.036

16. Pires J, Paula CD de, Souza VGL, Fernando AL, Coelhoso I. Understanding the barrier and mechanical behavior of different nanofillers in chitosan films for food packaging. Polymers, 2021;13(5):721. Doi: 10.3390/polym13050721

17. Daniel SCGK, Tharmaraj V, Sironmani TA, Pitchumani K. Toxicity and immunological activity of silver nanoparticles. Appl Clay Sci, 2010;48(4):547-551. Doi: 10.1016/j.clay.2010.03.001

18. Select committee on GRAS substances [Internet], [cited 2024 Apr 1]. Available from: https://www.cfsanappsexternal.fda.gov/scripts/fdcc/?set=SCOGS&sort=Sortsubstance&order=ASC&startrow=1&type=basic&search=bentonite

19. Hou Y, Wu P, Zhu N. The protective effect of clay minerals against damage to adsorbed DNA induced by cadmium and mercury. Chemosphere, 2014;95:206-212. Doi: 10.1016/j.chemosphere.2013.08.069

20. Plachá D, Rosenbergová K, Slabotínský J, Kutláková KM, Študentová S, Martynková GS. Modified clay minerals efficiency against chemical and biological warfare agents for civil human protection. J Hazard Mater, 2014;271:65-72. Doi: 10.1016/j.jhazmat.2014.01.059

21. Breitrück A, Sparmann G, Mitzner S, Kerkhoff C. Establishment of a novel extracorporeal bowel model to study luminal approaches to treat inflammatory bowel disease. Dis Model Mech, 2013;6(6):1487-1493. Doi: 10.1242/dmm.011734

22. Xu P, Dai S, Wang J, Zhang J, Liu J, Wang F, et al. Preventive obesity agent montmorillonite adsorbs dietary lipids and enhances lipid excretion from the digestive tract. Sci Rep, 2016;6(1):19659. Doi: 10.1038/srep19659

23. Mahmoudi M, Adib-Hajbaghery M, Mashaiekhi M. Comparing the effects of Bentonite & Calendula on the improvement of infantile diaper dermatitis: a randomized controlled trial. Indian J Med Res, 2015;142(6):742. Doi: 10.4103/0971-5916.174567

24. Bayülken S, Başçetin E, Güçlü K, Apak R. Investigation and modeling of cesium (I) adsorption by Turkish clays: Bentonite, zeolite, sepiolite, and kaolinite. Environ Prog Sustain Energy, 2011;30(1):70-80. Doi: 10.1002/ep.10452

25. Sabzevari AG, Sabahi H, Nikbakht M. Montmorillonite, a natural biocompatible nanosheet with intrinsic antitumor activity. Colloids Surfaces B Biointerfaces, 2020;190:110884. Doi: 10.1016/j.colsurfb.2020.110884

26. Abduljauwad SN, Ahmed HuR, Moy VT. Melanoma treatment via non-specific adhesion of cancer cells using charged nano-clays in pre-clinical studies. Sci Rep, 2021;11(1):1-13. Doi: 10.1038/s41598-021-82441-8

27. Iliescu RI, Andronescu E, Ghitulica CD, Voicu G, Ficai A, Hoteteu M. Montmorillonite–alginate nanocomposite as a drug delivery system – incorporation and *in vitro* release of irinotecan. Int J Pharm, 2014;463(2):184-192. Doi: 10.1016/j.ijpharm.2013.08.043

28. Cervini-Silva J, Ramírez-Apan MT, Kaufhold S, Ufer K, Palacios E, Montoya A. Role of Bentonite clays on cell growth. Chemosphere, 2016;149:57-61. Doi: 10.1016/j.chemosphere.2016.01.077

29. Dehzad MJ, Ghalandari H, Nouri M, Askarpour M. Antioxidant and anti-inflammatory effects of curcumin/turmeric supplementation in adults: a GRADE-assessed systematic review and dose–response meta-analysis of randomized controlled trials. Cytokine, 2023;164:156144. Doi: 10.1016/j.cyto.2023.156144

30. Anand P, Sundaram C, Jhurani S, Kunnumakkara AB, Aggarwal BB. Curcumin and cancer: an "old-age" disease with an "age-old" solution. Cancer Lett, 2008;267(1):133-164. Doi: 10.1016/j.canlet.2008.03.025

31. Atabaki M, Shariati-Sarabi Z, Tavakkol-Afshari J, Mohammadi M. Significant immunomodulatory properties of curcumin in patients with osteoarthritis; a successful clinical trial in Iran. Int Immunopharmacol, 2020;85:106607. Doi: 10.1016/j.intimp.2020.106607

32. Pivari F, Mingione A, Brasacchio C, Soldati L. Curcumin and type 2 diabetes mellitus: prevention and treatment. Nutrients, 2019;11(8):1837. Doi: 10.3390/nu11081837

33. Tang M, Taghibiglou C. The mechanisms of action of curcumin in Alzheimer's disease. J Alzheimer's Dis, 2017;58(4):1003-1016. Doi: 10.3233/JAD-170188

34. Malhotra L, Goyal HK V, Jhuria S, Dev K, Kumar S, Kumar M, et al. Curcumin rescue p53Y220C in BxPC-3 pancreatic adenocarcinomas cell line: Evidence-based on computational, biophysical, and *in vivo* studies. Biochim Biophys Acta Gen Subj, 2021;1865(2):129807. Doi: 10.1016/j.bbagen.2020.129807

35. Bimonte S, Barbieri A, Palma G, Luciano A, Rea D, Arra C. Curcumin inhibits tumor growth and angiogenesis in an orthotopic mouse model of human pancreatic cancer. Biomed Res Int, 2013;2013. Doi: 10.1155/2013/810423

36. Korać P, Antica M, Matulić M. MiR-7 in cancer development. Biomedicines, 2021;9(3):325. Doi: 10.3390/biomedicines9030325

37. Li W, Wang Z, Xiao X, Han L, Wu Z, Ma Q, et al. Curcumin attenuates hyperglycemia-driven EGF-induced invasive and migratory abilities of pancreatic cancer via suppression of the ERK and AKT pathways. Oncol Rep, 2019;41(1):650-658. Doi: 10.3892/or.2018.6833

38. Basha R, Connelly SF, Sankpal UT, Nagaraju GP, Patel H, Vishwanatha JK, et al. Small molecule tolfenamic acid and dietary spice curcumin treatment enhances antiproliferative effect in pancreatic cancer cells via suppressing Sp1, disrupting NF-kB translocation to nucleus and cell cycle phase distribution. J Nutr Biochem, 2016;31:77-87. Doi: 10.1016/j.jnutbio.2016.01.003

39. Abbaspour H, Safipour AA. Curcumin inhibits the expression of ornithine decarboxylase and adenosine deaminase genes in MCF-7 human breast cancer cells. Arch Biol Sci, 2018;70(4):639-645. Doi: 10.2298/ABS180209025A

40. Bachmeier BE, Mohrenz IV, Mirisola V, Schleicher E, Romeo F, Höhneke C, et al. Curcumin downregulates the inflammatory cytokines CXCL1 and -2 in breast cancer cells via NFκB. Carcinogenesis, 2008;29(4):779-789. Doi: 10.1093/carcin/bgm248

41. Mbese Z, Khwaza V, Aderibigbe BA. Curcumin and its derivatives as potential therapeutic agents in prostate, colon and breast cancers. Molecules, 2019;24(23):4386. Doi: 10.3390/molecules24234386

42. Khor PY, Aluwi MFFM, Rullah K, Lam KW. Insights on the synthesis of asymmetric curcumin derivatives and their biological activities. Eur J Med Chem, 2019;183:111704. Doi: 10.1016/j.ejmech.2019.111704

43. Karataş D, Tekin A, Bahadori F, Çelik MS. Interaction of curcumin in a drug delivery system including a composite with poly (lactic-co-glycolic acid) and montmorillonite: a density functional theory and molecular dynamics study. J Mater Chem B, 2017;5(40):8070-8082. Doi: 10.1039/C7TB01964E

44. Bimonte S, Barbieri A, Palma G, Rea D, Luciano A, D'Aiuto M, et al. Dissecting the role of curcumin in tumour growth and angiogenesis in mouse model of human breast cancer. Biomed Res Int, 2015;878134. Doi: 10.1155/2015/878134

45. Li N, Wang Z, Zhang Y, Zhang K, Xie J, Liu Y, et al. Curcumin-loaded redox-responsive mesoporous silica nanoparticles for targeted breast cancer therapy. Artif cells, nanomedicine, Biotechnol, 2018;46(Suppl.2):921-935. Doi: 10.1080/21691401.2018.1473412

46. Kumari P, Paul M, Bobde Y, Soniya K, Kiran Rompicharla SV, Ghosh B, et al. Albumin-based lipoprotein nanoparticles for improved delivery and anticancer activity of curcumin for cancer treatment. Nanomedicine, 2020;15(29):2851-2869. Doi: 10.2217/nnm-2020-0232

47. Ghosh S, Dutta S, Sarkar A, Kundu M, Sil PC. Targeted delivery of curcumin in breast cancer cells via hyaluronic acid modified mesoporous silica nanoparticle to enhance anticancer efficiency. Colloids Surfaces B Biointerfaces, 2021;197:111404. Doi: 10.1016/j.colsurfb.2020.111404

48. Mukhopadhyay R, Sen R, Paul B, Kazi J, Ganguly S, Debnath MC. Gemcitabine co-encapsulated with curcumin in folate decorated PLGA nanoparticles; a novel approach to treat breast adenocarcinoma. Pharm Res, 2020;37:1-19. Doi: 10.1007/s11095-020-2758-5

49. Ji P, Wang L, Chen Y, Wang S, Wu Z, Qi X. Hyaluronic acid hydrophilic surface rehabilitating curcumin nanocrystals for targeted breast cancer treatment with prolonged biodistribution. Biomater Sci, 2020;8(1):462-472. Doi: 10.1039/C9BM01605H

50. Li L, Aggarwal BB, Shishodia S, Abbruzzese J, Kurzrock R. Nuclear factor-κB and IκB kinase are constitutively active in human pancreatic cells, and their down-regulation by curcumin (diferuloylmethane) is associated with the suppression of proliferation and the induction of apoptosis. Cancer Interdiscip Int J Am Cancer Soc, 2004;101(10):2351-2362. Doi: 10.1002/cncr.20605

51. Li W, Sun L, Lei J, Wu Z, Ma Q, Wang Z. Curcumin inhibits pancreatic cancer cell invasion and EMT by interfering with tumor-stromal crosstalk under hypoxic conditions via the IL-6/ERK/NF-κB axis. Oncol Rep, 2020;44(1):382-392. Doi: 10.3892/or.2020.7600

52. Guo W, Ding Y, Pu C, Wang Z, Deng W, Jin X. Curcumin inhibits pancreatic cancer cell proliferation by regulating Beclin1 expression and inhibiting the hypoxia-inducible factor-1α-mediated glycolytic pathway. J Gastrointest Oncol, 2022;13(6):3254. Doi: 10.21037/jgo-22-802

53. Jadid MFS, Shademan B, Chavoshi R, Seyyedsani N, Aghaei E, Taheri E, et al. Enhanced anticancer potency of hydroxytyrosol and curcumin by PLGA-PAA nano-encapsulation on PANC-1 pancreatic cancer cell line. Environ Toxicol, 2021;36(6):1043-1051. Doi: 10.1002/tox.23103

54. Mansouri K, Rasoulpoor S, Daneshkhah A, Abolfathi S, Salari N, Mohammadi M, et al. Clinical effects of curcumin in enhancing cancer therapy: a systematic review. BMC Cancer, 2020;20:1-11. Doi: 10.1186/s12885-020-07256-8

Acta Pharm. Sci. Vol 63:(2), 2025
Original article
DOI: 10.23893/1307-2080.APS6325

Evolution of plasma trace element status in children treated with low-protein diets related to Maple Syrup Urine Disease (MSUD) and Urea Cycle Disorder (UCD)

Özlem ARAZ*, Halit ÇAM

Istanbul University-Cerrahpasa, Cerrahpasa Faculty of Medicine, Istanbul, Türkiye

ABSTRACT

The main treatment for Urea Cycle Disorder (UCD) and Maple syrup urine disease (MSUD) is low-protein diets and element deficiencies may develop related to dietary therapy. This study aimed to determine plasma trace element levels in patients with MSUD and UCD and to compare these results with those established in a healthy pediatric population not undergoing any dietary treatment. The study was conducted with 30 patients diagnosed with MSUD and UCD, and a control group of 30 health age-matched children. Dietary treatment involved a natural protein-restricted diet supplemented with a special formula, depending on the specific metabolic defect. Significant differences were observed between patients and control values for magnesium, selenium, and copper ($p<0.05$). These results reinforce that patients under dietary treatment should be regularly monitored for these elements. Furthermore, fortifying these elements in special formulas (as they are the sources of essential amino acids) should be considered.

Keywords: trace element, children, MSUD, UCD, protein-restricted diet

INTRODUCTION

MSUD is an autosomal recessive inherited metabolic disorder (IMD) caused by a deficiency in branched-chain α-ketoacid dehydrogenase (BCKD), resulting in the

*Corresponding author: Özlem ARAZ
E-mail: oz_araz@hotmail.com
ORCIDs:
Özlem ARAZ: 0009-0000-3675-8209
Halit ÇAM: 0000-0002-2611-9515
(Received 6 Jun 2024, Accepted 2 Jul 2024)

accumulation of branched-chain amino acids (BCAAs) such as leucine (LEU), isoleucine (ILE), and valine (VAL), along with their corresponding α-ketoacids (BCKAs)[1]. The increase in BCAAs prevents the transport of large neutral amino acids to the brain and leads to increases in neurotransmitter synthesis and myelination[2]. MSUD has had a worldwide incidence, occurring in one in 185,000 live births[3]. Although the exact incidence in Türkiye is not known, as MSUD is not currently included in the newborn screening program, it is estimated to affect as many as 1 in 50,000 newborns, particularly due to the high rate of consanguineous marriages[4].

MSUD treatment involves dietary leucine restriction, BCAA-free medical foods, moderate supplementation with isoleucine and valine, and regular clinical and biochemical monitoring[1]. Nutrition therapy plays a crucial role in restoring and maintaining metabolic homeostasis in MSUD[5]. In the diet, the most toxic effect is primarily caused by leucine. Therefore, priority is given to leucine content in the nutrition plan. When leucine is provided, usually isoleucine and valine are also provided. In cases where they cannot be provided, supplements are given[3]. In the diet, energy intake is provided from fruits (<30 mg leucine/100 g and 0.3-1 g protein/100 g) and vegetables (<100 mg leucine/100 g) with low leucine content, commercially available products with low leucine content (≤0.5 g protein/100 g), sugar, liquid oil, and starch[6].

Urea cycle disorders (UCDs) are congenital metabolic errors resulting from defects in one of the six enzymes or two transporters involved in the detoxification of ammonia into urea, which is excreted in the urine[7]. The overall incidence of urea cycle disorders occurs in approximately 1:35.000 births and all, except for OTC deficiency, are autosomal recessive. Loss of function of the urea cycle causes the problem of inability to excrete ammonium produced during protein catabolism. The resulting hyperammonemia is harmful to the brain[8].

The maintenance dietary treatment of UCD involves providing a low-protein diet, supplementing with essential amino acids as necessary, and offering appropriate nutritional support to prevent catabolic stress[9].

Despite this supplemented diet, patients with IMDs on low-protein diets are at risk of deficiency in several micronutrients. Deficiencies in selenium especially in phenylketonuria have been reported[10,11]. Selenium deficiency was also reported in patients with UCD, despite their selenium intake being higher than the Recommended Daily Allowance (RDA)[12]. These findings suggest a potential issue of reduced selenium bioavailability in IMDs. In addition, deficiencies in various micronutrients have been reported in patients with MSUD due to protein restriction. In a case report, skin lesions related to zinc deficiency were noted in an infant diagnosed with MSUD[13].

The objective of this study was to compare plasma levels of cobalt, copper, zinc, selenium, manganese, molybdenum, and magnesium between children undergoing low-protein dietary treatment and their age-matched healthy children without any dietary treatment. The aim was to explore potential deficiencies and their etiology, as well as to assess their association with nutritional status.

METHODOLOGY

Study design and sampling

The study was conducted between January 2015 and May 2017 in Istanbul University Cerrahpasa Medical Faculty. The patient group consisted of individuals undergoing protein-restricted dietary treatment; 19 had MSUD, and 11 had UCD, all of whom were being followed up by the Pediatric Nutrition and Metabolism Department. Inclusion criteria were: being under 18 years of age, undergoing low-protein nutrition therapy due to congenital protein metabolism disorders, attending regular check-ups, having good dietary compliance, and not having malabsorption. Exclusion criteria were: being under bad metabolic control, having malabsorption, not attending regular check-ups, and having poor dietary compliance. Results from these patients were compared with control values established in 30 healthy children who applied to the Healthy Child Polyclinic. Exclusion criteria for control group were: the existence of chronic or acute disease, pharmacological treatments, the use of food supplements containing trace elements, and special diets.

Dietary treatment

Dietary treatment involves a natural protein-restricted diet supplemented with a special formula containing different amino acids, vitamins and trace elements depending on the patient's specific metabolic disorder and age. Participants were asked to complete 3-day food diaries before blood samples were taken for monitoring trace elements. Food records were analyzed using the Nutrition Information System (BEBIS) program to quantify the average nutrient intake[14].

Biochemical analysis

Five milliliters of venous blood were drawn after an overnight fasting and blood was centrifuged for 10 minutes at 3000 rpm. The plasma was isolated and preserved in covered lithium heparin tubes, then stored at -20°C until the measurement of trace elements was conducted. Plasma levels of cobalt, copper, zinc, selenium, manganese, molybdenum, and magnesium were examined utilizing ICP-MS (Inductively Coupled Plasma – Mass Spectrometry) at the Forensic

Toxicology Laboratory of Istanbul University Cerrahpasa Faculty of Medicine, Forensic Medicine Institute. The study protocol strictly adhered to all relevant national regulations, institutional policies, and ethical principles outlined in the Helsinki Declaration. Approval was secured from the Ethical Committee of Cerrahpasa Medical Faculty (01.07.2014/No:83045809/604.01.01), and informed consent was obtained from the parents of all participating patients.

Statistical analysis

Descriptive statistics including mean, standard deviation, median, minimum, and maximum values, as well as frequency and percentage, were utilized in the data analysis. The distribution of variables was assessed using the Kolmogorov-Smirnov test. For the analysis of quantitative independent variables, the Mann-Whitney U test was employed, while the Chi-square test was used for qualitative independent variables. Statistical analyses were performed by using Statistical Package for Social Sciences version 22.0 (SPSS Inc., Chicago, IL, USA).

RESULTS and DISCUSSION

The characteristics of the diet group and control group included in the study are shown in Table 1. There was no significant difference ($p>0.05$) in the ages and gender distribution of patients in the diet and control groups.

Table 1. Age and gender distributions of patients in the diet and control groups

		Control Group (n=30)	Diet Group (n=30)	P
Age	Mean ± SD Median	7.0 ± 4.6 7.0	5.7 ± 5.0 5.0	0.312 [m]
Gender	Male (n, %) Female (n, %)	14 (%46.7) 16 (%53.3)	18 (%60) 12 (%40)	0.301 [x^2]

*m= Mann Whitney U test, x^2= chi-square test

Table 2 shows the concentration of plasma Mg, Mn, Co, Cu, Zn, Se and Mo in the diet and control groups. Statistical analysis showed that the diet group was significantly lower than the control group with regards to Mg, Cu, and Se levels ($p=0.008$, $p=0.001$, and $p<0.001$, respectively). Moreover, no significant differences in Mn, Co, Zn, or Mo levels were observed in the diet group, as compared to the control group ($p>0.05$) (Table 2).

Table 2. Comparison of plasma trace element concentration in diet and control groups

	Control Group (n=30)		Diet Group (n=30)			
	Mean ± SD	Median	Mean ± SD	Median	P	
Mg (x10⁴) (µg/L)	1.3 ± 0.2	1.4	1.2 ± 0.2	1.2	0.008	m
Mn (µg/L)	9.9 ± 10.2	6.3	7.8 ± 5.8	6.5	0.918	m
Co (µg/L)	1.0 ± 1.1	0.7	0.8 ± 0.3	0.7	0.482	m
Cu (µg/L)	1162.0 ± 217.6	1170.0	970.1 ± 192.4	945.9	0.001	m
Zn (µg/L)	607.4 ± 92.5	623.1	648.8 ± 158.5	630.1	0.294	m
Se (µg/L)	64.8 ± 23.1	61.8	26.4 ± 35.4	13.3	0.000	m
Mo (µg/L)	0.2 ± 0.7	0.1	1.0 ± 2.7	0.1	0.281	m

*m= Mann Whitney U test

Average daily oral nutrient intake and energy were calculated for patients with dietary treatment and control group (Table 3). Since the natural protein-restricted diet is a common treatment for these disorders, significant differences were observed between the values of IMDs and control groups compared to natural protein intake ($p<0.05$). In the IMDs and control groups, there was no significant difference in daily energy intake ($p>0.05$). Fat consumption in the IMDs group was significantly lower than in the control group ($p<0.05$). The carbohydrate consumption in the IMDs group was significantly higher than that in the control group ($p<0.05$).

In the IMD group and the control group, there was no significant difference in the dietary intake of magnesium ($p>0.05$) (Table 3). However, the plasma magnesium level of the IMD group was found to be significantly lower than that of the control group ($p<0.05$) (Table 3). For iron and zinc, the daily intake of patients with dietary treatment and the control group (iron: 13.5 ± 6.6 mg/day, 9.4 ± 4.0 mg/day; zinc: 8.5 ± 5 mg/day, 8 ± 2.9 mg/day, respectively) was slightly higher than the recommended daily allowances (RDAs) (iron: 7-11 mg/day; zinc: 4.3-7.4 mg/day, respectively) (Table 3).

Table 3. Comparison of energy and nutrient intake with diet in the IMDs and control groups

	Control Group (n=30)		IMDs Group (n=30)			
	Mean ± SD	Median	Mean ± SD	Median	P	
Energy (kcal)	1443.1 ± 367	1498.9	1396.6 ± 478.4	1336.5	0.836	m
Natural protein (gram)	55.6 ± 18.7	56.0	4.9 ± 2.0	4.5	0.000	m
Fat (gram)	68.7 ± 20.4	70.8	56.9 ± 17.8	57.7	0.025	m
Carbohydrate (gram)	146.4 ± 45.4	144.5	185.8 ± 74.1	192.6	0.028	m
Mg (mg)	213.1 ± 73.5	202.8	195.9 ± 107.0	184.2	0.132	m
Fe (mg)	9.4 ± 4.0	8.6	13.5 ± 6.6	12.5	0.009	m
Zn (mg)	8.0 ± 2.9	8.1	8.5 ± 5.0	7.1	0.416	m

*m= Mann Whitney U test

Results of different elements according to the type of disease in IMD patients under dietary treatment are shown in Table 4. Plasma Mg, Mn, Co, Cu, Zn, and Mo values did not differ significantly between the MSUD and UCD groups ($p>0.05$). However, in the UCD group, plasma Se value was significantly lower than in the MSUD group ($p<0.05$) (Table 4).

Table 4. Comparison of plasma trace element amounts in MSUD and UCD groups.

	Control Group (n=30)		IMDs Group (n=30)			
	Mean ± SD	Median	Mean ± SD	Median	P	
Energy (kcal)	1443.1 ± 367	1498.9	1396.6 ± 478.4	1336.5	0.836	m
Natural protein (gram)	55.6 ± 18.7	56.0	4.9 ± 2.0	4.5	0.000	m
Fat (gram)	68.7 ± 20.4	70.8	56.9 ± 17.8	57.7	0.025	m
Carbohydrate (gram)	146.4 ± 45.4	144.5	185.8 ± 74.1	192.6	0.028	m
Mg (mg)	213.1 ± 73.5	202.8	195.9 ± 107.0	184.2	0.132	m
Fe (mg)	9.4 ± 4.0	8.6	13.5 ± 6.6	12.5	0.009	m
Zn (mg)	8.0 ± 2.9	8.1	8.5 ± 5.0	7.1	0.416	m

*m= Mann Whitney U test

The amounts of energy, fat, magnesium, and zinc intake through diet did not show significant differences between the MSUD and UCD groups (p>0.05). However, in the UCD group, the intake of natural protein, essential amino acids, and iron through the diet was significantly lower compared to the MSUD group (p<0.05) (Table 5).

Table 5. Comparing the amounts of energy and nutrient intake in diets of MSUD and UCD groups

	MSUD (n=19)		UCD (n=11)			
	Mean ± SD	Median	Mean ± SD	Median	P	
Energy (kcal)	1498.3 ± 538.6	1711.0	122 0 ± 296.7	1266.0	0.067	m
Natural Protein (gram)	4.3 ± 1.9	4.1	6.1 ± 1.7	6.0	***0.010***	m
Essential amino acids (gram)	36.8 ± 22.5	35.6	9.1 ± 1.9	9.1	***0.000***	m
Fat (gram)	57.4 ± 18.9	59.2	56.0 ± 16.3	53.8	0.651	m
Carbohydrate (gram)	198.2 ± 85.5	213.5	164.3 ± 44.1	163.8	0.168	m
Mg (mg)	219.3 ± 126.6	193.0	155.4 ± 38.6	134.8	0.168	m
Fe (mg)	15.5 ± 7.4	14.6	10.1 ± 2.9	10.0	***0.027***	m
Zn (mg)	9.7 ± 5.9	7.5	6.3 ± 1.6	6.0	***0.077***	m

*m= Mann Whitney U test

Since a natural protein-restricted diet is frequently employed in the treatment of IMDs, patients with these disorders may experience deficiencies in vitamins and trace elements[15]. Trace elements play a crucial role in metabolic processes and oxidation-reduction reactions within the central nervous system, potentially influencing cognitive function. The treatment of IEMs involves restricting dietary intake of natural protein, which is balanced with a special formula fortified with trace elements, mineral salts, and vitamins[16]. The present study aimed to investigate the levels of trace elements (Zn, Cu, Mn, Se, Co, Mg, Mo) in children with MSUD and UCD, as well as in their age-matched healthy children without dietary intervention.

Previous studies have noted deficiencies in certain trace elements among individuals with IMDs, particularly those with phenylketonuria (PKU)[15,17].

This study found plasma selenium levels were significantly lower in the diet group than in the control group (p<0.05). Similar to this report, Tondo (2010) found significant differences in selenium levels between IMDs ongoing dietary

treatment and control subjects[12]. The study revealed that the average dietary selenium intake among PKU patients exceeded RDA values slightly. However, selenium deficiency was also evident in patients with UCD and organic acidurias, despite their selenium intake surpassing RDA levels[12]. These findings suggest a potential issue of reduced selenium bioavailability in both PKU and other IMD patients, as their average selenium intake exceeded the RDAs. In some studies, selenium deficiency has been reported, associated with decreased selenium intake[10] which has also been documented in patients with PKU due to low-protein diet therapy[11,15].

Van Bakel et al. observed significantly lower selenium levels in plasma samples from children with phenylketonuria compared to healthy children[17]. Unlike the current study and other studies in the literature, no significant differences were observed in plasma selenium levels among the PKU and mild hyperphenylalaninemia (m-HPA) patients and the control group[18].

Selenium deficiencies appear significant due to its involvement in numerous antioxidant metabolic pathways and hormone metabolism[17]. Reduced antioxidant capacity was observed in individuals with PKU, prompting consideration of selenium supplements in relation to oxidative stress parameters[19]. Selenium deficiency has been suggested to be associated with impaired antioxidant function and alterations in thyroid hormone levels[20-23].

Treated PKU patients exhibited decreased glutathione peroxidase activity due to low plasma selenium levels, leading to oxidative stress[24]. Furthermore, DNA damage has been reported, indicating elevated production of reactive species[25-27]. This condition has been linked to increased free radical generation and reduced levels of antioxidant micronutrients[28,29]. These findings resulted in adding selenium, vitamins, and oligo elements to phenylalanine-free mixtures for PKU[30]. Additionally, selenium deficiency in PKU patients has been associated with some impaired cognitive functions[31].

Some studies have associated oxidative stress with zinc deficiency[32] and selenium deficiency[20,21, 33]. Sitta and colleagues demonstrated that long-term supplementation of selenium and carnitine can rectify protein and lipid oxidative damage and reinstate glutathione peroxidase activity[19].

In the current study, plasma copper levels were found to be significantly lower in IMD patients compared to the control group. This contrasts with the findings of Gropper et al., who demonstrated no difference in plasma copper levels between children with PKU (19.2 μmol/L) and the control group (18.7 μmol/L)[34].

The other element that showed significantly lower values in IMD patients under dietary treatment was Mg. Nevertheless, no significant difference was observed in the dietary intake of magnesium between the IMDs group and the control group ($p>0.05$). This result can be attributed to the redistribution of mineral metabolic pools and disruption in intestinal absorption.

A study conducted with PKU patients concluded that exhibits interactive associations with PKU, and serum magnesium levels decrease in PKU patients. Accordingly, this reduction in serum Mg levels in PKU patients may stem from decreased tubular reabsorption and increased urinary excretion[35].

To our knowledge, apart from Tondo's study[12], no studies have been carried out on trace element status in patients with MSUD and UCD. The major limitation of this study, is the correlation between nutrient intake and status is intricate, influenced by factors like nutrient bioavailability, interactions, and individual metabolism. Another limitation is that throughout the study, advancements in markers of nutritional status have been identified. For instance, while all studies reported plasma selenium concentrations as the status indicator, more recently, plasma selenoprotein P (SEPP1) has been regarded as a more informative marker of status. Since studies on this subject are generally conducted in children with PKU, there is not enough data in the literature on trace element levels in patients with UCD and MSUD.

In conclusion, patients with IMDs on protein-restricted diets are at risk of deficiency in magnesium, selenium, and copper. Due to the restricted intake of natural protein, the MSUD and UCD formulas provide a high percentage of the daily requirements for micronutrients. All these results show the importance of evaluating trace element intake levels in the nutritional follow-up of such patients and the necessity of supplementing these trace elements in case of deficiency. Additionally, there is a need to enrich formulas with trace elements, which serve as essential amino acid sources.

STATEMENT OF ETHICS

Our study was approved by Istanbul University Cerrahpasa Medical Faculty's local ethics committee (Ethical approval no: 83045809/604.01.01, Date: 01.07.2014).

CONFLICT OF INTEREST STATEMENT

The authors declared no conflict of interest.

AUTHOR CONTRIBUTIONS

The authors contributed to the work equally.

FUNDING SOURCES

The Research Fund of Istanbul University supported the present work. Project No: 47337.

ACKNOWLEDGMENTS

This article is based on the master's thesis prepared at Istanbul University Health Sciences Institute Cerrahpasa Faculty of Medicine Department of Child Health and Diseases Nutrition Program.

REFERENCES

1. Strauss KA, Carson VJ, Soltys K, Young ME, Bowser LE, Puffenberger EG, et al. Branched-chain α-ketoacid dehydrogenase deficiency (maple syrup urine disease): treatment, biomarkers, and outcomes. Mol Genet Metab, 2020;129(3):193-206. Doi: 10.1016/j.ymgme.2020.01.006

2. Banjar HR. A smart monitoring system for self-nutrition management in pediatric patients with inherited metabolic disorders: maple syrup urine disease (MSUD). Healthcare, 2023;11(2):178. Doi: 10.3390/healthcare11020178

3. Blackburn PR, Gass JM, Vairo FPE, Farnham KM, Atwal HK, Macklin S, et al. Maple syrup urine disease: mechanisms and management. Appl Clin Genet, 2017;10:57-66. Doi: 10.2147/tacg.s125962

4. Simon E, Wendel U, Schadewaldt P. Maple syrup urine disease-treatment and outcome in patients of Turkish descent in Germany. Turk J Pediatr, 2005;47(1):8-13.

5. Frazier DM, Allgeier C, Homer C, Marriage BJ, Ogata B, Rohr F, et al. Nutrition management guideline for maple syrup urine disease: an evidence- and consensus-based approach. Mol Genet Metab, 2014;112(3):210-217. Doi: 10.1016/j.ymgme.2014.05.006

6. Marriage B. Nutrition management of patients with inherited disorders of branched-chain amino acid metabolism. In: Acosta BP, editor. Nutrition management of patients with inherited metabolic disorders. Sudbury: Jones and Bartlett Publishers; 2010. p. 175-236.

7. Brusilow SW, Horwich AL. Urea cycle enzymes. In: Scriver CR, Beaudet AL, Sly WS, Valle D, editors. The metabolic and molecular bases of inherited disease. 8th ed. New York: Mc Graw-Hill; 2001. p. 1909-1963.

8. Francini-Pesenti F, Gugelmo G, Lenzini L, Vitturi N. Nutrient intake and nutritional status in adult patients with inherited metabolic diseases treated with low-protein diets: a review on urea cycle disorders and branched chain organic acidemias. Nutrients, 2020;12(11):3331. Doi: 10.3390/nu12113331

9. Adam S, Almeida MF, Assoun M, Baruteau J, Bernabei SM, Bigot S, et al. Dietary management of urea cycle disorders: European practice. Mol Genet Metab, 2013;110(4):439-445. Doi: 10.1016/j.ymgme.2013.09.003

10. Lombeck I, Ebert KH, Kasperek K, Feinendegen LE, Bremer HJ. Selenium intake of infants and young children, healthy children and dietetically treated patients with phenylketonuria. Eur J Pediatr, 1984;143(2):99-102. Doi: 10.1007/BF00445794

11. Darling G, Mathias P, O'Regan M, Naughten E. Serum selenium levels in individuals on PKU diets. J Inherit Metab Dis, 1992;15(5):769-773. Doi: 10.1007/BF01800019

12. Tondo M, Lambruschini N, Gomez-Lopez L, Gutierrez A, Moreno J, García-Cazorla A, et al. The monitoring of trace elements in blood samples from patients with inborn errors of metabolism. J Inherit Metab Dis, 2010;33(Suppl. 3):S43-49. Doi: 10.1007/s10545-009-9015-8

13. Uaariyapanichkul J, Saengpanit P, Damrongphol P, Suphapeetiporn K, Chomtho S. Skin lesions associated with nutritional management of maple syrup urine disease. Case Rep Dermatol Med, 2017;2017(1):3905658. Doi: 10.1155/2017/3905658

14. Bebispro for Windows [software]. Turkish Version (Bebis 4). Stuttgart, Germany; 2004. Data based on: Bundeslebensmittelschlüssel (BLS) 11.3 and USDA 15.

15. Acosta PB, Yannicelli S. Plasma micronutrient concentrations in infants undergoing therapy for phenylketonuria. Biol Trace Elem Res, 1999;67(1):75-84. Doi: 10.1007/BF02784277

16. Millet P, Vilaseca MA, Valls C, Pérez-Dueñas B, Artuch R, Gómez L, et al. Is deoxypyridinoline a good resorption marker to detect osteopenia in phenylketonuria? Clin Biochem, 2005;38(12):1127-1132. Doi: 10.1016/j.clinbiochem.2005.09.002

17. Van Bakel MM, Printzen G, Wermuth B, Wiesmann UN. Antioxidant and thyroid hormone status in selenium-deficient phenylketonuric and hyperphenylalaninemic patients. Am J Clin Nutr, 2000;72(4):976-981. Doi: 10.1093/ajcn/72.4.976

18. Artuch R, Colomé C, Sierra C, Brandi N, Lambruschini N, Campistol J, et al. A longitudinal study of antioxidant status in phenylketonuric patients. Clin Biochem, 2004;37(3):198-203. Doi: 10.1016/j.clinbiochem.2003.10.017

19. A, Vanzin CS, Biancini GB, Manfredini V, de Oliveira AB, Wayhs CA, et al. Evidence that L-carnitine and selenium supplementation reduces oxidative stress in phenylketonuric patients. Cell Mol Neurobiol, 2011;31(3):429-436. Doi: 10.1007/s10571-010-9636-3

20. Wilke BC, Vidailhet M, Favier A, Guillemin C, Ducros V, Arnaud J, et al. Selenium, glutathione peroxidase (GSH-Px) and lipid peroxidation products before and after selenium supplementation. Clin Chim Acta, 1992;207(1-2):137-142. Doi: 10.1016/0009-8981(92)90157-l

21. Sierra C, Vilaseca MA, Moyano D, Brandi N, Campistol J, Lambruschini N, et al. Antioxidant status in hyperphenylalaninemia. Clin Chim Acta, 1998;276(1):1-9. Doi: 10.1016/s0009-8981(98)00091-6

22. Martinez-Cruz F, Pozo D, Osuna C, Espinar A, Marchante C, Guerrero JM. Oxidative stress induced by phenylketonuria in the rat: prevention by melatonin, vitamin E, and vitamin C. J Neurosci Res, 2002;69(4):550-558. Doi: 10.1002/jnr.10307

23. Ercal N, Aykin-Burns N, Gurer-Orhan H, McDonald JD. Oxidative stress in a phenylketonuria animal model. Free Radic Biol Med, 2002;32(9):906-911. Doi: 10.1016/s0891-5849(02)00781-5

24. Reilly C, Barrett JE, Patterson CM, Tinggi U, Latham SL, Marrinan A. Trace element nutrition status and dietary intake of children with phenylketonuria. Am J Clin Nutr, 1990;52(1):159-165. Doi: 10.1093/ajcn/52.1.159

25. Sirtori LR, Dutra-Filho CS, Fitarelli D, Sitta A, Haeser A, Barschak AG, et al. Oxidative stress in patients with phenylketonuria. Biochim Biophys Acta, 2005;1740(1):68-73. Doi: 10.1016/j.bbadis.2005.02.005

26. Ribas GS, Sitta A, Wajner, M, Varnas, CR. Oxidative stress in Phenylketonuria: what is the evidence? Cell Mol Neurobiol, 2011;31(5):653-662. Doi: 10.1007/s10571-011-9693-2

27. Dobrowolski SF, Phua YL, Vockley J, Goetzman E, Blair HC. Phenylketonuria oxidative stress and energy dysregulation: Emerging pathophysiological elements provide interventional opportunity. Mol Genet Metab, 2022;136(2):111-117. Doi: 10.1016/j.ymgme.2022.03.012

28. Colomé C, Artuch R, Vilaseca MA, Sierra C, Brandi N, Lambruschini N, et al. Lipophilic antioxidants in patients with phenylketonuria. Am J Clin Nutr, 2003;77(1):185-188. Doi: 10.1093/ajcn/77.1.185

29. Rocha JC, Martins MJ. Oxidative stress in phenylketonuria: future directions. J Inherit Metab Dis, 2012;35(3):381-398. Doi: 10.1007/s10545-011-9417-2

30. Bortoluzzi VT, Dutra Filho CS, Wannmacher CMD. Oxidative stress in phenylketonuria-evidence from human studies and animal models, and possible implications for redox signaling. Metab Brain Dis, 2021;36(4):523-543. Doi: 10.1007/s11011-021-00676-w

31. Gassió R, Artuch R, Vilaseca MA, Fusté E, Colome R, Campistol J. Cognitive functions and the antioxidant system in phenylketonuric patients. Neuropsychology, 2008;22(4):426-431. Doi: 10.1037/0894-4105.22.4.426

32. Eide DJ. The oxidative stress of zinc deficiency. Metallomics, 2011;3(11):1124-1129. Doi: 10.1039/c1mt00064k

33. Barretto JR, Silva LR, Leite ME, Boa-Sorte N, Pimentel H, Purificação AC, et al. Poor zinc and selenium status in phenylketonuric children and adolescents in Brazil. Nutr Res, 2008;28(3):208-211. Doi: 10.1016/j.nutres.2007.12.009

34. Gropper SS, Acosta PB, Clarke-Sheehan N, Wenz E, Cheng M, Koch R. Trace element status of children with PKU and normal children. J Am Diet Assoc, 1988;88(4):459-465.

35. Gok F, Ekin S, Dogan M. Evaluation of trace element and mineral status and related to levels of amino acid in children with phenylketonuria. Environ Toxicol Pharmacol, 2016;45:302-308. Doi: 10.1016/j.etap.2016.06.014

Acta Pharm. Sci. Vol 63:(2), 2025
Original article
DOI: 10.23893/1307-2080.APS6326

Evaluation of the antimicrobial activity and cytotoxicity of *Rhaponticoides iconiensis* seed extract

Sumeyye OZYAMAN[1*], Gamze Nur KOSOVALI[2], Ibrahim OZTURKCI[3], Merve SIMSAR[4]

1 Istanbul Medipol University, Graduate School of Health Sciences, Department of Histology and Embryology, Istanbul, Türkiye
2 Bahcesehir University, School of Medicine, Istanbul, Türkiye
3 MEF University, Computer Science and Engineering, Istanbul, Türkiye
4 Marmara University, Institute of Health Sciences, Istanbul, Türkiye

ABSTRACT

The goal of this study is to evaluate the antimicrobial and cytotoxic activities of aqueous extract from *Rhaponticoides iconiensis* seed. The Soxhlet extraction method was used to extract the seed in distilled water. It was tested for antimicrobial activities against pathogenic bacteria Escherichia coli using the disc diffusion method. Additionally, the cytotoxic activity of the seed extract on the MCF7 breast cancer cell line was evaluated by MTT (3-(4,5-dimethylthiazol-2-yl)-2,5-diphenyltetrazolium bromide) assay. *R. iconiensis* showed strong antibacterial activity against Escherichia coli compared to Cefotaxime antimicrobial agents. Additionally, an effective *in vitro* cytotoxic activity against the MCF7 is observed ($p<0.01$). The present study is the first report of endemic *Rhaponticoides iconiensis* seeds exhibiting potential antimicrobial activity and cytotoxicity, and it requires further investigation and characterization. These findings may be applied as a guideline for selecting Turkish medicinal plant species for further pharmacological and phytochemical studies.

Keywords: *Rhaponticoides iconiensis*, antimicrobial, cytotoxicity, cancer, phytotherapy

*Corresponding author: Sumeyye OZYAMAN
E-mail: sumeyye.ozyaman@medipol.edu.tr
ORCIDs:
Sumeyye OZYAMAN: 0000-0002-6077-7423
Gamze Nur KOSOVALI: 0009-0003-1642-9952
Ibrahim OZTURKCI: 0009-0005-0858-7226
Merve SIMSAR: 0009-0002-8460-5447
(Received 6 Jun 2024, Accepted 21 Jul 2024)

INTRODUCTION

Several plants are regarded as potential candidates for drugs due to their drug-like characteristics[1]. Since Türkiye is included in three different flora regions, plant diversity is of great importance. Many plants belonging to these regions are distributed among the plant communities in Türkiye[2,3]. It is known that there are approximately 9000 different natural plant species in Türkiye and 30% of these plants are endemic. Although there are many endemic plants, this diversity of plants cannot be utilized sufficiently[4].

Cancer is the primary cause of mortality in every nation worldwide[5]. Based on 2019 estimates, the World Health Organization (WHO) indicated that in 112 of 183 countries, cancer was the first or second most common cause of death before the age of 70, and in 23 countries, it was the third or fourth leading cause[6]. Although there is a significant decrease in stroke and coronary heart disease death rates compared to cancer, this is still the leading cause of death[7]. GLOBOCAN 2020 estimated that cancer claimed 10 million lives with 19.3 million new cases diagnosed in 2020[8].

Asteraceae is a vast and globally distributed family of flowering plants, with over 1,100 genera and 2,500 species. Within this family, *Centaurea L.* genus is among the largest and the most significant genera within the Asteraceae family and the *Rhaponticoides* genus is a member of the Asteraceae family. *Rhaponticoides iconiensis* (*R. iconiensis*), a species within this genus, is endemic to Konya, Türkiye[9]. It is widely used as herbal medicine due to its various properties[6]. In Türkiye, there are 8 species belonging to the *Rhaponticoides* genus with 7 of them being endemic. These species are known by the Turkish name 'Tülüşah'[4,10]. In our study, we focused on *R. iconiensis* which is one of these species.

There are few studies that reported chemical composition and bioactivity of *R. iconiensis*. Paşayeva et al. showed the antioxidant and antidiabetic activity of *R. iconiensis* flower[11]. Additionally, antioxidant properties, total phenol amounts and flavonoid amounts of the endemic *Rhaponticoides* species were determined. The mean percentage of DPPH (2,2-diphenyl-1-picrylhydrazyl) antioxidant free radical scavenging effect values is presented[12]. The antioxidant properties, enzyme inhibition, and levels of phenolics and flavonoids in methanol extracts (obtained via maceration and Soxhlet extraction) and extracts of water (prepared through infusion) were assessed of leaves, roots, and flower heads of *R. iconiensis*. It was reported that the leaf extracts of *R. iconiensis* had higher levels of phenolic and flavonoid compounds compared to

the flower and root extracts. Also, the extract had 87 compounds, including hydroxybenzoic, hydroxycinnamic, and acylquinic acids, anthocyanins, flavones and flavanones. On the other hand, it has been indicated that *R. iconiensis* might be a valuable source of natural enzyme inhibitors for developing new drugs to address global health issues because of its enzyme inhibitory effects[13].

Despite all aforementioned data, there is no study evaluated effect of *R. iconiensis* seed extract. We aimed to uncover the antimicrobial activity and cytotoxicity of aqueous *R. iconiensis* seed extract.

METHODOLOGY

Plant material

The endemic *R. iconiensis* (Hub.-Mor.) M.V. Agab. & Greuter (Voucher No. 11.048) used in our studies was obtained from the Nezahat Gökyiğit Botanical Garden with its species identification confirmed. A very small population of *R. iconiensis* was found between the canal and the highway near the village of Orta Karaören, 18 km from Seydisehir, by the expert of the subject Prof. Dr. Mecit Vural.

Solvent extraction of plants

R. iconiensis seeds were weighed to 10 g in a Soxhlet extractor thimble and placed in the extraction apparatus. Seeds were extracted in a 250 ml conical flask based on the feed-to-solvent ratio [1:10 (w/v)]. The extraction was performed on 10 g of seed using 100 ml of water. A heating mantle was utilized to reflux the mixture for extraction periods spanning from 6 to 8 hours[13]. Once the extraction time was completed, the extract solution was cooled at room temperature. It was subsequently filtered using cone filter paper (Whatman no.1) and left in a water bath[14]. Powder sample was measured and stored at -4°C for further analysis.

Cell culture and cell line

For the assessment of the anticancer activity of the seeds, MCF7 human breast cancer cell line was used. L929 mouse fibroblast were used as a negative control in the study. MCF7 and L929 cells were cultured in Dulbecco's Modified Eagle Medium/Nutrient Mixture (DMEM) medium supplemented with 10% FBS (Fetal Bovine Serum), 1% penicillin-streptomycin (P4458; Sigma, USA) and 1% L-glutamine at 37°C with 5% CO_2 in a humidified incubator. Cells were suspended in medium with 1% penicillin-streptomycin (P4458; Sigma, USA) and 1% L-glutamine. Then, cells were counted (at a density of 2×10^4 cells/ml), transferred into a 96-well plate, and incubated for 24 hours prior to the addi-

tion of extract. The seed extracts were dissolved in cell culture medium, then diluted to different serial concentrations. The cells were treated with 10, 50, 100 μg/ml dilutions of the seed extracts and 1% Triton-x was added as a positive control. Untreated cells given the same volume of medium considered as the control.

Cell viability assay

For cell viability assay, it was measured using the standard colorimetric MTT (3-(4, 5-dimethylthiazol-2-yl)-2, 5-diphenyl tetrazolium bromide) assay technique. After 24 hours incubation, 10 μL of MTT solution (5 mg/ml) was dispensed into each well and incubated for 4 hours. Subsequently, 100 μL of DMSO was added to each well to dissolve the formazan crystals. Then absorbance readings were recorded at 570 nm using a microplate reader for each cell line. The cytotoxicity was determined by comparing the absorbance levels between the serial dilutions and the control samples[15].

Antimicrobial assay

Escherichia coli (*E. coli*) (ATCC 25922) was obtained from the Department of Clinical Microbiology, Faculty of Medicine at Istanbul University. The organisms were kept in Nutrient agar at 4°C until analyses.

Disc diffusion method

The antimicrobial effect of *R. iconiensis* was tested according to the disc diffusion Kirby-Bauer technique, which complies with the standards recommended by CLSI, 2015[16]. To prepare the bacterial inoculum, the bacterial strain was suspended in sterile dH_2O, and the turbidity was adjusted to approximately 10^6 CFU/ml, equivalent to 0.5 McFarland standards[17]. Nutrient agar (4018102; Biolife, Italy) was used for antimicrobial activity. Next, 28 g of agar was dissolved in 1 liter of dH_2O, autoclaved and allowed to cool. Then, 20 ml of agar was poured into petri dishes. The sterile swab was immersed in the standardized bacterial suspension and utilized to uniformly inoculate the bacteria onto Nutrient agar plates. The plates were left to air dry for 5 minutes and Whatman no.1 filter paper was utilized to produce discs with a diameter of 6 mm. These discs were sterilized via autoclaving and subsequently dried in a hot air oven at 80°C for one hour. Circular discs measuring 6 mm in diameter were created by punching through a sheet of filter paper. Each disc was impregnated with 20 μl each of 1 g/ml *R. iconiensis* aqueous extract, Cefotaxime antimicrobial agents (dissolved in dH_2O) as a positive control, or dH_2O alone as a negative control. Following impregnation, all papers were dried, and the discs were maintained under sterile conditions until further use. Then, all discs were positioned on

the plates with flamed forceps and delicately pressed to guarantee complete contact with the agar. The plates were subsequently placed in an incubator at 37°C for a period of 24 hours. After incubation, the areas surrounding the discs where bacterial growth was impeded were measured and recorded in millimeters. The experiments were replicated six times to ensure consistency and reliability.

Statistical analysis

Statistical evaluations of the results were performed using the ANOVA test with GraphPad InStat (GraphPad Software Inc., San Diego, CA, USA). Tests were conducted with a 95% confidence interval, and $p<0.05$ was considered significant. Data averages for the groups are presented as means ± standard deviation (SD). To determine the concentration necessary for a 50% reduction in cell viability (IC_{50}), regression analysis was used, and graphs were prepared using Microsoft Office Excel 2017.

RESULTS and DISCUSSION

Many studies show that plants have a potential for use in traditional medicines in numerous countries worldwide. Moreover, plants are identified as a crucial source for discovering new cytotoxic compounds, with many polyphenolic flavonoids having antitumor effects[18]. Every part of the plant, including the leaf, flower, seed, and rhizome, is known to be used for both nutritional and medicinal purposes[19]. Extracts from plant flowers, fruits, and seeds have shown a variety of biological activities in numerous studies[20,21]. Despite the limited research has been conducted on endemic *R. iconiensis* to investigate its biological activities with some parts of it, there is an absence of studies regarding the activity of the seed. Herein, we document the cytotoxic and antimicrobial effects of seed samples from the endemic *R. iconiensis* species to elucidate their biological activities.

Cytotoxic activity findings

In our study, MTT test was performed to reveal the cytotoxic effects of the aqueous seed of endemic *R. iconiensis* species on the MCF7 breast cancer cell line.

Breast cancer is the leading cause of death and the most prevalent type of cancer among women globally, with over 10 million new cases identified annually. The disease's progression, prognosis, and treatment outcomes are influenced by its heterogeneity. According to the WHO, breast cancer has the highest prevalence worldwide. In 2018, breast cancer caused to 2.09 million diagnoses

and 627,000 deaths among women. Moreover, around 1.7 million new cases were reported in 2020, resulting in an estimated 627,000 deaths[22]. Therefore, we showed that *R. iconiensis* could be a new potential candidate for MCF7 breast cancer cell line.

In a study, it is investigated the methanol extracts and sub-extracts derived from the leafy stems and flowers of *R. iconiensis*. Their cytotoxic effects were examined on A549, Colo 205, HepG2, Beas-2b and MCF7 cell lines using the MTT assay. The constituents of *R. iconiensis* extracts were identified and quantified using LC–MS/MS. Consequently, while the methanol extracts had no cytotoxicity against A549 cells, they showed cytotoxic effects on HepG2, Colo 205, MCF-7, and Beas-2b cell lines[23]. To determine whether seed of it has anti-cancer effect, we first explored the cytotoxicity of aqueous *R. iconiensis in vitro* and we showed the decreased % viability rate of the MCF7 cell line, and the results were statistically significant with increasing dose (Figure 1).

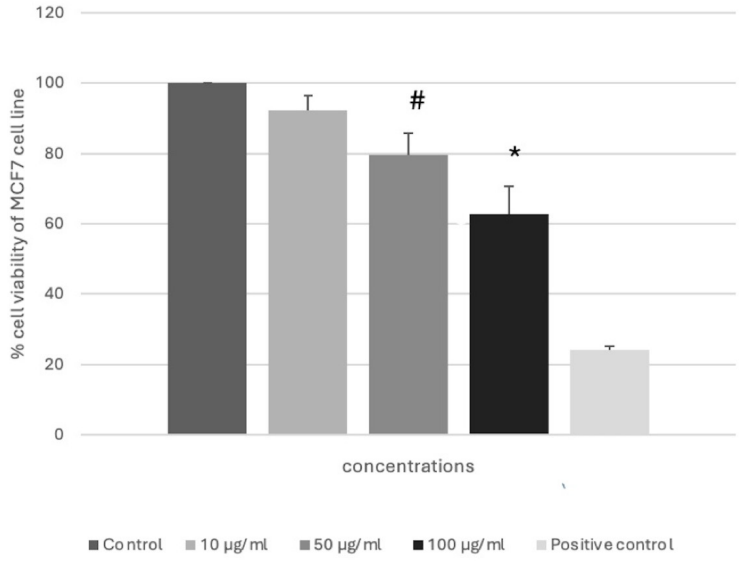

*p<0.01 compared to the control group

Figure 1. Representing the percentage (%) cell viability of *R. iconiensis* on MCF7 cell line. p<0.05. Values in the groups are expressed as mean (X) ± standard deviation (SD).

To investigate the cytotoxic effects of *R. iconiensis,* it was tested on healthy cell lines. After treating the L929 mouse fibroblast cells with different concentration of seed extract, there was no significant difference in viability of L929 compared to control (Figure 2).

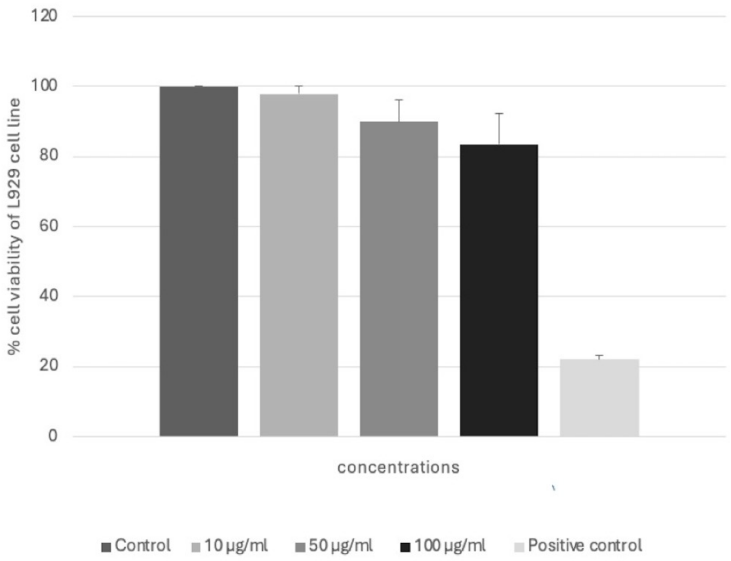

Figure 2. Representing the percentage (%) cell viability of *R. iconiensis* on L929 cell line. Results compared to control group. Values in the groups are expressed as mean (X) ± standard deviation (SD).

The IC_{50} (the dose that inhibits cell growth by 50%) value of *R. iconiensis* was found 56.33 µg/ml in MCF7 cell line. Tugay et al. provided that sub-extracts of leafy stem and flowers of *R. iconiensis* were most effective against MCF7 cancer cell line[23]. In a study, the cytotoxic effects of methanol extracts from the stem and flowers of *R. iconiensis* were showed against the A-549, HEPG2, MCF7, COLO-205, and BEAS-2b cell lines by MTT and SRB methods[24]. Hence, in present study we have proven that seed extracts of *R. iconiensis* have cytotoxic effect on MCF7 cell line.

Consequently, *R. iconiensis* showed cytotoxic effect on MCF7 cell line depending on increasing doses [50 µg/ml ($p<0.05$) and 100 µg/ml ($p<0.01$)] while it has not showed reduction in cell viability on L929 mouse fibroblast cell line.

Antimicrobial activity findings

The type of *E. coli* used in molecular biology labs is a model commensal bacterium that is prevalent in the mammalian intestine. However, some strains of this species can cause serious illnesses in humans[25]. Given this, the purpose of the present study was to determine the antimicrobial activity of *R. iconiensis* against *E. coli* and its antimicrobial activity has been demonstrated compared to Cefotaxime antimicrobial agents (Table 1). Paşayeva et al. reported the similar positive results, and they showed the antimicrobial effect with the microdilution method using leafy stem extracts of *R. iconiensis*[26].

Table 1. Zones of inhibitions as shown by aqueous *R. iconiensis* seed extract against *E. coli.* Data represents Mean ± Standard error of mean (n=6).

Disc diffusion zone diameters (cm) ± SD			
Microorganism	**Positive control (Cefotaxime)**	***R. iconiensis***	**Negative control (dH_2O)**
E. coli	4.9 ± 0,25	3,2 ± 0,2	—

*(— = no zone)

In summary, we have described robust antimicrobial activity and cytotoxic effect of seed samples from the endemic *R. iconiensis* which is extracted in distilled water by Soxhlet extraction method, we used only aqueous extract and focused exclusively on a single cell line and one bacterial strain. Hence, additional research encompassing a wider variety of cell lines and bacterial strains will provide a more thorough comprehension of their therapeutic potential.

STATEMENT OF ETHICS

No need for ethical approval for this study.

CONFLICT OF INTEREST STATEMENT

The authors state that they have no conflicts of interest.

AUTHOR CONTRIBUTIONS

All authors contributed to the work equally.

FUNDING SOURCES

No financial support was received for the study.

ACKNOWLEDGMENTS

This research was funded by the Bayrampasa Science Center.

REFERENCES

1. Bernhoft A. A brief review on bioactive compounds in plants. In: Norwegian Academy of Science and Letters. Bioactive compounds in plants - benefits and risks for man and animals. Proceedings of a symposium; 2008, Nov 13-14; Oslo, Norway. Norwegian Academy of Science and Letters; 2010. p. 11-17.

2. Svenning JC, Skov F. The relative roles of environment and history as controls of tree species composition and richness in Europe. J Biogeogr, 2005;32:1019-1033. Doi: 10.1111/j.1365-2699.2005.01219.x

3. Avcı M. Diversity and endemism in Turkey's vegetation. J Geography-Cografya Dergisi, 2005;13:27-55.

4. Güner A, Aslan S. List of plants of Turkey: (vascular plants). Nezahat Gökyiğit Botanical Garden Publications; 2012.

5. Bray F, Laversanne M, Weiderpass E, Soerjomataram I. The ever-increasing importance of cancer as a leading cause of premature death worldwide. Cancer, 2021;127:3029-3030. Doi: 10.1002/cncr.33587

6. World Health Organization. Global health estimates 2020: deaths by cause, age, sex, by country and by region, 2000–2019 [Internet]. Geneva: World Health Organization; 2020 [cited 6 Jun 2024]. Available from: https://www.who.int/data/gho/data/themes/mortality-and-global-health-estimates/ghe-leading-causes-of-death

7. Sung H, Ferlay J, Siegel RL, Laversanne M, Soerjomataram I, Jemal A, et al. Global cancer statistics 2020: GLOBOCAN estimates of incidence and mortality worldwide for 36 cancers in 185 countries. CA Cancer J for Clin, 2021;209-249. Doi: 10.3322/caac.21660

8. Anderberg A, Baldwin B, Bayer R, Breitwieser J, Jeffrey C, Dillon M, et al. The families and genera of vascular plants. In: Kubitzki K, editor. The families and genera of vascular plants. Vol. 8, Flowering plants. Eudicots. Asterales. Berlin: Springer-Verlag; 2007. p. 561-568.

9. Köse YB, İşcan G, Göger F, Akalın G, Demirci B, Başer KHC. Chemical composition and biological activity of *Centaurea baseri*: new species from Turkey. Chem Biodivers, 2016;13:1369-1379. Doi: 10.1002/cbdv.201600070

10. Cinbilgel I, Eren Ö, Duman H. *Rhaponticoides gokceoglui* (Asteraceae), a striking new species from Turkey. Phytotaxa, 2014;170(2). Doi: 10.11646/phytotaxa.170.2.5

11. Paşayeva L, Fatullayev H, Celik I, Unal G, Bozkurt NM, Tugay O, et al. Evaluation of the chemical composition, antioxidant and antidiabetic activity of *Rhaponticoides iconiensis* flowers: effects on key enzymes linked to type 2 diabetes *in vitro, in silico* and on alloxan-induced diabetic rats *in vivo*. Antioxidants, 2022;11:2284. Doi: 10.3390/antiox11112284

12. Hameed YAH, Bağcı Y. Biochemical studies on two endemic *Rhaponticoides* species (*R. aytachii, R. iconiensis*). Eur J Sci Educ, 2020;417-422.

13. Zheleva-Dimitrova D, Zengin G, Sinan KI, Yıldıztugay E, Mahomoodally MF, Ak G, et al. Identification of bioactive compounds from *Rhaponticoides iconiensis* extracts and their bioactivities: an endemic plant to Turkey flora. J Pharm Biomed Anal, 2020;190:113537. Doi: 10.1016/j.jpba.2020.113537

14. Alara OR, Abdurahman NH, Ukaegbu CI. Soxhlet extraction of phenolic compounds from *Vernonia cinerea* leaves and its antioxidant activity. J Appl Res Med Aromat Plants, 2018;11:12-17. Doi: 10.1016/j.jarmap.2018.07.003

15. Mosmann T. Rapid colorimetric assay for cellular growth and survival: application to proliferation and cytotoxicity assays. J Immunol Methods, 1983;65:55-63. Doi: 10.1016/0022-1759(83)90303-4

16. Clinical and Laboratory Standards Institute (CLSI). Methods for dilution antimicrobial susceptibility tests for bacteria that grow aerobically, Approved Standard, 10th ed. National Committee for Clinical Laboratory Standards, Wayne, USA, 2015; p. 88.

17. Cockerill FR, Wikler MA, Alder J, Dudley MN, Eliopoulos GM, Ferraro MJ, et al. Methods for dilution antimicrobial susceptibility tests for bacteria that grow aerobically. Approved Standard, 9th ed. Wayne; 2012.

18. Sak K. Characteristic features of cytotoxic activity of flavonoids on human cervical cancer cells. Asian Pac J Cancer Prev, 2014;15(19):8007-8019. Doi: 10.7314/apjcp.2014.15.19.8007

19. Sahu B, Sahu M, Sahu M, Yadav M, Sahu R, Sahu C. An updated review on *Nelumbo nucifera* Gaertn: chemical composition, nutritional value and pharmacological activities. Chem Biodivers, 2024;21(5):e202301493. Doi: 10.1002/cbdv.202301493

20. Keskin C. Antioxidant, anticancer and anticholinesterase activities of flower, fruit and seed extracts of *Hypericum amblysepalum* HOCHST. Asian Pac J Cancer Prev, 2015;16(7):2763-2769. Doi: 10.7314/apjcp.2015.16.7.2763

21. Zhang X, Bai Y, Wang Y, Wang C, Fu J, Gao L, et al. Anticancer properties of different solvent extracts of *Cucumis melo* L. seeds and whole fruit and their metabolite profiling using HPLC and GC-MS. Biomed Res Int, 2020;5282949. Doi: 10.1155/2020/5282949

22. World Health Organization. Accessed 6 June 2024. https://www.who.int/news-room/fact-sheets/detail/breast-cancer

23. Tugay O, Paşayeva L, Demirpolat E, Şahin M. Comparative evaluation of cytotoxicity and phytochemical composition of *Centaurea iconiensis (Rhaponticoides iconiensis*). Iran J Sci Technol Trans A: Sci, 2021;45:65-75. Doi: 10.1007/s40995-020-01030-y

24. Demirpolat E, Paşayeva L, Tugay O. Comparative evaluation of the cytotoxic effects of stem and flower extracts of *Rhaponticoides iconiensis* (Hub.-Mor.) M.V.Agab. & Greuter. Proceedings, 2017;1(10):1057. Doi: 10.3390/proceedings1101057

25. Kaper JB, Nataro JP, Mobley HL. Pathogenic *Escherichia coli*. Nat Rev Microbiol, 2004;2 (2):123-140. Doi: 10.1038/nrmicro818

26. Paşayeva L, Ince U, Fatullayev H, Ceylan C, Tugay O. Hypoglycemic, antioxidant, antimicrobial activities and phytochemical analyses of *Rhaponticoides iconiensis* leafy stem extracts. Vegetos, 2021;34:592-599. Doi: 10.1007/s42535-021-00250-w

Acta Pharm. Sci. Vol 63:(2), 2025
Original article
DOI: 10.23893/1307-2080.APS6327

Determination of antioxidant activities of rosehip (*Rosa canina* L.) fruits grown in Sivas province

Yakup GÖKÇEL[1], Eda SÖNMEZ GÜRER[2*], Ayhan ALTINTAŞ[3]

1 Sivas Cumhuriyet University, Faculty of Pharmacy, Sivas, Türkiye
2 Sivas Cumhuriyet University, Faculty of Pharmacy, Department of Pharmacognosy, Sivas, Türkiye
3 Anadolu University, Faculty of Pharmacy, Department of Pharmacognosy, Eskisehir, Türkiye

ABSTRACT

Rosa canina L., belonging to the Rosaceae family, is the most common *Rosa* species found in T*ürkiye*. Known commonly as rosehip, it is widely used in various traditional medicines. This study investigates the antioxidant activities of ethanol and water extracts of rosehip (*Rosa canina* L.) fruit samples naturally grown in Sivas. Using DPPH and ABTS assays, we measured the antioxidant capacities of the samples and compared results based on the solvents. Findings show that the ethanol extract exhibited a higher antioxidant capacity, with an IC_{50} value of 13.28 ± 1.3 µg/mL in the DPPH assay and 24.98 ± 5.3 µg/mL in the ABTS assay, compared to the water extract with IC_{50} values of 18.099 ± 2.4 µg/mL and 38.47 ± 6.1 µg/mL, respectively. These results suggest that rosehip fruits could serve as effective sources for antioxidant-rich pharmaceutical products, with ethanol extracts demonstrating a stronger antioxidant effect than water extracts.

Keywords: *Rosa canina*, antioxidant activity, rosehip, DPPH, ABTS

INTRODUCTION

Rosa canina, belonging to the Rosaceae family, refers to the fruits of wild rose species that can grow in almost all regions of Türkiye. *Rosa canina*, which also

*Corresponding author: Eda SÖNMEZ GÜRER
E-mail: edagurer@cumhuriyet.edu.tr
ORCIDs:
Yakup GÖKÇEL: 0009-0005-0026-7682
Eda SÖNMEZ GÜRER: 0000-0003-0319-6312
Ayhan ALTINTAŞ: 0000-0002-9413-0636
(Received 1 Nov 2024, Accepted 3 Dec 2024)

grows in Northeast Africa and Eurasia, is widely distributed in the Anatolian region. It grows wild along the edges of forests, ponds, shrublands, and grasslands[1,2]. Among the over 30 *Rosa* species in Türkiye, *Rosa canina* is the most widespread and is especially suited for processing due to its distribution and fruit characteristics. It is often found along forest edges, fields, and roadsides, especially in Türkiye's colder, more mountainous regions[3,4]. Regionally, rosehip is also known by various names: wild rose, dog rose; Askil, Civil, Gül burnu, Gül elması, İp burması, İp burnu, İt burnu, Kuşburnu, Kuşburni, Asker gülü, İt gülü[5,6]. Rosehip is a highly beneficial food source with a rich nutritional value, commonly preferred by the public for various health purposes. Traditionally, rosehip fruits have been used for generations to treat kidney stones, gastroenteritis, hypertension, and respiratory infections[7,8]. Rosehip fruits contain vitamins C, P, A, B1, B2, E, and K and are used to produce products such as jam, marmalade, juice, and tea. Besides its anti-inflammatory properties, rosehip is an excellent natural source of vitamin C and lycopene. Due to its nutritional composition, rosehip supplementation has shown beneficial effects in managing chronic conditions such as osteoarthritis, rheumatoid arthritis, and cancer[9,10]. Due to its nutritional content, rosehip supplements have positive effects on certain chronic diseases such as osteoarthritis, rheumatoid arthritis and cancer[10].

The fruits are rich in phenolic compounds such as apigenin, phloroglucinol, quercetin, gallic acid, and caffeic acid, with smaller amounts of catechin, resveratrol, and chlorogenic acid. The high antioxidant activity of rosehip is attributed to its ascorbic acid, beta-carotene, tocopherol, anthocyanin, and other phenolic compounds. Studies report the phenolic compounds anti-inflammatory, antioxidant, anticarcinogenic, antimicrobial, and antimutagenic properties. Additionally, rosehip fruits contain high amounts of Ca, Mg, Fe, Ag, Cu, Mn, Na, P, Sr, Zn, and pectin[3,8,11-14].

Oxidative stress occurs due to an imbalance between free radicals and antioxidants in the human body, a factor known to play a significant role in human health. Accumulation of free radicals in the body, reaching high levels, can damage cellular components such as lipids, proteins, and DNA, leading to neuronal dysfunction, chronic diseases, and even death. Experimental studies show that oxidative stress plays a critical role in the progression of diseases such as cancer, cardiovascular diseases, neurodegenerative disorders, aging, and age-related diseases. The damage caused by oxidative stress can be prevented by endogenous (superoxide dismutase, catalase, and glutathione) and exogenous (phenolic acids, flavonoids, and vitamins) antioxidant systems[15-17]. While antioxidants are naturally produced by some plants and animals, this process differs

in humans, making a balanced and regular diet crucial for sufficient antioxidant levels[18]. In this study, the antioxidant activities of rosehip fruits obtained from the *Rosa canina* plant naturally growing in the Zara district of Sivas province and prepared with ethanol and water solvents were investigated, with results compared and interpreted according to the solvents used.

METHODOLOGY

Plant material

In this study, the fruits obtained from the *Rosa canina* L. plant were collected fresh from the Esenler Village region of Zara, Sivas, in September 2022. These fruits were then dried under suitable conditions and prepared for experimental use. Species identification was conducted by Assoc. Prof. Dr. Mustafa Sevindik.

Chemicals

All chemicals and reference standards utilized in the experimental protocols were obtained from Sigma Chemical Co. (St. Louis, MO, USA). The chemicals used were of analytical grade.

Extraction

The dried fruits were ground into coarse powder. A sample of 5g of plant material was weighed and placed into an Erlenmeyer flask, to which 50 mL of ethanol was added. The flask was then sealed and left to macerate at room temperature, with occasional shaking to ensure thorough maceration. After 24 hours, the macerate was filtered, new solvent (50 mL) was added to the plant material, and the maceration was continued for three days. The collected macerates were then concentrated using a rotary evaporator at a low temperature (40°C) under vacuum[19]. The extracts were combined in dark-colored, capped glass containers and stored at -20°C in a refrigerator until use in experimental studies, with percentage yield calculations recorded.

For the water extract, an infusion process was used. A sample of 5g of plant material was weighed and placed into Erlenmeyer flasks, to which 50 mL of hot distilled water was added. The flask was sealed and left to stand at room temperature for 10–15 minutes with occasional shaking. After this period, the extract was filtered, and another 50 mL of hot distilled water was added to the plant material. After three repetitions, the collected extracts were placed in a lyophilizer (freeze-dryer) to ensure complete removal of water. After four days, the remaining extract in the freeze-dryer was transferred to a dark-colored, capped glass container, and the percentage yield was calculated. Extracts were stored at -20°C in a refrigerator until used in experimental studies.

For biological activity, stock solutions at a concentration of 1 mg/mL were prepared from each extract. The stock solution for the ethanol extract was prepared in DMSO (dimethyl sulfoxide), and for the water extract, it was prepared in distilled water.

Determination of antioxidant activity

DPPH (2,2-diphenyl-1-picrylhydrazyl) radical-scavenging activity

The DPPH free radical method[20] is a practical and highly reliable technique for determining the free radical scavenging capacity of antioxidants. DPPH is a stable nitrogen radical that is commercially available; its ethanol solution appears purple and is measured at an absorbance of 517 nm. When antioxidants are introduced into the DPPH solution, they reduce DPPH, changing the solution from purple to yellow. This reaction is monitored using a spectrophotometer[21,22].

For this test, the stock solution of each sample was prepared in methanol (MeOH) at a concentration of 1 mg/mL. After filtration, 200 µL of the clear stock solutions were transferred to the first column of a 96-well microtitration plate. Using a multi-channel pipette, eight serial dilutions were made in equal amounts of MeOH, and the mixtures were vortexed for 5 minutes. The DPPH stock solution was prepared by dissolving 2 mg of DPPH in 25 mL of MeOH, yielding a final concentration of 80 µg/mL. To each well, 100 µL of the DPPH solution was added to initiate the reaction, which was then incubated in the dark at room temperature for 30 minutes[23,24]. Ascorbic acid at the same concentration was used as a positive control, DPPH + MeOH as the negative control, and MeOH alone as the blank. The UV absorbance was read at 517 nm using a microplate spectrophotometer (Epoch) at room temperature[24].

The % inhibition value of DPPH was calculated using the following formula[25,26]:

$$\% \text{ Inhibition} = [(A \text{ Control} - A \text{ Sample}) / A \text{ Control}] \times 100$$

ABTS (2,2'-Azino-bis-3-ethylbenzothiazoline-6-sulfonic acid) radical-scavenging activity

The ABTS radical-scavenging activity, which follows the standard TEAC (Trolox Equivalent Antioxidant Capacity) method, was performed by optimizing the procedures established by Papandreou et al. (2006), Re et al. (1999), and Ardağ (2008)[27-29].

In the experimental protocol, a solution of 7 mM ABTS in distilled water (50 mL) was mixed with a 2.45 mM potassium persulfate solution (25 mL) and left

in the dark for 12–16 hours to form the radical cation. This blue-green ABTS radical solution was diluted with ethanol to a 1:80 ratio until an absorbance of 0.8–0.7 was achieved at 734 nm. Standard Trolox solutions were prepared at concentrations of 3, 2, 1, 0.5, 0.25, and 0.125 mM. Then, 10 µL of each sample was mixed with 990 µL of the prepared ABTS solution, and absorbance was measured at 734 nm. The absorbance results were used to create a linear regression equation for Trolox[24,26,30].

To perform the assay, 1 mL of the ABTS radical solution was added to numbered Eppendorf tubes, followed by 10 µL of each sample solution (100 µg/mL extract). Absorbance readings were taken at 734 nm at both 1 and 6 minutes. The difference in absorbance values between the first (A1) and sixth minute (A6) was calculated to yield ΔA values. Using these values, the percentage of inhibition was calculated using the formula below, and inhibition was plotted against sample concentration.

$$\% \text{ inhibition} = [(A6-A1)/A1] \times 100$$

$$\% \text{ inhibition} = (\Delta A/A1) \times 100$$

The TEAC method, initially developed by Miller et al., measures the decrease in absorbance of the ABTS radical solution in the presence of antioxidants[24,27,29-32].

Statistics

The results were expressed as mean ± standard deviation, and the statistical evaluation and calculations were performed using the GraphPad Data Analysis program. Data were analyzed at a 95% confidence level, and a p-value less than 0.05 was considered statistically significant.

RESULTS and DISCUSSION

This study initially involved the preparation of ethanol and water extracts of *Rosa canina* fruits, followed by the determination of extraction yields. By measuring the amounts used initially and the final amounts obtained, the extraction yields were calculated as percentages. It was found that the yield of the ethanol extract was higher at 10.41%, while the yield of the water extract was comparatively lower at 6.54% (Table 1).

Table 1. Yield values of *Rosa canina* fruit extracts

Extract	Yield %
Ethanol extract	10.41%
Water extract	6.54%

Antioxidant activity determination results

The antioxidant capacities of ethanol and water extracts from *Rosa canina* fruits were assessed using DPPH and ABTS radical-scavenging manual methods, with ascorbic acid, BHT (Butylated Hydroxytoluene), and Trolox as standard substances.

DPPH method activity results

The ability of the extracts to decolorize the DPPH solution was measured, with absorbance values obtained from the Elisa spectrophotometer indicating the extracts capacity to reduce DPPH radicals and overall antioxidant activity. Results showed that the antioxidant capacity of the ethanol extract was higher than that of the water extract, although the water extract still exhibited moderate to high antioxidant capacity. Specifically, the DPPH radical-scavenging activity of the ethanol extract had an IC_{50} value of 13.28 ± 1.3 µg/mL, while the water extract had an IC_{50} value of 18.099 ± 2.4 µg/mL. Table 2 shows the DPPH radical-scavenging activities of the extracts and standard solutions.

Table 2. DPPH radical-scavenging activity values of standard antioxidants and *Rosa canina* fruit extracts

Extracts/Standard Substances	IC_{50} (µg/mL)
Ethanol	13.28 ± 1.3
Water	18.099 ± 2.4
Ascorbic acid	5.35 ± 0.9
BHT	7.65 ± 1.8
Trolox	5.77 ± 1.6

ABTS method activity results

The ability of the extracts to scavenge ABTS radicals was measured spectrophotometrically and compared to standard solutions. Findings indicated that the antioxidant capacity of the ethanol extract was higher than that of the water extract. Specifically, the ABTS radical-scavenging activity of the ethanol extract had an IC_{50} value of 24.98 ± 5.3 µg/mL, while the water extract exhibited an IC_{50} value of 38.47 ± 6.1 µg/mL. Table 3 details the ABTS radical-scavenging activities of the extracts and standard solutions.

Table 3. ABTS radical-scavenging activity values for standard antioxidants and *Rosa canina* fruit extracts

Extracts/Standard Substances	IC_{50} (µg/mL)
Ethanol	24.98 ± 5.3
Water	38.47 ± 6.1
Ascorbic acid	7.48 ± 2.6
BHT	6.94 ± 1.1
Trolox	5.22 ± 0.9

In this study, the antioxidant activities of ethanol and water extracts of *Rosa canina* fruits were evaluated using the DPPH and ABTS methods, revealing that the ethanol extract demonstrated a stronger free radical inhibition capacity compared to the water extract. This result likely stems from the higher concentration of phenolic compounds in the ethanol extract. It is well-documented that the antioxidant activities of plant extracts are largely influenced by the diversity and quantity of phenolic and flavonoid compounds they contain. Secondary metabolites, through functional groups such as phenols and hydroxyls, donate hydrogen and electrons to radicals, playing a role in the reduction of oxidative compounds and consequently exhibiting antioxidant activity[33].

One study highlighted the antioxidant effects of extracts from *Rosa canina*, *Rosa sempervirens*, and *Pyrocantha coccinea*. When assessing the ability to protect against DNA damage, *Rosa canina* exhibited the highest level of protection, followed by *Rosa sempervirens* and *Pyrocantha coccinea*. Furthermore, among these species, the extract of *Rosa canina* was found to significantly reduce reactive oxygen species (ROS) in endothelial cells. Such findings suggest that *Rosa canina* extract could potentially serve as a dietary supplement to prevent pathological conditions arising from oxidative stress[34].

Another study found that the vitamin C content of *Rosa canina* is considerably higher than that found in citrus fruits, with some sources indicating that it has the highest vitamin C content among fruits and vegetables, ranging from 30 to 1300 mg per 100 g[35,36]. In a study aimed at confirming the antioxidant effects of *Rosa canina*, the vitamin C content, which partially contributes to its antioxidant properties, was determined. Extracts were prepared separately from the peel, seeds, and entire fruit, with the antioxidant capacity measured using the DPPH method. The results revealed significant vitamin C content and potent antioxidant properties in *Rosa canina*. Notably, the peel extract showed the highest antioxidant capacity (IC_{50} = 2.05 μg/mL), followed by the whole fruit extract (IC_{50} = 2.59 μg/mL)[37].

Further research involving dried wild *Rosa canina* fruits with three extracts (water, 50% ethanol, and 70% ethanol, all (v/v)). The content of ascorbic acid, tannins, and total phenolics was determined, and antioxidant strength was assessed using DPPH, ABTS, FRAP, and CUPRAC methods. The highest ascorbic acid content was found in the 70% ethanol (v/v) extract, the highest tannin content in the water extract, and the highest phenolic content in the 50% ethanol (v/v) extract. Overall, *Rosa canina* was recognized as a potent source of antioxidants[38]. Using total antioxidant status (TAS) kits, the TAS value of ethanol extracts obtained from the fruits of *Rosa canina* L. collected from Türkiye was determined to be 4.602 mmol/L. As a result, *R. canina* showed high antioxidant activities[39].

A similar study analyzed the antioxidant composition of ethanol extracts of *Rosa canina* fruits using HPLC-UV-MS and investigated their cytotoxic effects on HepG2 and SH-SY5Y cells. The results indicated that *Rosa canina* provides substantial protection against oxidative damage. Additionally, the antioxidant effect was attributed to compounds such as flavonoids, tannins, terpenoids, xanthonoids, and glycerol glucosides. Given its abundance of antioxidant components, *Rosa canina* has been suggested as a potential additive in the food industry and as a dietary component to help control certain cancer types[13]. In a study, it was observed that the highest ascorbic acid content was in the 70% ethanol extract, the highest tannin content was in the water extract, and the highest phenolic content was in the 50% ethanol extract. The results showed that *Rosa canina* L. can be considered as a rich source of antioxidants and has a serious potential as food and herbal cosmetic preparations[38]. A study conducted in Russia revealed that pelargonidin-3,5-diglucoside, an anthocyanin derivative prepared from *Rosa canina*, has a significant radioprotective effect[40].

Rosa canina fruits, which is widely used among the public, should be considered for further in-depth studies to isolate and produce active compounds effective in mitigating damage caused by free radicals. This study is expected to contribute to the existing literature by determining the antioxidant activities of *Rosa canina* fruits, which hold an important position in both domestic and international markets. The findings demonstrate the potential for using the studied extracts as natural sources of antioxidants with health benefits. Additionally, the inclusion of *Rosa canina* extracts in the development of innovative products may contribute significantly to the formulation of value-added food and cosmetic products.

STATEMENT OF ETHICS

Not applicable.

CONFLICT OF INTEREST STATEMENT

The authors declare no conflict of interest.

AUTHOR CONTRIBUTIONS

All authors contributed equally to the article. All authors have read and approved the final published version of the manuscript.

FUNDING SOURCES

Not applicable.

ACKNOWLEDGMENTS

We would like to thank Assoc. Prof. Dr. Mustafa SEVİNDİK for identifying the plant.

REFERENCES

1. Selahvarzian A, Alizadeh A, Baharvand PA, Eldahshan OA, Rasoulian B. Medicinal properties of *Rosa canina* L. Herb Med J, 2017;2(2):71-79. Doi: 10.22087/hmj.v3i2.703

2. Güler S. Doğu Anadolu bölgesinde doğal yayılış gösteren kuşburnu (*Rosa* L.) türleri, yetiştirme teknikleri ve kullanım alanları. Doğu Anadolu Ormancılık Araştırma Müdürlüğü Dergisi, 1997;0(1):40-59.

3. Ercisli S. Rose (*Rosa* spp.) germplasm resources of Turkey. Genet Resour Crop Evol, 2005;52(6): 787-795. Doi: 10.1007/s10722-003-3467-8

4. Yılmaz H, Bulut Y, Kelkit A. Peyzaj Planlama Çalışmalarında *Rosa canina*'nın Kullanım Alanları. Rosehip Symposium; 1996; Gümüşhane, Türkiye.

5. Anşin R. Doğu Karadeniz Bölgesinde Yetişen Doğal Rosa L. Taksonları. Rosehip Symposium; 1996; Gümüşhane, Türkiye.

6. Öz M. *Rosa pimpinellifolia* L. ve *Rosa canina* L. kuşburnu türlerinin çiçek, yaprak, gövde ve meyvelerinde uçucu yağ analizleri ve biyolojik aktiviteleri. [Doctoral Thesis]. Trabzon: University of Karadeniz Technical; 2016.

7. Ayati Z, Amiri MS, Ramezani M, Delshad E, Sahebkar A, Emami SA. Phytochemistry, traditional uses and pharmacological profile of rose hip: a review. Curr Pharm Des, 2019;24(35):4101-4124. Doi: 10.2174/1381612824666181010151849

8. Deliorman Orhan D, Hartevioğlu A, Küpeli E, Yeşilada E. *In vivo* anti-inflammatory and antinociceptive activity of the crude extract and fractions from *Rosa canina* L. fruits. Int J Ethnopharmacol, 2007;112(2):394-400. Doi: 10.1016/j.jep.2007.03.029

9. Doğan A, Kazankaya A, Çelik F, Uyak C. Kuşburnunun Halk Hekimliğindeki Yeri ve Bünyesindeki Bileşenler Açısından Yararları. II. National Grapefruits Symposium; 2006; Tokat, Türkiye.

10. Fan C, Pacier C, Martirosyan D. Rose hip (*Rosa canina* L): a functional food perspective. Functional Foods in Health and Disease, 2014;4(12):493-509. Doi: 10.31989/ffhd.v4i12.159

11. Başgel S, Erdemoğlu SB. Determination of mineral and trace elements in some medicinal herbs and their infusions consumed in Turkey. Science of the Total Environment, 2006;359(3):82-89. Doi: 10.1016/j.scitotenv.2005.04.016

12. Böhm V, Fröhlich K, Bitsch R. Rosehip –– a "new" source of lycopene? Mol Aspects Med, 2003;24(6):385-389. Doi: 10.1016/S0098-2997(03)00034-7

13. Fetni S, Bertella N, Ouahab A, Zapater JMM, Fernandez SPT. Composition and biological activity of the Algerian plant *Rosa canina* L. by HPLC-UV-MS. Arabian J of Chem, 2020;13(1):1105-1119. Doi: 10.1016/j.arabjc.2017.09.013

14. Stanila A, Diaconeasa Z, Roman I, Sima N, Maniutiu D, Roman A, et al. Extraction and characterization of phenolic compounds from rose hip (*Rosa canina* L.) using liquid chromatography coupled with electrospray Ionization - mass Spectrometry. Not Bot Horti Agrobo, 2015;43(2):349-354. Doi: 10.15835/nbha43210028

15. Negreanu-Pirjol BS, Oprea OC, Negreanu-Pirjol T, Roncea FN, Prelipcean AM, Craciunescu O, et al. Health benefits of antioxidant bioactive compounds in the fruits and leaves of *Lonicera caerulea* L. and *Aronia melanocarpa* (Michx.) Elliot. Antioxidants, 2023;12(4):951. Doi: 10.3390/antiox12040951

16. Pilipović K, Jurišić Grubešić R, Dolenec P, Kučić N, Juretić L, Mršić-Pelčić J. Plant-based antioxidants for prevention and treatment of neurodegenerative diseases: Phytotherapeutic potential of *Laurus nobilis*, *Aronia melanocarpa* and Celastrol. Antioxidants, 2023;12(3):746 Doi: 10.3390/antiox12030746

17. Silva RMG da, Alves CP, Barbosa FC, Santos HH, Adão KM, Granero FO, et al. Antioxidant, antitumoral, antimetastatic effect and inhibition of collagenase enzyme activity of *Eleutherine bulbosa* (Dayak onion) extract: *in vitro*, *in vivo* and *in silico* approaches. J Ethnopharmacol, 2024;318:117005. Doi: 10.1016/j.jep.2023.117005

18. Watanabe Y, Nakanishi H, Goto N, Otsuka K, Kimura T, Adachi S. Antioxidative properties of ascorbic acid and acyl ascorbates in ML/W Emulsion. J Am Oil Chem Soc, 2010;87(12):1475-1480. Doi: 10.1007/s11746-010-1632-8

19. Mata AT, Proença C, Ferreira AR, Serralheira MLM, Nogueira JMF, Araujo MEM. Antioxidant and antiacetylcholinesterase activities of five plants used as Portuguese food spices. Food Chem, 2007;103(3):778-786. Doi: 10.1016/j.foodchem.2006.09.017

20. Cuendet M, Hostettmann K, Potteratt O, Dyatmiko W. Iridoid glucosides with free radical scavenging properties from *Fagraea blumei*. Helv Chim Acta, 1997;80. Doi: 10.1002/hlca.19970800411

21. Eren E. Bazı soğansı bitkilerin antioksidan aktivitelerinin belirlenmesi. [Master's Thesis]. Sakarya: University of Sakarya; 2011.

22. Frankel EN, Meyer AS. The problems of using one-dimensional methods to evaluate multifunctional food and biological antioxidants. J Sci Food Agric, 2000;80(13):1925-1941. Doi: 10.1002/1097-0010(200010)80:13%3C1925::AID-JSFA714%3E3.0.CO;2-4

23. Chandra Shekhar T, Anju G. Antioxidant activity by DPPH radical scavenging method of *Ageratum conyzoides* Linn. leaves. American J Etnomed, 2014;1(4):244-249.

24. Koçyiğit M, İzol E, Haspolat YK. Phytochemicals in honey and health effect. In: Honeybees, plants and health. Orient Publications; 2023. p. 85-96.

25. Arıkan H. *Inula graveolens* (L.) Desf. bitkisi üzerinde farmakognozik çalışmalar. [Master's Thesis]. Eskişehir: University of Anadolu; 2019.

26. Dündar E. *Centaurea babylonica* L. bitkisi üzerinde farmakognozik araştırmalar. [Master's Thesis]. Eskişehir: University of Anadolu; 2017.

27. Ardağ A. Antioksidan kapasite tayin yöntemlerinin analitik açıdan karşılaştırılması. [Master's Thesis]. Aydın: University of Adnan Menderes; 2008.

28. Papandreou MA, Kanakis CD, Polissiou MG, Efthimiopoulos S, Cordopatis P, Margarity M, et al. Inhibitory activity on Amyloid-β aggregation and antioxidant properties of *Crocus sativus* stigmas extract and its crocin constituents. J Agric Food Chem, 2006;54(23):8762-8768. Doi: 10.1021/jf061932a

29. Re R, Pellegrini N, Proteggente A, Pannala A, Yang M, Rice-Evans C. Antioxidant activity applying an improved ABTS radical cation decolorization assay. Free Radic Biol Med, 1999;26(9-10):1231-1237. Doi: 10.1016/S0891-5849(98)00315-3

30. Gökgöz Y. Burdur ili pazarlarında satılan bazı meyvelerin antioksidan kapasitelerinin belirlenmesi. [Master's Thesis]. Burdur: University of Mehmet Akif Ersoy; 2015.

31. Miller M, Rao JKM, Wlodawer A, Gribskov MR. A left-handed crossover involved in amidohydrolase catalysis. FEBS Lett, 1993;328(3):275-279. Doi: 10.1016/0014-5793(93)80943-O

32. Rice-Evans CA, Miller NJ. Total antioxidant status in plasma and body fluids. Methods in Enzymology, 1994;234:279-293. Doi: 10.1016/0076-6879(94)34095-1

33. Cheung SCM, Szeto YT, Benzie IFF. Antioxidant protection of edible oils. Plant Foods for Human Nut, 2007;62(1):39-42. Doi: 10.1007/s11130-006-0040-6

34. Kerasioti E, Apostolou A, Kafantaris I, Chronis K, Kokka E, Dimitriadou C, et al. Polyphenolic composition of *Rosa canina*, *Rosa sempervivens* and *Pyrocantha coccinea* extracts and assessment of their antioxidant activity in human endothelial cells. Antioxidants, 2019;8(4):92. Doi: 10.3390/antiox8040092

35. Demir F, Özcan M. Chemical and technological properties of rose (*Rosa canina* L.) fruits grown wild in Turkey. J Food Eng, 2001;47(4):333-336. Doi: 10.1016/S0260-8774(00)00129-1

36. Ziegler S, Meier B, Sticher O. Fast and selective assay of *l* -ascorbic acid in Rose hips by RP-HPLC coupled with electrochemical and/or spectrophotometric detection. Planta Med, 1986;52(05):383-387. Doi: 10.1055/s-2007-969192

37. Georgieva S, Angelov G, Boyadzhieva S. Concentration of vitamin c and antioxidant activity of rosehip extracts. Journal of Chemical Technology and Metallurgy, 2014;49(5):451-454.

38. Taneva I, Petkova N, Dimov I, Ivanov I, Denev P. Characterization of Rose hip (*Rosa canina* L.) fruits extracts and evaluation of their *in vitro* antioxidant activity. Journal of Pharmacognosy and Phytochemistry, 2016;5(2):35-38.

39. Pehlivan M, Mohammed FS, Sevindik M, Akgül H. Antioxidant and oxidant potential of *Rosa canina*. Eurasian J Forest Science, 2018;6(4):22-25. Doi: 10.31195/ejejfs.475286

40. Jagetia GC, Baliga MS. The evaluation of the radioprotective effect of chyavanaprasha (an ayurvedic rasayana drug) in mice exposed to lethal dose of gamma-radiation: a preliminary study. Phytother Res, 2004;18(1):14-18. Doi: 10.1002/ptr.1298

Acta Pharm. Sci. Vol 63:(2), 2025
Original article
DOI: 10.23893/1307-2080.APS6328

Preparation and *in-vitro* evaluation of Paclitaxel-loaded sericin nanoparticles planned for pulmonary drug delivery system

Mustafa EGLA[1], Nawal A. RAJAB[2*]

1 University of Al-Turath, School of Pharmacy, Department of Pharmaceutics, Baghdad, Iraq
2 University of Baghdad, School of Pharmacy, Department of Pharmaceutics, Baghdad, Iraq

ABSTRACT

One of the most popular and successful antineoplastic drugs, Paclitaxel (PTX), comes from natural sources and is distinguished by its high lipophilicity. Sericin is a naturally occurring hydrophilic protein which become a popular choice for creating scaffolds for tissue engineering or drug delivery systems using nanocarriers. This work aimed to create and analyze sericin nanoparticles loaded with PTX to deliver lung drugs which synthesized utilizing a desolvation technique and were extensively analyzed to determine their physicochemical features, including particle size, Polydispersity index (PDI), entrapment efficiency, zeta potential, and *in vitro* drug release profile. Additionally, *in vitro* aerosolization were conducted to assess the effectiveness of aerosolization and the possibility of delivering drugs to the lungs using PTX-loaded sericin nanoparticles. Cytotoxicity research was performed on these nanoparticles using the A-549 lung cell line. The findings indicated that the sericin nanoparticles loaded with PTX had appropriate particle size, negative zeta potential, high entrapment efficiency, prolonged drug release behavior, and compelling aerosolization features. Moreover, the cytotoxicity assays on cancer cells demonstrated that the sericin nanoparticles loaded with PTX had anticancer solid properties. In conclusion, the PTX-loaded sericin nanoparticles that have been produced show significant potential as an innovative pulmonary drug delivery system for cancer treatment.

*Corresponding author: Nawal A. RAJAB
E-mail: dr.nawalayash@copharm.uobaghdad.edu.iq
ORCIDs:
Mustafa EGLA: 0009-0009-7033-283X
Nawal A. RAJAB: 0000-0003-1812-2244
(Received 19 Apr 2024, Accepted 15 Aug 2024)

Keywords: Paclitaxel, sericin, protein nanoparticles, aerosols, pulmonary drug delivery system

INTRODUCTION

Lung cancer is the first leading cause of cancer-related deaths worldwide, with an estimated 1.79 million deaths (18% of total deaths due to cancer in 2020). It is also the second most frequent type of malignancy, with more than 2.21 million cases, 11.4% of cancer cases, diagnosed annually. Small and non-small cell lung cancer (NSCLC) are the two types of lung cancer; NSCLC makes up 80–85% of all lung cancer cases[1].

Currently available conventional treatment methods include immunotherapy, chemotherapy, radiation, and surgery. Chemotherapy is a key treatment strategy for metastatic lung malignancies, helping to manage symptoms and increase patient survival. The cornerstone of chemotherapy for lung cancer is the intravenous delivery of chemotherapeutic drug[2].

Anticancer medications cause systemic toxicity, which includes nausea, vomiting, hair loss, and fatigue, as well as ineffective drug accumulation at tumorous sites and undesirable distributions in normal organs. Systemic drug administration eventually kills both cancerous and nearby healthy cells (lacks targeting capability)[3]. As a result, creating a treatment plan that can maximize effectiveness while reducing systemic adverse effects is imperative.

Nebulization is a method of delivering medication directly to the lungs through inhaling a fine mist. This method has been shown to be effective in treating a variety of respiratory diseases, including asthma, chronic obstructive pulmonary disease (COPD), and cystic fibrosis. Nebulization is also being investigated as a potential method for delivering chemotherapy drugs to the lungs in the treatment of lung cancer[4].

Because of its tailored administration and lower risk of systemic adverse effects, inhaled chemotherapy is seen to be a very promising treatment for non-small cell lung cancer. The advantage of using inhaled chemotherapy originate from the usage of a lower amount of the therapeutic agents which despite of that provide a high drug concentration at the cancerous cells which minimize the side effects of these agents because a lower concentration of antineoplastic drugs reaches the systemic circulation in comparison with other routes of drug administration like oral or IV routes. Lastly, compared to intravenous injection, it might also improve the patient's compliance[5].

One of the most popular and successful antineoplastic drugs, Paclitaxel (PTX), comes from natural sources and is distinguished by its high lipophilicity. It is a pseudoalkaloid whose nucleus is a taxane ring. By blocking the microtubule depolymerization of free tubulins, PTX's anti-proliferative mechanism is utilized to treat a variety of tumors, including ovarian, breast, prostate, and non-small cell lung cancer (NSCLC). Research has demonstrated that PTX suppresses the migration, proliferation, and release of collagenase associated with angiogenesis[6].

Because of their high drug loading capacity, stability *in vitro* or *in vivo*, controlled release, and ability to maximize the availability of the drug at its intended site of action for therapeutic benefit, nanocarriers are a class of drug delivery systems that have the potential to minimize the degradation of therapeutic agents. They have also attracted much attention in the field of tumor therapy. When a medication is administered to the site of therapeutic action, often smaller doses are required to get clinically effective results[7].

Safety concerns are a top priority when creating innovative drug delivery systems for the inhalation route. For a drug to be delivered locally through inhalation, excipients included in the composition of an inhaled formulation must be well-tolerated by the respiratory system[8].

Natural polymers have garnered interest as viable materials for nanocarriers due to their superior biocompatibility, *in vivo* biodegradability, and plentiful renewable supplies[9].

A naturally occurring hydrophilic protein called sericin is extracted from silkworm cocoons. Its excellent biocompatibility with cells and tissues, biodegradability, lack of immunogenicity, and variety of bioactivities have made it a popular choice for creating scaffolds for tissue engineering or drug delivery systems using nanocarriers[10].

This study aimed to develop self-assembled PTX-loaded sericin nanoparticles (NPs) made from protein sericin and poloxamer 407 by the modified desolvation method. Poloxamer 407 is self-assembled as a hydrophobic core (PPG) loaded with paclit and a hydrophilic corona made from Pconjugatedates to the hydrophilic protein (sericin). The formulated nanoparticles were then evaluated for their feasibility as carriers for the pulmonary delivery of PTX.

METHODOLOGY

Paclitaxel and sericin (lyophilized) were procured from Wuhan Senwayer Century Chemical Co., China. Dialysis membrane M.wt. 100 kDa was procured from HiMedia laboratories in Mumbai, India. Dimethylsulfoxide (DMSO) and methanol were procured from BDH Chemicals, Ltd., Liverpool, England. Poloxamer 407 was procured from Sigma-Aldrich, Germany.

Analytical quantification of PTX using HPLC

PTX's Quantification was determined by an HPLC method adapted from reference[8]. The chromatographic system (SIL-20A HPLC, Shimadzu, Japan) included an autosampler, a variable wavelength detector, and a quaternary pump. Shim-pack VP-ODS column C18 (5 µm, 250 mm x 6 mm) (Shimadzu, Japan) was used for the separations. The ultrapure water/acetonitrile (47:53 v/v) mobile phase was supplied at a 1.0 mL/min flow rate. At 227 nm, the Quantification was carried out. PTX produced a six-point standard curve between 25 and 1000 ng/mL, used for Quantification within a validated standard curve. The detection and quantification limits were 6.0 ng/mL and 11.0 g/mL, respectively, based on the linear regression value of $R^2 = 0.999$.

Preparation of PTX-loaded sericin NPs

PTX-loaded sericin NPs were prepared according to the previously reported procedure with modifications. Briefly, sericin powder, poloxamer 407, and PTX were dissolved in 1mL of DMSO at a final concentration of 1, 4.5, and 0.6% (w/v), respectively. The three materials were wholly dissolved using a bath sonicator for 15 min. Subsequently, the resultant solution mixture was added dropwise to 10 mL of deionized water under stirring at 1000 rpm using a magnetic stirrer (Vision Scientific, Korea), permitting the construction of PTX-loaded sericin NPs by self-assembly. Using cellulose dialysis tubes, the resulting NP suspension has been dialyzed against deionized water (100 kDa for 72 h, with frequent changes of deionized water every 4–6 h), allowing the formation of SNPs by self-assembly[11].

Particle size/ polydispersity index analysis

The particle size and PDI of PTX-loaded sericin NPs was measured using the dynamic light scattering (DLS) method (Zetasizer, Malvern, UK). The particle size and PDI of one milliliter of each preparation was measured using the Zetasizer. We used quartz cuvettes and set the instrument refractive index at 1.33. The temperature was 25°C, and the scattering angle was 90°. We conducted the experiments three times[12].

Measurement of zeta potential

The surface charge of the chosen NP formulation was calculated in terms of zeta potential by calculating their electrophoretic mobility. A Malvern instrument (Zetasizer, Malvern, UK) connected to a laser Doppler anemometer conducted the measurement. The instrument used a scattering angle of 90°[13]. We performed each test three times in the experiments.

Assessment of entrapment efficiency (EE%)

To determine the EE% of the generated self-assembled NP formulations, we combined 1 mL of NP suspension with 9 mL of methanol and sonicated it for 5 min using a bath sonicator (Powersonic 410, Hwashin Technology, Korea). This is considered "the actual drug content," determined by the HPLC method described earlier. In addition, we determined "the entrapped drug" by taking another 1 mL of the NP suspension and subjecting it to ultra-centrifugation for 60 min at 20,000 RPM at four °C using a cooling centrifuge (Eppendorf AG, Germany). The remaining supernatant was thrown away; then the remainder was dissolved in 10 mL of methanol and sonicated for 5 min in a bath sonicator to determine the amount of entrapped PTX using the HPLC method described earlier[14]. We performed all tests in triplicate. The EE% of each formulation was calculated using the equation below:

$$EE\% = \frac{Amount\ of\ entrapped\ drug}{\text{Actual drug content}} \text{ X } 100$$

Transmission electron microscopy (TEM)

The diluted sample was stained with phospho-tungstic acid, dropped on a copper grid, dried at 60°C, and then loaded onto the TEM holder to be imaged with a TEM detector (Joel JEM 1230; Tokyo, Japan). A clean petri dish with a copper grid hexagonal 200-mesh was attached to carbon tape for TEM examination[15].

In-vitro release study

The *in-vitro* drug release performance of PTX from self-assembled sericin-based PTX NPs was investigated using the dialysis technique. In summary, a previously soaked dialysis bag was filled with 1 mL of NP dispersion, equivalent to 0.5 mg of PTX (the molecular weight cutoff was 8.0 to 14 kDa). After being hermetically sealed, the dialysis bag was incubated at 37 ± 0.5°C with moderate shaking (100 rpm) in 75 mL of acetate buffer (pH = 5.4) containing brij-35 (0.5% w/v). Two mL of the media were removed at each scheduled time and replaced with freshly released media that had been pre-warmed to 37°C. Centrifuging the extracted release medium for 15 min at 12,000 rpm was done. The supernatant was collected for analysis using the HPLC method described earlier[16].

The release of marketed PTX (Abraxane®) and free PTX was performed as follows: 10 mg of lyophilized powder was dispersed in 2 mL deionized water, and from this suspension 1mL (equal to 0.5 mg of PTX) was placed in a dialysis bag, and one the release same as the colloidal dispersion of NPs. For free PTX, 5 mg was dispersed in 10 mL deionized water; from this suspension, 1 mL was taken and placed in the dialysis bag as in the method described for colloidal dispersion NPs and marketed product. The formula used to determine the release rate was RR% = (Wi/W total) × 100%, where Wi is the quantity of PTX measured at the given time, and W total is the entire amount of PTX loaded in the dialysis bag. A similarity factor (f2) was used to statistically verify the data obtained from the two release profiles using the equation below:

$$f2 = 50.\log\{100.[1 + \frac{1}{n}\sum_{t=1}^{n}(Rt - Tt)^2]^{-0.5}\}$$

Where (n) is the number of dissolution time points. (Rt) Moreover, (Tt) are the reference (Abraxane® or free drug) and test (PTX loaded sericin NPs) release values at time t, respectively. The two release profiles are considered similar when f2 values are greater than 50 (50–100); otherwise, the profiles are not similar[17].

Attenuated total reflectance infrared spectroscopy (ATR-FTIR)

The drug's compatibility with the excipients was validated by ATR–FTIR (Shimadzu). An IR Affinity-1S spectrophotometer with an ATR accessory was used to determine the spectra of pure PTX, excipients, a 1:1:1 physical combination (PTX: sericin: poloxamer 407), and the optimum formulation. FTIR/ATR spectra [4000–600 cm^{-1}] were collected with a resolution of 4 cm^{-1} by co-adding 256 scans for each spectrum at room temperature[18].

Differential scanning calorimeter (DSC)

The thermal behavior and thermotropic properties of pure PTX, poloxamer 407, pure sericin, and PTX-loaded sericin NPs (lyophilized) were evaluated using differential scanning calorimetry (DSC/TA-60 instrument from Shimadzu, Japan), equipped with the intercooler two cooling system. Nitrogen was utilized as a blank gas, and samples weighing 3-5 mg were heated in aluminum pans with scanning temperatures ranging from 50-250°C at a scanning rate of 10°C per minute[19].

***In-vitro* aerosol dispersion performance by the Next Generation Impactor™ (NGI)**

By US Pharmacopeia (USP) Chapter <601> specifications on aerosols[20], the *in vitro* aerosol dispersion properties of PTX loaded sericin NPs were determined

using (NGI) (M170 NGI: MSP Corporation, Shoreview, MN, USA) equipped with a stainless-steel induction port (USP throat), which used to connect the device to nebulizer reservoir (Omron NE-U780, Omron Healthcare UK Ltd, UK) through a customized rubber mouthpiece and equipped. Seven specialized stainless steel insert cups are included with the NGI. The NGI was linked to a Copley HCP5 vacuum pump via a Copley TPK 2000 critical flow controller, and a Copley DFM 2000 flow meter (Copley Scientific, UK) was used to measure and modify the airflow rate, Q, before each experiment[21]. Tween 80 was applied to every cup's particle collecting surface to guarantee effective particle capture and avoid inter-stage losses brought on by particle bounce. In order to do this, each of the eight NGI collection cups was submerged in an ethanol solution containing 1% Tween 80. The coated cups were then put under the fume hood to evaporate the ethanol thoroughly[22].

For the NGI flow rate of 60 L/min, the effective cutoff diameters for each impaction stage were calibrated by the manufacturer and stated as Stage 1 (8.06 μm), Stage 2 (4.46 μm); Stage 3 (2.82 μm); Stage 4 (1.66 μm); Stage 5 (0.94 μm); Stage 6 (0.55 μm); and Stage 7 (0.34 μm)[23].

The aerosolization starts by placing 2 ml of NP suspension (equivalent to 1 mg PTX) in a nebulizer cup and nebulizing for 10 min (according to European and Indian guidelines)[24,25] at 25°C, 65% relative humidity, and 60 L/min flow rate.

Each stage of the NGI, the induction port, and the nebulizer device were rinsed with 10 mL of the respective HPLC mobile phase and collected for quantitative analysis by HPLC[26]. The experiment was done in triplicate (n=3), and data are represented as mean ± SD. The mass median aerodynamic diameter (MMAD), geometric standard deviation (GSD), fine particle fraction (FPF), respirable fraction (RF), and emitted dose (ED) were using CITDAS software (Version 3)[27].

The fine particle fraction (FPF), respirable fraction (RF), and emitted dose (ED) were calculated as follows[28].

$$FPF\% = \frac{Mass\ deposited\ on\ stage\ 2\ through\ stage\ 7}{Initial\ mass\ loaded\ in\ nebulizer} \text{ X } 100$$

$$RF\% = \frac{Mass\ deposited\ on\ stage\ 2\ through\ stage\ 7}{Initial\ mass\ on\ all\ stages} \text{ X } 100$$

$$ED\% = \frac{Mass\ recoverd\ from\ NGI}{Initial\ mass\ in\ nebulizer} \text{ X } 100$$

In vitro cytotoxicity assay

The antitumor activity of Paclitaxel before and after loading with sericin-based NPs as well as blank NPs was performed by the Central laboratory in the Al-Mustansiriya University using the following procedures.

Cell culture

Human lung adenocarcinoma cell line A-549 was obtained from the American Type Culture Collection (ATCC). The cells were grown as monolayers in RPMI 1640 medium, supplemented with 10% FBS, 100 IU/mL penicillin, and 100µg/mL streptomycin sulfate at 37°C with 5% CO2 under fully humidified conditions[29].

MTT assay

A-549 cells were seeded in 96-well plates at a density of 5000 viable cells per well and incubated for 24 h to allow cell attachment. After 24 h of incubation at 37°C with 5% CO2, the growth medium was replaced with 100µL medium containing either free PTX solution in DMSO, PTX–loaded sericin NPs, or blank NPs (same amount as PTX–loaded sericin NPs) equivalent to PTX concentrations ranging from 0.1, 0.3, 0.5, 1.0, 3.0, 5.0, 10.0, and 30.0nM of PTX to each well then incubated at 37°C for 72 h. After 72 h of incubation with each compound, 20.0 µL of the MTT (3-(4, 5-dimethylthiazolyl-2)-2, 5-diphenyltetrazolium bromide) dye (MTT was dissolved in phosphate–buffered saline (PBS) at 5.0 mg/mL) 180µL of fresh growth medium were added to each 96–well then kept in an incubator for four h at 37°C for the formation of formazan crystals. After incubation, MTT was aspirated off, and DMSO (100µL) was added to each well to dissolve the formazan crystals after mild shaking for 15 min. The absorbance of the soluble formazan dye was measured at 570 nm using a microplate reader. Absorbance was measured at 570 nm using a microplate reader. Untreated cells were taken as control with 100% viability, and cells without the addition of MTT were used as blanks to calibrate the spectrophotometer to zero absorbance[30, 31].

Statistical analysis

The experiment's results were reported as the mean ± standard deviation (SD). The samples were analyzed using one-way analysis of variance (ANOVA) to see if there was a significant difference between studied formulations at a significance threshold of $p<0.05$[31].

RESULTS AND DISCUSSION

Preparation and characterization of the prepared NPs

The desolvation and accompanying dialysis procedures were used to create NPs. During the desolvation process, adding a DMSO mixture containing PTX, poloxamer 407, and protein sericin into the aqueous phase caused fast miscibility of DMSO with water, and then NPs were synthesized by spontaneous self-assembly. Paclitaxel was successfully incorporated into the core of self-assembled nanoparticles composed from hydrophobic (poly PPG) copolymers of poloxamer 407, as shown in Figure 1, which highlights the TEM of PTX-loaded sericin NPs. TEM confirms the spherical morphology of NPs, absence of particle aggregation, and core-shell structure. The particles appeared to be solid in structure with rounded outlines (i.e., hydrophobic core presumably containing PTX and a hydrophilic corona (poly PEG) to which hydrophilic protein is conjugated physically); this assumption is the same putative structure proposed by researchers Mandal et al.[11]. Because the corona-forming PEG chain block offers steric protection against non-specific absorption by the phagocytic system and permits prolonged residence in the lung, this is particularly advantageous for local delivery to the lung[32]. The size of formulated PTX-loaded sericin NPs was 145.0 nm with nearly homogeneous and uniform particle distribution in solvent without any aggregation (PDI of 0.25). The EE% of PTX-loaded sericin NPs was 82%.

Zeta potential measurements can determine the stability of a system by assessing the surface charges on particles. Large zeta potential values in absolute numbers often denote more stable systems. PTX-loaded sericin NPs in this study have a zeta potential of -30.16 ± 3.9 mV, suggesting that it has enough surface charge to be stable. Since the polypropylene oxide and polyethylene oxide segments in Poloxamer 407's structure were both nonionic, the presence of the protein sericin should cause the shift in the NPs' surface charge. The sericin structure has several negatively charged functional groups generated from various amino acid residues. The deprotonation of these carboxylate groups, which results in COO- groups, gave PTX-loaded sericin NPs their negative charge[33].

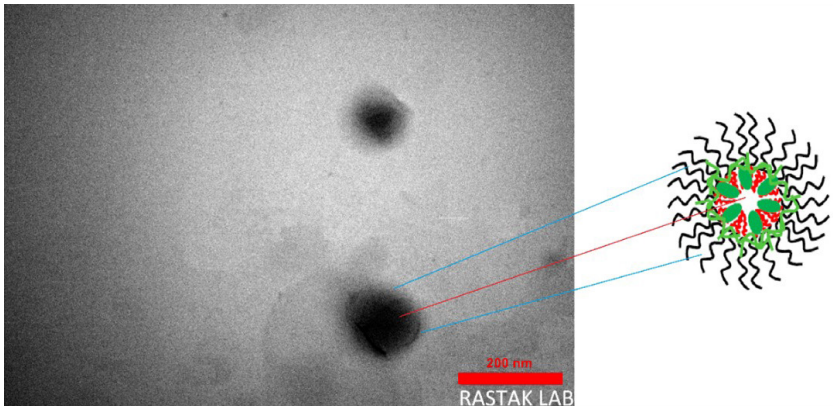

Figure 1. TEM of PTX-loaded sericin NPs merged with putative core-shell self assembles structure

In-vitro release study of PTX loaded sericin NPs

The release profile study of PTX-loaded sericin NPs, marketed (Abraxane®) and free PTX, was shown in Figure 2. In contrast to Abraxane®, which only releases 76% of the medication after the same time, PTX NPs demonstrated a 68% PTX release after 24 h in acidic solutions that mimicked the tumor microenvironment. Because of PTX's strong affinity toward the hydrophobic interior of the NPs, the formulation under study and Abraxane® showed a delayed and prolonged release of the drug. The drug included in these NPs may be released gradually owing to their capacity as drug reservoirs[34]. Although the drug release from Abraxane® was higher than observed in PTX NPs, both of them had similar release profiles (f_2=65). The *in vitro* release profile for free PTX suspension showed only 40% drug release throughout 24 h. The PTX loaded in NPs showed significantly higher release ($p<0.05$) than pure PTX suspension. The calculated similarity factor (f_2=36) indicates the difference between these profiles. The elaboration of this result relies on the fact that NPs have a larger surface area compared to the pure drug, which allows for more interactions with the surrounding environment; this, in turn, enhances PTX solubility and thus facilitates faster release of the drug. PTX is known for its poor solubility, but when encapsulated in NPs, it can be enhanced, leading to more efficient release from the NPs[35].

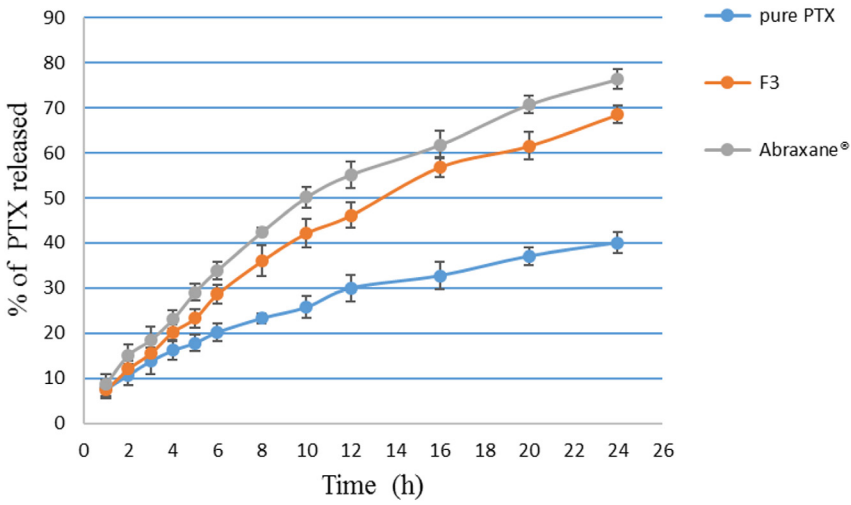

Figure 2. *In Vitro*, the release profile of PTX NPs was compared with the marketed product (Abraxane®) and Pure PTX in acetate buffer (pH 5.4) at 37°C.

ATR-FTIR analysis

FTIR spectroscopy was used to examine the functional group components and structural alterations that occurred during the creation of NPs. Figure 3 displays the IR spectrum of PTX, poloxamer 407, sericin, and the physical combination of PTX, sericin, and poloxamer 407 (1:1:1), and PTX-loaded sericin NPs.

The characteristic peaks in the FTIR spectrum of pure PTX are found at 3400–3500 cm^{-1} (N-H stretching), 3307 cm^{-1} (O-H stretching), 1734 cm^{-1} (C=O) stretching of ester, 1707 cm^{-1} (C=O) stretching of amide, 1645 cm^{-1} (C-C) stretching, 1242 cm^{-1} (C-N) stretching, 1176 cm^{-1} (NC-O) stretching, and 1072 cm^{-1} (C-O) stretching[36]. The spectrum of poloxamer 407 shows a band at 2881 cm^{-1} (C–H) stretching vibration, a band at 1467 cm^{-1} (C–H) bending vibration, and its distinctive band at 1109 cm^{-1} (C-O) stretching[37]. Sericin showed characteristic bands of C=O stretching at 1649 cm^{-1} and N-H bending at 1539 cm^{-1} of amides I and II, respectively, and broadband peaked at 3342 cm^{-1} owing to the stretching of the N-H bond of amides in conjunction with the absorption of the O-H groups[38]. The majority of the distinctive peaks for both the drug and the protein were visible in the physical mix spectrum: PTX: sericin: poloxamer 407 at a ratio of 1:1:1, suggesting that there was no drug-excipient interaction. The absence of all the primary peaks in the FT-IR spectrum of the optimum PTX-loaded sericin NP formulation is caused by PTX becoming entrapped in the self-assembled sericin-based PTX NPs. The following bands, which correspond to the properties of poloxamer 407, were seen in the optimized for-

mulation: a band at 2883 cm^{-1} from C-H stretching vibration, a band at 1467 cm^{-1} from C-H bending vibration, and a distinctive band at 1112 cm^{-1} from C-O stretching. In addition, while they have moved to higher wavenumbers 1647 and 1535 cm^{-1}, respectively—the distinctive bands of the sericin N-H bond of amides 3362 cm^{-1}, amide I, and II are still discernible, indicating the existence of the protein in the structure of the NPs.

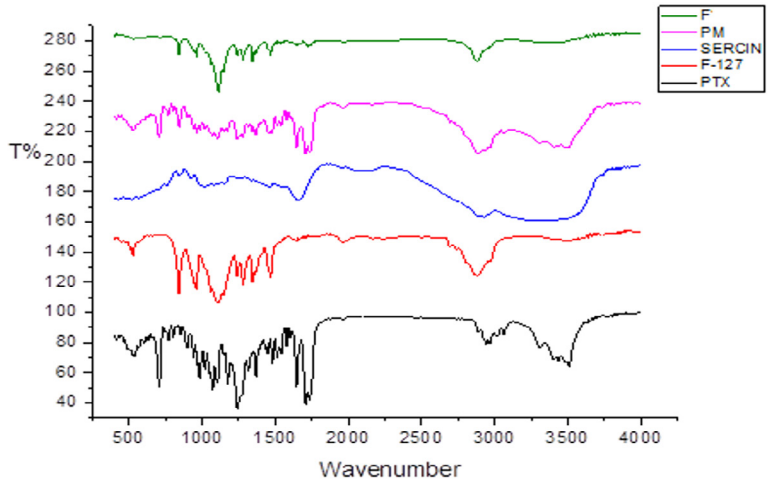

Figure 3. FTIR absorption spectrum of pure PTX, sericin, poloxamer 407, physical mixture, and optimized formulation

DSC analysis

The thermal analysis of PTX-loaded sericin NPs is shown in Figure 4. The DSC profile of PTX shows an endothermic effect at T peak = 220°C due to melting, indicating its pure crystalline state[39]. The DSC profile of poloxamer 407 also shows an endothermic effect at T peak = 60°C due to melting[40]. The DSC profile of sericin shows a broad endothermic effect at T peak = 122°C associated with order → disorder transitions, which can be considered thermal signatures of protein (irreversible) denaturation[41].

DSC profile of PTX-loaded sericin NPs shows the endothermic peaks of poloxamer 407 and sericin (shifted to lower melting temperatures) due to the presence of the other excipients with an additional peak of mannitol (added as a cryoprotectant) at T peak = 157°C. Conversely, there was no peak for PTX at 122°C, suggesting that PTX undergoes conversion to amorphous form (molecularly dispersed) during formulation[42]. These effects in the DSC curve of PTX-loaded sericin NPs confirm the presence of the protein in the structure of NPs.

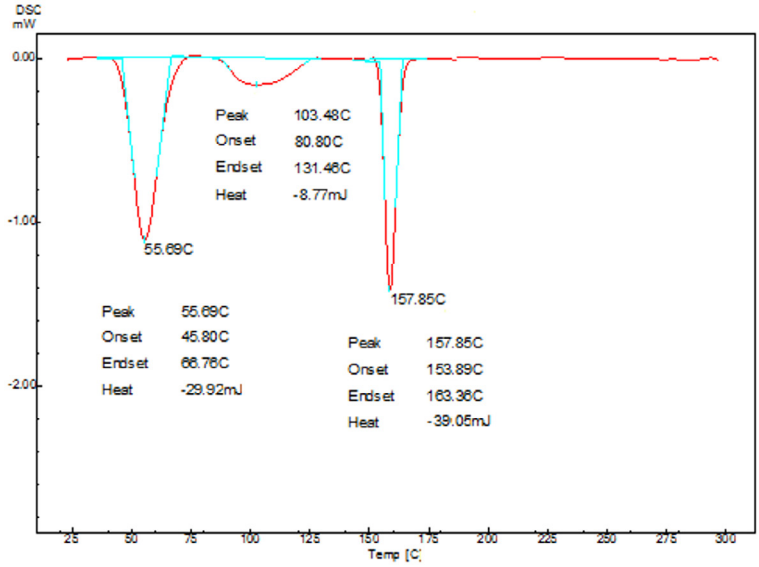

Figure 4. DSC profile of PTX-loaded sericin NPs

In-vitro aerosol dispersion performance by the Next Generation Impactor™

Nebulizers that can deliver formulations as minute droplets that will be deposited in the lung airways based on their aerodynamic qualities, such as MMAD and FPF, can be used in the pulmonary route of administration. These aerodynamic characteristics of nebulized particles reflect the *in vivo* deposition profile in the alveolar portion of deep lung regions and the airways[43].

The aerosol dispersion properties of PTX-loaded sericin NPs were evaluated using the Next Generation Impactor™ (NGI™) coupled with the Omron NE-U780 (Omron Healthcare UK Ltd, UK) nebulizer device. They are presented in Figure 5 and Table 1.

The data obtained indicated that the particle size distribution's normalcy, as shown by the MMAD (3.72μm) and GSD (2.06μm), was within the optimal range for pulmonary administration (1–5 and 1-3μm, respectively)[27]. The loaded dose in the device was emitted by an average extent of 81.5%, the average FPF% was about 54.83%, and the average RF% was 74.26%.

Table 1. Aerodynamic properties of PTX-loaded sericin NPs

Formulation	MMAD (μm)	GSD (μm)	FPF%	RF%	ED%
PTX-NPs	3.72 ± 1.08	2.06 ± 0.85	54.83 ± 2.05	74.26 ± 2.96	81.50 ± 2.23

It is expected that the particles on Stages 5-7, which had significant particle deposition and aerodynamic diameter values of less than 1 μm, would deposit in the deep lung alveolar region through a mechanism of deposition known as diffusion, or Brownian motion. The particles deposited on Stages 1-4 would primarily deposit through sedimentation owing to gravity settling in the middle-to-deep lung regions.

The hydrophilic polymer in the NPs' outer shell and the smallest particle size of PTX-loaded sericin NPs allowed for a repulsive steric interaction between the particles, effectively decreasing the overall adhesive forces. This allowed for more effective aerosolization and stabilization of the colloidal suspension in the air, which allowed the NPs to reach deeper stages of the NGITM device[44].

NPs that demonstrate the best in-vitro aerosol lung deposition can be inhaled to facilitate local delivery of PTX to the deep lungs. This allows the NPs to deposit in almost all lung regions, allowing for treatment of the entire tissue and minimizing adverse events and exposure to other organs.

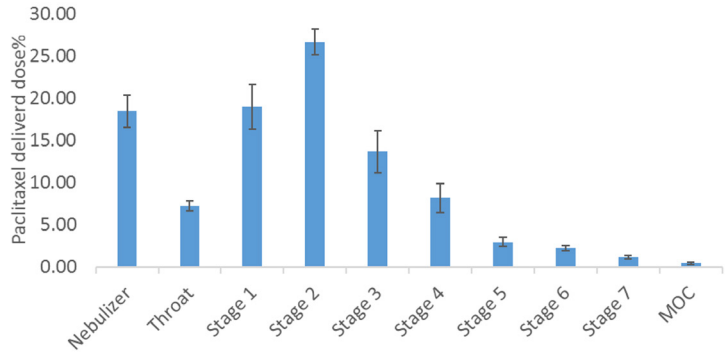

Figure 5. The aerosol dispersion performance of the nebulized NPs as the % deposition on each NGI™ stage

In-vitro cytotoxicity

The MTT assay was used to examine and compare the *in vitro* cytotoxicity of PTX-loaded sericin NPs with that of unloaded blank NPs and free PTX using the human lung cancer cell line A-549. As demonstrated in Figure 6, no significant ($p>0.05$) cytotoxic activity was seen for the drug-free NPs at dif-

ferent concentrations compared to others, suggesting that the synthetic blank NPs are harmless in cell culture. At all concentrations used (0.1-30 nM), PTX-loaded sericin NPs significantly ($p<0.05$) outperform pure PTX and blank NPs in terms of cytotoxicity on the A-549 cancer cell line 72 hours after exposure. This indicates that the cells can cleave PTX, allowing the freed PTX to reduce cellular viability. PTX-loaded sericin NPs can enter cancer cells by endocytosis and avoid the efflux pumps that cause PTX therapeutic resistance, which is one reason for their superiority over free PTX. Moreover, unlike free PTX, which clears out quickly, PTX-loaded nanoparticles can release the drug gradually and maintain therapeutic levels for more time. Its continuous release profile may improve the medication's ability to kill cancer cells[45].

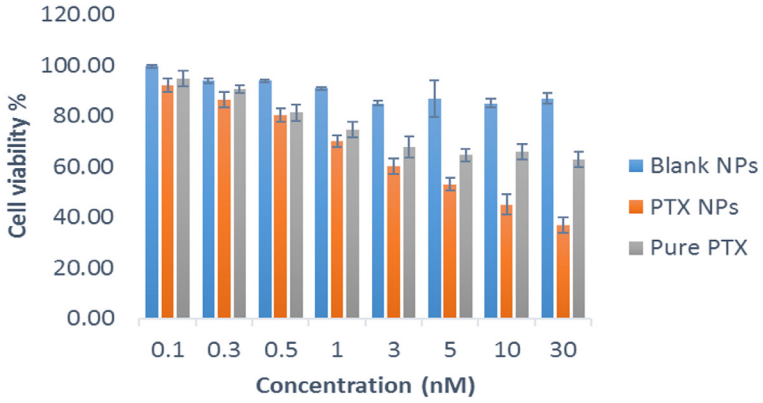

Figure 6. Viability of A-549 cells after 72 h of cell culture with different concentrations of PTX

It successfully manufactured PTX-loaded sericin NPs using desolvation and related dialysis processes with spherical morphology of the particles, the lack of particle aggregation, and the core-shell structure with a consistent surface charge. When compared to the reference PTX, it had extended-release behavior. DSC analysis revealed that PTX was amorphous, and FTIR data showed no chemical interaction with the excipients. These particles improved PTX *in vitro* cytotoxicity on lung cancer cells and demonstrated strong aerosol performance *in vitro*. According to the physicochemical and *in vitro* evaluation findings, NPs of PTX have great potential as a pulmonary delivery mechanism.

STATEMENT OF ETHICS

This study does not require ethical permission to be carried out.

CONFLICT OF INTEREST STATEMENT

The authors declare that there are no conflicts of interest regarding the publication of this manuscript.

AUTHOR CONTRIBUTIONS

All authors contributed equally to the article.

FUNDING SOURCES

This research received no specific grant from any funding agency in the public, commercial, or not-for-profit sectors.

ACKNOWLEDGMENTS

The authors thank the Department of Pharmaceutics at the College of Pharmacy Baghdad University for supporting this research article.

REFERENCES

1. Chhikara BS, Parang K. Global Cancer Statistics 2022: the trends projection analysis. Chem Biol Lett, 2023;10(1):451.

2. Cai H, Wang Y, Qin D, Cui Y, Zhang H. Advanced surgical technologies for lung cancer treatment: Current status and perspectives, Eng Regen, 2023;4(1):55-67. Doi: 10.1016/j.engreg.2022.12.001

3. Bhattacharya S. Development of 5-FU loaded poly lactic-co-glycolic acid nanoparticles for lung cancer treatment. Iraqi J Pharm Sci, 2022;31(1):130-143. Doi: 10.31351/vol31iss1pp130-143

4. Storti C, Le Noci V, Sommariva M, Tagliabue E, Balsari A, Sfondrini L. Aerosol delivery in the treatment of lung cancer. Curr Cancer Drug Targets, 2015;15(7):604-612. Doi: 10.2174/1568009615666150602143751

5. Wauthoz N, Rosière R, Amighi K. Inhaled cytotoxic chemotherapy: clinical challenges, recent developments, and future prospects. Expert Opin Drug Deliv, 2021;18(3):333-354. Doi: 10.1080/17425247.2021.1829590

6. Sharifi-Rad J, Quispe C, Patra JK, Singh YD, Panda MK, Das G, et al. Paclitaxel: application in modern oncology and nanomedicine-based cancer therapy. Oxid Med Cell Longev, 2021;2021:3687700. Doi: 10.1155/2021/3687700

7. Nasser ST, Abdulrassol A, Ghareeb M. Design, preparation and *in-vitro* evaluation of novel ocular antifungal nanoemulsion using posaconazole as a model drug. Technology, 2021;11(3):1-7. Doi: 10.25258/ijddt.11.3.00

8. Rosière R, Van Woensel M, Mathieu V, Langer I, Mathivet T, Vermeersch M, et al. Development and evaluation of well-tolerated and tumor-penetrating polymeric micelle-based dry powders for inhaled anticancer chemotherapy. Int J Pharm, 2016;501(1-2):148-159. Doi: 10.1016/j.ijpharm.2016.01.073

9. Huang L, Tao K, Liu J, Qi C, Xu L, Chang P, et al. Design and fabrication of multifunctional sericin nanoparticles for tumor targeting and pH-responsive subcellular delivery of cancer chemotherapy drugs. ACS Appl Mater Interfaces, 2016;8(10):6577-6585. Doi: 10.1021/acsami.5b11617

10. Seo S-J, Das G, Shin H-S, Patra JK. Silk sericin protein materials: characteristics and applications in food-sector industries. Int J Mol Sci, 2023;24(5):4951. Doi: 10.3390/ijms24054951

11. Mandal BB, Kundu S. Self-assembled silk sericin/poloxamer nanoparticles as nanocarriers of hydrophobic and hydrophilic drugs for targeted delivery. Nanotechnology, 2009;20(35):355101. Doi: 10.1088/0957-4484/20/35/355101

12. Toma NM, Abdulrasool AA. Formulation and evaluation of montelukast sodium nanoparticles for transdermal delivery. Int J Drug Deliv Technol, 2021;11(2):530-538.

13. Ali HH, Hussein AA. Oral nanoemulsions of candesartan cilexetil: formulation, characterization and *in vitro* drug release studies. AAPS Open, 2017;3(4):1-16. Doi: 10.1186/s41120-017-0016-7

14. Al-Sawaf OF, Jalal F. Novel probe sonication method for the preparation of meloxicam bilosomes for transdermal delivery: part one. J Res Med Dent Sci, 2023;11(6):5-12.

15. Salih O, Muhammed E. Preparation, evaluation, and histopathological studies of ondansetron-loaded invasomes transdermal gel. J Res Pharm, 2024;28(1):289-303. Doi: 10.29228/jrp.696

16. Wu Z, Zou X, Yang L, Lin S, Fan J, Yang B, et al. Thermosensitive hydrogel used in dual drug delivery system with Paclitaxel-loaded micelles for *in situ* treatment of lung cancer. Colloids Surf B Biointerfaces, 2014;122:90-98. Doi: 10.1016/j.colsurfb.2014.06.052

17. Abdulqader AA, Rajab NA. Preparation and characterization of posaconazole as a nanomicelles using d-α-tocopheryl polyethylene glycol 1000 succinate (TPGS). Iraqi J Pharm Sci, 2023;32(Suppl.):26-32. Doi: 10.31351/vol32issSuppl.pp26-32

18. Jasim IK, Abd Alhammid SN, Abdulrasool AA. Synthesis and evaluation of B-cyclodextrin based nanosponges of 5-Fluorouracil by using ultrasound assisted method. Iraqi J Pharm Sci, 2020;29(2):88-98. Doi: 10.31351/vol29iss2pp88-98

19. Abdullah TM, Al-Kinani KK. Topical propranolol hydrochloride nanoemulsion: a promising approach drug delivery for infantile hemangiomas. Iraqi J Pharm Sci, 2023;32:300-315. Doi: 10.31351/vol32issSuppl.pp300-315

20. Li X, Vogt FG, Hayes D Jr, Mansour HM. Design, characterization, and aerosol dispersion performance modeling of advanced spray-dried microparticulate/nanoparticulate mannitol powders for targeted pulmonary delivery as dry powder inhalers. J Aerosol Med Pulm Drug Deliv, 2014;27(2):81-93. Doi: 10.1089/jamp.2013.1078

21. Meenach SA, Anderson KW, Hilt JZ, McGarry RC, Mansour HM. High-performing dry powder inhalers of Paclitaxel DPPC/DPPG lung surfactant-mimic multifunctional particles in lung cancer: physicochemical characterization, *in vitro* aerosol dispersion, and cellular studies. AAPS PharmSciTech, 2014;15(6):1574-1587. Doi: 10.1208/s12249-014-0182-z

22. Faramarzi P, Haririan I, Ghanbarzadeh S, Yaqoubi S, Hamishehkar H. Development of carrier-free montelukast dry powder inhalation formulation. Pharm Ind, 2015;77(10):1535-1542.

23. Meenach SA, Anderson KW, Hilt JZ, McGarry RC, Mansour HM. Characterization and aerosol dispersion performance of advanced spray-dried chemotherapeutic PEGylated phospholipid particles for dry powder inhalation delivery in lung cancer. Eur J Pharm Sci, 2013;49(4):699-711. Doi: 10.1016/j.ejps.2013.05.012

24. Boe J, Dennis J, O'Driscoll B, Bauer T, Carone M, Dautzenberg B, et al. European Respiratory Society Guidelines on the use of nebulizers: guidelines prepared by a European Respiratory Society Task Force on the use of nebulizers. Eur Respir J, 2001;18(1):228-242. Doi: 10.1183/09031936.01.00220001

25. Katiyar S, Gaur S, Solanki R, Sarangdhar N, Suri J, Kumar R, et al. Indian guidelines on nebulization therapy. Indian J Tuberc, 2022;69(Suppl.):1-191. Doi: 10.1016/j.ijtb.2022.06.004

26. Sahib MN, Abdulameer SA, Darwis Y, Peh KK, Tan YTF. Solubilization of beclomethasone dipropionate in sterically stabilized phospholipid nanomicelles (SSMs): physicochemical and *in vitro* evaluations. Drug Des Devel Ther, 2012;6:29-42. Doi: 10.2147/DDDT.S28265

27. Shiehzadeh F, Tafaghodi M, Dehghani ML, Mashhoori F, Bazzaz BSF, Imenshahidi M. Preparation and characterization of a dry powder inhaler composed of PLGA large porous particles encapsulating gentamicin sulfate. Adv Pharm Bull, 2019;9(2):255-265. Doi: 10.15171/apb.2019.029

28. Sahib MN, Darwis Y, Peh KK, Abdulameer SA, Tan YTF. Rehydrated sterically stabilized phospholipid nanomicelles of budesonide for nebulization: physicochemical characterization and *in vitro, in vivo* evaluations. Int J Nanomedicine, 2011;6:2351-2366. Doi: 10.2147/IJN.S25363

29. Salim Al-Khfajy W, Abdulrazzaq MH, Al-Mashhadani Z. Synergistic effects of 2-Deoxy-D-glucose and cinnamic acid with erlotinib on NSCLC cell line. Iraqi J Pharm Sci, 2023;32(Suppl.):136-144. Doi: 10.31351/vol32issSuppl.pp136-144

30. Jiménez-López J, Bravo-Caparrós I, Cabeza L, Nieto FR, Ortiz R, Perazzoli G, et al. Paclitaxel antitumor effect improvement in lung cancer and prevention of the painful neuropathy using large PEGylated cationic liposomes. Biomed Pharmacother, 2021;133:111059. Doi: 10.1016/j.biopha.2020.111059

31. Akram S, Al-Shammari AM, Sahib HB, Jabir MS. Papaverine enhances the oncolytic effects of Newcastle disease virus on breast cancer *in vitro* and *in vivo*. Int J Microbiol, 2023;3324247. Doi: 10.1155/2023/3324247

32. Gill KK, Nazzal S, Kaddoumi A. Paclitaxel-loaded PEG_{5000}–DSPE micelles as a pulmonary delivery platform: formulation characterization, tissue distribution, plasma pharmacokinetics, and toxicological evaluation. Eur J Pharm Biopharm, 2011;79(2):276-284. Doi: 10.1016/j.ejpb.2011.04.017

33. Carissimi G, Lozano-Pérez AA, Montalbán MG, Aznar-Cervantes SD, Cenis JL, Víllora G. Revealing the influence of the degumming process in the properties of silk fibroin nanoparticles. Polymers, 2019;11(12):2045. Doi: 10.3390/polym11122045

34. Al-Edhari GH, Al Gawhari FJ. Study the effect of formulation variables on preparation of nisoldipine-loaded nano bilosomes. Iraqi J Pharm Sci, 2023;32(Suppl.):271-282. Doi: 10.31351/vol32issSuppl.pp271-282

35. Averineni RK, Shavi GV, Gurram AK, Deshpande PB, Arumugam K, Maliyakkal N, et al. PLGA 50:50 nanoparticles of Paclitaxel: development, *in vitro* antitumor activity in BT-549 cells and *in vivo* evaluation. Bull Mater Sci, 2012;35:319-326. Doi: 10.1007/s12034-012-0313-736

36. Pedro IDR, Almeida OP, Martins HR, de Alcântara Lemos J, de Barros ALB, Leite EA, et al. Optimization and *in vitro/in vivo* performance of Paclitaxel-loaded nanostructured lipid carriers for breast cancer treatment. J Drug Deliv Sci Technol, 2019;54:101370. Doi: 10.1016/j.jddst.2019.101370

37. Alkufi HK, Kassab HJ. Formulation and evaluation of sustained-release sumatriptan mucoadhesive intranasal in-situ gel. Iraqi J Pharm Sci, 2019;28(2):95-104. Doi: 10.31351/vol28iss2pp95-104

38. Saha J, Mondal M, Sheikh MK, Habib M. Extraction, structural and functional properties of silk sericin biopolymer from Bombyx mori silk cocoon waste. J Text Sci Eng, 2019;9(2). Doi: 10.4172/2165-8064.1000390

39. Jangid AK, Pooja D, Jain P, Gupta N, Ramesan S, Kulhari H. Self-assembled and pH-responsive polymeric nanomicelles impart effective delivery of Paclitaxel to cancer cells. RSC Adv, 2021;11(23):13928-13999. Doi: 10.1039/D1RA01574E

40. Al Khalidi MM, Jawad FJ. Enhancement of aqueous solubility and dissolution rate of etoricoxib by solid dispersion technique. Iraqi J Pharm Sci, 2020;29(1):76-87. Doi: 10.31351/vol29iss1pp76-87

41. Balcão VM, Harada LK, Jorge LR, Oliveira JM Jr, Tubino M, Vila MM. Structural and functional stabilization of sericin from *Bombyx mori* cocoons in a biopolysaccharide film: bioorigami for skin regeneration. J Braz Chem Soc, 2020;31(4):833-848. Doi: 10.21577/0103-5053.20190247

42. Egla M, Hammid S. Design of zolmitriptan liquisolid orodispersible tablets and their *in vitro* evaluation. J Chem Pharm Res, 2016;8(11):232-242. Doi: 10.22159/ijpps.2017v9i1.15656

43. Elbatanony RS, Parvathaneni V, Kulkarni NS, Shukla SK, Chauhan G, Kunda NK, et al. Afatinib-loaded inhalable PLGA nanoparticles for localized therapy of non-small cell lung cancer (NSCLC) development and *in-vitro* efficacy. Drug Deliv Transl Res, 2021;11:927-943. Doi: 10.1007/s13346-020-00802-8

44. Sahib MN, Darwis Y, Khiang PK, Tan YTF. Aerodynamic characterization of marketed inhaler dosage forms: high-performance liquid chromatography assay method for the determination of budesonide. Afr J Pharm Pharmacol, 2010;4(12):878-884.

45. Song RF, Li XJ, Cheng XL, Fu AR, Wang YH, Feng YJ, et al. Paclitaxel-loaded trimethyl chitosan-based polymeric nanoparticles for the effective treatment of gastroenteric tumors. Oncol Rep, 2014;32(4):1481-1488. Doi: 10.3892/or.2014.3344

Acta Pharm. Sci. Vol 63:(2), 2025
Original article
DOI: 10.23893/1307-2080.APS6329

Production of short-chain fatty acids in polyphenol-rich foods by *in vitro* human digestive system

Esma OĞUZ[1*], Burcu İrem OMURTAG KORKMAZ[2], Ömer Faruk MIZRAK[3]
Esra YILDIRIM SERVİ[4], Mustafa YAMAN[5]

1 Marmara University, Institute of Health Sciences, Department of Nutrition and Dietetics, Istanbul, Türkiye
2 Marmara University, Faculty of Health Sciences, Department of Nutrition and Dietetics, Istanbul, Türkiye
3 Istanbul Sabahattin Zaim University, Faculty of Health Sciences, Department of Nutrition and Dietetics, Istanbul, Türkiye
4 Istanbul Sabahattin Zaim University, Faculty of Engineering and Natural Sciences, Department of Molecular Biology and Genetics, Istanbul, Türkiye
5 Istanbul Sabahattin Zaim University, Faculty of Engineering and Natural Sciences, Department of Molecular Biology and Genetics, Istanbul, Türkiye

ABSTRACT

The study examines how specific polyphenols influence *in vitro* human digestion, focusing on their effects on short-chain fatty acids (SCFAs) profiles and antioxidant capacities. Aronia, Cornelian cherry, green tea, and Turkish coffee were digested, and changes in SCFAs and antioxidants were analyzed. Results showed variations in SCFAs levels before and after digestion, with Turkish coffee displaying the lowest acetic acid levels post-digestion (16 ± 0.4 mg/100 g) and green tea showing the highest propionic acid levels (742 ± 19.6 mg/100 g). Cornelian cherry exhibited the greatest increase in butyric acid levels after digestion (4.7 ± 0.12 mg/100 g). Additionally, Turkish coffee showed the highest increase in total phenolic content (TPC) post-digestion, while Cornelian cherry had the highest increase in total antioxidant capacity (TAC). Overall, the findings suggest that polyphenols may positively impact digestion and potentially exhibit prebiotic effects.

*Corresponding author: Esma OĞUZ
E-mail: esma.oguz@marmara.edu.tr
ORCIDs:
Esma OĞUZ: 0009-0001-4817-5999
Burcu İrem OMURTAG KORKMAZ: 0000-0001-7918-6212
Ömer Faruk MIZRAK: 0000-0002-0389-5626
Esra YILDIRIM SERVİ: 0000-0001-5094-5828
Mustafa YAMAN: 0000-0001-9692-0204
(Received 1 Apr 2024, Accepted 19 Aug 2024)

Keywords: polyphenols, *in vitro* human digestion, HPLC, short-chain fatty acids

INTRODUCTION

Polyphenols constitute the predominant category among secondary metabolites devoid of energetic properties, encompassing approximately 8,000 distinct compounds that have been identified[1,2,3]. Polyphenols, including flavonols, flavones, flavanones, flavanols, phenolic acids, lignans, and stilbenes, harbor bioactive compounds associated with advantageous physiological impacts, including potential anticancer and anti-inflammatory attributes[4,5].

Referred to as 'essential elements for longevity,' polyphenols play a significant role in health[6]. While numerous studies in the literature document the bioactivity of polyphenols, understanding of the mechanisms driving their health effects is limited due to their poor oral bioavailability[7].

The absorption and bioavailability of dietary polyphenols in the body determine their health benefits[8]. Bioactive compounds undergo transformations as they progress through the gastrointestinal (GI) tract, leading to the generation of various metabolites. In the colon, certain polyphenols undergo fermentation mediated by the gut microbiota, consequently leading to elevated concentrations of short-chain fatty acids (SCFAs). This process specifically affects the microbiota utilized by the host[9]. SCFAs generated within the colonic environment during the fermentation of dietary fiber and specific food components serve various functions with positive effects on health[10,11].

Polyphenols act as metabolic prebiotics[12]. Phenolics that remain unabsorbed in the colon exhibit effects similar to "prebiotics"[13]. Typically, dietary polyphenols exhibit limited bioavailability, with approximately 90-95% evading absorption in the intestine and instead reaching the colon[14]. Unabsorbed molecules undergo biotransformation, being deconjugated, depolymerized, and metabolized into phenolic metabolites with reduced molecular weight, which are then absorbed by colonic microbiota[15].

There is increasing interest in the enzymatic modification of phenolic compounds mediated by lactic acid bacteria (LAB), with several studies showcasing the capability of diverse LAB strains to carboxylate, demethylate, de-esterify, and glycosylate dietary polyphenols[16,17]. LAB can be used to convert polyphenols into bioavailable and bioactivated compounds[18].

Polyphenols, found in legumes, cereals, vegetables, olives, fruits, and various other dietary sources, significantly contribute to overall dietary intake[19]. Notable examples of polyphenol-rich foods, distinguished by their unique flavors, cultural significance, and rich polyphenolic content, include Aronia (*Aronia melanocarpa*), Turkish coffee (*Coffea arabica*), green tea (*Camellia sinensis*), and Cornelian cherry (*Cornus mas* L.).

The aim was to analyze the polyphenols found in Cornelian cherry, Aronia, green tea, and Turkish coffee during *in vitro* digestion and to evaluate their effects on SCFAs, along with their antioxidant properties.

METHODOLOGY

Chemicals

Methanol (product code: 106009), Folin–Ciocalteu reagent (product code: 109001), ammonium acetate (NH_4Ac) (product code: 101116), sodium carbonate (Na_2CO_3) (product code: 106392) and Copper (II) chloride ($CuCl_2$) (product code: 102739) were obtained from Merck (Darmstadt, Germany). Alpha-amylase (1.5 U/mg, from Aspergillus oryzae powder) (product code: 86250),), pancreatin (from porcine pancreas, meeting 8 × USP specifications) (product code: P7545), pepsin (≥250 U/mg solid, from porcine gastric mucosa, lyophilized powder) (product code: P7000), bovine serum albumin, KCl (product code: 58221), lipase (100–500 U/mg protein, from porcine pancreas Type II) (product code: L3126NaCl (product code: S9888), $CaCl_2{\cdot}2H_2O$ (product code: 223506), urea, uric acid, mucin, $NaHCO_3$ (product code: S6014), acetonitrile (ACN) (product code: 34851), bile salts mixture, neocuproine (Nc) (product code: N1501), Trolox (6-hydroxy-2,5,7,8–22 tetramethylchroman-2-carboxylic acid), gallic acid, and 1,1-diphenyl-2-picrylhydrazyl (DPPH) were obtained from Sigma-Aldrich (St. Louis, MO, USA).

The sample preperation

The fresh Cornelian cherry and Aronia fruits purchased for the study were processed into a puree using a 32-mm pore pulper machine. The lyophilization processes were carried out using the G-Ray 125 freeze-dry machine through sublimation[20]. Turkish coffee and green tea were purchased in boxes. For the Turkish coffee, 6 g of coffee was mixed with 65 mL of water and thoroughly blended before being brewed using a coffee machine[21]. Green tea, consisting of 1.5 g, was prepared by adding 200 mL of boiling water and thoroughly mixing.

In vitro digestion procedure

The method outlined by Lee et al. was slightly adapted for *in vitro* digestion. Each sample containing 5 g of polyphenols (Aronia, Turkish coffee, green tea, and Cornelian cherry) was placed in 50 mL Falcon tubes[22]. *In vitro* human digestion was simulated by adding solutions mimicking those in the oral, gastric, intestinal digestion (Figure 1).

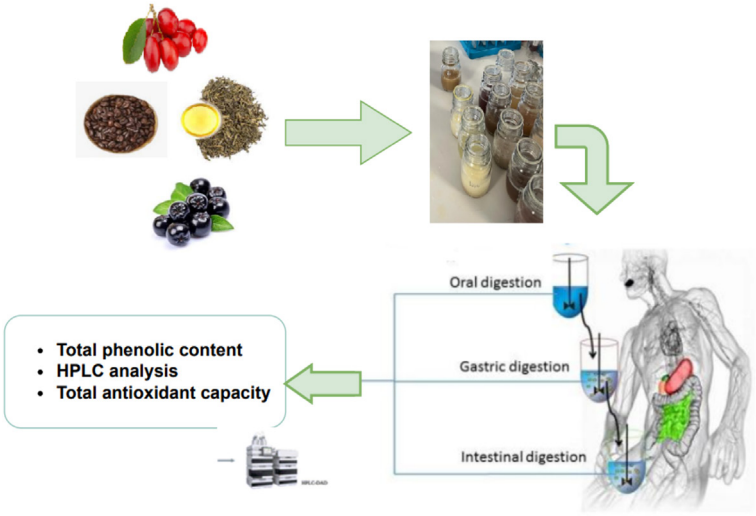

Figure 1. Dynamic changes in polyphenol products of Aronia, Cornelian cherry, green tea, Turkish coffee during the *in vitro* gastrointestinal digestion

For the oral medium, NaCl, urea, uric acid, α-amylase, and mucin were dissolved in deionized water, with the pH adjusted to 6.8 ± 0.2. The gastric medium included HCl, $CaCl_2.H_2O$, bovine serum albumin, pepsin, and mucin, with a pH of 1.5 ± 0.02. The small intestine medium contained KCl, $CaCl_2.2H_2O$, bovine serum albumin, pancreatin, and lipase, adjusted to pH 8.0 ± 0.2. Lastly, the bile solution was composed of $NaHCO_3$, $CaCl_2.2H_2O$, bovine serum albumin, and bile, with a pH of 7.0 ± 0.2. In each case, deionized water was used to make up the volume, and HCl or NaOH was used to adjust the pH[22].

Five mL of salivary solution were added to the samples and incubated in a shaking water-bath (5 min, 37°C). Then, 12 mL of gastric juice was added to the samples and incubated at the same temperature for 30 min. Subsequently, 12 mL of duodenal juice and 6 mL of bile juice were added to the mixture obtained after the addition of gastric juice. The mixture underwent an incubation period in a shaking water-bath (2 hours, 37°C)[22].

The liquid agar for *Escherichia coli (E. coli)* was prepared by mixing 2.5 g of Mueller–Hinton broth with 100 mL of deionized-distilled water (DDW), while the liquid medium for *Lactobacillus plantarum* (*L. plantarum)* involved combining 5.5 g of Lactobacilli MRS Broth with 100 mL of double-distilled water (DDW). Frozen (-80°C*) E. coli* and *L. plantarum* were heated to 37°C. For 1% of the *E. coli* and *L. plantarum* stocks, 1 mL was added to 100 mL of suitable sterile liquid medium. The *E. coli* and *L. plantarum* liquid medium solutions were incubated at 37°C for 12 hours to activate them. For activated *E. coli* and *L. plantarum*, 100 mL of sterile liquid medium was again inoculated and incubated at 37°C for an additional 12 hours. *E. coli* was allowed to grow for 24 hours, and *L. plantarum* for 72 hours at 37°C. After incubation, the final number of *E. coli* and *L. plantarum* colonies was log 10^8-10^{10} colony-forming units (CFU). For the large intestine digestion phase, 38 mL of liquid agar containing *E. coli* and *L. plantarum* solutions were added to samples that had undergone small intestine digestion. The samples were then incubated (4 hours, 37°C)[22].

HPLC analysis

The prepared samples were filtered through a 0.45-µm syringe tip cellulose acetate filter, transferred into 2-mL amber screw-cap vials, and then subjected to HPLC. The HPLC analysis for SCFAs determination, following the method by De Baere et al., was adapted for this study[23]. A Shimadzu Nexera-i HPLC system equipped with a Shimadzu DAD detector was utilized for separation of acetic acid, butyric acid, and propionic acid. The mobile phase consisted of methanol: water: acetonitrile (42:56:2 v/v/v), with detection at 210 nm. An Inersil ODS-3 column (5µm, 4.6x250 mm) was used in a column oven (30°C) with a flow rate (0.8 mL/min).

Total phenolic content analysis

The Folin-Ciocalteu method was employed to determine the total phenolic content (TPC) of the samples[24]. Pre-digestion samples underwent extraction with an extraction solution, followed by centrifugation. Then, 0.1 mL of the centrifuged samples was mixed with 0.75 mL of 6% Na_2CO_3 and 0.75 mL of Folin reagent. Post-digestion, samples were again extracted and centrifuged, and the process was repeated similarly. After incubating in the absence of light at room temperature (90 min), absorbance (760 nm) was determined using a UV-visible spectrophotometer (Shimadzu UV-1700 UV–Vis, Japan). Absorbance values were compared to a gallic acid calibration curve (mg/L-1 gallic acid equivalent [GAE]).

Total antioxidant capacity

The DPPH (1,1-diphenyl-2-picrylhydrazyl) assay was used to evaluate the Total Antioxidant Capacity (TAC), with Trolox as the standard. Each assay was conducted in triplicate for the samples. The procedure followed the method outlined by Karunakaran and Kumaran[25]. Initially, 3.9 mL of 0.1 mM DPPH in methanol was combined with 100 µL of sample extract or standard solution. The blank sample comprised 100 µL of an 80% methanol solution and 3.9 mL of the DPPH solution. Following incubation at room temperature in the absence of light (30 min), absorbance was determined utilizing a UV-visible spectrophotometer, referencing against a blank measurement (at 517 nm).

Data analysis

Analyses were conducted using Minitab 18 software, involved applying one-way analysis of variance (ANOVA) and Tukey post hoc tests to determine any significant differences ($p<0.05$). Triplicate analyses were conducted.

RESULTS and DISCUSSION

The effect of polyphenols on SCFAs

The production of SCFAs by microbiota in colon is essential for various physiological processes, extending beyond the intestinal environment to affect peripheral tissues following absorption[26]. Acetic, propionic, and butyric acid are the primary fermentation products, significantly contributing to the overall SCFAs pool. Acetic acid serves as an essential energy substrate, being metabolized and absorbed by organs. Propionic acid exhibits potential in reducing fatty acid levels in both the liver and plasma, thereby inhibiting cholesterol synthesis. Butyric acid maintains the immune function of the intestinal mucosa and suppresses cytokine production[27].

In this study, Aronia, Cornelian cherry, green tea, and Turkish coffee were subjected to analysis for their acetic, propionic, and butyric acid contents pre- and post-*in vitro* digestion. The data depicted in Table 1, demonstrated variations in the levels of SCFAs among these polyphenol-rich foods. Prior to digestion, Cornelian cherry and green tea exhibited the lowest acetic acid values, while Aronia displayed the highest. Upon *in vitro* digestion, Turkish coffee showed the lowest acetic acid levels, with a notable increase observed in green tea. Similarly, the initial propionic acid levels were lowest in Cornelian cherry and highest in Turkish coffee, with a substantial increase noted in green tea post-digestion. As for butyric acid, Cornelian cherry and green tea had the lowest initial values, whereas Aronia displayed the highest. Following digestion, Turkish coffee exhibited the lowest butyric acid levels, while Aronia demonstrated the most significant increase.

Table 1. Content of acetic, propionic and butyric acids in different types of polyphonels

Polyphonels	Acetic Acid (mg/100g)		Propionic Acid (mg/100g)		Butyric Acid (mg/100g)	
	Pre-digestion	Post-digestion	Pre-digestion	Post-digestion	Pre-digestion	Post-digestion
Aronia	0.53 ± 0.03^{a}	66.5 ± 1.8^{b}	0.24 ± 0.00^{c}	285 ± 7.5^{b}	2.1 ± 0.05^{a}	4.7 ± 0.12^{a}
Cornelian Cherry	0.19 ± 0.00^{c}	62.4 ± 1.65^{b}	0.15 ± 0.00^{d}	279 ± 7.1^{b}	0.18 ± 0.00^{c}	3.7 ± 0.09^{b}
Green Tea	0.17 ± 0.01^{c}	177 ± 4.7^{a}	0.32 ± 0.01^{b}	742 ± 19.6^{a}	0.17 ± 0.04^{c}	3.7 ± 0.09^{b}
Turkish Coffee	0.47 ± 0.02^{b}	16 ± 0.4^{c}	1.30 ± 0.04^{a}	58.5 ± 1.5^{c}	0.39 ± 0.01^{b}	1.14 ± 0.00^{c}

Outcomes are represented ± standard deviation (n=3). The distinct symbols within the same column displayed indicate a significant difference in mean values (ANOVA, Tukey's test, $p<0.05$).

The investigation into the digestion process conducted *in vitro* demonstrated an increase in the acetic, butyric, and propionic acid content of these polyphenol-containing foods compared to their levels before digestion. Phenolic compounds have a limited absorption in the intestine, with 5 to 10% of the total ingested polyphenols undergoing absorption. Complex phenolics that remain unabsorbed in the small intestine undergo biotransformation by resident microbiota in the colon into smaller molecular weight metabolites, facilitating potential absorption[15]. Throughout this procedure, SCFAs are generated, accompanied by notable alterations in the composition of gut microbiota[15]. During *in vitro* gastrointestinal digestion, Aronia, green tea, coffee, and Cornelian cherry exhibited elevated levels of SCFAs (propionic, butyric, acetic acid). This observation may be connected to the effects of processes such as digestion, absorption, and metabolism on the bioavailability[28]. Moreover, gut microbiota exerts a crucial influence on the biotransformation of polyphenols, a process vital for their bioavailability[29,30]. Polyphenols may promote an increase in SCFAs production by exerting a prebiotic effect[31]. It has been found that unabsorbed phenolic compounds and their derivatives in the colon possess 'prebiotic-like' effects[32]. *In vitro* gastrointestinal digestion of Aronia, green tea, coffee, Cornelian cherry exhibited prebiotic potential by promoting the production of SCFAs. Recent studies by Moorthy et al. and Alves-Santos et al. support this study's findings, confirming that polyphenol intake affects gut microbial composition and enhances host health by promoting homeostasis, exhibiting prebiotic properties[31,33]. Polyphenolic compounds, including anthocyanins and

phenolic acids, are noted to promote fermentation, leading to an elevation in SCFAs concentration[34,35]. In the study, green tea was found to contain elevated levels of acetic and propionic acids, whereas Aronia demonstrated increased concentrations of butyric acid following digestion. In line with this study, Rha et al. suggest that specific stable polyphenols found in green tea have higher bioaccessibility in the gastrointestinal system, and their health-regulating effects are based on interactions with gut microbes[36]. The antioxidant properties of green tea and Aronia polyphenols may have created a synergistic effect.

The results of our *in vitro* digestion experiments reveal that polyphenol-rich foods significantly influence the digestive system, aligning with existing literature that highlights their potential to enhance SCFAs production and exert prebiotic effects. This finding corroborates previous studies, such as those by Sorrenti et al. and Dou et al., which have demonstrated that polyphenols can positively modulate gut microbiota and fermentation processes, thereby supporting gastrointestinal health and function[37,38]. Our data extends these observations by confirming that diverse polyphenol sources, including those analyzed in our study, contribute to increased SCFA levels and exhibit prebiotic properties, reinforcing the role of dietary polyphenols in promoting beneficial microbial activity and overall digestive health.

The effect of polyphenols on TAC and TFC

The evaluation and comparison of TAC and TPC of polyphenols pre- and post-digestion revealed significant alterations (Figure 2). Aronia exhibited the highest TPC values initially, while green tea had the lowest. Turkish coffee showed the most considerable increase in TPC post-digestion, whereas green tea and Cornelian cherry displayed the lowest increments. Regarding TAC, Aronia had the highest initial value, while Cornelian cherry and green tea had the lowest. Post-digestion, Aronia demonstrated the highest increase in TAC, whereas Turkish coffee showed the lowest enhancement.

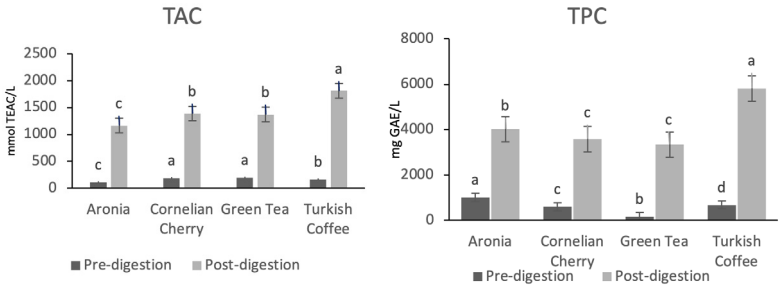

Figure 2. TPC and TAC values of the polyphenols before and after *in vitro* digestion. The distinct symbols displayed indicate a significant difference.

The findings indicated that TAC and TPC levels of polyphenols were higher following *in vitro* digestion in comparison to pre-digestion levels. The increased TAC and TFC of polyphenols subsequent to *in vitro* digestion might be associated with enzymatic hydrolysis in the stomach and intestines as well as the increase in content[39]. Particularly noteworthy was the substantial enhancement observed in both TPC values and TAC of coffee following gastrointestinal processing. These results align with prior research by Campos-Vega et al., which suggests that colonic fermentation enhances the antioxidant capacity of polyphenols derived from coffee grounds through the release of phenolic compounds[40]. Furthermore, coffee's active compounds can be metabolized by gut bacteria, potentially enhancing their antioxidant properties and beneficial effects.

Vamanu et al. endorse the notion that the phenolic acids present in coffee grounds are instrumental in its observed antioxidant properties[41]. The evaluation of antioxidant activities in coffee indicates that the active compounds possessing antioxidant capabilities withstand complete neutralization by digestive enzymes within the GI tract, facilitating their passage to the colon and maintenance of their bioactive effects, as evidenced in the study by de Cosío-Barron et al.[42]. This highlights the high bioaccessibility of polyphenolic compounds during digestion.

Aronia, green tea, Cornelian cherry, and coffee polyphenols on SCFAs production are emerging. Preclinical and *in vitro* studies suggest potential synergistic effects on gut health. This study explores the antioxidant effects of these polyphenols, with digestion enhancing their bioaccessibility. These polyphenols also demonstrate prebiotic activity by increasing the production of butyric, acetic, and propionic acids. Gastrointestinal digestion releases bound phenolic compounds, boosting TPC and TAC. Understanding the nutritional value and potential applications of these polyphenols in functional foods provides valuable insights for consumers and the food industry.

STATEMENT OF ETHICS

This study does not require any ethical approval.

CONFLICT OF INTEREST STATEMENT

The authors declare no conflict of interest.

AUTHOR CONTRIBUTIONS

Design: MY, BİPL. Acquisition of data: ÖFM, EYS, EO. Analysis of data: MY, EO. Drafting of the manuscript: EO. Critical revision of the manuscript: MY, BİOK, EO. Statistical analysis: EO. Supervision: MY, BİOK.

FUNDING SOURCES

No funding or other financial support was received.

ACKNOWLEDGMENTS

Not applicable.

REFERENCES

1. Swallah MS, Sun H, Affoh R, Fu H, Yu H. Antioxidant potential overviews of secondary metabolites (Polyphenols) in fruits. Int J Food Sci, 2020;2020:9081-9686. Doi: 10.1155/2020/9081686

2. Santhakumar AB, Battino M, Alvarez-Suarez JM. Dietary polyphenols: structures, bioavailability and protective effects against atherosclerosis. Food Chem Toxicol, 2018;113:49-65. Doi: 10.1016/j.fct.2018.01.022

3. Yamagata K, Tagami M, Yamori Y. Dietary polyphenols regulate endothelial function and prevent cardiovascular disease. Nutrition, 2015;31(1):28-37. Doi: 10.1016/j.nut.2014.04.011

4. Spencer JP, Abd El Mohsen MM, Minihane AM, Mathers JC. Biomarkers of the intake of dietary polyphenols: strengths, limitations and application in nutrition research. BJN, 2008;99(1):12-22. Doi: 10.1017/S0007114507798938

5. Tatipamula VB, Kukavica B. Phenolic compounds as antidiabetic, anti-inflammatory, and anticancer agents and improvement of their bioavailability by liposomes. Cell Biochem Funct, 2021;39(8):926-944. Doi: 10.1002/cbf.3667

6. Chandrasekara A, Shahidi F. Content of insoluble bound phenolics in millets and their contribution to antioxidant capacity. J Agric Food Chem, 2010;58(11):6706-6714. Doi: 10.1021/jf100868b

7. Xiao JB. Stability of dietary polyphenols: it's never too late to mend? Food Chem Toxicol, 2018;119:3-5. Doi: 10.1016/j.fct.2018.03.051

8. Catalkaya G, Venema K, Lucini L, Rocchetti G. Interaction of dietary polyphenols and gut microbiota: microbial metabolism of polyphenols, influence on the gut microbiota and implications on host health. Food Front, 2020;1(2):109-133. Doi: 10.1002/fft2.25

9. Trompette A, Gollwitzer ES, Yadava K, Sichelstiel AK, Sprenger N, Ngom-Bru C, et al. Gut microbiota metabolism of dietary fiber influences allergic airway disease and hematopoiesis. Nat Med, 2014;20(2):159-166. Doi: 10.1038/nm.3444

10. Chen XF, Chen X, Tang X. Short-chain fatty acid, acylation and cardiovascular diseases. Clin Sci, 2020;134(6):657-676. Doi: 10.1042/CS20200128

11. Bonif T, Catarino MD, Vilas-boas AA, Ribeiro TB, Campos DA, Teixeira JA, et al. Impact of circular Brewer's Spent Grain flour after *in vitro* Gastrointestinal Digestion on Human Gut Microbiota. Foods, 2022;11(15):2022:2279. Doi: 10.3390/foods11152279

12. Hui CL, Jenner AM, Low CS, Lee YK. Effect of tea phenolics and their aromatic fecal bacterial metabolites on intestinal microbiota. Res Microbiol, 2006;157(9):876-884. Doi: 10.1016/j.resmic.2006.07.004

13. González-Sarrías A, Larrosa M, Tomás-Barberán FA, Dolara P, Espín JC. NF-κB-dependent anti-inflammatory activity of urolithins, gut microbiota ellagic acid-derived metabolites, in human colonic fibroblasts. Br J Nutr, 2010;104(4):503-512. Doi: 10.1017/S0007114510000826

14. Singh AK, Cabral C, Kumar R, Ganguly R, Rana HK, Gupta A, et al. Beneficial effects of dietary polyphenols on gut microbiota and strategies to improve delivery efficiency. Nutrients, 2019;11(9):2216. Doi: 10.3390/nu11092216

15. Gowd V, Karim N, Shishir MRI, Xie L, Chen W. Dietary polyphenols to combat the metabolic diseases via altering gut microbiota. Trends Food Sci Technol, 2019;93:81-93. Doi: 10.1016/j.tifs.2019.09.005

16. Rossi M, Amaretti A, Leonardi A, Raimondi S, Simone M, Quartieri A. Potential impact of probiotic consumption on the bioactivity of dietary phytochemicals. J Agric Food Chem, 2013;61(40):9551-9558. Doi: 10.1021/jf402722m

17. Pereira-Caro G, Oliver CM, Weerakkody R, Singh T, Conlon M. Chronic administration of a microencapsulated probiotic enhances the bioavailability of orange juice flavanones in humans. Free Radic Biol Med, 2015;84:206-214. Doi: 10.1016/j.freeradbiomed.2015.03.010

18. Chiou Y, Wu J, Huang Q, Shahidi F, Wang Y, Ho C, et al. Metabolic and colonic microbiota transformation may enhance the bioactivities of dietary polyphenols. J Funct Foods, 2014;7:3-25. Doi: 10.1016/j.jff.2013.08.006

19. Cardona F, Andrés-Lacueva C, Tulipani S, Tinahones FJ, Queipo-Ortuño MI. Benefits of polyphenols on gut microbiota and implications in human health. JNB, 2013;24(8):1415-1422. Doi: 10.1016/j.jnutbio.2013.05.001

20. Celik ZM, Sargin M, Tamer HG, Gunes FE. The effect of lyophilized dried cornelian cherry (*Cornus mas* L.) intake on anthropometric and biochemical parameters in women with insulin resistance: a randomized controlled trial. Food Sci Nutr, 2023;11(12):8060-8071. Doi: 10.1002/fsn3.3725

21. Nakilcioğlu-Taş E. The effects of sugar addition and degree of roast on the bioactive compounds and antioxidant activity of Turkish-style coffee brews. IJPER, 2018;52(3):456-466. Doi: 10.5530/ijper.52.3.53

22. Lee SJ, Lee SY, Chung MS, Hur SJ. Development of novel *in vitro* human digestion systems for screening the bioavailability and digestibility of foods. J Funct Foods, 2016;22:113-121. Doi: 10.1016/j.jff.2016.01.005

23. De Baere S, Eeckhaut V, Steppe M, De Maesschalck C, De Backer P, Van Immerseel F, et al. Development of a HPLC–UV method for the quantitative determination of four short-chain fatty acids and lactic acid produced by intestinal bacteria during *in vitro* fermentation. J Pharm Biomed Anal, 2013;80:107-115. Doi: 10.1016/j.jpba.2013.02.032

24. Singleton VL, Rossi JA. Colorimetry of total phenolics with phosphomolybdic-phosphotungstic acid reagents. AJEV, 1965;16(3):144-158. Doi: 10.5344/ajev.1965.16.3.144

25. Kumaran A, Karunakaran JR. Antioxidant activities of the methanol extract of *Cardiospermum halicacabum*. Pharm Biol, 2006;44(2):146-151. Doi: 10.1080/13880200600596302

26. den Besten G, van Eunen K, Groen AK, Venema K, Reijngoud DJ, Bakker BM. The role of short-chain fatty acids in the interplay between diet, gut microbiota, and host energy metabolism. JLR, 2013;54(9):2325-2340. Doi: 10.1194/jlr.R036012

27. Laparra JM, Sanz Y. Interactions of gut microbiota with functional food components and nutraceuticals. Pharmacol Res, 2010;61(3):219-225. Doi: 10.1016/j.phrs.2009.11.001

28. Teng H, Chen L. Polyphenols and bioavailability: an update. Crit Rev Food Sci Nutr, 2019;59(13):2040-2051. Doi: 10.1080/10408398.2018.1437023

29. de Paulo Farias D, de Araujo FF, Neri-Numa IA, Pastore GM. Prebiotics: Trends in food, health and technological applications. Trends Food Sci Technol, 2019;93:23-35. Doi: 10.1016/j.tifs.2019.09.004

30. Gowd V, Karim N, Shishir MRI, Xie L, Chen W. Dietary polyphenols to combat the metabolic diseases via altering gut microbiota. Trends Food Sci Technol, 2019;93:81-93. Doi: 10.1016/j.tifs.2019.09.005

31. Alves-Santos AM, Sugizaki CSA, Lima GC, Naves MMV. Prebiotic effect of dietary polyphenols: a systematic review. J Func Foods, 2020;74:104169. Doi: 10.1016/j.jff.2020.104169

32. González-Sarrías A, Espín JC, Tomás-Barberán FA. Non-extractable polyphenols produce gut microbiota metabolites that persist in circulation and show anti-inflammatory and free radical-scavenging effects. Trends Food Sci Technol, 2017;69:281-288. Doi: 10.1016/j.tifs.2017.07.010

33. Moorthy M, Chaiyakunapruk N, Jacob SA, Palanisamy UD. Prebiotic potential of polyphenols, its effect on gut microbiota and anthropometric/clinical markers: a systematic review of randomised controlled trials. Trends Food Sci Technol, 2020;99:634-649. Doi: 10.1016/j.tifs.2020.03.036

34. Faria A, Fernandes I, Norberto S, Mateus N, Calhau C. Interplay between anthocyanins and gut microbiota. J Agric Food Chem, 2014;62(29):6898-6902. Doi: 10.1021/jf501808a

35. Gil-Sánchez I, Cueva C, Sanz-Buenhombre M, Guadarrama A, Moreno-Arribas MV, Bartolomé B. Dynamic gastrointestinal digestion of grape pomace extracts: bioaccessible phenolic metabolites and impact on human gut microbiota. J Food Compos Anal, 2017;68:41-52. Doi: 10.1016/j.jfca.2017.05.005

36. Rha CS, Seong H, Jung YS, Jang D, Kwak JG, Kim DO, et al. Stability and fermentability of green tea flavonols in *in-vitro*-simulated gastrointestinal digestion and human fecal fermentation. Int J Mol Sci, 2019;20(23):5890. Doi: 10.3390/ijms20235890

37. Sorrenti V, Ali S, Mancin L, Davinelli S, Paoli A, Scapagnini G. Cocoa polyphenols and gut microbiota interplay: bioavailability, prebiotic effect, and impact on human health. Nutr, 2020;12(7):1908. Doi: 10.3390/nu12071908

38. Dou Z, Chen C, Huang Q, Fu X. *In vitro* digestion of the whole blackberry fruit: bioaccessibility, bioactive variation of active ingredients and impacts on human gut microbiota. Food Chem, 2022;370:131001. Doi: 10.1016/j.foodchem.2021.131001

39. Zheng G, Deng J, Wen L, You L, Zhao Z, Zhou L. Release of phenolic compounds and antioxidant capacity of Chinese hawthorn "*Crataegus pinnatifida*" during *in vitro* digestion. J Funct Foods, 2018;40:76-85. Doi: 10.1016/j.jff.2017.10.039

40. Campos-Vega R, Vázquez-Sánchez K, López-Barrera D, Loarca-Piña G, Mendoza-Díaz S. Oomah BD. Simulated gastrointestinal digestion and *in vitro* colonic fermentation of spent coffee (*Coffea arabica* L.): bioaccessibility and intestinal permeability. Food Res Int, 2015; 77:156-161. Doi: 10.1016/j.foodres.2015.07.024

41. Vamanu E, Gatea F, Pelinescu DR. Bioavailability and bioactivities of polyphenols eco extracts from coffee grounds after *in vitro* digestion. Foods, 2020;9(9):1281. Doi: 10.3390/foods9091281

42. de Cosío-Barrón ACG, Hernández-Arriaga AM, Campos-Vega R. Spent coffee (*Coffea arabica* L.) grounds positively modulate indicators of colonic microbial activity. IFSET, 2020; 60:102286. Doi: 10.1016/j.ifset.2019.102286

Acta Pharm. Sci. Vol 63:(2), 2025
Original article
DOI: 10.23893/1307-2080.APS6330

Antimicrobial activity of European Pharmacopoeia quality essential oil combinations against oral pathogens

Sümeyye Elif KAHYA[1*], Damla KIRCI[2], Ayşe Esra KARADAĞ[1], Fatih DEMİRCİ[3]

1 Istanbul Medipol University, School of Pharmacy, Department of Pharmacognosy, Beykoz, Istanbul, Türkiye
2 Izmir Katip Çelebi University, Faculty of Pharmacy, Department of Pharmacognosy, Izmir, Türkiye
3 Anadolu University, Faculty of Pharmacy, Department of Pharmacognosy, Eskisehir, Türkiye

ABSTRACT

This study evaluates the antimicrobial activity of European Pharmacopeia quality essential oils from *Foeniculum vulgare* Mill., *Lavandula angustifolia* Mill., *Carum carvi* L., and *Pinus mugo* Turra in mouthwash formulations with various combinations. These essential oils are ethnobotanically recognized for treating throat infections. Antimicrobial testing was conducted using microdilution and disc diffusion methods against oral pathogens. The mouthwash formulations were created as binary and quadruple combinations of the four oils. Formulations contains essential oils in the range of 0.5-0.55 mg/mL. Among the seven combinations tested, the most potent were the *F. vulgare* - *P. mugo* (25 mm zone diameter) and *L. angustifolia* - *C. carvi* (30 mm zone diameter) blends against *Streptococcus mitis*. While none of the formulations were effective against *Moraxella catarrhalis*, all were generally effective against *S. mutans*. Consequently, it is suggested that the mouthwash formulations developed with these essential oils may be particularly useful in preventing dental caries.

Keywords: mouthwash, disc diffusion, essential oil, European Pharmacopeia

*Corresponding author: Sümeyye Elif KAHYA
E-mail: sumeyye.kahya@medipol.edu.tr
ORCIDs:
Sümeyye Elif KAHYA: 0009-0002-5024-0021
Damla KIRCI: 0000-0002-9881-164X
Ayşe Esra KARADAĞ: 0000-0002-3412-0807
Fatih DEMİRCİ: 0000-0003-1497-3017
(Received 13 Dec 2024, Accepted 28 Jan 2025)

INTRODUCTION

The oral cavity is considered one of the most extensively studied ecosystems in the human body. The oral cavity is highly susceptible to infections and various pathologies, with common issues including dental diseases, periodontitis, oral mucosa infections, and oral cancer[1].

Mouthwashes play a key role in reducing microbial plaque, which helps in maintaining oral hygiene[2]. Mouthwashes are oral solutions designed to rinse the mouth, eliminate bacteria, act as astringents, deodorize the oral cavity, and provide therapeutic benefits by alleviating infections. The efficacy of mouthwashes in controlling microbial plaque is important, but they should also be designed to offer a pleasant mouthfeel and flavor to encourage consistent use and consumer preference. They often contain antiseptics used for treating such infections[3]. Mouthwashes have the potential to function as targeted therapeutic agents by addressing either the host's inflammatory responses or specific pathogens. By focusing on pro-inflammatory pathways or specific bacterial targets, mouthwashes could effectively reduce inflammation and alleviate oral disease symptoms[4]. Many strategies focus on the biological activities of alternative natural products due to the increased microbial resistance of common antibiotics[5].

Essential oils in mouthwashes are effective against oral pathogens[6]. *In vitro* studies showed that an essential oil blend can more effectively eliminate *Staphylococcus aureus* and *Streptococcus* biofilms on hydroxyapatite discs than chlorhexidine[7]. Additionally, essential oils were reported to decrease plaque and bleeding scores when used by tooth brushing[8]. Additionally, it is well-established that essential oils possess antimicrobial effects on the gingiva while exhibiting low toxicity. It is highly significant in terms of enabling the development of new pharmaceutical formulations for oral hygiene[2].

There are several reports on antimicrobial activity of *Foeniculum vulgare* Mill. (fennel, bitter fennel oil) essential oil that belongs to Lamiaceae family[9,10]. Essential oil contains major 55.0 to 75.0% anethole according to European Pharmacopeia. Fennel essential oil known, along with active compounds within it, has shown strong inhibitory effects *in vitro* against a diverse range of bacterial and fungal pathogens. *Lavandula angustifolia* L. of the Lamiaceae family, is uses against insomnia and mental stress in the EMA monographs[11,12]. Also, previous studies demonstrated that lavender essential oil a wide range of bioactivities, including antibacterial, antifungal, antioxidant, and anti-inflammatory[10,13,14]. Lavender essential oil includes linalool (20-50%) and linaly acetate

(25-46%) as major components according to EMA monographs[12]. Caraway (*Carum carvi* L.), which are members of the Apiaceae family, widely used to flavor foods, enhance fragrances, and in medical preparations. Specifically, *C. carvi* essential oil is commonly found in liqueurs, mouthwashes, toothpastes, soaps, and perfumes due to its strong antimicrobial effects[15,16]. The main components of essential oil were reported limonene and carvone[17]. *Pine mugo* Turra, also named mountain pine, studies were examined the chemical composition of dwarf pine essential oil. The major components of the mountain pine essential oil were found as obtained δ-3-carene, α-pinene, β-phellandrene previously[18].

In this study, the potential antimicrobial effects of 4 different (*F. vulgare, L. angustifolia, C. carvi, P. mugo*) European Pharmacopoeia quality essential oils were evaluated. The *in vitro* antimicrobial activity of essential oils mouthwash formulations consisting of a blend in various proportions were studied. To the best of our knowledge, this is the first study on mouthwashes composed of seven different combinations of *Foeniculum vulgare, Lavandula angustifolia, Carum carvi*, and *Pinus mugo* essential oils.

METHODOLOGY

Materials

All essential oils were obtained from Caesar & Loretz GmbH (Germany). Antimicrobial test materials and excipients of the mouthwash formulations (sodium chloride, sodium bicarbonate, sodium saccharin and ethanol) were purchased from Sigma Aldrich (Germany).

Antimicrobial activity

The *in vitro* antibacterial activity was determined using the broth microdilution assay following the methods according to the Clinical and Laboratory Standards Institute (CLSI) to determine the minimum inhibitory concentrations (MIC)[19]. *Staphylococcus aureus* ATCC 6538, *Streptococcus mitis* NCIMB 13770, *Moraxella catarrhalis* ATCC 23245 and *Streptococcus mutans* ATCC 25125 strains were grown in Mueller Hinton Broth (MHB, Merck, Germany) in aerobic conditions at 37°C for 24 h. All microorganisms were adjusted to 1×10^8 CFU/mL using McFarland No: 0.5 in sterile saline (0.85%) solution. Stock solutions and serial dilutions of the test samples were prepared in dimethyl sulfoxide (DMSO). The minimum non-reproductive concentration was reported as minimum inhibitory concentration (MIC, as μg/mL). The MIC was calculated and reported as the mean of three repetitions compared to positive standards.

In addition, the *in vitro* antimicrobial activity of formulations was evaluated using the disc diffusion method following the methodology described by the Clinical and Laboratory Standards Institute (CLSI). The same human pathogenic strains were used here as well. The inoculation of the pathogens was performed using Mueller Hinton Broth (MHB, Merck, Germany) at 37°C under aerobic conditions for 24 h and standardized to 1×10^8 CFU/mL using McFarland No: 0.5 in sterile saline (0.85%). The mouthwash sample's stock solution was prepared in dimethyl sulfoxide (DMSO) at 10 mg/mL concentration, and the antibacterial evaluation was performed in triplicates[20], where the results were reported as average values.

Mouthwash formulations

The mouthwashes were prepared using combinations of the essential oils. Initially, the mouthwash solutions were formulated using 5.0-5.5% of essential oil. As sweetener saccharine sodium was applied. Furthermore, the essential oils were weighed and dissolved in ethanol while sodium chloride and sodium bicarbonate were added gradually using a mechanical stirrer (500 rpm, 30 minutes), respectively. The combination blend was filtered, and the volume of the filtrate was completed to 10 mL by using distilled water. No preservative was added since the mouthwashes included high content of ethanol (>15%), as well as essential oils (Table 1)[20].

Table 1. The mouthwash formulations containing the essential oils (EO)

Formulation code	*F. vulgare* EO (%)	*L. angustifolia* EO (%)	*C. carvi* EO (%)	*P. mugo* EO (%)	Sodium Chloride (%)	Sodium Bicarbonate (%)	Sodium Saccharine (%)	EtOH (%)	Distilled water
MF1	2.5	2.5	-	-	0.1	0.05	0.001	60	q.s. 10 mL
MF2	2.5	-	2.5	-	0.1	0.05	0.001	60	q.s. 10 mL
MF3	2.5	-	-	2.5	0.1	0.05	0.001	60	q.s. 10 mL
MF4	-	2.5	2.5	-	0.1	0.05	0.001	60	q.s. 10 mL
MF5	-	2.5	-	2.5	0.1	0.05	0.001	60	q.s. 10 mL
MF6	-	-	2.5	2.5	0.1	0.05	0.001	60	q.s. 10 mL
MF7	2.5	1	1	1	0.1	0.05	0.001	60	q.s. 10 mL

RESULTS and DISCUSSION

In this study, we report on the antibacterial activity of individual essential oils and combined mouthwash formulations. Seven different formulations exhibited the same amount of the excipients, however, in different concentrations of essential oils.

The essential oil of *F. vulgare* used in the study should contains at more than 55.0% anethole, 12.0% fenchone, and less than 6.0% estragole, according to Ph. Eur. monograph. The analysis study of the composition of essential oil of *F. vulgare*, cultivated from different places, reported predominant compounds estragole (60.01%-35.33%), anethole (22.15%-52.27%), and fenchone (6.50%-4.32%)[21]. The main components of the *L. angustifolia* essential oil obtained through steam distillation are monoterpenes such as linalool (20-50%) and linalyl acetate (25-46%)[22]. In the analysis of volatile components of *Lavandula aetheroleum* of main components was identified linalool (20.0-45.0%) and linalyl acetate (20.79-39.91%). According to the Ph. Eur., *C. carvi* essential oil should contain 50-65% carvone, 30-45% limonene, and a maximum of 2.5% of trans-dihydrocarvone and trans-carveol, respectively. The identification of the major components of *C. carvi* essential oil studies[23,24] was found to be consistent with the Ph. Eur. Essential oil of *C. carvi* obtained from the needles and twigs is used. This essential oil consists of monoterpene hydrocarbons such as α-pinene, δ-3-carene, myrcene, limonene, according to Ph. Eur. The phytochemical analysis studies showed that the major components were consistent with in the pharmacopeia[25,26].

In the present study, the antimicrobial activity of 4 different essential oils of pharmacopoeia quality at 1 mg/mL concentration was evaluated individually using the broth two-serial dilution method against oral pathogens, as shown Table 2. According to the result, essential oils at >1000 μg/mL concentration were comparatively ineffective against several oral pathogens as compared to the control group.

Table 2. Antimicrobial activity of Pharmacopeia quality essential oils

Essential oils	Minimum inhibitory concentration (mg/mL)			
	S. aureus	***S. mitis***	***M. catarrhalis***	***S. mutans***
F. vulgare	>1000	>1000	>1000	>1000
L. angustifolia	>1000	>1000	>1000	>1000
C. carvi	>1000	>1000	>1000	>1000
P. mugo	>1000	>1000	>1000	>1000
Tetracycline	8	0.5	8	0.5

Anethole was reported as the major component of *F. vulgare* essential oil, and its antimicrobial activity was found to be of low efficacy[27]. In contrast, the antimicrobial activity of *F. vulgare* essential oil was tested against various microorganisms, and the MIC value against *S. aureus* was found at concentration 250 mg/mL. Additionally, this study reported that the main components of essential oil were α-pinene, estragole, and β-pinene[28]. The results of this study differ when compared to our findings. The differences in the MIC values observed for the same microorganism could be attributed to the varying percentages of the compounds in the essential oils.

The antimicrobial effect of *L. angustifolia* essential oil was reported against human pathogens. Several studies have shown that *Lavandula* essential oil possesses significant antibacterial properties against a wide range of microorganisms. It was showed that formulations containing lavender essential oil demonstrate a stronger antimicrobial activity against *S. aureus*[29]. Other studies showed that *C. carvi* seems to have notable antibacterial activity[23,30,31]. Moreover, *P. mugo* essential oil was identified with outcomes varying based on the specific microbial pathogens targeted[26,32,33].

The oral cavity provides space for the colonization by various microorganisms that predominant components of microflora. The majority of the oral bacterial infections are polymicrobial so the combination of antimicrobial molecules should be combined. Currently, there is an increasing demand for mouthwashes formulated with combinations of essential oils. Studies demonstrated the effectiveness of Listerine® mouthwash, which is available in a combination of essential oils[34].

The antimicrobial effects of the formulations against four oral pathogens were determined using the disc diffusion test. As a result of, it was determined that the combination of *L. angustifolia-C. carvi* provided a selective antimicrobial effect

against *S. mutans* than other combinations (Table 3). Additionally, the combination of *F. vulgare-P. mugo* was effective against *S. mutans* bacteria. According to the experimental results, mouthwash combination of *F. vulgare-P. mugo, L. angustifolia-C. carvi,* and quadruple combination (*F. vulgare-L. angustifolia-C. carvi-P. mugo*) showed that the combination has a significantly antimicrobial effect (Figure 1). In the evaluation of the three combinations effective against *S. mutans*, the percentage concentrations of essential oils in the formulations are of particular interest. Both the *F. vulgare-P. mugo* and *L. angustifolia-C. carvi* formulations contain 0.25 mg/mL each of essential oil. The quadruple combination contains 0.25 mg/mL of *F. vulgare*, while the other essential oils are present at 0.1 mg/mL each. The results show that the effectiveness of the *L. angustifolia*, *C. carvi*, and *P. mugo* essential oils decreases at lower doses.

Table 3. Growth of inhibition zones of mouthwash formulations (in mm)

	S. mitis	***M. catarrhalis***	***S. mutans***	***S. aureus***
F. vulgare- L. angustifolia	18	-	17	8
F. vulgare-C. carvi	14	-	12	10
F. vulgare-P. mugo	12	-	25	7
L. angustifolia-C. carvi	12	-	30	8
L. angustifolia-P. mugo	14	-	17	8
C. carvi-P. mugo	10	-	18	8
F. vulgare-L. angustifolia C. carvi- P. mugo	19	-	22	9
Tetracycline	24	19	22	20

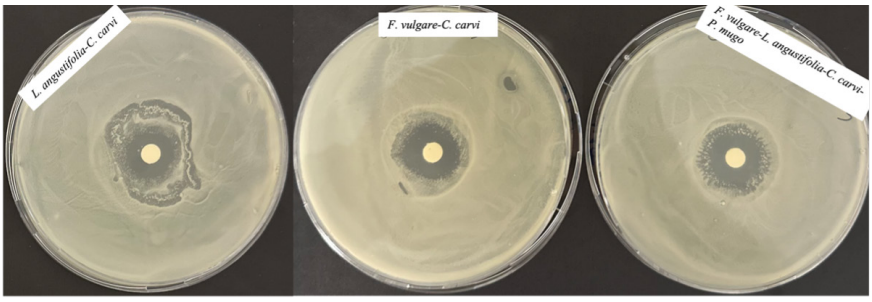

Figure 1. Disk diffusion test results against *S. mutans*

In the combination study of lavender essential oil with *Artemisia herba alba* and *Rosmarinus officinalis* essential oils, a synergistic effect was observed against the tested microorganisms[35]. A combination study of lavender and fennel essential oils also revealed an additive effect against *S. aureus*[10]. In our study, the combination of lavender and fennel essential oils showed greater effectiveness against *S. mitis* than the positive control in antimicrobial activity. Based on these findings, it can be inferred that the formulations exhibited a synergistic effect resulting from the various combinations. Essential oils used in the combinations found to have antibacterial activity exhibited a synergistic effect against *S. mutans*. Furthermore, it can be concluded that the combinations exhibiting a synergistic effect could be considered for use as mouthwashes. The first report on the antimicrobial activity of mouthwashes prepared from different combination of *F. vulgare*, *L. angustifolia*, *C. carvi*, and *P. mugo* essential oils. As a result, it is thought that mouthwash formulations developed with these pharmacopeia quality essential oils can be used especially in preventing dental caries.

STATEMENT OF ETHICS

Ethics approval is not required in this study, as no human and experimental animal samples is involved.

CONFLICT OF INTEREST STATEMENT

Declared none.

AUTHOR CONTRIBUTIONS

Data collection: A. E. Karadağ, D. Kırcı, S. E. Kahya; design of the study: A. E. Karadağ, D. Kırcı, F. Demirci, S. E. Kahya; analysis and interpretation of the data: A. E. Karadağ, S. E. Kahya; drafting the manuscript: A. E. Karadağ, S. E. Kahya.

FUNDING SOURCES

The authors declared that no financial support was received for the study.

ACKNOWLEDGMENTS

This study was presented at the 5th International Congress of Chemist and Chemical Engineers of B&H 2024, Sarajevo, Bosnia and Herzegovina.

REFERENCES

1. Coll PP, Lindsay A, Meng J, Gopalakrishna A, Raghavendra S, Bysani P, et al. The prevention of infections in older adults: oral health. J Am Geriatr Soc, 2020;68(2):411-416. Doi: 10.1111/jgs.16154

2. Claffey N. Essential oil mouthwashes: a key component in oral health management. J Clin Periodontol, 2003;30(5):22-24. Doi: 10.1034/j.1600-051X.30.s5.8.x

3. Sekita Y, Murakami K, Yumoto H, Amoh T, Fujiwara N, Ogata S, et al. Preventive effects of *Houttuynia cordata* extract for oral infectious diseases. Biomed Res Int, 2016;2016(1); 2581876. Doi: 10.1155/2016/2581876

4. Duane B, Yap T, Neelakantan P, Anthonappa R, Bescos R, McGrath C, et al. Mouthwashes: alternatives and future directions. Int Dent J, 2023;73(2):89-97. Doi: 10.1016/j.identj.2023.08.011

5. Jain I, Jain P. Comparative evaluation of antimicrobial efficacy of three different formulations of mouth rinses with multi-herbal mouth rinse. J Indian Soc Pedod Prev Dent, 2016;34(4):315-323. Doi: 10.4103/0970-4388.191409

6. Vlachojannis C, Chrubasik-Hausmann S, Hellwig E, Al-Ahmad A. A preliminary investigation on the antimicrobial activity of Listerine®, its components, and of mixtures thereof. Phytother Res, 2015;29(10):1590-1594. Doi: 10.1002/ptr.5399

7. Dudek-Wicher R, Junka AF, Migdał P, Korzeniowska-Kowal A, Wzorek A, Bartoszewicz M. The antibiofilm activity of selected substances used in oral health prophylaxis. BMC Oral Health 2022;22(1):509. Doi: 10.1186/s12903-022-02532-4

8. Alshehri FA. The use of mouthwash containing essential oils (LISTERINE®) to improve oral health: a systematic review. Saudi Dent J, 2018;30(1):2-6. Doi: 10.1016/j.sdentj.2017.12.004

9. Gulfraz M, Mehmood S, Minhas N, Jabeen N, Kausar R, Jabeen K, et al. Composition and antimicrobial properties of essential oil of *Foeniculum vulgare*. Afr J Biotechnol, 2008;7 (24):4364-4368.

10. Karadağ AE, Çaşkurlu A, Demirci B, Demirci F. Binary synergistic combinations of lavender and fennel essential oils with amoxicillin. Planta Med, 2023;89(8):800-807. Doi: 10.1055/a-1891-1119

11. European Pharmacopoeia 6.0 (2008b) Lavender oil. Council of Europe. 1/2008: 1338.

12. European Medicines Agency. Lavandula angustifolia L. European Medicines Agency; 2020.

13. Karavuş ŞN, Çaşkurlu A, Karadağ AE, Demirci F. Bioautography for evaluation of several *Lavandula* L. and *Origanum* species antimicrobial and antioxidant activity. Acta Pharm Sci, 2023;61(2):141-151. Doi: 10.23893/1307-2080.APS6110

14. Erland LA, Bitcon CR, Lemke AD, Mahmoud SS. Antifungal screening of lavender essential oils and essential oil constituents on three post-harvest fungal pathogens. Nat Prod Commun, 2016;11(4):523-527. Doi: 10.1177/1934578X1601100427

15. Blumenthal M, editor. The Complete German Commission E Monographs: therapeutic guide to herbal medicines. Austin (TX): American Botanical Council; 1999.

16. Javed R, Hanif MA, Rehman R, Hanif M, Tung BT. Caraway. In: Ahmad VU, editor. Medicinal plants of South Asia. 1st ed. Amsterdam: Elsevier; 2020. p. 87-100. Doi: 10.1016/B978-0-08-102659-5.00007-0

17. Rasooli I, Allameh A. Caraway (*Carum carvi* L.) essential oils. In: Preedy VR, editor. Essential oils in food preservation, flavor and safety. 1st ed. Amsterdam: Academic Press; 2016. p. 287-293. Doi: 10.1016/B978-0-12-416641-7.00032-8

18. Stevanovic T, Garneau FX, Jean FI, Gagnon H, Vilotic D, Petrovic S, et al. The essential oil composition of *Pinus mugo* Turra from Serbia. Flavour Fragr J, 2004;20(1):96-97. Doi: 10.1002/ffj.1390

19. CLSI, Methods for dilution antimicrobial susceptibility tests for bacteria that grow aerobically: Approved Standard, 2009;28:1-35. Wikler MA, Clinical and Laboratory Standards Institute. Methods for dilution antimicrobial susceptibility tests for bacteria that grow aerobically: approved standard. 8th ed. Wayne (PA): Clinical and Laboratory Standards Institute; 2009.

20. Karadağ AE, İpekçi E, Yağcılar AP, Demirbolat İ, Kartal M, Siafaka PI, et al. Antibacterial evaluation of *Elettaria cardamomum* (L.) Maton, *Lavandula angustifolia* Mill. and *Salvia fruticosa* Mill. essential oil combinations in mouthwash preparations. Nat Vol Essent Oil, 2020;7(1):9-17. Doi: https://doi.org/10.37929/nveo.685474

21. Abdellaoui M, Derouich M, El-Rhaffari L. Essential oil and chemical composition of wild and cultivated fennel (*Foeniculum vulgare* Mill.): a comparative study. S Afr J Bot, 2020;135: 93-100. Doi: 10.1016/j.sajb.2020.09.004

22. European Scientific Cooperative on Phytotherapy, editor. ESCOP monographs. 2nd ed. Lavandulae Flos, Lavandulae Aetheroleum. Stuttgart: Georg Thieme Verlag; 2009. p. 147-156.

23. Simic A, Rančic A, Sokovic MD, Ristic M, Grujic-Jovanovic S, Vukojevic J, et al. Essential oil composition of *Cymbopogon winterianus*. and *Carum carvi*. and their antimicrobial activities. Pharm Biol, 2008;46(6):437-441. Doi: 10.1080/13880200802055917

24. Raal A, Arak E, Orav A. The content and composition of the essential oil found in *Carum carvi* L. commercial fruits obtained from different countries. J Essent Oil Res, 2012;24(1):53-59. Doi: 10.1080/10412905.2012.646016

25. Mirković S, Tadić V, Milenković MT, Ušjak D, Racić G, Bojović D, et al. Antimicrobial activities of essential oils of different *Pinus* species from Bosnia and Herzegovina. Pharmaceutics, 2024;16(10):1331. Doi: 10.3390/pharmaceutics16101331

26. Semerdjieva B, Radoukova T, Cantrell CL, Astatkie T, Kacaniova M, Borisova D, et al. Essential oil composition of *Pinus heldreichii* Christ., *P. peuce* Griseb., and *P. mugo* Turra as a function of hydrodistillation time and evaluation of its antimicrobial activity. Ind Crops Prod, 2022;187(1):115484. Doi: 10.1016/j.indcrop.2022.115484

27. Miguel MG, Cruz C, Faleiro L, Simões MT, Figueiredo AC, Barroso JG, et al. *Foeniculum vulgare* essential oils: chemical composition, antioxidant and antimicrobial activities. Nat Prod Commun, 2010;5(2):1934578X1000500231. Doi: 10.1177/1934578X1000500231

28. Di Napoli M, Castagliuolo G, Badalamenti N, Maresca V, Basile A, Bruno M, et al. Antimicrobial, antibiofilm, and antioxidant properties of essential oil of *Foeniculum vulgare* Mill. le aves. Plants, 2022;11(24):3573. Doi: 10.3390/plants11243573

29. Hossain S, Heo H, De Silva BCJ, Wimalasena SHMP, Pathirana HNKS, Heo GJ. Antibacterial activity of essential oil from lavender (*Lavandula angustifolia*) against pet turtle-borne pathogenic bacteria. Lab Anim Res, 2017;33(3):195-201. Doi: 10.5625/lar.2017.33.3.195

30. Liu C, Cheng F, Aisa HA, Maiwulanjiang M. Comprehensive study of components and antimicrobial properties of essential oil extracted from *Carum carvi* L. seeds. Antibiotics, 2023;12(3):591. Doi: 10.3390/antibiotics12030591

31. Iacobellis NS, Lo Cantore P, Capasso F, Senatore F. Antibacterial activity of *Cuminum cyminum* L. and *Carum carvi* L. essential oils. J Agric Food Chem, 2005;53(1):57-61. Doi: 10.1021/jf0487351

32. Garzoli S, Masci VL, Caradonna V, Tiezzi A, Giacomello P, Ovidi E. Liquid and vapor phase of four conifer-derived essential oils: comparison of chemical compositions and antimicrobial and antioxidant properties. Pharmaceuticals, 2021;14(2):134. Doi: 10.3390/ph14020134

33. Mitić ZS, Jovanović B, Jovanović SČ, Mihajilov-Krstev T, Stojanović-Radić ZZ, Cvetković VJ, et al. Comparative study of the essential oils of four *Pinus* species: chemical composition, antimicrobial and insect larvicidal activity. Ind Crops Prod, 2018;111(1):55-62. Doi: 10.1016/j.indcrop.2017.10.004

34. Fine DH. Listerine: past, present and future – a test of thyme. J Dent, 2010;38:2-5. Doi: 10.1016/S0300-5712(10)70003-8

35. Moussii IM, Nayme K, Timinouni M, Jamaleddine J, Filali H, Hakkou F. Synergistic antibacterial effects of Moroccan *Artemisia herba alba, Lavandula angustifolia* and *Rosmarinus officinalis* essential oils. Synergy, 2020;10:100057. Doi: 10.1016/j.synres.2019.100057